AD621340

TECHNICAL REPORT NO. 1-682

RESPONSE OF HORIZONTALLY ORIENTED BURIED CYLINDERS TO STATIC AND DYNAMIC LOADING

by

Albert F. Dorris

CLEARINGHOUSE
FOR FEDERAL SCIENTIFIC AND TECHNICAL INFORMATION

Hardcopy	Microfiche		
$ —	$ 1.25	222	pp 48

ARCHIVE COPY

July 1965

Sponsored by

Defense Atomic Support Agency

DDC
OCT 4 1965

Conducted by

U. S. Army Engineer Waterways Experiment Station
CORPS OF ENGINEERS
Vicksburg, Mississippi

For Sale By
WATERWAYS EXPERIMENT STATION
$3.00

Qualified requesters may obtain copies of this report from DDC.

Destroy this report when it is no longer needed. Do not return
it to the originator.

The findings in this report are not to be construed as an official
Department of the Army position, unless so designated
by other authorized documents.

TECHNICAL REPORT NO. 1-682

RESPONSE OF HORIZONTALLY ORIENTED BURIED CYLINDERS TO STATIC AND DYNAMIC LOADING

by

Albert F. Dorris

July 1965

Sponsored by

Defense Atomic Support Agency

Conducted by

U. S. Army Engineer Waterways Experiment Station

CORPS OF ENGINEERS

Vicksburg, Mississippi

ARMY-MRC VICKSBURG, MISS

FOREWORD

This report was prepared in the Nuclear Weapons Effects Division, U. S. Army Engineer Waterways Experiment Station, under the sponsorship of the Defense Atomic Support Agency (DASA) as part of NWER Subtask 13.010, Response of Buried Structures to Ground Shock. The work was accomplished during the period February 1964 through May 1965. During this time, Mr. G. L. Arbuthnot, Jr., was Acting Chief of the Nuclear Weapons Effects Division, and Mr. W. J. Flathau was Acting Chief of the Protective Structures Branch.

This report was prepared by Captain Albert F. Dorris, CE, and is essentially a thesis submitted in partial fulfillment of the requirements for the degree of Doctor of Philosophy in Civil Engineering to the University of Illinois, Urbana, Illinois.

Directors of the Waterways Experiment Station during the period of this study were Colonel Alex G. Sutton, Jr., CE, and Colonel John R. Oswalt, Jr., CE. Mr. J. B. Tiffany was Technical Director.

SUMMARY

This was an experimental investigation into the response of small, shallow-buried (in dense, dry sand and stiff clay), aluminum cylinders to static (15-min rise time), rapid (13 msec), and dynamic (0.3 msec) plane-wave loading up to 500 psi. Th. cylinders had identical outside diameters of 3.5 in. and two thicknesses, 0.022 and 0.065 in. Hence, the cylinder stiffnesses, EI/R^3, were 1.7 and 45 (d/t = 159 and 54), respectively.

In stiff clay, the overpressure required to cause collapse increased very slowly with increasing depth of burial from zero to the deepest burial, three-quarters of the diameter. The hydrostatic buckling equation, $P_{cr} = 3\ EI/R^3$, was applicable for the cylinders tested.

In the dense d, the overpressure required to cause collapse increased greatly with increasing depth of burial from zero to one-eighth of the diameter. Below this depth it was not possible to collapse even the most flexible cylinders under the available 500-psi pressure. The hoop compression theory was verified. A ductility factor of about 7 was found to be conservative for cylinders buried at depths greater than one-eighth their diameter in the dense sand.

The recorded strains were nonelastic in many cases and it was shown that large yielding does not necessarily define collapse. Stress and moment were found to be nonlinear functions of overpressure, whereas thrust was generally found to be a linear function of overpressure. The differences between static and rapid loading in the elastic response of the cylinder were found to be small.

Diameter changes recorded prior to collapse for the static tests were small, less than 5 percent of the diameter.

UNIVERSITY OF ILLINOIS

THE GRADUATE COLLEGE

May 11, 1965

I HEREBY RECOMMEND THAT THE THESIS PREPARED UNDER MY

SUPERVISION BY ALBERT FRANCIS DORRIS

ENTITLED RESPONSE OF HORIZONTALLY ORIENTED BURIED CYLINDERS TO STATIC AND DYNAMIC LOADING

BE ACCEPTED IN PARTIAL FULFILLMENT OF THE REQUIREMENTS FOR

THE DEGREE OF DOCTOR OF PHILOSOPHY IN CIVIL ENGINEERING

s/ N. M. Newmark
In Charge of Thesis

s/ N. M. Newmark
Head of Department

Recomn ndation concurred in†

s/ George K. Sinnamon
s/ John D. Haltiwanger
s/ W. J. Trjitzinsky
s/ M. T. Davisson
s/ William C. Schnobrich

Committee on Final Examination†

† Required for doctor's degree but not for master's.

D517

RESPONSE OF HORIZONTALLY ORIENTED BURIED CYLINDERS TO STATIC AND DYNAMIC LOADING

BY

ALBERT FRANCIS DORRIS
B.S., United States Military Academy, 1959
M.S., University of Illinois, 1963

THESIS

Submitted in partial fulfillment of the requirements
for the degree of Doctor of Philosophy in Civil Engineering
in the Graduate College of the
University of Illinois, 1965

Urbana, Illinois

ACKNOWLEDGMENT

This thesis is based upon experimental studies conducted at the University of Illinois and the U. S. Army Engineer Waterways Experiment Station (WES). The tests conducted at Illinois were sponsored by the Department of Civil Engineering.

These studies were conducted under the general direction of Dr. N. M. Newmark, Professor and Head of the Department of Civil Engineering, and under the direct supervision of Professor G. K. Sinnamon of the Department of Civil Engineering.

Acknowledgment is made to 1st Lt. A. J. Hendron, Jr., and Mr. W. J. Flathau for their comments and encouragement, and to Mr. W. H. Sadler, Jr.,who assisted in all phases of the study at WES.

TABLE OF CONTENTS

TABLE OF CONTENTS (CONT'D)

TABLE OF CONTENTS (CONT'D)

TABLE OF CONTENTS (CONT'D)

NOTATION

a	Radius of the intrados of the cylinder
A	Area of the cross section perpendicular to the ring center line
AR	Arching ratio
b	Radius of the extrados of the cylinder
C_u	Uniformity coefficient, D_{60}/D_{10}
d	Outside diameter of cylinder
D_r	Relative density, $\frac{e_{max} - e}{e_{max} - e_{min}}$
D_{10}	Soil grain diameter of which 10 percent of the soil weight is finer
D_{60}	Soil grain diameter of which 60 percent of the soil weight is finer
e	Void ratio, $\frac{V_v}{V_s}$
e_{max}	Maximum void ratio
e_{min}	Minimum void ratio
e_o	Initial void ratio
E	Modulus of elasticity of the cylinder, Young's modulus
E'	Modulus of soil reaction, equal to $k_s R$, psi
E_s	Modulus of elasticity of the soil
g	Acceleration of gravity
G_s	Specific gravity of the solids
h	Thickness of the cylinder wall
I	Moment of inertia of the cross section of the cylinder wall per unit length, in.^{4}/in., I_y

k Spring constant, load divided by deflection

k_ℓ Coefficient of elastic soil reaction, psi per strain

k_m Coefficient of soil reaction ("subgrade modulus")

k_s Modulus of passive resistance of the enveloping earth, psi per inch of deflection, $lb/in.^3$

k_z Radial elastic support

K_o Coefficient of earth pressure at rest

ℓ Cylinder length

M_c Bending moment at the cylinder crown, constrained soil modulus

M_{cs} Constrained secant modulus of soil

M_y Bending moment, M

n Buckling mode number or order; number of half-waves

N_y Thrust or normal force in the cylinder, lb/in.

p Pressure, psi

p_a Vertical pressure on a horizontal plane through the cylinder crown

p_c, p_{cr}, p_f, p_h, p_ℓ, p_m, p_t Critical buckling pressure

p_o Critical buckling pressure in lowest mode for a ring subjected to hydrostatic pressure.

P Vertical force, lb

P_{so} Overpressure on surface of soil, psi

P_{sof} Overpressure on surface of soil when cylinder collapsed

q Ratio of average horizontal force (or pressure) to average vertical force (or pressure) applied to the cylinder

q_u Unconfined compressive strength

Q Vertical shear force in soil between surface and cylinder crown

Q' Vertical shear force in soil between cylinder crown and spring line

Q'' Oblique shear force in soil between cylinder crown and spring line

r Radius of a cylinder element

R Radius of the cylinder middle surface

S_r Degree of saturation

S, S_1 Relative stiffness

t Time

T_c Period of vibration in the compressive mode

T_f Period of vibration in the first flexural mode

TD Typical descriptor of relative stiffness

V Total volume of soil sample

V_o Initial volume

V_s Volume of soil solids

V_v Volume of voids

w Radial displacement of the cylinder; water content

x, y, z Cylinder coordinates, spatial cordinates

Z Vertical distance from soil surface to cylinder crown

γ Unit weight of soil, specific weight

γ_d Dry unit weight

Δ_h Horizontal deflection (increase in diameter)

Δ_v Vertical deflection (decrease in diameter)

ΔV Volume change

ϵ Unit strain

ϵ_e Strain on extrados of the cylinder

ϵ_i Strain on intrados of the cylinder

θ Circular angle

ν Poisson's ratio of the cylinder

ν_s Poisson's ratio of the soil

σ Stress

σ_y Stress in the y or tangential direction

σ_{y1} Lower or first yield stress

σ_{y2} Upper yield stress (result in 0.2 percent permanent strain)

σ_1 Vertical stress

σ_3 All-around confining stress

ϕ Angle of internal friction

LIST OF TABLES

LIST OF FIGURES

RESPONSE OF HORIZONTALLY ORIENTED BURIED CYLINDERS

TO STATIC AND DYNAMIC LOADING

CHAPTER 1. INTRODUCTION

1.1 Background

The art of designing buried structures to resist nuclear blast loading is still (1965) in its infancy. A desirable way of augmenting the development and evaluation of particular protective structures designs is to conduct full-scale tests; however, the moratorium on full-scale surface tests in effect since 1 November 1958 eliminates this approach in studying the response of shallow-buried structures to overpressure-induced disturbances. Unfortunately, even if full-scale tests had been permitted since 1958, it is doubtful that sufficient data would be available from such tests alone to formulate economical and practical designs for most design situations. Laboratory and analytical studies still would have been needed to supplement such programs. Because of the limitations imposed by the moratorium, special emphasis has by necessity been placed on analytical studies and laboratory tests of small-scale structures for the purpose of developing usable design methods.

At the moment there is a lack of well-documented experimental data and field experience with which to compare current thought and analytical theory. The most advanced design manual, Principles and Practices for Design of Hardened Structures by Newmark and Haltiwanger (1962, under revision),* and the current source book of underground phenomena and effects of nuclear weapons, Nuclear Geoplosics by Stanford Research

* Authors and dates refer to list of references at end of text.

Institute (1964), point out a multitude of unknowns in the state of the art.

1.2 Problem Under Study

Buried cylindrical or ring configurations are ideal geometries to resist external loads effectively and are thus well suited to protect personnel and appurtenances for various facilities such as NIKE and ICBM hardened sites. They are also favored as entrances and escape routes for protective structures buried deep in rock. Additionally, almost all communication and utility conduits, existing and planned, are cylindrical in shape. Currently, these structures are being designed largely on the basis of engineering hypotheses supplemented by the field experience gained with buried conduits and tunnel liners subjected to static loading. There is virtually no experimental validation of the current dynamic design criteria. Because of the uncertainties, the current design procedures are only stop-gap measures which await the results of controlled experimental investigations for confirmation or refutation.

The problems of designing shallow-buried protective structures for overpressure-induced loading from large-yield weapons differ from those associated with other underground cylindrical structures in at least two major ways: (1) The live load is large compared with the dead load, and the structure must be designed primarily for the live load; (2) the criteria for failure, together with the factor of safety, must lead to the least expensive structure which couples cost and use to fulfill requirements. A factor of safety of 4 is common in culvert design as indicated by Armco Drainage and Metal Products, Inc. (1958, p 70). This factor is sufficiently large to take care of many unknowns. However, a factor this large is economically infeasible for the design of most protective structures.

1.3 Objective of the Study

The objective of this investigation was to study experimentally the phenomena associated with the failure of horizontally oriented, circular cylinders buried at various shallow depths in several soil media and subjected to either static or dynamic overpressures.

1.4 Scope of the Investigation

It would be desirable to study a wide range of cylinder types by varying such parameters as material properties of the cylinder, cylinder dimensions, soil media, depths of burial, overpressure characteristics, and combinations of instrumentation transducers. Experimentally, very little ultimate strength work has been done to study buried cylindrical structures in the collapse range.

An evaluation of all the parameters and combinations in detail would be far beyond the scope of any single investigation. The parameters selected for study are outlined below:

1. In order to examine the extreme range in soil media, two soils were selected: a dense, dry sand and a highly plastic clay placed at such a water content that the consistency ranged from stiff to very stiff as defined by Terzaghi and Peck (1948, p 31).
2. In order to examine the effect of depth of burial, five shallow depths, ranging from zero to 2-5/8 in. or 3/4 diameter (d), were investigated.
3. In order to examine overpressure effects, three pressure-time signatures were used, ranging from a quasi-static rise time of 10 to 15 min, to a rapid

rise time of 13 msec, and up to a dynamic rise time of 0.3 msec.

4. In order to examine a range in structural stiffness, two circular cylinder geometries (two wall thicknesses and three nominal yield strengths) were employed. The outside diameter, length, and end conditions were kept constant.

Since underground cylindrical structures have long been used as tunnels, culverts, sewers, and pipes, a great deal of qualitative knowledge is available covering all aspects of the soil-structure system, e.g. arching, longitudinal beam action, live load distribution, ring loading, and ring response. Fig. 1.1 illustrates some of the concepts of load transfer from the soil surface to the underground structure.

This test program was planned to investigate ring response, and the emphasis was not on the associated phenomena such as arching. These will be discussed only as they contribute to an understanding of the ring response.

Forty-six cylinders were tested during the investigation. For each rapid or dynamic test (plane wave loading), a corresponding static test was performed for comparison. The entire program is summarized in Table 5.1.

The 30 cylinders designated as groups A, B, and C were tested under static and rapid loading in the blast-loading facility at the University of Illinois. The 16 cylinders in groups D and E were tested under static and dynamic loading at the U. S. Army Waterways Experiment Station (WES).

CHAPTER 2. DEVELOPMENT OF PRESENT STATE OF KNOWLEDGE

2.1 Culvert, Pipe, and Tunnel Contribution

It is not the writer's purpose to cite all of the potentially applicable work, but rather to categorize the development of current schools of thought and to summarize the more pertinent references describing the development of design and analysis procedures for buried cylinders.

2.1.1 Talbot, Cain, Marston

Talbot (1908) tested cast-iron, plain concrete, and reinforced concrete pipes to failure. He recognized both the beneficial effect of lateral confinement (p 22) and the ability of the concrete rings to retain their circular configuration until final failure occurred when the concrete crushed (p 65). The idealized load distribution which he considered is shown in Fig. 2.1a. In view of the fact that the load distribution was not uniform, that the actual value of q (the average horizontal pressure divided by the average vertical pressure) was not determinable, and that cracking would not be acceptable for permanent installations, Talbot recommended the use of the formula $M_c = 0.25p_aR^2$ for design, i.e. the maximum bending moment (at the crown), M_c, with $q = 0$ where p_a is the average pressure on a horizontal plane through the crown, and R the mean radius of the pipe. Any surplus strength offered by the side restraint would be "considered merely an additional margin of safety" (Talbot (1908)).

Braune, Cain, and Janda (1929) explored the possibility that the horizontal pressure was not distributed all the way to the top of the ring (Fig. 2.1b). Using the results of pressure cell measurements on the surface of relatively flexible rings, they (in Appendix II written by Cain) tried to arrive at applicable values of θ, the circular angle, and q. Cain also discussed (p 173) the reasons why deflections determined by a uniform radial load theory would never agree with measured values. This theory treats the horizontal passive soil resistances as if they were active soil forces.

Marston (1930) summarized his own work on arching and gave some guidelines to define the differences between flexible and rigid conduits. He considered flexible conduits as having cross-sectional shapes that can be distorted sufficiently to change their vertical or horizontal dimensions more than 3 percent before causing materially injurious cracks; rigid conduits cannot sustain such distortions.

2.1.2 Spangler

Spangler (1938) used a friction tape technique to measure the pressure distribution on the outside of flexible metal pipes. He developed a hypothetical distribution of pressure, Fig. 2.1c, based on the maximum unit horizontal pressure being equal to the modulus of passive resistance, k_s, of the fill material multiplied by one-half the horizontal diameter change. Spangler used e for this, but for distinction within this report the term k_s shall be used. He stated that deflection of a flexible culvert is the phenomenon of primary interest "because failure of flexible pipes occurs by excessive deflection rather than excessive stress." Spangler's design formula (Iowa Formula) for good bedding, Fig. 2.1c, also shows the relative influence of the pipe parameter, EI, and the influence of the passive soil resistance parameter, $0.061\, k_s R^4$, where E is the modulus of elasticity of the pipe, I is the moment of inertia of the pipe wall, and R is the mean radius of the cylinder.

Spangler (1948) reviewed the state of knowledge of underground conduits and pointed out the lack of knowledge concerning the modulus of passive resistance, k_s . He also indicated that the load distribution on a horizontal plane at the level of the cylinder crown, p_a , is approximately uniform over the breadth of the pipe. Spangler (1956, pp 1054-9) discussed the validity of assuming a condition of plane strain or plane stress for pipeline problems. He concluded that it is not possible to determine which most nearly applies, and used the somewhat simpler plane stress assumption which is not dependent upon Poisson's ratio, ν , of the cylinder. Spangler (1960, Chapter 25) further discussed the Iowa Formula and tentatively recommended that for flexible culverts the deflection should not exceed 5 percent of the diameter. Typical values for the modulus of passive resistance were mentioned. Spangler indicated that the modulus of passive resistance is strongly influenced by the size of the pipe and gave recommended values for design.

2.1.3 Watkins

Watkins and Spangler (1958) examined the Iowa Formula from a dimensional analysis or similitude point of view. It was concluded that the modulus of passive resistance is not a property of the soil alone; and, further, that the product of the modulus of passive resistance, k_s , times the pipe radius is a constant for a given soil. This quantity, k_sR , was termed the modulus of soil reaction, E' .

Watkins (1959) attempted to correlate the modulus of soil reaction to properties that are easily measured. His work indicated that the modulus was related to the compression index for a given soil. Watkins (1960) pointed to buckling of the pipe wall, before an excessive diameter change has occurred, as a potential failure mechanism for buried conduit systems. Watkins (1963) suggested that the hydrostatic buckling equation, $p_o = \frac{3EI}{R^3}$ (where p_o is the critical buckling pressure in psi), be applied as a conservative estimate of the buckling failure phenomenon. This and the work of Brockenburgh (1963) influenced the U. S. Steel Corporation to produce a new corrugation profile for their flexible culverts. Watkins and Nielson (1964) developed a test apparatus, modpares device, to measure the modulus of soil reaction. It was found that this quantity is not a constant, but rather decreases with increasing conduit deflection.

Watkins (1964) again pointed out the importance of the soil in influencing structural response, and illustrated the possibility of buckling for a very flexible ring carefully embedded in a well-compacted, granular fill.

2.1.4 Schafer, Barnard, White

Schafer (1948) stated that an average safe maximum deflection for conduits is 20 percent of the vertical diameter. Application of a factor of safety of 4 to the deflection criterion leads to a design deflection of 5 percent. He developed an empirical deflection equation, examined the Iowa Formula, and concluded that it gave undue value to the side-support factor, k_s, for large-diameter structures.

Barnard (1957) pointed out that apparent bending stresses in steel pipe based on elastic theory are not of importance in themselves when the ductility of the material in the shell permits deformation without failure. Localized bending stresses which appear to pass the yield point of the material are not proper criteria for failure.

White and Layer (1960) proposed the ring compression theory,

Fig. 2.1d, as a rational design tool. They argued that the ring bending stiffness need only be sufficient (1) to prevent buckling, (2) to resist the uneven loads in minimum cover installations, and (3) to permit easy handling and erection. White (1961) described a 21-ft-diameter corrugated culvert designed by using the ring compression theory, and indicated that the primary factor for average corrugated metal conduits is compressive strength.

2.1.5 Meyerhof

Meyerhof and Baikie (1963) performed tests to failure on quarter sections of curved steel sheets bearing against dense sand backfill. They showed that for small values of the subgrade modulus and the flexural rigidity of the plates, the sheets would fail by buckling; but, for larger values of these parameters the sheets would fail by yielding of the section. The ring compression theory was supported. Their buckling theory, discussed in Chapter 3, indicates that the hydrostatic theory is overly conservative. Meyerhof and Fisher (1963) discussed several field experiences and concluded that failures due to excess deflection were a consequence of unsuitable backfill material or poorly compacted soil. They urged the use of competent backfill so that the ring compression theory could be applied.

2.1.6 Large Field Structures

Terzaghi (1943) observed experimental sections of the Chicago subway tunnels in clay, and concluded that a nearly uniform distribution of pressure should be assumed. Terzaghi (1942, p 207) further suggested that the bending moments would be insignificant even in a fairly thick shell because the deformation of the tube automatically reduces the moments.

Peck and Peck (1949) discussed observations made on large-diameter, flexible steel culverts. They concluded that if the soil is adequately compacted, a moderate deformation will establish a state of nearly uniform all-around pressure.

Lane (1960) described the observation made of tunnel test sections at Garrison Dam. In the flexible sections, the ratio of the horizontal to vertical load ranged from 0.8 to 1.1. However, higher bending moments were observed in the flexible ribs than could be explained by the small differences between the measured horizontal and vertical thrusts. Thus, the moment was apparently dependent on things other than the overall loading, such as the construction procedures.

2.2 Protective Structures Research

2.2.1 Dynamic Theory

A number of complex solutions have been generated for mathematical continuum models which are tractable within the classical theory of elasticity. Palmer and Lankford (1963) compared several solutions and recommended the approach taken by Yoshihara and others (1963) as being very promising. Albritton and others (1965) reported the results of an experimental pilot study of a stiff, buried cylinder and an extensive analysis of the mathematical and physical limitations of the currently available continuum theories.

Mow (1964) reviewed various dynamic analyses and concluded that "under the assumption of earth media being elastic, homogeneous and isotropic, the dynamic-stress concentration factors for all cylindrical-cavity cases, whether elastically lined or unlined, are all about 10 to 20 percent higher than those for their corresponding static cases." The verification of this analytical prediction could reduce the problem (when a step pulse or instantaneously applied input assumption is applicable) to the simpler static case with an arbitrary 20 percent increase in design equations.

As a consequence of the work of Merritt and Newmark (1962) and Melin and Sutcliffe (1959), Newmark and Haltiwanger (1962) outlined the only theory known to the writer which takes into account the nonelastic behavior of the cylinder.

No directly applicable theory of dynamic buckling is known.

2.2.2 Static Theory

In addition to the mechanics' theories already mentioned in connection with culverts, Section 2.1, several possible elastic continuum theories exist. Palmer and others (1963) compared a number of these and suggested using the solution of Savin (1961) for a lined hole in an infinite plate. Other similar solutions can be found for the static case which evolve as limiting portions (longtime or steady state) of the dynamic analyses where they approach the static case.

2.2.3 Ultimate Strength Laboratory Tests

Bulson (1962) tested 56 thin tubes to failure under static loading up to 100 psi. Overpressure and dial deflections were the only measurements made, but these were sufficient to describe the failure mode as buckling. The failures at the deepest burial, 3/4d , in the dense sand point to a failure mode heretofore unrecognized for fully buried cylinders. Bulson (1963, a and b, and 1965) extended the work to square cylinders and (1964) summarized all of his previous tests.

Donnellan (1964) conducted nondestructive tests on instrumented cylinders and destructive tests on noninstrumented cylinders buried in dense, dry, 20-30 Ottawa sand. The loading was quasi-static up to a maximum of 160 psi. Only the overpressure was monitored during the ultimate strength tests.

Whitman and Luscher (1962) and Luscher (1963) statically tested small aluminum tubes surrounded by dense sand and symmetrically loaded in a triaxial type device. As a result, Luscher and Höeg (1964) concluded that the major contribution of the sand to the system was to force the cylinder to respond in higher buckling modes. Luscher and Höeg (1964) also conducted buried tube tests which yielded failure conditions similar to those of the fully symmetric situation.

2.2.4 Nondestructive Laboratory Tests

A number of tests have been conducted to verify elastic theories and to form a basis for predicting the ultimate strength of a cylinder.

Allgood and Gill (1964) made a series of static and dynamic tests up to a maximum of 25-psi overpressure on a 24-in.-diameter steel cylinder buried in dense sand. All response was in the elastic range of the cylinder material. They found that the form of the deflection, thrust, and moment distribution was much the same under both types of loading. Some differences were noted: The maximum thrust under dynamic loading was about 14 percent higher than for static loading; the crown deflection under dynamic loading was about twice that under static loading. Allgood (1965), in attempting to summarize the case of a thin metal cylinder buried at shallow depths in a uniform, noncohesive soil, concluded that the net arching (reduction in vertical load below that at the surface) across a thin metal cylinder is negligible.

Robinson (1962) presented the results of a series of static tests up to a maximum of 100-psi overpressure on 6-in.-diameter tubes buried in dense, dry Ottawa sand. Robinson (1964) extended the earlier tests by including more strain gages. Four test sections were used at a depth of burial of 15 in., 2-1/2d. The results were nonsymmetric in response and showed a great amount of scatter in the moments.

2.2.5 Full Scale Tests

Albright and others (1960) described the response of large-diameter, buried conduit sections located at the 100-psi pressure range of Shot Priscilla (1957) in Operation PLUMBBOB, a full-scale field test. The sections were selected by means of modified static design procedures, and all survived the blast loading.

Williamson and Huff (1961) described the response of 20-ft long, 7-ft diameter, 10-gauge structural-plate pipes buried at a 10-ft depth of cover and subjected to a pressure of 250 psi from Shot Smoky of Operation PLUMBBOB. Again the structures survived with very small deformations and virtually no damage.

McDonough (1959) described tests on drum-shaped structural models buried at depths of from 0 to 20 ft and subjected to the effects of air-induced pressures resulting from large detonations. The compressibility of the structure relative to the surrounding soil appeared to govern the amount of load that was transmitted to the structure.

2.3 Similitude Studies

The American Machine and Foundry Company (1962) and Murphy and Young (1962) examined the feasibility of modeling the soil-structure interaction problem, and developed similitude relations.

Murphy and others (1963) demonstrated the feasibility of using small-scale modeling for qualitative results. Young and Murphy (1964) tested their similitude requirements on stiff aluminum cylinders buried in dry Ottawa sand, and concluded that the requirements were satisfied within the range of parameters investigated.

Dowell (1964) continued the work with stiff cylinders, but experienced difficulty as a result of sidewall friction in the testing device.

2.4 Bibliographies and Design Manuals

Van Horn and Tener (1963) and Merkle (1963) prepared annotated bibliographies on the subject of soil-structure interaction. Each chapter of the five volume set of Nuclear Geoplosics by Stanford Research Institute (1964) contains an excellent bibliography. The Effects of Nuclear Weapons by U. S. Atomic Energy Commission (1964) covers the general field of nuclear weapons, and the Proceedings of the Symposium on Soil-Structure Interaction by University of Arizona (1964) presents the most up-to-date research.

Design manuals appeared in 1957 with the U. S. Army Corps of Engineers series EM 1110-345-413 to -421. American Society of Civil Engineers (1961) and Newmark and others (1961) developed design recommendations. Newmark and Haltiwanger (1962, under revision) outlined design procedures for hardened sites.

CHAPTER 3. THEORETICAL CONSIDERATIONS

Various theoretical solutions and concepts are presented in this chapter and are compared with the test results in Chapter 6. The non-availability of a dynamic buckling theory together with the theoretical indication that the dynamic response for a step pulse is only 10 to 20 percent greater than the static response suggests that static theory may be applicable for the elastic case.

3.1 Definition of Failure

A protective structure fails when it can no longer perform the function for which it was designed. For the shell under consideration, Fig. 3.1, failure is an inability to keep the ring from collapsing. This could come about by (1) the vertical diameter decreasing to such an extent, say 20 percent, that the crown would reverse curvature and plunge to the invert, Fig. 3.2a; (2) a section of the wall becoming unstable before a large-diameter change has occurred (and buckling inward into the cavity with a large amplitude) as a consequence of the interaction between thrust and moment (a) before any fiber in the cross section has yielded, (b) after some fibers have yielded in bending but before the whole cross section has yielded in thrust, (c) at some time after the whole cross section has yielded in thrust (hoop compression). Fig. 3.2b, c, and d show some observed modes of failure.

Large, i.e. greater than 5 percent, changes in diameter will not occur (if the cylinder is emplaced in a competent backfill) before one of the failure mechanisms in (2) above has triggered the structural collapse. The backfilling around protective structures should be carefully controlled; therefore, the tests of the present investigation were conducted in well-compacted and -controlled sand and clay specimens.

Because the cylinder tends to readjust itself under load, it may be assumed that the bending moments are negligible in the development of a buckling criterion. Hence, failures (2)(a) and (2)(b) mentioned previously can be considered one condition describing the elastic membrane response of the cross section.

As long as the wall acts as a ductile member, yielding will not constitute failure other than as it precipitates inelastic buckling.

3.2 Elastic Buckling

3.2.1 Soil Medium Approximated by Water

A first approximation to the problem of a uniform soil-surrounded cylinder can be made by the use of the equation for hydrostatic buckling of a ring, Fig. 3.3. Since this mathematical model assumes that the medium possesses no shear strength, it should serve as a lower bound for the buckling value for uniform radial loading. Seely and Smith (1952, p 612) arrived at the classical relation

$$p_h = (n^2 - 1) \frac{EI}{R^3} \qquad n \geq 2 \qquad 3.1$$

where p_h = uniform collapsing (critical) pressure (force per unit area) for the ring section

n = buckling mode number, an integer

E = modulus of elasticity of the cylinder material

I = moment of inertia (per unit length) of the ring cross section

R = mean radius of the ring

The minimum value for p_h, other than zero, is

$$p_o = 3\,\frac{EI}{R^3} \qquad 3.2$$

Timoshenko and Gere (1961, p 292) indicated that the buckling forms of higher order can be obtained only by introducing certain additional constraints. For $n = 3$, $p_h = 8\,\frac{EI}{R^3}$ or $2.7\,p_o$. For $n = 4$, $p_h = 15\,\frac{EI}{R^3}$ or $5\,p_o$. Williamson and Huff (1961, p 42) used $15\,\frac{EI}{R^3}$ as their buckling criterion.

The hydrostatic value for the critical buckling pressure is based on the external forces remaining normal to the surface of the ring when buckling occurs. Boresi (1955, p 101) has shown that the coefficient on $\frac{EI}{R^3}$ in equation 3.2 is 4.5 for the fundamental buckling mode if the external forces are assumed to remain directed toward the original center of the ring instead of normal to the surface. Bodner (1958) showed that the coefficient is 4 for a constant-directional-pressure force system.

The foregoing observations indicate some of the potential weaknesses in the hydrostatic assumption. A slightly different assumption in the action of the surface traction could change the critical buckling pressure by 50 percent.

Anderson and Boresi (1962) investigated a nonuniform load distribution of the form $p = p_a \sin^2\theta$, Fig. 3.4, where p_a is the peak pressure at the crown. For centrally directed forces, p_{cr} (average) $= 4.5\,\frac{EI}{R^3}$, which was identical with the uniform load case where p_{cr} (average) is the total load divided by the circumference. This implies that the specific load distribution may not be overly critical in some cases.

For the test specimens of cylinder groups A, B, D, and E, $p_o = 135$ psi and for group C, $p_o = 5.1$ psi from equation 3.2 for the lowest mode.

Other investigators, e.g. Donnellan (1964), have tested cylindrical shells in which the longitudinal boundaries were supported and as a result the theoretical buckling equation became a function of the cylinder length, ℓ . Timoshenko and Gere (1962, p 478) derived the expression for a simply supported shell, $w = \frac{\partial^2 w}{\partial x^2} = 0$ where w is the deflection of the middle surface in the radial direction and x is the cylinder coordinate in the longitudinal direction, Fig. 3.1.

$$p_t = \frac{Eh}{R(n^2 - 1)\left(1 + \frac{n^2 \ell^2}{\pi^2 R^2}\right)} + \frac{EI}{(1 - \nu^2)R^3}\left(n^2 - 1 + \frac{2n^2 - 1 - \nu}{1 + \frac{n^2 \ell^2}{\pi^2 R^2}}\right) \qquad 3.3$$

where p_t is the theoretical buckling pressure, and h is the wall thickness. The number of half-waves, n , into which the shell buckles increases as the length of the shell decreases and as the thickness of the shell decreases. Taking the limit of equation 3.3 as the length becomes long (approaches infinity) yields the equation for a long tube or structure

$$p_t = \frac{(n^2 - 1)}{(1 - \nu^2)} \frac{EI}{R^3} \qquad 3.4$$

where ν is Poisson's ratio of the cylinder material.

For a value of $\nu = 0.3$, equation 3.4 for a long cylindrical shell differs from equation 3.1 for a ring by only 10 percent.

Armenàkas and Herrmann (1963) reanalyzed the shell case and presented convenient graphs to allow rapid assessment of the critical buckling number n corresponding to values of ℓ/R .

3.2.2 Soil Medium Approximated by Elastic Support

Cheney (1963, p 41) derived an expression for the critical buckling pressure (p_c) of a ring with radial elastic support, Fig. 3.5.

$$p_c = (n^2 - 1)\frac{EI}{R^3} + \frac{k_z R}{n^2 - 1} \qquad n \geq 2 \qquad 3.5$$

in which

$$n_{cr} = \sqrt{1 + \sqrt{\frac{k_z R^4}{EI}}} \geq 2 \qquad 3.6$$

This leads to a convenient approximation

$$p_c = 2\sqrt{k_z \frac{EI}{R^2}} \qquad 3.7$$

where k_z is the spring constant in psi per in. of radial deflection. Cheney (1964) pointed out that equation 3.7 underestimates the buckling load no more than by 10 percent for n greater than 5 and less than 1 percent for n greater than 10. For vanishing values of k_z and for n less than 5, the exact expression, equation 3.5, must be used because equation 3.7 is not suited to small values of the spring constant or n.

The great difficulty involved in applying this type of equation is the evaluation of an appropriate spring constant, k_z, for the soil. To facilitate comparison, equation 3.7 can be rewritten as

$$p_c = 2\sqrt{k_z R}\sqrt{\frac{EI}{R^3}} \qquad 3.8$$

Meyerhof and Baikie (1963, p 13) arrived at an elastic buckling equation by modifying the theory of flat plates on an elastic foundation. Their equation may be written as

$$p_m = \frac{(n + 1)^2 - 1}{1 - v^2}\frac{EI}{R^3} + \frac{(1 - v^2)\, k_m R}{(n + 1)^2 - 1} \qquad 3.9$$

where k_m is the coefficient of soil reaction ("subgrade modulus").

For large values of n this can be reduced to

$$p_m = 2\sqrt{\frac{k_m EI}{(1 - \nu^2)R^2}} \qquad 3.10$$

or

$$p_m = 2\sqrt{\frac{k_m R}{(1 - \nu^2)}}\sqrt{\frac{EI}{R^3}} \qquad 3.11$$

Equation 3.11 differs from Cheney's equation, 3.8, only by the factor $(1 - \nu^2)$.

Luscher and Höeg (1964, p 35) used an approach of Hetényi (1946) to arrive at an equation for critical buckling pressure (p_ℓ).

$$p_\ell = 2\left(\sqrt{\frac{k_\ell R^3}{EI} + 1} - 1\right)\frac{EI}{R^3} \qquad 3.12$$

where

$$n_{cr} = \sqrt[4]{\frac{k_\ell R^3}{EI} + 1} \qquad 3.13$$

These can be simplified for higher order buckling modes to

$$p_\ell = 2\sqrt{k_\ell \frac{EI}{R^3}} = 2\sqrt{k_\ell}\sqrt{\frac{EI}{R^3}} \qquad 3.14$$

and

$$n_{cr} = \sqrt[4]{k_\ell \frac{R^3}{EI}} \qquad 3.15$$

where k_ℓ = coefficient of elastic soil reaction (having the units psi per strain). Luscher and Höeg (1964, p 143) expressed k_ℓ in terms of the constrained tangent modulus of the soil and the thickness of the soil support. For the Ottawa sand which they used, the equation was written as

$$p_\ell = 780\left[\frac{EI}{R^3} f(R)\right]^{5/6} \qquad 3.16$$

where $f(R)$ is a function of the depth of burial.

Newmark and Merritt (1963) considered a similar problem.

All of the above can be summarized by the following:

$$p_c = 2\sqrt{k_z R}\sqrt{\frac{EI}{R^3}} \geq \frac{3EI}{R^3} \qquad 3.8$$

$$p_m = 2\sqrt{\frac{k_m R}{(1-v^2)}}\sqrt{\frac{EI}{R^3}} \qquad 3.11$$

$$p_\ell = 2\sqrt{k_\ell}\sqrt{\frac{EI}{R^3}} \qquad 3.14$$

The application of this type of formula revolves around an ability to arrive at an appropriate value of the coefficient of soil reaction. This will be discussed in Chapter 6.

3.2.3 Soil Medium Approximated by an Elastic Medium

Forrestal and Herrmann (1964) derived a buckling equation for a long cylindrical shell subjected to uniform external pressure exerted by a surrounding elastic medium, Fig. 3.6. The solution for the unbonded case (shear stresses between the shell and the medium are absent) can be expressed as

$$p_f = \frac{(n^2-1)}{(1-v^2)}\frac{EI}{R^3} + \frac{E_s}{(1+v_s)(1-2v_s)(n+1)+n} \qquad 3.17$$

where p_f is the critical buckling pressure, E_s is the Young's modulus of the medium, and v_s is the Poisson's ratio of the medium. Solutions for the bonded case were also presented but were more complicated and did not give results which varied greatly from those for the unbonded case.

3.3 Inelastic Action

After the cross section has yielded in hoop compression, it can continue to yield or strain for some time before structural collapse. It is hypothesized that such failure can be defined by the judicious choice of a ductility factor. Newmark and Haltivanger (1962) defined this factor, μ, as the ratio of the maximum deflection to the deflection at yield. Ductility factors for compression members have been assumed to be in the range 1.3 to 1.5.

3.4 Characteristic Ring Parameter

In order to compare the results of various tests run by different investigators, it is necessary to have a parameter by which the ring can be adequately described. Various groupings have been used, e.g. radius to thickness ratio, diameter to thickness ratio, and these quantities weighted in some fashion by the modulus of elasticity.

The quantity $\frac{EI}{R^3}$ appears as a parameter in all of the aforementioned buckling equations and appears to be a convenient index for the elastic action of rings.

Stiffness can be defined as the force required to produce a unit deflection. For a large variety of loading configurations this is a function of $\frac{EI}{R^3}$. Fig. 3.7 illustrates a number of these loading conditions, many of which were investigated by Lane (1960, p 287).

Point load, P (Fig. 3.7a):

$$\frac{P}{\Delta_v} = 6.7 \frac{EI}{R^3} \qquad 3.18$$

60° triangle (Fig. 3.7b):

$$\frac{p(2R)}{\Delta_v} = 29 \frac{EI}{R^3} \qquad 3.19$$

90° triangle (Fig. 3.7c):

$$\frac{p(2R)}{\Delta_v} = 22 \frac{EI}{R^3} \qquad 3.20$$

120° triangle (Fig. 3.7d):

$$\frac{p(2R)}{\Delta_v} = 19 \frac{EI}{R^3} \qquad 3.21$$

180° triangle (Fig. 3.7e):

$$\frac{p(2R)}{\Delta_v} = 18 \frac{EI}{R^3} \qquad 3.22$$

Parabolic (Fig. 3.7f):

$$\frac{p(2R)}{\Delta_v} = 14 \frac{EI}{R^3} \qquad 3.23$$

Uniform (Fig. 3.7g):

$$\frac{p(2R)}{\Delta_v} = 12 \frac{EI}{R^3} \qquad 3.24$$

Side support (Fig. 3.7h):

$$\frac{p(2R)}{\Delta_v} = 12\ (1 - q)\ \frac{EI}{R^3} \qquad 3.25$$

Uniform radial (Fig. 3.3a):

$$\frac{p(2R)}{\Delta_v} = 2 \frac{Eh}{R} \qquad 3.26$$

where Δ_v is the decrease in vertical diameter, q is the ratio of the horizontal to the vertical pressure, and h is the ring wall thickness.

It also appears that the parameter $\frac{EI}{R^3}$ may provide a means for differentiating between so-called stiff and flexible buried cylinders. The Iowa Formula (Fig. 2.1c) can be rewritten as

$$\frac{p(2R)}{\Delta_h} = \frac{0.061(k_s R) + \frac{EI}{R^3}}{0.083} \qquad 3.27$$

where Δ_h is the increase in horizontal diameter. If a flexible structure is defined as one whose stiffness, $\frac{EI}{R^3}$, has less than a 10 percent influence on elastic deformation relative to the influence of the soil, then, from equation 3.27, a stiff structure is one in which

$$\frac{EI}{R^3} > 0.61(k_s R) \tag{3.28}$$

In a dense sand medium (with $k_s R = E' = 1000$ as suggested by Watkins and Nielson (1964, p 173)), a cylinder is stiff if $\frac{EI}{R^3} > 610$ psi from equation 3.28. In a clay (with $E' = 900$), it is stiff if $\frac{EI}{R^3} > 550$ psi. These stiffness values are greater than those required to prevent buckling for overpressures lower than 1500 psi.

Other approaches have been suggested to arrive at relative stiffness. Meyerhof and Baikie (1963) indicated that the relative stiffness, S , of a culvert with respect to the soil is

$$S = \sqrt[4]{\frac{EI}{(1 - \nu^2)k_m}} \tag{3.29}$$

or

$$S = \sqrt[3]{\frac{2(1 - \nu_s^2)EI}{(1 - \nu^2)E_s}} \tag{3.30}$$

where ν_s is Poisson's ratio of the soil. Davisson* suggested that relative stiffness, S_1 , could be expressed as

$$S_1 = \sqrt[3]{\frac{EI}{RE_s}} \tag{3.31}$$

and that a typical discriptor, TD , would be

$$TD = \frac{R}{S_1} \tag{3.32}$$

No numerical limits have been established to differentiate between stiff and flexible structures on the basis of these equations.

---

* Private communication with M. T. Davisson, Professor, Department of Civil Engineering, University of Illinois, June 1964.

Qualitatively, a flexible structure may be thought of as one which deforms (vertical change or volumetric change) more than the medium replaced would have. However, this concept has its greatest applicability in the assessment of overall arching.

Flexibility, in the structural sense that it will deform sufficiently to mobilize the passive resistance of the side-supporting soil, appears to be assured for a structure made of ductile material whose value of $\frac{EI}{R^3}$ is less than about 600 psi.

CHAPTER 4. EXPERIMENTAL PROCEDURE

4.1 Description of Cylinders

4.1.1 Considerations in Selection of Design

A number of practical considerations were influential in the selection of the cylinder material and the geometric dimensions for the tests.

Aluminum was selected for the cylinder material because it, in general, is not strain-rate sensitive according to Steidel and Makerov (1960) and Smith (1963). It has a face-centered, cubic, crystalline, lattice structure and exhibits a continuous stress-strain curve with no sharp yielding zone. Steel was rejected because of its unpredictable yield strength under dynamic loading. Massard and Collins (1958) and Wright and Hall (1964) have proposed methods of taking this strain-rate effect into account, but it was considered best to avoid adding this parameter to the study. Plastics are made of long chain molecules which possess no ordered geometric pattern of structure, and hence are not only strain-rate sensitive but also experience a brittle failure under rapid loading as indicated by Dietz and McGarry (1956) and Hall (1958).

The relative size of the cylinders was dictated by the dimensions of the University of Illinois 2-ft-diameter, 500-psi, loading device. As a result, it can be assumed that for shallow burial no load was lost due to the effect of sidewall friction, and hence that the free-field vertical soil pressure immediately above the cylinder was equal to the surface overpressure. Measurements by Hanley (1963) have shown this to be a reasonable assumption.

The specific cross-sectional dimensions were determined by consideration of two factors. First, it was essential to have specimens that would fail under the maximum available pressure. In this regard, it was also desirable to take full advantage of the high pressure capability available by concentrating on specimens which would be too strong for ultimate strength studies in other facilities. Second, in view of the high cost of specimen preparation and the desirability of testing a large number of cylinders, commercially available tubing was sought.

The length was governed by the desire to have a somewhat realistic proportion between length and diameter, and by the need for enough length to smooth out any local disturbances caused by the presence of either the outside strain gages or end walls. Also, the length should be long enough to allow two-dimensional behavior and short enough to fit conveniently into the tank.

The closure plates (end caps) for the ends of the cylinder were designed so that no axial loading would be transferred to the cylinder, while at the same time retaining free radial motion.

4.1.2 Cylinder Material

Although all of the cylinders are made of aluminum, alloys with three different, nominal yield strengths were involved. The stress-strain properties of the materials were experimentally obtained and are discussed in Appendix A. The modulus of elasticity, E , was found to be a constant value, 10×10^6 psi. Two yield values were determined: a lower yield point, σ_{y1} (which is hard to define and probably no more accurate than ± 10 percent), corresponding to the first noticeable deviation from elastic behavior; and an upper yield point, σ_{y2} , corresponding to the stress which would result in 0.2 percent permanent strain. These values are summarized in Table 4.1.

4.1.3 Cylinder Geometry

The outside diameter, d , for all cylinders was 3.5 in. Micrometer measurements of the horizontal and vertical diameters prior to each test indicated that the greatest deviation was ±0.5 percent. The larger diameter was oriented vertically for the test. The length, ℓ , was a constant 10.5 in., making the length-to-diameter ratio for all cases equal to 3. Two wall thicknesses were used, 0.065 in. and 0.022 in. No deviation in thickness was found to be greater than ±0.001 in. A longitudinal section of a cylinder is shown in Fig. 4.1, and the geometric values are summarized in Table 4.1.

4.1.4 End Conditions

The conditions at the ends of the cylinder represent a free boundary. The end caps prevented the transfer of any axial load to the cylinder and the clearance of 0.05 in. at each end was sufficient to allow for radial motion. One layer of commercial, paper masking tape was used to hold the cylinder in place between the end caps during handling and placement in the soil.

4.1.5 Natural Period of Vibration

In dynamic problems it is sometimes necessary to know the natural period of vibration of the structure for all loading conditions except a step pulse. For circular, cylindrical structures buried underground the procedure for determining the period is not well established. However, a good approximation can be made by finding the period of a cylinder in air and making appropriate corrections to account for the soil.

The natural period of the pure radial vibration of a complete ring is given by Timoshenko and Young (1955, p 426) as

$$T_c = 2\pi\sqrt{\frac{\gamma R^2}{Eg}} \qquad 4.1$$

where

T_c = natural compressive period

γ = specific weight

R = radius of the center line of the ring

E = modulus of elasticity

g = acceleration due to gravity

For this study $\gamma = 169$ lb/ft^3 , E = 10 × 10^6 psi, g = 32.2 ft/sec^2 , and R = 1.72 in. (groups A, B, D, E) or 1.74 in. (group C). The calculations yield for all cylinders

$$T_c = 0.06 \text{ msec} \qquad 4.2$$

For comparison, consider the period of the fundamental mode of flexural vibration given by Timoshenko and Young (1955, p 429) as

$$T_f = 2\pi\sqrt{\frac{5}{36}\frac{\gamma AR^4}{EgI}} \qquad 4.3$$

where

T_f = natural flexural period

A = area of the cross section perpendicular to the ring center line

I = moment of inertia of the cross section perpendicular to the ring center line

This may be rewritten as

$$T_f = \frac{R}{h}\sqrt{\frac{5}{3}}\, 2\pi\sqrt{\frac{\gamma R^2}{Eg}} \qquad 4.4$$

where h = thickness of the ring.

The substitution of equation 4.1 into equation 4.4 yields

$$T_f = \frac{R}{h}\sqrt{\frac{5}{3}} \quad T_c \qquad 4.5$$

For this study h = 0.065 in. (groups A, B, D, E) or 0.022 in. (group C). The calculations yield

$$T_f = 1.9 \text{ msec, groups A, B, D, and E} \qquad 4.6$$

$$T_f = 5.6 \text{ msec, group C} \qquad 4.7$$

The soil acts in two ways to modify the foregoing expressions for the natural period. It tends to stiffen, and at the same time to add mass to the structure. The effect of the mass of soil, virtual mass, which must be accelerated along with the buried structural elements can be treated in the manner suggested by Merritt and Newmark (1964, p 23); but, the deflections observed in this study for the small cylinders were of such small magnitude that it is unlikely that any appreciable amount of additional mass should be included. The stiffening effect is even less susceptible to quantitative assessment.

4.2 Description of Soil

4.2.1 Considerations in Selection of Test Soils

Although considerable thought is being given to what soil parameters govern soil-structure interaction, no complete answer is presently available. Therefore, it was desirable to use soils at each end of the spectrum,* and at the same time soils whose shear strength and

* 1st Lt. A. J. Hendron, Jr., Ph.D., "A Short Technical Note on the Extremes in Soil Types in Regard to Dynamic Soil-Structure Interaction," Vicksburg, Miss., July 22, 1964.

stress-strain properties could be documented for future reference. A new soil environment was built for every cylinder; hence, the in-place properties of the soils used had to be reproducible. Dense, dry sand and a clay of high plasticity were selected. The sand was uniformly graded because a given density was thought to be more reproducible in a uniformly graded sand than in a well-graded sand.

4.2.2 Sangamon River and Cook's Bayou No. 1 Sands

The Sangamon River sand has been used extensively in tests at the University of Illinois. It was used in a dense (D_r = 78%), dry condition as the soil environment for the testing of cylinder groups A, B, and C. The Cook's Bayou No. 1 sand (D_r = 79%) has been used for several experiments at WES; extensive, dynamic one-dimensional and triaxial tests are planned in the near future to expand the knowledge of its properties. It was used for group E. The characteristics of both sands, together with the placement techniques employed, are outlined in Appendix B.

4.2.3 Buckshot Clay

This particular clay (CH) was selected for the group D cylinders because of the experience at WES in its use. However, even with this kind of knowledge available, great difficulty was experienced in developing placing methods adaptable to this study. The properties and placement techniques are discussed in Appendix C.

4.3 Loading Devices

Experimental work in this area has required the development of new testing machines.

4.3.1 Illinois

The equipment used in the first stage of this study was originally developed by Egger (1957) and later modified to permit simulation of blast loading by Sinnamon and others (1961). Its capabilities are described by Sinnamon and Newmark (1961), and it has recently been used by Hanley (1963) to study the interaction between sand and vertically oriented cylinders.

The container is a vertical cylinder 26-3/4 in. high and 23-1/4 in. in diameter. A 1/32-in.-thick neoprene diaphragm is placed over the soil surface to prevent gas penetration. Then a spacer ring is positioned, followed by the static or dynamic loading head. The device is illustrated in Fig. 4.2. Both the static and dynamic loads are provided by a compressed gas system. Although the equipment is capable of producing rise times in the neighborhood of 3 msec by using helium gas, this study was conducted with nitrogen gas because it is less expensive and because the 3 msec rise time apparently offered little advantage over the 13 msec rise time (rapid) with nitrogen gas. A typical overpressure-time relation is shown in Fig. 4.3. No reflection of the incident wave on the bottom was noted.

4.3.2 <u>WES</u>

Cylinder groups D and E were tested in the Small Blast Load Generator (SBLG) facility at WES. This was the first extensive experimental program completed in the SBLG and hence a number of problems in technique had to be resolved during the course of the investigation. The dynamic overpressure is applied by the detonation of two parallel lines of PETN in the form of primacord. The effective overpressure-time relation (dynamic) is shown in Fig. 4.3. The early part of the curve was obtained by averaging the maximum and minimum points in adjacent oscillations.

Although the amplitude of the oscillations varied as much as ±50 percent from the average, the impulse was so small (10,000 and 20,000 cps ringing) that the approximation in Fig. 4.3 is justified. The high-frequency signals were probably caused by the nonshock isolated gage mounts. The pressure distribution on the surface is within ±10 percent of being a plane wave according to Kennedy and Sadler (1965).

The loader is a cylindrical ring device, 46-3/4 in. in diameter. For these tests an average soil replacement depth of 2 ft was used. The layout is shown in Fig. 4.4. The static tests of group D were run with a rigid concrete base (III). The static tests of group E along with the dynamic tests of both D and E were conducted with a pseudo-infinite base (II) to avoid the dynamic disadvantages of the rigid base.

The "infinite" base is a column of sand extending 9 ft below the floor level. This column had been previously loaded many times to 500 psi, and no further compaction was observed. Two feet of sand above floor level was replaced for each sand test. For the dynamic clay tests, a rubber diaphragm was inserted at floor level to separate the lower sand column from the upper 2 ft of clay.

The operation of the loading device has been outlined by Boynton Associates (1960), and the U. S. Army Engineer Waterways Experiment Station (1963) and an evaluation study is being made by Kennedy and Sadler (1965).

4.4 Instrumentation

4.4.1 General

Metal film strain gages were used to measure hoop strain on the inside and outside of the cylinders (Fig. 4.1). Static deflection gages were made from brass shim stock and individually calibrated. The transducers and techniques are discussed in Appendix D.

4.4.2 Illinois

The instrumentation used is pictured in Fig. 4.5. The active strain gage on the cylinder was one arm of a four-arm bridge. The dummy gages were mounted on isolated metal strips outside the test tank. Multi-conductor cable was used initially, but it was found that two-conductor shielded cable provided a better barrier to spurious noise in the system.

The eight hoop strain gages were hooked to a bank of Consolidated Electrodynamics Corporation (CEC) carrier amplifiers, Type 1-127. A 12-channel CEC, direct-write, recording oscillograph Type 5-124 with available paper speeds of 0.5, 2, 8, 32, and 128 in./sec was used. The two deflection gages each formed two arms of a bridge and were fed through DANA d-c amplifiers to the oscillograph. For the static tests, the slowest paper speed was used. A timing trace of 2 cps and one reference (dead) trace completely utilized all of the available channels. The overpressure was read on an auxiliary Bourdon gage with the timing trace interrupted at predesignated pressure levels. Modifications were made for the rapid tests. The output of the strain gage amplifiers was split so that it was placed on both the oscillograph and a Honeywell 8100 tape recorder (as a back-up record). Additional DANA amplifiers were used to drive the tapes. The time base frequency was increased to 500 cps. The output of a Kistler Instrument Corporation, piezoelectric, pressure transducer, which was in series with a Kistler calibrator and charge amplifier, was used to record pressure. The recording paper was driven at the fastest speed possible, 128 in./sec.

The frequency response of the oscillograph system was limited to that of the CEC 7-364 galvanometers, 500 cps. The tape system had a frequency response of at least 3000 cps and a few records reproduced directly from the tape indicated that no frequencies higher than 500 cps were present.

4.4.3 WES

The equipment used for group E (the first test series at WES) and the evaluation of the overpressure-time signature is shown in Fig. 4.6. The Wheatstone bridge was set up as in the Illinois tests. The Sensor Analog Module (SAM) amplifiers used are d-c, and hence the dynamic frequency response was again limited by the galvanometer capabilities, 2500 cps (CEC 7-362).

After the group E tests were completed, the SBLG facility instrumentation was moved to a separate area. The layout used for the group D tests is shown in Fig. 4.7. In this case, DANA amplifiers coupled with galvo drivers were used.

Overpressure was monitored by a pair of 1000-psi Norwood pressure transducers, Model 211C. Additional pressure transducers were used and their output recorded on tape to gain higher frequency response (20,000 cps) in order to describe adequately the high-frequency characteristics of the pressure-time signature.

4.4.4 Sources of Error

Potential sources of error are present throughout the system: (1) inexact strain gage placement (±2%); (2) variation in gage factor and resistance (±1%); (3) amplifier nonlinearity (±2%); (4) galvanometer nonlinearity (±1%); and (5) properties of the pressure transducers (±5%). These imply a confidence limit of no better than ±11 percent in the instrumentation system.

CHAPTER 5. PRESENTATION OF EXPERIMENTAL RESULTS

5.1 Method of Presentation

5.1.1 Cylinder Coding

Table 5.1 outlines the overall testing program for the 46 specimens and identifies each cylinder with its respective soil environment, depth of burial, and type of loading. The notation used, e.g. A-3, to identify each cylinder (and thus each test) has general meaning. The alphabetic term, A, was used to identify the original 12-ft tube from which the test cylinder was cut and can be related to the stress-strain curves of Appendix A. Cylinders with a numerical designation 1 through 5 were tested statically, while those designated 6 through 10 were tested either rapidly or dynamically. In Tables 5.2 through 5.11 the tests are presented by group (A, B, C, D, E), static first, in the order of increasing depth of burial within the group.

5.1.2 Tables of Data

The digitized strain values were taken from the oscillograph records at points corresponding to specific values of the overpressure to obtain a cause-and-effect relation. In the dynamic tests, peak strain values were recorded. These experimental strain values, together with diameter-change values (for static tests only), are listed in Tables 5.2 to 5.11 with respect to overpressure.

Use of a dash instead of a number indicates that the results were lost due to instrumentation difficulties. The values of stress, thrust, and moment are also listed in the tables. The gage locations are identified in Fig. 4.1.

5.1.3 Data Plots

The values of strain were, in general, not plotted directly in Figs. 5.1 to 5.43 because an appropriate scale to show the large inelastic values would have masked the much smaller elastic strains. The stress to cause yield and the thrust to cause yield are shown by horizontal dotted lines in each figure. "First yield" (σ_{y1}) represents the stress at a point where the slope of the stress-strain curve departs from the initial elastic slope (E). The yield value corresponding to 0.2 percent permanent strain is the "0.2 percent offset yield" (σ_{y2}). The diagonal dotted line labeled "uniform radial load" represents the theoretical relation derived for a uniform radial load equivalent in magnitude to the overpressure, Fig. 2.1d.

Stress, thrust, moment, and diameter change (static tests only) are plotted as ordinates with respect to the surface overpressure as the abscissa.

The symbols used to identify a gage location are presented on each figure and are consistent throughout. The inside gages are represented by open symbols and the outside gages by closed symbols. The cross sections are identified by the applicable open symbol.

5.2 Computations

5.2.1 Moment and Thrust Computation

The moment and thrust at a cross section were calculated from

$$M_y = \int_{-h/2}^{h/2} \sigma_y \, z dz \qquad 5.1$$

$$N_y = \int_{-h/2}^{h/2} \sigma_y \, dz \qquad 5.2$$

where M_y is the moment in the y or tangential direction, Fig. 3.1, in units of pounds (inch-pounds per inch), and N_y is the thrust or in-plane force in the tangential direction in units of pounds per inch. For the elastic case these can be reduced to

$$M_y = (\epsilon_e - \epsilon_i) \frac{Eh^2}{12} \qquad 5.3$$

$$N_y = (\epsilon_e + \epsilon_i) \frac{Eh}{2} \qquad 5.4$$

where ϵ_e is the exterior strain, and ϵ_i is the interior strain at the cross section in inches per inch. Compressive strains and thrust are considered positive in the presentation. Moment tending to compress the external fibers is positive.

5.2.2 Computer Program

To reduce the large mass of strain data to applicable stress, thrust, and moment values, a program (13-G1-Z5010) was written in FORTRAN for the WES, GE 225 computer. The aluminum stress-strain curves of Appendix A were input in a discrete number of linear segments and a "table lookup was utilized to compute the elastic and inelastic stress. The strain distribution was assumed to be linear across the section, Singer (1951, p 409), so that the expressions for moment and thrust, equations 5.1 and 5.2, could be numerically integrated for the nonelastic case. The program assumes that the material stress-strain properties are the same in both tension and compression and that any unloading takes place along the original load curve.

5.2.3 Computation of q

Values of q are listed in Tables 5.2 to 5.11. As used in this context, q is not a coefficient of earth pressure, but merely defines the ratio of the average thrust at the crown and invert divided by the average thrust at the spring line. Values of q are plotted in Figs. 6.1 to 6.3.

5.3 Mode of Failure

All of the cylinders that failed, failed by a catastrophic snap-through (caving) of the crown. A noise was heard at the moment of failure and all of the strain gage traces were instantaneously driven off the oscillograph, either by being overranged or by shorting out electrically. The last recorded strains in the tables are those at the moment of failure.

The failed cylinders are shown in Figs. 5.44 and 5.45. The distorted cross section of two cylinders which did not fail are shown in Fig. 5.46 (the strain gage wires are evident in D-6), and the postfailure clay configuration is illustrated in Fig. 5.47. A plot of overpressure at failure versus depth of burial is shown in Fig. 5.48.

5.4 Stress, Moment, and Thrust

The cylinder groups are presented in the order A, B, C, E, and D because the first four groups were in a sand medium and the last in clay.

5.4.1 A Group

The static test data are presented in Table 5.2 and plotted in Figs. 5.1 through 5.6. An air line broke at 400 psi during test A-3. Fig. 5.4, test A-3A, presents the data up to that point. The line was repaired, the gages were rezeroed, and a second test, A-3B, Fig. 5.5, was run up to 500 psi. The values of stress, thrust, and moment listed for test A-3B were computed by the computer program on the assumption of no residual strain. Sample calculations based on the more realistic assumption of residual strains from test A-3A indicated that the listed values are no more than about 10 percent low.

The deflection gages were not suitable for the rapid testing, and hence data from them do not appear in Table 5.3 nor in Figs. 5.7 through 5.11.

5.4.2 B Group

The static test data are presented in Table 5.4 and plotted in Figs. 5.12 through 5.17. The B group was the first group to be tested, and B-1 was the first cylinder. Test B-1A, Fig. 5.12, terminated at 300 psi because no higher pressure was attainable with the loading device. A subsequent modification in the O-ring configuration allowed the device to attain its 500-psi static capacity. Test B-1 was rerun, test B-1B, Fig. 5.13, and the cylinder failed at 315-psi overpressure.

The rapid test data are presented in Table 5.5 and plotted in Figs. 5.18 through 5.22.

5.4.3 C Group

The static test data are presented in Table 5.6 and plotted in Figs. 5.23 through 5.27. The rapid test data are presented in Table 5.7 and plotted in Figs. 5.28 through 5.32.

5.4.4 E Group

The static tests were run as duplicates to check the tests of the A group. Test data are presented in Table 5.8 and plotted in Figs. 5.33 through 5.35. The dynamic results (peak strain values) are presented in Table 5.9 and plotted in Figs. 5.36 and 5.37. The initial pressure rise of the dynamic pressure wave, Fig. 4.3, approximates a step pulse. For this region a strain-pressure relation is unmanageable. Therefore, the dynamic results are plotted with respect to the circular angle θ

(Fig. 4.1) for the various overpressures attained. No failures resulted from the maximum available, nominal overpressure of 250 psi.

5.4.5 D Group (Clay)

The static test data are presented in Table 5.10 and plotted in Figs. 5.38 through 5.42. The dynamic results are presented in Table 5.11 and plotted with respect to the circular angle θ in Fig. 5.43. The values of stress, thrust, and moment were computed by the computer program on the assumption of no initial strain. Sample calculations, which took into account the strains impressed during placement, indicated that the values listed in Tables 5.10 and 5.11 are no more than about 10 percent low.

CHAPTER 6. ANALYSIS AND INTERPRETATION OF TEST RESULTS

Initially this discussion will concern Figs. 5.1 through 5.48; then other detailed comparisons of pertinent aspects of the data will be treated.

6.1 Overall Structural Response

6.1.1 A Group (Sangamon Sand)

Fig. 5.1, test A-1 (Z = 0 in.), depicts the structural response of a relatively stiff cylinder as it progresses toward failure under static loading. This is a typical case only for cylinders buried at depths approaching zero depth of burial. It is evident that the stress curves are not linear functions of the applied pressure even in the elastic range of the cylinder material; the lower stresses (those tending to tension) are the ones most susceptible to nonlinear behavior. The agreement of the stress levels for gages 2 and 4, and 2a and 4a indicates that the cylinder experienced generally symmetric response about the vertical axis. The crown and invert at this very shallow burial did not exhibit this agreement in response. The stress at many gage points was greater than the first yield stress of the cylinder material. Only the stress recorded for the outside gage at the crown, 1a , tended to pass the 0.2 percent offset yield stress of the material (at incipient failure).

Thrust is a more nearly linear function of overpressure than the stress at any gage point. The thrusts at the four cross sections are nearly equal below 150 psi; but at high pressures the thrust at the invert is considerably lower than the thrust at the crown or spring line for the case of shallow burial.

The decidedly nonlinear variation of moment with overpressure above 100 psi is the consequence of the cylinder readjusting itself under load and probably of the load distribution changing. It is important to note how the magnitude of the spring line moment decreases for input pressure greater than 200 psi. It is at this pressure that the stresses exceeded the first yield stress of the structural material. The change in sign of the crown moment is of concern. For the structure to assume an elliptical shape (with the major axis horizontal), it would seem that the crown moment would have to be positive throughout the loading. However, this is not the case for pressure levels below 210 psi. Coupled with this, the diameter changes are extremely small for the first 210 psi of loading. This type of reversal of curvature at the crown was not an isolated occurrence. It is shown in the results of test A-5 in Fig. 5.2 and in other cylinders which are very close to the surface boundary and susceptible to collapse. There are a number of possible explanations for this phenomenon.

1. The vertical axis was slightly greater than the horizontal axis, and this by itself may have influenced the sign of the moment prior to incipient failure. However, if this were significant it would have influenced the moments at deeper depths of burial.
2. The external strain gages and their respective protective covering could cause load concentrations away from the gage locations by activating local arching. But, this would not be the case with the depth of burial, Z , equal to zero.

3. Nonuniformity in the soil medium could cause uneven stress distribution. Again, this should be a random occurrence, while the phenomenon is systematic.
4. The tendency to buckle in a mode other than the lowest mode could cause local moment anomalies. Higher order buckling modes would have node points occurring in a random fashion even though collapse came by a full snap-through (caving) of the crown. But, here too the occurrence would be random.
5. The proximity of the crown to the surface boundary at very shallow burial, relative to the proximity of other points, is much more significant than at deeper depths of burial. The load at the crown is fixed, but local arching could have caused an uneven load distribution. At the deeper depths enough soil would be present to smooth out the local variations.

DaDeppo (1963, p 30) concluded that the magnitude of initial deformation in arches was important in controlling the flexural response. He was most concerned with variation in the initial shape induced by backfilling. However, the conclusion would apply regardless of how the variations in initial shape came about. Random deviations of the cylinder from circularity could result in random moment response. But, the moment response in the present investigation was systematic and repeatable.

Robinson (1964) recorded moments on a cylinder at every 45-degree point, and they were all of the same sign. He felt that this was due to local arching of the soil at the contact between the external strain gages and the soil. However, the data were not reproducible.

It is the writer's opinion that the most plausible explanation of the negative moment is directly related to the proximity of the surface boundary causing local arching to neighboring elements of the cylinder. The buildup in pressure and subsequent nonuniform loading become less significant at the higher pressures. At depths greater than 1/4d (d/4) the crown moment is positive, Fig. 6.1. This indicates that the crown response is greatly influenced by the surface boundary at depths shallower than d/4 . Overall arching can be applied to the crown at depth, but not at very shallow burial.

Test A-5 (Z = 3/16 in.), Fig. 5.2, agrees very well with test A-1 (Z = 0 in.), Fig. 5.1, both qualitatively and quantitatively, with two exceptions. First, the overpressure required to cause failure is higher for A-5. Second, the invert moment is negative in A-5 and positive in A-1. Again, for the elliptical geometry one would expect this moment always to be positive. However, it appears to be positive or negative in a random variation. This could be a result of geometric imperfections, incipient high buckling modes, or the character and nonuniformity of the soil bedding. The latter, nonuniformity of the soil bedding, appears to be the most reasonable explanation at pressure levels below 300 psi. In many tests, A-5 (Z = 3/16 in.), A-2 (Z = 7/16 in.), etc., the moment at the invert changed from negative to positive at pressures greater than 300 psi. The significance of the initial bedding decreases as the pressure level increases. An exception is test A-4 (Z = 1-3/4 in.).

Also in test A-5 (Z = 3/16 in.) a vertical diameter increase was recorded at 50 and 100 psi. This is compatible with both the crown and invert moments being negative at that pressure.

Donnellan (1964, p 29) recorded an outward displacement of the radius at the invert of one of his shallow-buried cylinders. The present study recorded only diameter changes, and it is not possible to tell if half a diameter (the radius) increased while the other half decreased.

Test A-2 (Z = 7/16 in.), Fig. 5.3, follows the trends observed at the shallower depths except that no failure was experienced at the maximum machine loading capability of 500 psi. Additionally, the large positive bending moment at the crown observed just prior to failure in tests A-1 (Z = 0 in.) and A-5 (Z = 3/16 in.) was not encountered in this test. Also, the rate of change of moment with pressure decreased, indicating local arching.

Again at about 200 psi the rate of vertical diameter change begins to appear more rapid than below 200 psi. This is probably a result of the cylinder material reaching its yield value at several locations. The moments continue to decrease at overpressures above 200 psi.

Test A-3A (Z = 7/8 in.), Fig. 5.4, exhibits virtually identical thrust values at all four cross sections at pressure below 150 psi. However, at higher levels it establishes the generally observed trend of the spring line having the highest thrust, followed by the crown, with the invert experiencing the least amount of thrust. This is probably a consequence of the bedding providing a soil environment different from that around the crown.

The test (A-3A) was aborted at 400 psi by a broken gas line. The pressure went to zero, the line was repaired, the gages were rezeroed on the oscillograph, and a second test, A-3B, was run without touching the cylinder or the soil. From Fig. 5.5 it can be seen that some aspects of the structural response changed as much as 100 percent as a result of this cycling of the load. This gives a graphic illustration of how initial, geometric deformations (plastic set in this case) can affect moments. The crown moment is much larger on the second cycle, and the invert moment has changed character greatly.

Test A-4 (Z = 1-3/4 in.), Fig. 5.6, underwent similar response to that of test A-3A (Z = 7/8 in.) with the exception of the invert moment which continued to remain large throughout the test.

The only variable changed between the static tests, A-1 through A-5, and the rapid tests ([illegible] msec rise time to 500 psi), A-6 through A-10, Figs. 5.7 through 5.11, was the rise time. The rapid tests in general verified the static tests, but several differences can be seen. First, the pressure necessary to cause collapse was somewhat higher in the rapid tests. This may have been due to a true increase in capacity or to the possibility that some creep mechanism was involved which resulted in failure appearing at a slightly higher pressure in the rapid tests. Second, the values of the thrust are about 20 percent higher in the rapid tests. This may have been due to inertial effects in the soil adding load to the structure. Third, the crown moment is initially positive up to about 100 psi in all rapid tests. For very shallow burial, the moment changed sign and was negative to about 250 psi; then it became positive again. Apparently, the pressure wave struck and depressed the crown, causing the initial positive moment. This occurred at about 3 msec which was slightly greater than the natural period of vibration in the first flexural mode, equation 4.6. This, of course, is much later than would be expected if equation 4.6 were directly applicable.

Although the symmetry around the vertical axis was good, test A-9

(Z = 3/16 in.), Fig. 5.8, illustrates how the spring-line moments can differ by as much as 100 percent (at 150 psi) while the spring-line thrusts agree well. Also, it can be seen that the disparity is not constant during the whole loading cycle, but rather tends to decrease as the cylinder material yields. Also, the moment changes produce deformations which tend to reduce disparities. Test A-7 (Z = 7/8 in.), Fig. 5.10, is a good illustration of the general response.

It is of interest to plot various responses of the group together, as shown in Fig. 6.1. The average spring-line thrust was calculated (refer to Tables 5.2 and 5.3) and the results of all ten tests plotted. It can be seen that all of the test results fall close together and exhibit a linear increase with respect to pressure, and that the rapid test results lie slightly higher (for a given pressure level) than the static results. Data from those cylinders which failed fall right along with those from cylinders which did not fail, indicating that thrust by itself (without some link with depth of burial) will not be an adequate failure criterion for very shallow depths of burial.

The crown moment plot shows how closely the rapid and static tests agree at pressures above 100 psi. The crown moments are always positive at depths greater than $d/4$.

The average of the crown and invert thrusts was divided by the average spring-line thrust to form the ratio q . This is plotted in Fig. 6.1. After experiencing a large range in values at pressures below 200 psi, the ratio settles into a band between 0.6 and 0.8. The values are least accurate in the lower pressure regions and are most influenced by the initial conditions created by the soil placement. Disregarding the few very high values, the trend is to start at about 0.4 (which is approximately equal to the coefficient of earth pressure at rest), increase to about 1.0 as the cylinder began to deform, and then decrease slightly and become relatively constant.

The vertical diameter changes in the static tests are also plotted together. There is a decrease in diameter change with depth of burial for a given overpressure that is noticeable at pressure levels above 250 psi. This reflects the stiffening effect of the soil as the depth of burial increases.

6.1.2 B Group (Sangamon Sand)

The B group differs from the A group only in the value of the yield stresses. The B group had about twice the yield value of the A group.

The pressure causing failure was consistently higher in the B group, Table 5.1, indicating that the yield stress probably had some influence on the collapse pressure. However, this influence does not appear to be large in these tests.

In tests B-1A and B-1B (Z = 0 in.), Figs. 5.12 and 5.13, the effect of cycling is again seen in the character and magnitude of the crown moment. It is also significant that the effect of the cycling is not very pronounced at other locations (which did not yield during first loading). Other studies, Dorris and Albritton (1965) and Albritton and others (1965), have also shown that cycling may not affect the reproducibility more than about 20 percent as long as the cylinder material remains elastic.

Test B-3 (Z = 1-3/4 in.), Fig. 5.16, and test B-4 (Z = 2-5/8 in.), Fig. 5.17, again show that the results are reproducible. They also indicate that moment increases at a decreasing rate (but remains large until the material begins to yield).

The rapid tests, Figs. 5.18 through 5.22, yielded much the same information as the static tests. Tests B-9 (Z = 1-3/4 in.) and B-10 (Z = 2-5/8 in.), Figs. 5.21 and 5.22, illustrate the smoothing out of response that can be expected with deeper depths of burial.

A summary of the B group response is plotted in Fig. 6.2. As with the A group, the spring-line thrust is generally linear with pressure up to a level equivalent to first yielding of the material. The values of rapid test thrusts are larger than those for the static case. The vertical diameter changes fall into a pattern with each other and are lower than those of the A group, Fig. 6.1, at pressures greater than 200 psi. The q values settle into a band between 0.5 and 0.8 for pressures greater than 300 psi.

6.1.3 C Group (Sangamon Sand)

The C group of cylinders was only one-twentieth (1/20) as stiff as the A and B groups. The yield stress was high enough that all of the cylinder strains recorded were below the level corresponding to 0.2 percent permanent strain. The pressures required to induce failure were lower than in the A and B groups by a factor of 2 or 3. But, again, at depths greater than one-eighth the diameter no failures occurred. The moments in the C group were substantially smaller, and the moment scale for plotting was changed by an order of magnitude from that used for the B group.

Test C-1 (Z = 0 in.), Fig. 5.23, experienced negative moments at all four cross sections and the vertical diameter increased at pressures above 25 psi. This was probably caused by the propensity for collapse in a high-order buckling mode.

The variability in moment response is even more evident in these very flexible cylinders at shallow burial. Tests C-4 (Z = 3/16 in Fig. 5.24, and C-2 (Z = 7/16 in.), Fig. 5.26, both experienced positive moments at the spring line and the horizontal diameter decreased in C-4. Donnellan (1964, p 26) also recorded inward movement at the spring line of some flexible cylinders. This may be another manifestation of a tendency toward a high-order buckling mode.

The crown thrust was larger than that at the spring line in most of the C group tests. But, q was still less than 1.0 in most cases, Fig. 6.3. The invert thrust was low and probably reflects a decrease in vertical pressure between the crown and invert. This also shows up in a lower arching ratio, Section 6.4.

Rapid tests C-6 through C-9, Figs. 5.28 through 5.31, exhibited the same type curvature changes at shallow burial as the A and B groups. The initial peak positive moment occurred at about 3.5 msec which is about half the natural flexural period given by equation 4.7. Test C-10 (Z = 7/8 in.), Fig. 5.32, is a good example to validate the argument for application of the ring compression theory to flexible cylinders which are not affected by the surface boundary.

Test C-9 (Z = 7/16 in.), Fig. 5.31, exhibited the largest applied pressure, 550 psi, encountered during this investigation. This was the only test in which the maximum pressure deviated from 500 psi. The response ended as usual when the pressure peaked, but the cylinder collapsed about a minute later as the pressure was about to be manually decayed. A stability problem is, of course, very sensitive to slight disturbance, but this also points to a possible creep effect reducing the resistance to buckling.

The average spring-line thrust values, Fig. 6.3, show more scatter than the previous two groups, but the exclusion of test C-2 (Z = 7/16 in.) reduces the spread considerably. Although no characteristics of the test indicated a difference, the results are not in line with the rest of the C group.

The values for the rapid tests are higher than those for the static. The q values for pressures greater than 300 psi lie in a band between about 0.7 and 1.0 with the exception of test C-2. In this test the q values are higher because the spring-line thrusts were lower than the rest of the C group.

6.1.4 E Group (Cook's Bayou Sand)

The cylinders used in the E group were identical with those of the A group except that they were cut from a different tube (same nominal material) and hence had a slightly different yield (Appendix A). The three static tests were run as a verification of the reproducibility of the A group results and for comparison with dynamic tests E-4, E-5, and E-6.

The thrust, moment, and diameter change results of E-3 (Z = 0 in.) are plotted together with companion values from test A-1 in Fig. 5.33. The values for thrust are comparable, but the spring-line thrusts of the E group are higher than those of the A group. The diameter change values also are higher and only the spring-line moments are compatible. E-3 failed at 205 psi, whereas A-1 failed at 270 psi. This is reasonably good agreement for such a buckling failure, but the thrust and diameter change trends suggest that the response was more unfavorable in the E test. Different sands were used in the two tests but they have about the same strength and deformation characteristics (Appendix B). If anything, the Cook's Bayou sand (E group) is slightly stiffer than the Sangamon sand

(A, B, and C groups). As a result, it is felt that the variation in response is a function of the two different methods of placing the sand around the cylinders. The Sangamon River sand was vibrated and rodded in, whereas the Cook's Bayou sand was sprinkled into place. This illustrates one of the difficulties inherent in comparing results from tests in which different placement techniques were used. Conservative conclusions must be drawn.

Test E-2 (Z = 7/16 in.), Fig. 5.34, exhibits the same trends as E-1, and the similarity of the thrust with A-2 is evident. Also, at pressures above 300 psi the moments show closer agreement. It is interesting to note again how the large moments tend to decrease as the cylinder material yields and loading progresses.

Test E-1 (Z = 7/8 in.), Fig. 5.35, exhibits even better agreement with its A group counterpart. However, the large crown moment at pressures below 250 psi and the greater diameter changes of the E group indicate that sprinkling placement of the sand gave a lower density and less restraint.

The recorded values of peak strain on the intrados and extrados for E-5 (Z = 7/16 in.) and E-4 (Z = 7/8 in.), Fig. 5.36, are compared with the values recorded for the static tests at the same 250-psi level (maximum dynamic pressure available). A large amount of ductility is evident in the dynamic tests. Using the analysis outlined by Newmark and Haltiwanger (1962) for a step pulse input of 250 psi and an equivalent elastoplastic resistance function for the cylinders, a theoretical ductility factor of 7 and a theoretical maximum strain of 5100 μin./in. were calculated. This theoretical strain agrees well with the observed strains which ranged between 5000 and 6000 μin./in.

The moment and thrust values are shown in Fig. 5.37. The peak thrusts are uniform around the cylinders for all three dynamic tests at the 250-psi pressure level used. The thrust values for the static and rapid tests are also very consistent with each other, whereas the moment values are widely scattered at the crown and invert.

6.1.5 D Group (Buckshot Clay)

The D group cylinders were buried in clay, but were identical with those of the A and E groups in material and geometry with the exception of a slight change in yield points (Appendix A) resulting from use of different tubes.

The static tests, Figs. 5.38 through 5.42, indicate higher bending moments and larger diameter changes than occurred in sand. The thrust values follow about the same trend as in sand. Generally, symmetric response was recorded and hence opposite gages acted as a check on each other.

The thrusts recorded in several tests, e.g., D-4 (Z = 1-3/4 in.) and D-5 (Z = 2-5/8 in.), were higher at the 45-degree cross section than at the spring line. The instability may very well be concentrated between this level and the crown.

The moments are a highly nonlinear function of overpressure and tend to decrease as the material yielded at high pressure levels, Fig. 5.41.

Ultimate-strength dynamic testing with the WES type Heaviside input is essentially a "go-no go" process. The true failure pressure can only be bracketed between a known collapse and a known survival. A tight bracket would require many tests and be extremely expensive. At the same time it would not be truly reliable because of the inherent scatter in stability problems.

The experience with sand indicated that the rapid and dynamic failure pressures would be relatively close to the static values. This proved to be the case also in clay, and the static failure pressures served as the basis for estimating required dynamic overpressures. The overpressures obtained were not always close to those requested because of variabilities in the loading apparatus. However, a reasonable bracket was obtained for two representative depths of burial, 7/8 in. and 1-3/4 in.

The results obtained from those cylinders which survived are plotted in Fig. 5.43. Results from those cylinders which failed are also plotted to shed more light on what occurred. However, these data should be considered only as guides. They were obtained from the records at incipient failure. This was extremely hard to define for the dynamic tests in which the cylinders failed.

Some instrumentation difficulties were encountered and the data from half the strain gages, Table 5.11, in test D-10 ($Z = 7/8$ in.) were lost because an oscillograph malfunctioned. However, the thrust values of D-8 ($Z = 7/8$ in.) and D-6 ($Z = 1\text{-}3/4$ in.) are relatively uniform. The peak moments are at the crown and are positive in sign. The permanent deformations in D-6 and D-10 can be seen from the end views of Fig. 5.46. The strains far exceeded yield in most cases, both in tension and compression, and resulted in high bending moments.

6.2 <u>Diameter Change</u>

The diameter changes were small for all tests. In order to verify the validity of the diameter change gages, the cylinder diameters were measured to the nearest one-thousandth of an inch with outside micrometers, both before and after the test (when possible). These results are plotted in Fig. 6.4 along with the peak diameter change indicated by the diameter change gages. Reasonable verification is evident.

A vertical Collins gage was included in test E-5, and its peak output substantiates the trends.

Several observations can be made based on Fig. 6.4. The horizontal deflection stiffness, P_{so}/Δ_h , appears to be independent of the buckling stiffness, $\frac{EI}{R^3}$; but, it varies a great deal with the soil environment. The Sangamon River and Cook's Bayou sands differ by a factor of 2 for horizontal stiffness. The clay is less stiff by an order of magnitude.

Using these empirical values for horizontal stiffness, it is possible to calculate subgrade moduli from the Iowa Formula,

$$\Delta_h = \frac{0.166\, p_a R^4}{EI + 0.061 k_s R^4} \qquad 6.1$$

where

Δ_h = horizontal diameter increase, in.

p_a = vertical pressure on top of the cylinder, psi

R = cylinder radius, in.

E = modulus of elasticity of the cylinder, psi

I = moment of inertia of the cylinder cross section, $in.^4$

k_s = modulus of passive resistance of the soil, $lb/in.^3$

This can be solved for $k_s R$, E' , in terms of the other parameters where E' is called the modulus of soil reaction.

$$E' = \frac{1}{0.061}\left[(0.166\, R)\frac{p_a}{\Delta_h} - \frac{EI}{R^3}\right]$$

Substituting $R = 1.75$ yields

$$E' = \frac{1}{0.061}\left(0.2905\frac{p_a}{\Delta_h} - \frac{EI}{R^3}\right) \quad 6.2$$

Using the average values of $\frac{P_{so}}{\Delta_h}$ calculated from the results plotted in Fig. 6.4 as $\frac{p_a}{\Delta_h}$, values of E' can be calculated. This assumes no change with depth of burial and is essentially true within the scatter for the range of shallow depths investigated. A trend of increasing stiffness with depth is true of the vertical stiffness. A typical calculation follows.

$$E' \text{ for the A group} = \frac{1}{0.061}\left[0.2905(32{,}900) - 45\right]$$

$$= \frac{1}{0.061}\left(9550 - 45\right) = \frac{9505}{0.061} = 155{,}900 \text{ psi} \quad 6.3$$

$$k_s \text{ for the A group} = \frac{E'}{R} = \frac{155{,}900}{1.75} = 89{,}100 \text{ lb/in.}^3 \quad 6.4$$

Also, from equation 6.2 one can compute

E' for the B group = 125,100 psi

k_s for the B group = 71,600 lb/in.^{3}

E' for the C group = 127,100 psi

k_s for the C group = 72,600 lb/in.^{3}

E' for the E group = 57,300 psi

k_s for the E group = 32,700 lb/in.^{3}

E' for the D group = 6,500 psi

k_s for the D group = 3,700 lb/in.^{3}

These calculations verify how little influence the buckling stiffness of the cylinders has on the deformations in competent soils such as these, under the assumptions of this mathematical model. The deformations are controlled by the stiffness of the soil. For example, in the computations for equation 6.3 the cylinder buckling stiffness, $\frac{EI}{R^3}$, is a negligible term relative to the horizontal soil stiffness $\frac{p_a}{\Delta_h}$.

The calculated soil parameter, k_sR , is of the same order of magnitude as the moduli from the one-dimensional consolidation and triaxial tests at roughly the same pressures (Appendixes B and C).

Up to this point everything has been analyzed in terms of the overpressure, P_{so} , on the surface. Here it was assumed that the pressure, p_a , at the level of the cylinder crown was equal to the surface pressure. This is true by definition only when the cylinder is at zero depth of burial. However, the assumption is satisfactory within the limits discussed in Section 6.3.

6.3 Arching Ratio

Overall arching may be assessed by summing forces in the vertical direction above the cylinder. The thrust at the spring line represents a vertical force as does the surface pressure integrated over the area. The arching ratio, AR , is defined as the average spring-line thrust divided by the overpressure times the radius.

$$AR = \frac{N_y \text{ (avg)}}{P_{so}R} \qquad 6.5$$

These ratios have been calculated from the results of the static tests and are plotted in Fig. 6.5.

The A and B groups verified one another well below 200 psi. At that pressure level the A group cylinders began to yield, the moments began to decrease, and hence the cylinders stiffened as a result of approaching more closely a compression mode. The arching ratio increased until such time as the whole cross section yielded, at about 300 psi.

After that, the arching ratio decreased.

It appears that the B group began to stiffen at 450 to 500 psi. The moments decreased and the arching ratio began to increase. If the trend were to continue at higher pressure, it would be compatible with the A group behavior.

The E group began with a higher arching ratio than the A group, but at pressures above 250 psi they are similar. These groups had the same buckling stiffness, $\frac{EI}{R^3} = 45$, but as has been pointed out the soil placement techniques differed. This indicates that initial soil differences (densities in the immediate vicinity of the cylinder, Appendix B) created by placement techniques may not be important after the soil-structure system has readjusted under 200-psi overpressure.

It is the writer's opinion that it is appropriate to express cylinder response in terms of the pressure, p_a , on a horizontal plane through the crown. As a consequence, a correction to P_{so} would be applicable only if the arching ratio at a given depth varied significantly from the arching ratio at zero depth. This does not occur for the cylinders tested as Fig. 6.5 indicates (although this indication is not conclusive because of the scatter in data for these shallow burials). Hence p_a and P_{so} were considered interchangeable.

This does not negate the facts that the arching ratios do differ from group to group at zero depth of burial, and that the arching ratio at zero depth is not necessarily 1.0. For any study of the arching ratio for real structures at depth, it would be necessary first to study the response of the structure at zero depth where a known loading exists. Apparently, load can be dissipated between the level of the crown and the level of the spring line.

6.4 Ultimate Strength

The collapse pressure, P_{sof} , is plotted in Fig. 6.6 with respect to the stiffness parameter $\frac{EI}{R^3}$. The tests of the present investigation, Table 5.1, cover only a small part of the practical range of stiffness and pressure. In order to make the picture as complete as possible, results of other investigations in dense, dry sand are also indicated. The depth of burial is listed next to the symbol in terms of the cylinder diameter, d .

A dotted line indicates the yield value of a high-strength steel in hoop compression for a smooth cylinder. This establishes the upper bound limit of applicability of the elastic buckling theory and hence defines the area of concern for elastic buckling. Above this line the membrane response is inelastic and would be treated in terms of a ductility factor rather than stiffness.

In Figs. 6.7 through 6.10, the collapse pressure has been formed into a nondimensional parameter, $P_{sof}R^3/EI$. The test results are plotted in this form with respect to $\frac{EI}{R^3}$. A different set of theoretical equations is shown in each of Figs. 6.7 through 6.10. It was mentioned in Chapter 3 that the theoretical equations all contain the cylinder stiffness parameter, $\frac{EI}{R^3}$, as an independent variable.

Open symbols in Figs. 6.6 through 6.10 refer to tests which did not result in failure. Although these tests do not indicate the pressure at which the cylinder would have failed, they are pertinent because they do document areas where failure did not occur.

The amount of data available with which to correlate the clay results is very slight. Luscher and Höeg (1964, p 231) reported a series, $\frac{EI}{R^3} = 0.011$, that experienced failure very similar to their sand tests which were two orders of magnitude higher than the theoretical pressure predicted by the hydrostatic equation, $p_o = 3 \frac{EI}{R^3}$, Fig. 6.7. The results of the present investigation, $\frac{EI}{R^3} = 45$, indicate that the failure pressure for cylinders in clay increases very slowly with increasing depth of burial, Fig. 5.48. The hydrostatic equation is in reasonable agreement with these results, Fig. 6.7, and the results of a test on a stiffer cylinder, $\frac{EI}{R^3} = 82$, conducted by Dorris and Albritton (1965). On the basis of this, it appears that the hydrostatic buckling equation should be retained for claylike soil media until such time as more experimental evidence fills in the gap between the available data points.

Although far from complete, the data available from tests in dense, dry sand are more plentiful. The present investigation in dense sand showed considerable increase in failure pressure with increase in depth of burial down to d/8 , Fig. 5.48. Below this depth failure could not be precipitated with the pressure available, 500 psi. Donnellan (1964, p 42) experienced failures a d/8 but none at d/4 at 160 psi. However, the conclusion that below some critical depth in dense sand, elastic buckling will not occur is precluded by the results of Bulson (1962) and Luscher and Höeg (1964). But, this conclusion may very well apply to cylinders which are stiffer than some critical stiffness.

The theoretical analysis developed by Luscher and Höeg (1964, p 143), equation 3.16, is plotted in Fig. 6.8 for several depths of burial. It takes into account the change in soil stiffness with depth and pressure, and predicts the possibility of elastic buckling at depths greater than d/4 for very flexible structures. The equation fits the author's experimental data and that reported by Bulson (1962) fairly well. For depths greater than d/4 , the equation indicates that buckling will not occur before yield of the material for the cylinders used in the present investigation. Hence, this appears to be potentially an adequate design equation for interpolation.

However, for extrapolation of the data a much more conservative approach is in order. A lower bound for these data at zero depth of burial is established by equation 3.8, Fig. 6.9. Substituting $k_z R = 400$ in equation 3.8,

$$p_c = 40\sqrt{\frac{EI}{R^3}} \text{ , psi} \qquad 6.6$$

where E is in units of psi, I is in units of in.^{3} and R is in units of in. Although the theoretical equation has the hydrostatic buckling value, $3\frac{EI}{R^3}$, as a lower bound, it is not possible to say that this would be true for the actual conditions. For a stiff cylinder at very shallow burial, the soil could be a less desirable environment than water because of the nonuniform loading occurring through the soil.

Equation 3.8 with $k_z R = 1400$ fits the writer's data at d/8 , Fig. 6.9, and is a lower bound to the data available for more flexible cylinders. Hence, it appears that

$$p_c = 75\sqrt{\frac{EI}{R^3}} \text{ , psi} \qquad 6.7$$

would provide a more realistic lower bound to the buckling value than the hydrostatic equation used alone. The units are the same as in equation 6.6.

It is evident that the foregoing values of $k_z R$ are much smaller than those calculated for sand from the Iowa Formula in Section 6.2.

Equation 3.8 with $k_zR = 37{,}000$ fits the $d/8$ no-failure data of the flexible cylinders, and is also shown in Fig. 6.9. It is possible that this may be an appropriate equation for the high overpressure region. This value of k_zR is still lower than those calculated from equation 6.2. If k_zR = 37,000 or higher, it is apparent that buckling will not occur before yield for many practical values of cylinder stiffness (greater than about 1.7) when the cylinder is buried at a depth below $d/8$. Hence, the theoretical variation of the dense sand properties with respect to pressure may be important only for design pressures below about 500 psi.

The theoretical equation, 3.17, which utilizes Poisson's ratio and Young's modulus of the soil is plotted in Fig. 6.10 for comparison. It follows the general trend of the available test data, but no definite conclusions can be drawn.

A comparison of the results of the A and B groups, Table 5.1, indicates that the cylinder strength may play a part in the buckling values. This is probably a reflection of the decrease in effective buckling stiffness which occurs when part of the cross section yields. However, the failure values between the groups did not differ by more than 25 percent although the yield values varied by a factor of 2.

The catastrophic manner in which the cylinders failed is probably a consequence of the large amount of strain energy in the cylinders at incipient collapse. Figs. 5.44 and 5.45 depict the failed cylinders. The irregularities in the postbuckling shapes were caused by the cylinder crowns striking the longitudinal rods (which connected the end caps) as they caved in. The postcollapse configuration in clay is shown in Fig. 5.47.

CHAPTER 7. SUMMARY, CONCLUSIONS, AND RECOMMENDATIONS

7.1 Summary

Forty-six, small, horizontally oriented cylinders were tested in two kinds of soil media: dense, dry sand and stiff clay. The applied overpressure, vertical, and horizontal diameter changes for the static tests and hoop strains were measured. The cylinders were all made of aluminum. Three alloys were involved having yield stress values of 7,500, 12,700, and 42,100 psi. The cylinders had identical outside diameters of 3.5 in. and two thicknesses, 0.022 and 0.065 in. Hence, the cylinder stiffnesses, $\frac{EI}{R^3}$, were 1.7 and 45 (d/h = 159 and 54), respectively.

The test structures were buried at depths ranging from zero to three-quarters of the outside diameter, 2-5/8 in. Three overpressure rise times were used: a static rise time (10 to 15 min), a rapid rise time (13 msec), and a dynamic rise time (0.3 msec).

The relations between stress, thrust, moment, and diameter change were plotted and analyzed with respect to the surface overpressure. The pressure necessary to cause collapse was established and compared with several theoretical solutions and with the results of other investigations. The horizontal and vertical stiffnesses as indicated by the diameter changes were analyzed and compared with theoretical concepts.

It was not possible to collapse cylinders of either stiffness when buried in sand at depths equal to or greater than one-eighth the diameter, 7/16 in., under the available 500-psi pressure. In stiff clay, however, it was possible to define collapse even at the deepest burial, three-quarters of the diameter or 2-5/8 in.

7.2 Conclusions

All of the conclusions are based on the assumption of the plane-wave loading which was used during this investigation.

7.2.1 Cylinders in Dense, Dry Sand

The difference between static and rapid loading in the elastic response of the cylinder is small (within 20 percent). The rapid loading was observed, Figs. 6.1 through 6.3, to cause larger thrusts.

Inelastic strains are much higher under dynamic loading than under static or rapid loading at the same pressure, Fig. 5.36. However, a cylinder buried at a depth greater than one-eighth its diameter can sustain large inelastic bending strains without experiencing structural failure or collapse.

Based on an equivalent elastoplastic resistance function for the cylinder and an approximate step-pulse loading, a ductility factor of about 7 was found to be conservative for the dynamic tests. No failures occurred, so it is not possible to say what the ductility factor to define failure would be.

Thrust is generally a linear function of surface overpressure. It is largest at the spring line, smaller at the crown, and smallest at the invert. For overpressures greater than 200 psi, the average value of the horizontal force divided by the vertical force on the cylinder is about 0.8. However, the hoop compression theory appears to be adequate for design.

Moment is generally a nonlinear function of surface overpressure. It tends to increase at a decreasing rate (probably governed by local arching from point to point around the circumference of the cylinder), until the cylinder material begins to yield. Thereafter, the moments tend to decrease. The moments are larger in the stiffer cylinders. A depth of burial of one-eighth the diameter is a critical depth for the sign of the crown moment. At shallower depths the curvature increases, whereas for deeper depths the moment is positive and the curvature tends to decrease.

For zero depth of burial, the pressure to cause buckling failure can be defined by

$$p_{cr} = 40\sqrt{\frac{EI}{R^3}}\text{ , psi} \qquad 7.1$$

where E is in units of psi, I is in units of in.^{3}, and R is in units of in. This is an empirical fit of equation 3.8 to the test data with $k_z R = 400$, Fig. 6.9. For depths of burial equal to or greater than one-eighth the diameter, the pressure to cause buckling failure can be bounded until more experimental data becomes available by

$$p_{cr} = 75\sqrt{\frac{EI}{R^3}} \qquad 7.2$$

where the units are the same as those in equation 7.1. This is equation 3.8 with $k_z R = 1400$. Failure occurs (at the shallow burial) by a sudden snap-through of the crown. The result is a complete collapse. But, no collapse could be induced at depths greater than one-eighth the diameter for $\frac{EI}{R^3} \geq 1.7$ for pressures up to 500 psi.

Depths of burial greater than one-eighth the diameter probably have more significant effects (on elastic buckling) than indicated by the allowable pressures from equation 7.2. However, since the effects of the depths were not satisfactorily defined because no failures occurred, they can only be considered as an additional factor of safety. Equation 7.2 represents points where no failure occurred and does not define failure.

However, this is a more realistic equation than the hydrostatic prediction. It is hypothesized that equation 7.2 is still overly conservative for values of $\frac{EI}{R^3}$ greater than about 1.7.

It is not possible at present to identify adequately the appropriate soil properties controlling cylinder collapse with soil properties obtained from standard laboratory tests.

The technique used to place the sand in the vicinity of the cylinder can affect the response of the cylinder and apparent deformation stiffness by as much as 50 percent. However, the pressure required to cause collapse differs by only ± 25 percent. Sprinkling in the vicinity of the cylinder is less effective than vibrating or rodding.

The arching ratio (defined as the average spring-line thrust divided by the overpressure times the radius) for cylinders buried with the crown tangent to the soil surface is not necessarily 1.0.

7.2.2 Cylinders in Stiff Clay

Collapse of the cylinder occurs by a sudden snap-through of the crown. Regardless of the depth of burial, this mode of failure occurs even at the maximum depth tested, three-quarters of the diameter.

Only a small increase in failure pressure results from an increase in depth of burial. The hydrostatic buckling equation

$$P_{cr} = 3 \frac{EI}{R^3} \qquad 7.3$$

was appropriate for the cylinders used, Fig. 6.7, and should be slightly conservative for cylinders buried at depths greater than one-eighth the diameter. This equation implies a low value of $k_z R$.

Moments and deformations of the cylinder were much larger than in sand at comparable pressures. They were both highly nonlinear functions of pressure.

7.3 Recommendations for Future Study

High pressure tests (500 psi or greater) should be conducted in dense sand with cylinder stiffnesses, $\frac{EI}{R^3}$, between 0.1 and 1.0 for the purpose of establishing failure pressures for depths of burial greater than one-eighth the cylinder diameter. Materials with high yield strengths, such as high-strength steel or aluminum, would best serve the purpose. Elastic buckling could be isolated relative to the buckling stiffness without consideration of the reduced stiffness due to yielding.

Some ultimate strength tests should be conducted with relatively large (2-ft-diameter) cylinders in the WES Large Blast Load Generator to investigate the possibility of size effects. These should have the same value of $\frac{EI}{R^3}$ as some smaller diameter cylinders discussed in the literature, or else small companion cylinders should be tested concurrently.

A cylinder with $\frac{EI}{R^3} = 220$ should be tested at zero depth of burial in dense sand at pressure greater than 500 psi to extend the range of knowledge of equation 7.1.

The work on elastic buckling should be done with static loading (but fast enough that longtime effects such as creep do not enter) to gain the most for the least cost. Selective dynamic testing should then be done to assure the applicability of the knowledge gained from the static tests.

Once the limits of the buckling problem are established, then dynamic studies should be conducted to determine an appropriate magnitude for the ductility factor to define collapse in the nonelastic region of cylinder response. Since yielding is not a proper criterion for failure, it is doubtful that the studies of the elastic response of cylinders will shed much light on the ultimate strength except when buckling governs.

Once the dense, dry sand-cylinder interaction is fully understood, other soil environments such as medium density (relative density of 50 percent), and partially saturated sands should be investigated. It may then be possible to develop a single equation which can take into account the significant soil properties in a realistic manner.

Concurrent with the foregoing, an attempt should be made to determine the pressure distribution on the surface of the buried cylinder from the measured strains. The solution by Riley (1965) for WES which expresses the load in a Fourier series with undetermined coefficients could be used.

REFERENCES

Albright, G. H., LeDoux, J. C., and Mitchell, R. A. (1960), Evaluation of Buried Conduits as Personnel Shelters, WT-1421, Sandia Base, New Mexico: Defense Atomic Support Agency.

Albritton, G. E., Kirkland, J. L., Kennedy, T. E., and Dorris, A. F. (1965), The Elastic Response of Buried Cylinders--Critical Literature Review and Pilot Study, Miscellaneous Paper, Vicksburg, Mississippi: U. S. Army Engineer Waterways Experiment Station (in preparation).

Allgood, J. R. (1965), The Behavior of Shallow-Buried Cylinders, Technical Report R 344, Port Hueneme, California: U. S. Naval Civil Engineering Laboratory.

Allgood, J. R., and Gill, H. L. (1964), Static and Blast Loading of Small Buried Cylinders, Technical Report R 332, Port Hueneme, California: U. S. Naval Civil Engineering Laboratory.

Aluminum Company of America (1960), Alcoa Structural Handbook, Pittsburgh, Pa.: Alcoa.

Aluminum Company of America (1962), Alcoa Aluminum Handbook, Pittsburgh, Pa.: Alcoa.

American Machine & Foundry Company (1962), Study of the Use of Models to Simulate Dynamically Loaded Underground Structures, AFSWC-TDR-62-3, Kirtland Air Force Base, New Mexico: Air Force Special Weapons Center.

American Society for Testing and Materials (1961), ASTM Standards 1961, Part 3, Philadelphia, Pa.: ASTM, pp 165-181.

American Society of Civil Engineers (1961), Design of Structures to Resist Nuclear Weapons Effects, No. 42, New York: ASCE.

Anderson, R. H., and Boresi, A. P. (1962), "Equilibrium and Stability of Rings Under Nonuniformly Distributed Loads," Proceedings of the Fourth U. S. National Congress of Applied Mechanics, Vol. 1, New York: The American Society of Mechanical Engineers.

Armco Drainage & Metal Products, Inc. (1958), Handbook of Drainage and Construction Products, Middletown, Ohio: Armco.

Armenàkas, A. E., and Herrmann, G. (1963), "Buckling of Thin Shells Under External Pressure," Journal of the Engineering Mechanics Division, Proceedings of the American Society of Civil Engineers, Vol. 89, No. 3552, Ann Arbor: ASCE.

Barnard, Russell E. (1957), "Design and Deflection Control of Buried Steel Pipe Supporting Earth Loads and Live Loads," Proceedings of the American Society for Testing Materials, Vol. 57, Philadelphia, Pa.: American Society for Testing Materials.

Bodner, Sol R. (1958), "On the Conservativeness of Various Distributed Force Systems," Journal of the Aeronautical Sciences, Vol. 25, No. 2, New York: Institute of the Aeronautical Sciences, Inc.

Boresi, A. P. (1955), "A Refinement of the Theory of Buckling of Rings Under Uniform Pressure," Journal of Applied Mechanics, Vol. 22, New York: The American Society of Mechanical Engineers.

Boynton Associates (1960), Operation Manual for 250 PSI 4-Foot Diameter Dynamic Load Generator, La Canada, California: Boynton Associates.

Braune, G. M., Cain, W., and Janda, H. F. (1929), "Earth Pressure Experiments on Culvert Pipe," Public Roads, Vol. 10, No. 9, Washington, D. C.: U. S. Government Printing Office.

Brockenbrough, R. L. (1963), The Influence of Wall Stiffness on the Design of Corrugated Metal Culverts, Project No. 57.12-400(3), Monroeville, Pennsylvania: United States Steel, Applied Research Laboratory.

Bulson, P. S. (1962), Deflection and Collapse of Buried Tubes, Report Res. 7/1, Christchurch, Hampshire, England: Military Engineering Experimental Establishment.

Bulson, P. S. (1963a), Buried Square Tubes Under Surface Pressure (1), Report Res. 48.3/2, Christchurch, Hampshire, England: Military Engineering Experimental Establishment.

Bulson, P. S. (1963b), Buried Square Tubes Under Surface Pressure (2), Report Res. 48.3/3, Christchurch, Hampshire, England: Military Engineering Experimental Establishment.

Bulson, P. S. (1964), Buried Tubes Under Surface Pressure, Report Res. 48.3/4, Christchurch, Hampshire, England: Military Engineering Experimental Establishment.

Bulson, P. S. (1965), Blast Loading of Buried Square Tubes, Report Res. 48.3/5, Christchurch, Hampshire, England: Military Engineering Experimental Establishment.

Carroll, W. F. (1963), Vertical Displacements of Spread Footings on Clay: Static and Impulsive Loadings. Technical Report No. 3-599, Vicksburg, Mississippi: U. S. Army Engineer Waterways Experiment Station.

Cheney, J. A. (1963), "Bending and Buckling of Thin-Walled Open-Section Rings," Journal of the Engineering Mechanics Division, Proceedings of the American Society of Civil Engineers, Vol. 89, No. 3665, Ann Arbor: ASCE.

Cheney, J. A. (1964), "Bending and Buckling of Thin-Walled Open-Section Rings," discussion closure, Journal of the Engineering Mechanics Division, Proceedings of the American Society of Civil Engineers, EM 6, No. 4160, Ann Arbor: ASCE

DaDeppo, D. A. (1963), Influence of Initial Deformation on the Bending of Arches, Technical Note N-462, Port Hueneme, California: U. S. Naval Civil Engineering Laboratory.

Davisson, M. T. (1964), discussion in Proceedings of the Symposium on Soil-Structure Interaction, Tucson: University of Arizona, p 599.

Dietz, A. G. H., and McGarry, F. J. (1956), "The Effects of Speed in the Mechanical Testing of Plastics," Symposium on Speed of Testing, Philadelphia, Pa.: ASTM.

Donnellan, B. A. (1964), "The Response of Buried Cylinders to Quasi-Static Overpressures." Ph. D. dissertation, Department of Civil Engineering, University of Illinois.

Dorris, A. F., and Albritton, G. E. (1965), Response of a Prototype Communications Conduit to Static and Dynamic Loading, Technical Report, Vicksburg, Mississippi: U. S. Army Engineer Waterways Experiment Station (in preparation).

Dowell, D. C. (1964), "Response of Statically and Dynamically Loaded Cylinders Embedded in Granular Materials." Ph.D. dissertation, Department of Engineering Mechanics, Iowa State University of Science and Technology.

Egger, W. (1957), 60 Kip Capacity, Slow or Rapid Loading Apparatus, SRS 158, Urbana, Illinois: Department of Civil Engineering, University of Illinois.

Forrestal, M. J., and Herrmann, G. (1964), "Buckling of a Long Cylindrical Shell Surrounded by an Elastic Medium," paper presented at the ASCE Structural Engineering Conference and Annual Meeting, October 12-23, 1964, Conference Preprint 108.

Hall, H. W. (1958), "Mechanical Properties of Plastics at High Speeds of Stressing," International Symposium on Plastics Testing and Standardization, ASTM Special Technical Publication No. 247, Philadelphia, Pa.: ASTM.

Hanley, J. T. (1963), "Interaction Between a Sand and Cylindrical Shells Under Static and Dynamic Loading." Ph.D. dissertation, Department of Civil Engineering, University of Illinois.

Hendron, A. J. (1963), "The Behavior of Sand in One-Dimensional Compression." Ph.D. dissertation, Department of Civil Engineering, University of Illinois.

Hetényi, M. (1946), Beams on Elastic Foundation, Ann Arbor: The University Of Michigan Press.

Jackson, J. G., Jr., and Hadala, P. F. (1964), Dynamic Bearing Capacity of Soils, Report 3, Technical Report No. 3-599, Vicksburg, Mississippi: U. S. Army Engineer Waterways Experiment Station.

Kane, H., Davisson, M. T., Olson, R. E., and Sinnamon, G. K. (1964), A Study of the Behavior of a Clay Under Rapid and Dynamic Loading in the One-Dimensional and Triaxial Tests, RTD TDR-63-3116, Kirtland Air Force Base, New Mexico: Air Force Weapons Laboratory.

Kennedy, T. E., and Sadler, W. H., Jr. (1965), An Evaluation of the Small Blast Load Generator, Miscellaneous Paper, Vicksburg, Mississippi: U. S. Army Engineer Waterways Experiment Station (in preparation).

Lane, K. S. (1960), "Evaluation of Test Results," Garrison Dam Test Tunnel, Reprinted from Transactions, Vol. 125, Part I, No. 3022, New York: ASCE.

Luscher, U. (1963), Study of the Collapse of Small Soil-Surrounded Tubes, AFSWC-TDR-63-6, Kirtland Air Force Base, New Mexico: Air Force Special Weapons Center.

Luscher, U., and Höeg, K. (1964), The Interaction Between a Structural Tube and the Surrounding Soil, RTD TDR-63-3109, Kirtland Air Force Base, New Mexico: Air Force Weapons Laboratory.

McDonough, G. F., Jr. (1959), "Dynamic Loads on Buried Structures." Ph.D. dissertation, Department of Civil Engineering, University of Illinois.

McNulty, J. W. (1965), An Experimental Study of Arching in Sand, Technical Report No. 1-674, Vicksburg, Mississippi: U. S. Army Engineer Waterways Experiment Station.

Marston, A. (1930), "The Theory of External Loads on Closed Conduits in the Light of the Latest Experiments," Iowa State College of Agricultural and Mechanic Arts Official Publication, Bulletin 96, Vol. XXVIII, No. 38, Ames, Iowa: Iowa Engineering Experiment Station.

Massard, J. M., and Collins, R. A. (1958), The Engineering Behavior of Structural Metals Under Slow and Rapid Loading, SRS 161, Urbana, Illinois: Department of Civil Engineering, University of Illinois.

Melin, J. W., and Sutcliffe, S. (1959), Development of Procedures for Rapid Computation of Dynamic Structural Response, SRS 171, Urbana, Illinois: Department of Civil Engineering, University of Illinois.

Merkle, D. H. (1963), Project 1080 Research Summary, RTD TDR-63-3023, Kirtland Air Force Base, New Mexico: Air Force Weapons Laboratory.

Merritt, J. L., and Newmark, N. M. (1962), Design of Underground Structures to Resist Nuclear Blast, Vol. II, SRS 149, Urbana, Illinois: Department of Civil Engineering, University of Illinois.

Merritt, J. L., and Newmark, N. M. (1964), "Effects of Underground Structures and Equipment," Nuclear Geoplosics, Part 5, Menlo Park, California: Stanford Research Institute.

Meyerhof, G. G., and Baikie, L. D. (1963), "Strength of Steel Culvert Sheets Bearing Against Compacted Sand Backfill," Culverts and Slope Protection--Four Reports, Record No. 30, Washington, D. C.: Highway Research Board.

Meyerhof, G. G., and Fisher, C. L. (1963), "Composite Design of Underground Steel Structures," The Engineering Journal, Vol. 46, No. 9, Montreal, Canada: Engineering Institute of Canada.

Mow, C. C. (1964), Dynamic Response of Lined and Unlined Underground Openings, Memorandum RM-3962-PR, Santa Monica, California: The Rand Corporation.

Murphy, G., and Young, D. F. (1962), A Study of the Use of Models to Simulate Dynamically Loaded Underground Structures, AFSWC-TDR-62-2, Kirtland Air Force Base, New Mexico: Air Force Special Weapons Center.

Murphy, G., Young, D. F., and Martin, C. W. (1963), Use of Models to Predict the Dynamic Response of Dynamically Loaded Underground Structures, RTD TDR-63-3064, Kirtland Air Force Base, New Mexico: Air Force Weapons Laboratory.

Newmark, Hansen and Associates (1961), Protective Construction Review Guide-Hardening, Vol. 1, prepared for the Office of the Assistant Secretary of Defense.

Newmark, N. M., and Haltiwanger, J. D. (1962), Principles and Practices for Design of Hardened Structures, AFSWC-TDR-62-138, Kirtland Air Force Base, New Mexico: Air Force Special Weapons Center.

Newmark, N. M., and Merritt, J. L. (1963), Design of Tests of Nearly Invulnerable Structures in Granite (U), (Operation Piledriver), DASA 1399, Urbana, Illinois: Newmark, Hansen and Associates (SECRET FRD).

Palmer, D. M., and Lankford, J., Jr. (1963), The Experimental and Theoretical Study of Buried Cylinders Under Dynamic Loading, Technical Memorandum No. 1, Tallahassee, Florida: Recon, Inc.

Palmer, D. M., Root, R. M., Lankford, J., Jr., and Troutner, T. C. (1963), The Experimental and Theoretical Study of Buried Cylinders Under Static Loading, Technical Report No. 15, Tallahassee, Florida: Recon, Inc.

Peck, O. K., and Peck, R. B. (1949), "Experience with Flexible Culverts Through Railroad Embankments," Contributions to Proceedings of the Second International Conference on Soil Mechanics and Foundation Engineering, U of I Bulletin No. 53, Urbana, Illinois: University of Illinois.

Perry, C. C., and Lissner, H. R. (1962), The Strain Gage Primer, 2nd ed., New York: McGraw-Hill Book Company, Inc.

Prakash, S. (1962), "Behavior of Pile Groups Subjected to Lateral Loads." Ph.D. dissertation, Department of Civil Engineering, University of Illinois.

Riley, W. F. (1965), Stress and Strain Distributions in a Long Cylindrical Shell with Arbitrary Pressure and Shear Loadings Imposed on the Outer Surface, Chicago: IIT Research Institute.

Robinson, R. R. (1962), The Investigation of Silo and Tunnel Linings, AFSWC-TDR-62-1, Kirtland Air Force Base, New Mexico: Air Force Special Weapons Center.

Robinson, R. R. (1964), Analytical and Experimental Investigations of Silo and Tunnel Linings, RTD TDR-63-3085, Kirtland Air Force Base, New Mexico: Air Force Weapons Laboratory.

Savin, G. N. (1961), Stress Concentration Around Holes, New York: Pergamon Press.

Schafer, G. E. (1948), "Schafer on Underground Conduits," Transactions of the American Society of Civil Engineers, Vol 113, No. 2337, New York: ASCE.

Seely, F. B., and Smith, J. O. (1952), Advanced Mechanics of Materials, 2nd ed., New York: John Wiley & Sons, Inc.

Singer, F. L. (1951), Strength of Materials, New York: Harper & Brothers.

Sinnamon, G. K., and Newmark, N. M. (1961), Facilities for Dynamic Testing of Soils, SRS 244, Urbana, Illinois: Department of Civil Engineering, University of Illinois.

Sinnamon, G. K., Schamaum, J. T., and Hanley, J. T. (1961), Feasibility

Study of a Facility for Laboratory Investigations of Effects of Dynamic Loads on Soils and Buried Structures, Urbana, Illinois: Department of Civil Engineering, University of Illinois.

Smith, J. E. (1963), "Tension Tests of Metals at Strain Rates up to 200 Sec," Materials Research & Standards, Vol. 3, No. 9, Philadelphia, Pa.: ASTM.

Spangler, M. G. (1938), "The Structural Design of Flexible Pipe Culverts," Public Roads, Vol. 18, No. 12, Washington D. C.: U. S. Government Printing Office.

Spangler, M. G. (1948), "Underground Conduits - An Appraisal of Modern Research," Transactions of the American Society of Civil Engineers, Vol. 113, No. 2337, New York: ASCE.

Spangler, M. G. (1956), "Stresses in Pressure Pipelines and Protective Casing Pipes," Journal of the Structural Division, Proceedings of the American Society of Civil Engineers, Vol. 82, No. 1054, Ann Arbor: ASCE.

Spangler, M. G. (1960), Soil Engineering, 2nd ed., Scranton, Pa.: International Textbook Company.

Stanford Research Institute (1964), Nuclear Geoplosics, Parts 1-5, Menlo Park, California.

Steidel, R. F., and Makerov, C. E. (1960), "The Tensile Properties of Some Engineering Materials at Moderate Rates of Strain," ASTM, Bulletin No. 247, Philadelphia, Pa.: ASTM.

Talbot, A. N. (1908), "Tests of Cast-Iron and Reinforced Concrete Culvert Pipe," University of Illinois, Engineering Experiment Station, Bulletin No. 22, Urbana, Illinois: Engineering Experiment Station.

Tener, R. K. (1964), Model Study of a Buried Arch Subjected to Dynamic Loading, Technical Report No. 1-660, Vicksburg, Mississippi: U. S. Army Engineer Waterways Experiment Station.

Terzaghi, K. (1942), "Shield Tunnels of the Chicago Subway," Journal of the Boston Society of Civil Engineers, Vol. XXIX, No. 3, Boston: Boston Society of Civil Engineers.

Terzaghi, K. (1943), "Liner-Plate Tunnels on the Chicago (Ill.) Subway," Transactions of the American Society of Civil Engineers, Vol. 108, No. 2200, New York: ASCE.

Terzaghi, K., and Peck, R. B. (1948), Soil Mechanics in Engineering Practice, New York: John Wiley & Sons, Inc.

Timoshenko, S. P., and Gere, J. M. (1961), Theory of Elastic Stability, 2nd ed., New York: McGraw-Hill Book Company, Inc.

Timoshenko, S., and Young, D. H. (1955), Vibration Problems in Engineering, 3rd ed., Princeton, New Jersey: D. Van Nostrand Company, Inc.

University of Arizona (1964), Proceedings of the Symposium on Soil-Structure Interaction, Tucson, Arizona.

U. S. Atomic Energy Commission (1964), The Effects of Nuclear Weapons, Revised ed., Washington, D. C.

U. S. Army Corps of Engineers (1957), Design of Structures to Resist the Effects of Atomic Weapons, EM 1110-345-413 to -421, Washington, D. C.: Office of the Chief of Engineers.

U. S. Army Engineer Waterways Experiment Station (1963), Manual of Laboratory Tests for Soils for Use on Civil Works Projects, looseleaf volume prepared and distributed for the Office, Chief of Engineeers, Vicksburg, Mississippi: U. S. Army Engineer Waterways Experiment Station.

U. S. Army Engineer Waterways Experiment Station (1963), Status Report for Blast Load Generator Facility, Vicksburg, Mississippi: U. S. Army Engineer Waterways Experiment Station.

Van Horn, D. A., and Tener, R. K. (1963), A Study of Loads on Underground Structures, Project 434-S, Ames, Iowa: Iowa Engineering Experiment Station.

Watkins, R. K. (1959), "Influence of Soil Characteristics on the Deformation of Embedded Flexible Pipe Culverts," in Embedded Flexible Metal Pipe Culverts, presented at the 38th Annual Meeting of the Highway Research Board, Bulletin 223, Washington, D. C.

Watkins, R. K. (1960), "Failure Conditions of Flexible Culverts Embedded in Soil," Highway Research Board Proceedings, Vol. 39, Washington, D. C.: Highway Research Board.

Watkins, R. K. (1963), "Some Observations on the Ring Buckling of Buried Flexible Conduits," Culverts and Slope Protection--Four Reports, Record No. 30, Washington, D. C.: Highway Research Board.

Watkins, R. K. (1964), "Structural Design Trends in Buried Flexible Conduits," Proceedings of the Symposium on Soil-Structure Interaction, Tucson: University of Arizona.

Watkins, R. K., and Nielson, F. D. (1964), "Development and Use of the Modpares Device," Journal of the Pipeline Division, Proceedings of the American Society of Civil Engineers, Vol. 90, No. 3782, Ann Arbor: ASCE.

Watkins, R. K., and Spangler, M. G. (1958), "Some Characteristics of the Modulus of Passive Resistance of Soil: A Study in Similitude," Highway Research Board Proceedings, Vol. 37, Washington, D. C.: Highway Research Board.

White, H. L. (1961), "Largest Metal Culvert Designed by Ring Compression Theory," Civil Engineering, Vol. 31, No. 1, New York: American Society of Civil Engineers.

White, H. L., and Layer, J. P. (1960), "The Corrugated Metal Conduit as a Compression Ring," Highway Research Board Proceedings, Vol. 39, Washington, D. C.: Highway Research Board.

Whitman, R. V., Getzler, Z., and Höeg, K. (1962), Static Tests upon Thin Domes Buried in Sand, Report No. 12, Research Project R 62-41, Cambridge: Department of Civil Engineering, Massachusetts Institute of Technology.

Whitman, R. V., and Healy, K. A. (1962), "Shear Strength of Sand During Rapid Loading," Journal of the Soil Mechanics Division, Proceedings of the American Society of Civil Engineers, Vol. 88, No. 3102, Ann Arbor: ASCE.

Whitman, R. V., and Luscher, U. (1962), "Basic Experiment into Soil-Structure Interaction," Journal of the Soil Mechanics and Foundations Division, Proceedings of the American Society of Civil Engineers, Vol. 88, No. 3366, Ann Arbor: ASCE.

Williamson, R. A., and Huff, P. H. (1961), Test of Buried Structural-Plate Pipes Subjected to Blast Loading, WT-1474, Los Angeles, California: Holmes & Narver, Inc.

Wright, R. N., and Hall, W. J. (1964), "Loading Rate Effects in Structural Steel Design," Journal of the Structural Division, Proceedings of the American Society of Civil Engineers, Vol. 90, No. 4084, Ann Arbor: ASCE.

Yoshihara, T., Robinson, A. R., and Merritt, J. L. (1963), Interaction of Plane Elastic Waves with an Elastic Cylindrical Shell, SRS 261, Urbana, Illinois: Department of Civil Engineering, University of Illinois.

Young, D. F., and Murphy, G. (1964), "Dynamic Similitude of Underground Structures," Journal of the Engineering Mechanics Division, Proceedings of the American Society of Civil Engineers, Vol. 90, No. 3938, Ann Arbor: ASCE.

Table 4.1

Geometric and Material Properties of Test Cylinders

$E = 10 \times 10^6$ psi; $\ell = 10.5$ in.; $d = 3.5$ in.; $\ell/R = 6$

Group	Aluminum	σ_{y1} (psi)	σ_{y2} (psi)	h (in.)	R (in.)	I (10^{-8} in.^{3})	EI (lb-in.)	$\frac{EI}{R^3}$ (psi)	$\frac{d}{h}$
A	D6061-0	5000	7600	0.065	1.72	2289	228.9	45.0	54
D	D6061-0	3400	6100	0.065	1.72	2289	228.9	45.0	54
E	D6061-0	4500	7400	0.065	1.72	2289	228.9	45.0	54
B	D5052-0	11,000	12,700	0.065	1.72	2289	228.9	45.0	54
C	D6061-T6	37,500	42,100	0.022	1.74	89	8.9	1.7	159

Table 5.1

Overall Testing Program and Overpressure, P_{so}, at Failure

			Depth of Burial													
			Z* = 0 in.		Z = 3/16 in.		Z = 5/16 in.		Z = 7/16 in.		Z = 7/8 in.		Z = 1-3/4 in.		Z = 2-5/8 in.	
Group	Soil	Loading	Cylinder	P_{so} psi	Cylinder	P_{so} psi	Cylinder	P_{so} psi	Cylinder	P_{so} psi	Cylinder	P_{so} psi	Cylinder	P_{so} psi	Cylinder	P_{so} psi
A	Sand	Static	A-1	270	A-5	325			A-2	500**	A-3	500**	A-4	500**		
A	Sand	Rapid	A-10	300	A-9	400			A-8	500**	A-7	500**	A-6	500**		
B	Sand	Static	B-1	315					B-5	500**	B-2	500**	B-3	500**	B-4	500**
B	Sand	Rapid	B-6	400					B-7	500**	B-8	500**	B-9	500**	B-10	500**
C	Sand	Static	C-1	95	C-4	195	C-5	500**	C-2	500**	C-3	500**				
C	Sand	Rapid	C-6	175	C-7	350	C-8	500	C-9	500	C-10	500**				
E	Sand	Static	E-3	205					E-2	400**	E-1	440**				
E	Sand	Dynamic	E-6	254**					E-5	262**	E-4	264**				
D	Clay	Static	D-1	95					D-2	130	D-3	100	D-4	190	D-5	180
D	Clay	Dynamic									D-10	97**	D-6	160**		
											D-8	116**	D-7	180		
											D-9	148				

Note: Depths of burial, Z , of 7/16 in. = 1/8d; 7/8 in. = 1/4d; 1-3/4 in. = 1/2d; 2-5/8 in. = 3/4d where d is outside diameter of the cylinder.

* Z = depth of burial.

** No failure.

Table 5.[illegible]

Strain, Stress, Thrust, Moment, and Deflection: Tests A-1, A-2, A-3A, A-3B, A-[illegible], A-5

Gage	Measurement	Overpressure, psi 50	100	150	200	250	275	300	325	[illegible]	[illegible]	[illegible]	[illegible]
					Test A-1 (2 - [illegible] in.)								
1	Strain, µin./in.	194	396	485	485	276	-523						
	Stress, psi	1940	3960	4850	4850	2760	-5102						
1a	Strain, µin./in.	20	53	145	408	1862	--						
	Stress, psi	200	530	1450	4080	7143	--						
1-1a	Thrust, lb/in.	70	146	205	290	3	--						
	Moment, in.-lb/in.	-0.61	-1.21	-1.20	-0.27	1.[illegible]	--						
3	Strain, µin./in.	44	88	141	141	132	123						
	Stress, psi	440	880	1410	1410	1320	1230						
3a	Strain, µin./in.	100	174	240	327	454	480						
	Stress, psi	1000	1740	2400	3270	4540	4800						
3-3a	Thrust, lb/in.	47	85	124	152	190	196						
	Moment, in.-lb/in.	0.20	0.30	0.35	0.65	1.13	1.26						
2	Strain, µin./in.	183	319	475	800	1440	1840						
	Stress, psi	1830	3190	4750	5864	6807	7125						
2a	Strain, µin./in.	-18	14	56	108	550	890						
	Stress, psi	-180	140	560	1080	5222	6022						
2-2a	Thrust, lb/in.	54	106	173	248	402	434						
	Moment, in.-lb/in.	-0.71	-1.07	-1.48	-1.79	-0.53	-0.37						
4	Strain, µin./in.	125	224	344	581	1041	1231						
	Stress, psi	1250	2240	3440	5360	6288	6623						
4a	Strain, µin./in.	9	51	102	191	404	510						
	Stress, psi	90	510	1020	1910	4040	5044						
4-4a	Thrust, lb/in.	44	89	145	248	363	388						
	Moment, in.-lb/in.	-0.41	-0.61	-0.85	-1.29	-0.64	-0.49						
DC1	Deflection, in.	0.001	0.001	0.003	0.007	0.017	0.037						
DC2	Deflection, in.	0.001	0.000	0.002	0.003	0.005	0.007						
1-1a;3-3a	Avg thrust, lb/in.	59	116	165	221	291	--						
2-2a;4-4a	Avg thrust, lb/in.	49	99	159	258	383	411						
	q	1.20	1.17	1.04	0.86	0.76	--						
					Test A-5 (2 - 3/16 in.)								
1	Strain, µin./in.	290	553	632	554	230		-516	-1290				
	Stress, psi	2900	5236	5568	5240	2380		-5062	-6688				
1a	Strain, µin./in.	0	0	133	401	1962		6820	--				
	Stress, psi	0	0	1330	4010	7201		9505	--				
1-1a	Thrust, lb/in.	94	179	242	307	391		445	--				
	Moment, in.-lb/in.	-1.02	-1.92	-1.59	-0.55	1.27		3.03	--				
3	Strain, µin./in.	141	236	281	298	272		262	262				
	Stress, psi	1410	2360	2810	2980	2720		2620	2620				
3a	Strain, µin./in.	10	10	36	106	182		259	298				
	Stress, psi	100	100	360	1060	1820		2590	2980				
3-3a	Thrust, lb/in.	49	80	104	131	148		169	182				
	Moment, in.-lb/in.	-0.46	-0.80	-0.86	0.68	-0.32		-0.01	0.13				
2	Strain, µin./in.	113	243	356	535	1005		2145	2620				
	Stress, psi	1130	2430	3560	5156	6285		7304	7561				
2a	Strain, µin./in.	0	31	78	164	523		1610	2080				
	Stress, psi	0	310	780	1640	5108		6942	7266				
2-2a	Thrust, lb/in.	37	89	139	207	375		464	482				
	Moment, in.-lb/in.	-0.60	-0.75	-1.00	-1.29	-0.35		-0.13	-0.10				
4	Strain, µin./in.	162	304	518	777	1790		2817	2690				
	Stress, psi	1620	3040	5080	5824	6621		7341	7377				
4a	Strain, µin./in.	-33	-11	0	55	329		1162	1578				
	Stress, psi	-330	-110	0	550	3290		6501	6812				
4-4a	Thrust, lb/in.	42	102	168	268	364		454	473				
	Moment, in.-lb/in.	-0.69	-1.18	-1.82	-2.00	-0.94		-0.29	-0.23				
DC1	Deflection, in.	-0.001	-0.009	0.001	0.005	0.017		0.039	0.091				
DC2	Deflection, in.	0.001	0.001	0.002	0.004	0.004		0.018	0.009				
1-1a;3-3a	Avg thrust, lb/in.	72	130	173	219	270		307	--				
2-2a;4-4a	Avg thrust, lb/in.	40	96	154	238	370		459	477				
	q	1.80	1.35	1.12	0.92	0.73		0.67	--				
					Test A-[illegible] (2 - 7/16 in.)								
1	Strain, µin./in.	191	397	507	536	559		796		1140	1440	1405	1377
	Stress, psi	1910	3970	5031	5140	5040		5853		[illegible]	[illegible]	7097	7211
1a	Strain, µin./in.	20	68	153	318	605		[illegible]		--	--	--	--
	Stress, psi	200	680	1530	3180	6008		7979		--	--	--	--
1-1a	Thrust, lb/in.	74	150	214	276	370		467		--	--	--	--
	Moment, in.-lb/in.	-0.94	-1.17	-1.25	-0.78	0.89		0.33		--	--	--	--
3	Strain, µin./in.	148	280	380	453	486		581		578	683	780	832
	Stress, psi	1480	2800	3800	4530	4860		5093		5329	5823	[illegible]	[illegible]
3a	Strain, µin./in.	7	47	80	140	208		314		477	780	1080	[illegible]
	Stress, psi	70	470	800	1400	2080		3140		4770	7703	[illegible]	[illegible]
3-3a	Thrust, lb/in.	57	107	149	184	223		271		333	389	393	[illegible]
	Moment, in.-lb/in.	-0.57	-0.83	-1.26	-1.03	-0.98		-0.70		-0.43	0.06	0.17	[illegible]
2	Strain, µin./in.	197	318	480	594	1080		--		--	--	--	--
	Stress, psi	1970	3180	4800	5031	6650		--		--	--	--	--
2a	Strain, µin./in.	-18	20	66	212	711		[illegible]		--	--	--	--
	Stress, psi	-180	200	660	2120	7709		7964		--	--	--	--
2-2a	Thrust, lb/in.	57	110	187	247	393		--		--	--	--	--
	Moment, in.-lb/in.	-0.74	-1.04	-1.80	-1.16	-0.24		--		--	--	--	--
4	Strain, µin./in.	238	380	594	813	1447		--		--	--	--	--
	Stress, psi	2380	3800	5940	5957	6613		--		--	--	--	--
4a	Strain, µin./in.	-43	-40	06	116	408		1352		[illegible]	--	--	--
	Stress, psi	-430	-400	[illegible]	1160	[illegible]		6777		[illegible]	--	--	--
4-4a	Thrust, lb/in.	69	117	188	278	380		--		--	--	--	--
	Moment, in.-lb/in.	-0.98	-1.42	-1.93	-1.96	-0.77		--		--	--	--	--
DC1	Deflection, in.	0.004	0.005	0.007	0.020	0.069		0.032		0.047	0.038	0.099	0.098
DC2	Deflection, in.	0.004	0.005	0.005	0.009	0.012		0.015		0.017	0.019	0.021	0.073
1-1a;3-3a	Avg thrust, lb/in.	66	129	182	231	307		359		--	--	--	--
2-2a;4-4a	Avg thrust, lb/in.	60	114	178	262	392		--		--	--	--	--
	q	1.10	1.13	1.02	0.89	0.77		--		--	--	--	--

(Continued)

Table [illegible] (Concluded)

Gage	Measurement	50	100	150	200	250	270	300	325	350	400	450	500
					Overpressure, psi								
Test A-3A (Z = 7/8 in.)													
1	Strain, μin./in.	88	169	213	199	213		389		840	1362		
	Stress, psi	880	1690	2130	1990	2130		3890		5934	6745		
1a	Strain, μin./in.	87	174	289	463	820		1380		2261	3125		
	Stress, psi	870	1740	2890	4630	5899		6759		7365	7033		
1-1a	Thrust, lb/in.	57	111	163	215	300		353		444	477		
	Moment, in.-lb/in.	0.00	0.02	0.27	0.93	1.36		0.80		0.47	0.37		
3	Strain, μin./in.	166	280	367	464	560		647		796	954		
	Stress, psi	1660	2800	3670	4640	5267		5595		5857	6135		
3a	Strain, μin./in.	31	55	80	128	185		222		332	473		
	Stress, psi	310	550	800	1280	1850		2220		3320	4730		
3-3a	Thrust, lb/in.	64	109	145	192	240		273		327	367		
	Moment, in.-lb/in.	-0.48	-0.79	-1.01	-1.18	-1.27		-1.26		-0.86	-0.41		
2	Strain, μin./in.	171	308	426	564	1450		2680		4150	--		
	Stress, psi	1710	3080	4260	5285	6815		7593		8337	--		
2a	Strain, μin./in.	-14	26	110	262	1170		2341		3745	--		
	Stress, psi	-140	260	1100	2620	6515		7409		8138	--		
2-2a	Thrust, lb/in.	51	109	174	266	435		488		525	--		
	Moment, in.-lb/in.	-0.65	-0.99	-1.11	[illegible]	[illegible]		-0.06		-0.07	--		
4	Strain, μin./in.	213	368	530	697	1198		2243		3545	4600		
	Stress, psi	2130	3680	5132	5683	6564		7355		8040	8558		
4a	Strain, μin./in.	-46	-20	33	113	435		1434		2601	3601		
	Stress, psi	-460	-200	330	1130	4350		6802		7550	8067		
4-4a	Thrust, lb/in.	54	113	183	250	378		462		507	540		
	Moment, in.-lb/in.	-0.91	-1.37	-1.74	-1.73	-0.62		-0.20		-0.17	-0.17		
DC1	Deflection, in.	0.005	0.007	0.009	0.013	0.021		0.029		0.039	0.048		
DC2	Deflection, in.	0.004	0.006	0.007	0.009	0.011		0.013		0.014	0.015		
1-1a:3-3a	Avg thrust, lb/in.	61	110	154	204	270		328		386	422		
2-2a:4-4a	Avg thrust, lb/in.	53	111	179	258	407		475		521	540		
	q	1.15	0.99	0.86	0.79	0.66		0.69		0.74	0.78		
Test A-3B (Z = 7/8 in.)													
1	Strain, μin./in.	-206	-244	-264	-257	-264		-198		-44	66	294	896
	Stress, psi	-2060	-2440	-2640	-2570	-2640		-1980		-440	660	2940	6033
1a	Strain, μin./in.	338	521	695	840	1070		1331		1689	2048	2620	3702
	Stress, psi	3380	5093	5679	5934	6339		6720		7005	7248	7561	8117
1-1a	Thrust, lb/in	43	90	132	167	205		258		327	369	422	476
	Moment, in.-lb/in.	1.92	2.69	3.16	3.27	3.35		3.05		2.32	1.82	1.11	0.64
3	Strain, μin./in.	79	122	175	216	271		306		376	507	655	814
	Stress, psi	790	1220	1750	2180	2710		3060		3760	5031	5609	5889
3a	Strain, μin./in.	55	117	184	234	296		362		474	621	817	1056
	Stress, psi	550	1170	1840	2340	2960		3620		4740	5536	5894	6315
3-3a	Thrust, lb/in.	44	78	117	147	184		217		276	344	374	397
	Moment, in.-lb/in.	-0.08	-0.02	0.03	0.06	0.09		0.20		0.35	0.18	0.10	0.15
2	Strain, μin./in	216	368	518	650	800		920		1200	2570	4010	--
	Stress, psi	2160	3680	5080	5600	5864		6075		6568	7534	8268	--
2a	Strain, μin./in.	69	131	220	302	392		488		742	1971	3302	4420
	Stress, psi	690	1310	2200	3020	3920		4880		5762	7206	7920	8470
2-2a	Thrust, lb/in.	93	162	240	298	341		366		401	479	526	--
	Moment, in.-lb/in.	-0.52	-0.83	-1.04	-0.95	-0.62		-0.37		-0.28	-0.12	-0.12	--
4	Strain, μin./in.	199	338	468	590	736		860		1020	1898	2842	4110
	Stress, psi	1990	3380	4680	5400	5751		5970		6251	7166	7680	8317
4a	Strain, μin./in.	47	100	174	234	315		388		515	1375	2300	3362
	Stress, psi	470	1000	1740	2340	3150		3880		5067	6755	7386	7950
4-4a	Thrust, lb/in.	80	142	209	264	315		346		375	453	490	529
	Moment, in.-lb/in.	-0.54	-0.84	-1.04	-1.14	-0.93		-0.65		-0.37	-0.15	-0.10	-0.13
DC1	Deflection, in.	0.007	0.011	0.013	0.016	0.020		0.022		0.026	0.034	0.043	0.053
DC2	Deflection, in.	0.004	0.007	0.008	0.009	0.011		0.013		0.014	0.015	0.016	0.017
1-1a:3-3a	Avg thrust, lb/in.	44	84	125	157	195		238		302	357	398	437
2-2a:4-4a	Avg thrust, lb/in.	87	152	225	281	328		355		388	466	508	529
	q	0.51	0.55	0.56	0.56	0.59		0.67		0.78	0.77	0.78	0.83
Test A-4 (Z = 1-3/4 in.)													
1	Strain, μin./in.	0	39	78	143	195		295		507	780	1142	1535
	Stress, psi	0	390	780	1430	1950		2950		5031	5829	6466	6883
1a	Strain, μin./in.	134	201	295	443	531		900		1290	1706	2226	2760
	Stress, psi	1340	2010	2950	4430	[illegible]		6040		6688	7019	7346	7636
1-1a	Thrust, lb/in.	44	78	121	190	261		330		391	425	454	474
	Moment, in.-lb/in.	0.47	0.57	0.76	1.06	1.35		1.02		0.53	0.42	0.29	0.26
3	Strain, μin./in.	166	280	402	543	744		963		1226	1480	1813	2035
	Stress, psi	1660	2800	4020	5191	5765		6151		6614	6839	7104	7241
3a	Strain, μin./in.	-38	-57	-76	-114	-123		-123		-104	-86	-38	38
	Stress, psi	-380	-570	-760	-1140	-1230		-1230		-1040	-860	-380	380
3-3a	Thrust, lb/in.	42	72	106	139	188		220		269	301	337	364
	Moment, in.-lb/in.	-0.72	-1.19	-1.68	-2.30	-2.68		-2.76		-2.67	-2.54	-2.26	-1.93
2	Strain, μin./in.	267	445	609	807	1275		2140		3322	4470	5650	6900
	Stress, psi	2670	4450	5485	5876	6676		7298		7930	8494	9023	9558
2a	Strain, μin./in.	-41	-41	-10	10	134		909		2029	3043	4110	5240
	Stress, psi	-410	-410	-100	100	1340		6056		7236	7789	8317	8854
2-2a	Thrust, lb/in.	73	131	192	241	331		443		493	529	565	598
	Moment, in.-lb/in.	-1.08	-1.71	-2.08	-2.19	-1.68		-0.41		-0.25	-0.25	-0.25	-0.24
4	Strain, μin./in.	194	296	445	571	765		1267		2238	3220	4293	5424
	Stress, psi	1940	2960	4450	5316	5802		6670		7352	7880	8407	8950
4a	Strain, μin./in.	-22	-11	34	122	290		793		1767	2688	3707	4726
	Stress, psi	-220	-110	340	1220	2900		5852		7083	7597	8119	8620
4-4a	Thrust, lb/in.	56	93	156	223	313		407		470	503	537	571
	Moment, in.-lb/in.	-0.76	-1.08	-1.45	-1.52	-1.03		-0.29		-0.09	-0.10	-0.10	-0.11
DC1	Deflection, in.	0.002	0.003	0.005	0.007	0.010		0.016		0.021	0.028	0.034	0.044
DC2	Deflection, in.	0.004	0.005	0.007	0.008	0.009		0.010		0.011	0.012	0.012	0.013
1-1a:3-3a	Avg thrust, lb/in.	43	75	114	165	225		279		330	363	396	419
2-2a:4-4a	Avg thrust, lb/in.	65	112	174	232	322		425		482	516	551	585
	q	0.66	0.67	0.66	0.71	0.70		0.66		0.68	0.70	0.72	0.72

Table 5.3

Strain, Stress, Thrust, and Moment; Tests A-6, A-7, A-8, A-9, A-10

Gage	Measurement	Overpressure, psi 50	100	150	200	250	300	350	400	450	500
	Test A-10 (Z = 0 in.)										
1	Strain, μin./in.	-149	432	894	1281	461	-4830				
	Stress, psi	-1490	4320	6029	6681	4610	-8676				
1a	Strain, μin./in.	309	51	26	309	3942	10400				
	Stress, psi	3090	510	260	3090	8235	10950				
1-1a	Thrust, lb/in.	52	157	259	365	465	234				
	Moment, in.-lb/in.	1.61	-1.34	-2.14	-1.02	0.95	8.24				
3	Strain, μin./in.	-80	151	330	446	423	503				
	Stress, psi	-800	1510	3330	4460	4230	5013				
3a	Strain, μin./in.	231	284	328	389	458	503				
	Stress, psi	2310	2840	3280	3890	4580	5013				
3-3a	Thrust, lb/in.	49	141	214	271	286	326				
	Moment, in.-lb/in.	1.09	0.47	-0.01	-0.20	0.12	0.00				
2	Strain, μin./in.	269	316	398	457	1630	2862				
	Stress, psi	2690	3160	3980	4570	6958	7691				
2a	Strain, μin./in.	-12	104	198	349	1235	1947				
	Stress, psi	-120	1040	1980	3490	6630	7193				
2-2a	Thrust, lb/in.	84	137	194	262	442	484				
	Moment, in.-lb/in.	-0.99	-0.75	-0.70	-0.38	-0.11	-0.18				
4	Strain, μin./in.	275	375	462	713	1338	2564				
	Stress, psi	2750	3750	4620	5711	6726	7531				
4a	Strain, μin./in.	-11	80	159	353	1014	1276				
	Stress, psi	-110	800	1590	3530	6241	6677				
4-4a	Thrust, lb/in.	86	148	202	322	423	464				
	Moment, in.-lb/in.	-1.01	-1.04	-1.07	-0.77	-0.18	-0.30				
1-1a:3-3a	Avg thrust, lb/in.	51	149	237	318	376	--				
2-2a:4-4a	Avg thrust, lb/in.	85	143	195	292	433	474				
	q	0.60	1.04	1.20	1.09	0.87	--				
	Test A-9 (Z = 3/16 in.)										
1	Strain, μin./in.	-207	445	1482	2667	2445	1748	1185	-1778		
	Stress, psi	-2070	4450	6840	7586	7466	7052	6542	-7076		
1a	Strain, μin./in.	324	162	-162	81	1462	5982	10042	--		
	Stress, psi	3240	1620	-1620	810	5825	9150	10830	--		
1-1a	Thrust, lb/in.	38	197	283	398	466	531	580	--		
	Moment, in.-lb/in.	1.87	-1.00	-2.86	-1.68	-0.22	0.74	1.42	--		
3	Strain, μin./in.	35	263	518	658	702	676	711	737		
	Stress, psi	350	2630	5080	5614	5692	5646	5707	5753		
3a	Strain, μin./in.	131	98	82	98	155	221	262	311		
	Stress, psi	1310	980	820	980	1550	2210	2620	3110		
3-3a	Thrust, lb/in.	54	117	195	237	264	279	297	314		
	Moment, in.-lb/in.	0.34	-0.58	-1.53	-1.75	-1.57	-1.29	-1.14	-0.94		
2	Strain, μin./in.	241	289	361	602	1133	2699	3687	4892		
	Stress, psi	2410	2390	3610	5454	6450	7603	8109	8702		
2a	Strain, μin./in.	25	0	199	373	772	2414	3634	4505		
	Stress, psi	250	0	1990	3730	5815	7449	8083	8512		
2-2a	Thrust, lb/in.	86	94	182	309	399	489	526	559		
	Moment, in.-lb/in.	-0.76	-1.02	-0.57	-0.62	-0.22	-0.05	-0.01	-0.07		
4	Strain, μin./in.	330	356	559	839	1449	3433	4399	5670		
	Stress, psi	3330	3560	5262	5933	6814	7984	8559	9031		
4a	Strain, μin./in.	-49	0	74	221	959	2754	3511	4770		
	Stress, psi	-490	0	740	2210	6144	7633	8170	8642		
4-4a	Thrust, lb/in.	91	116	204	304	425	508	540	575		
	Moment, in.-lb/in.	-1.33	-1.25	-1.67	-1.32	-0.24	-0.12	-0.10	-0.13		
1-1a:3-3a	Avg thrust, lb/in.	46	157	239	318	365	405	439	--		
2-2a:4-4a	Avg thrust, lb/in.	89	105	193	307	412	499	533	567		
	q	0.52	1.50	1.24	1.04	0.89	0.81	0.82	--		
	Test A-8 (Z = 7/16 in.)										
1	Strain, μin./in.	-220	422	906	1293	1188	1139	1355	1557	1698	1707
	Stress, psi	-2200	4220	6051	6690	6547	6454	6739	6900	7012	7019
1a	Strain, μin./in.	249	-28	166	443	1773	3574	5154	7094	9726	12303
	Stress, psi	2490	-280	1660	4430	7072	8054	8818	9618	10703	11569
1-1a	Thrust, lb/in.	9	128	299	385	444	480	511	545	584	618
	Moment, in.-lb/in.	1.65	-1.58	-1.55	-0.64	0.17	0.52	0.71	0.93	1.26	1.58
3	Strain, μin./in.	146	474	849	1236	1529	1804	2133	2437	--	--
	Stress, psi	1460	4740	5950	6631	6778	7097	7293	7461	--	--
3a	Strain, μin./in.	89	33	17	50	127	283	371	533	749	1004
	Stress, psi	890	330	170	500	1270	2830	3710	5147	5774	6223
3-3a	Thrust, lb/in.	76	165	250	308	349	390	414	435	--	--
	Moment, in.-lb/in.	-0.20	-1.55	-2.17	-2.02	-1.68	-1.14	-0.93	-0.72	--	--
2	Strain, μin./in.	381	429	620	787	2290	4080	5487	7348	9329	11333
	Stress, psi	3810	4290	5534	5841	7381	8303	8956	9723	10539	11252
2a	Strain, μin./in.	25	125	176	427	1586	3297	4581	[illegible]	7853	9564
	Stress, psi	250	1250	1760	4270	6923	7918	8549	9594	9931	10636
2-2a	Thrust, lb/in.	132	180	253	347	466	527	569	615	665	712
	Moment, in.-lb/in.	-1.25	-1.07	-1.41	-0.49	-0.16	-0.14	-0.14	-0.19	-0.21	-0.21
4	Strain, μin./in.	380	456	608	836	2155	3677	4945	6568	8242	9890
	Stress, psi	3800	4560	5480	5927	7307	8104	8728	9401	10091	10771
4a	Strain, μin./in.	0	100	201	437	1413	2926	4305	5685	7367	8611
	Stress, psi	0	1000	2010	4370	6786	7726	8413	9037	9731	10243
4-4a	Thrust, lb/in.	123	181	258	353	459	515	557	599	644	683
	Moment, in.-lb/in.	-1.34	-1.25	-1.29	-0.47	-0.19	-0.13	-0.11	-0.13	-0.13	-0.19
1-1a:3-3a	Avg thrust, lb/in.	43	147	275	347	397	435	463	490	--	--
2-2a:4-4a	Avg thrust, lb/in.	128	181	256	350	463	521	563	607	655	698
	q	0.34	0.81	1.07	0.99	0.86	0.83	0.82	0.81	--	--

(Continued)

Table 5.3 (Concluded)

Gage	Measurement	Overpressure, psi 50	100	150	200	250	300	350	400	450	500
					Test A-7 (Z = 7/8 in.)						
1	Strain, μin./in.	-155	103	415	675	766	831	1078	1389	1857	2338
	Stress, psi	-1550	1030	4150	5644	5804	5919	6353	6767	7139	7407
1a	Strain, μin./in.	251	275	461	769	1271	1547	2268	2972	3839	4365
	Stress, psi	2510	2750	4610	5809	6673	6892	7369	7751	8184	8443
1-1a	Thrust, lb/in.	31	123	285	372	406	422	453	475	499	516
	Moment, in.-lb/in.	1.43	0.61	0.16	0.06	0.31	0.35	0.33	0.34	0.37	0.36
3	Strain, μin./in.	-44	61	217	330	391	400	478	530	626	678
	Stress, psi	-440	610	2170	3300	3910	4000	4780	5133	5558	5649
3a	Strain, μin./in.	185	245	277	305	376	425	528	659	861	1106
	Stress, psi	1850	2450	2770	3050	3760	4250	5125	5616	5971	6403
3-3a	Thrust, lb/in.	46	99	161	206	249	268	324	352	375	392
	Moment, in.-lb/in.	0.81	0.65	0.21	-0.03	-0.05	0.09	0.12	0.18	0.15	0.27
2	Strain, μin./in.	258	371	436	662	1551	2650	4088	5510	6916	8047
	Stress, psi	2580	3710	4360	5521	6895	7577	8307	8965	9545	10011
2a	Strain, μin./in.	35	70	245	420	1348	2346	3799	5078	6426	7494
	Stress, psi	350	700	2450	4200	6734	7413	8164	8787	9343	9783
2-2a	Thrust, lb/in.	95	143	221	332	443	487	535	577	614	643
	Moment, in.-lb/in.	-0.79	-1.06	-0.67	-0.49	-0.06	-0.06	-0.05	-0.06	-0.07	-0.08
4	Strain, μin./in.	282	459	689	1025	2510	3765	5410	7107	8991	10289
	Stress, psi	2820	4590	5669	6260	7501	8148	8924	9624	10400	10910
4a	Strain, μin./in.	-16	66	212	475	2047	2915	4488	6044	7518	8681
	Stress, psi	-160	660	2120	4750	7247	7720	8503	9185	9793	10272
4-4a	Thrust, lb/in.	86	171	279	372	479	516	567	611	656	689
	Moment, in.-lb/in.	-1.05	-1.38	-1.33	-0.44	-0.09	-0.15	-0.15	-0.15	-0.21	-0.23
1-1a;3-3a	Avg thrust, lb/in.	39	111	223	289	328	345	389	414	437	454
2-2a;4-4a	Avg thrust, lb/in.	91	157	250	352	461	502	551	594	635	666
	q	0.43	0.71	0.89	0.82	0.71	0.69	0.71	0.70	0.69	0.68
					Test A-6 (Z = 1-3/4 in.)						
1	Strain, μin./in.	-90	-26	167	390	619	683	812	1057	1354	1793
	Stress, psi	-900	-260	1670	3900	5529	5658	5885	6316	6739	7088
1a	Strain, μin./in.	218	339	485	728	1059	1237	1480	1893	2321	2831
	Stress, psi	2180	3390	4850	5737	6320	6633	6839	7163	7398	7674
1-1a	Thrust, lb/in.	42	102	212	333	386	399	418	443	461	480
	Moment, in.-lb/in.	1.08	1.29	1.12	0.62	0.27	0.34	0.35	0.27	0.23	0.20
3	Strain, μin./in.	9	148	331	531	880	1159	1456	1937	2367	2875
	Stress, psi	90	1480	3310	5138	5005	6496	6820	7187	7423	7698
3a	Strain, μin./in.	106	90	8	-98	-229	-327	-425	-532	-581	-606
	Stress, psi	1060	900	80	-980	-2290	-3270	-425[illegible]	-5142	-5360	-5471
3-3a	Thrust, lb/in.	37	77	110	140	183	201	2[illegible]	239	264	292
	Moment, in.-lb/in.	0.34	-0.20	-1.14	-2.21	-3.17	-3.61	-3.98	-4.25	-4.25	-4.11
2	Strain, μin./in.	262	525	708	934	1389	2529	3592	5162	6144	7240
	Stress, psi	2620	5111	5702	6100	6767	7512	8063	8822	9227	9683
2a	Strain, μin./in.	-31	-41	123	260	743	1754	2774	4255	5215	6664
	Stress, psi	-310	-410	1230	2600	5764	7057	7644	8389	8844	9446
2-2a	Thrust, lb/in.	75	157	256	325	411	474	511	560	587	622
	Moment, in.-lb/in.	-1.03	-1.99	-1.70	-1.16	-0.37	-0.15	-0.15	-0.15	-0.13	-0.08
4	Strain, μin./in.	199	399	487	612	1161	2288	3421	5113	6307	7890
	Stress, psi	1990	3990	4870	5498	6499	7380	7979	8802	9294	9951
4a	Strain, μin./in.	0	68	158	305	1028	2092	3019	4535	5496	6899
	Stress, psi	0	680	1580	3050	6265	7272	7776	8526	8959	9542
4-4a	Thrust, lb/in.	65	152	210	291	415	476	512	563	593	634
	Moment, in.-lb/in.	-0.70	-1.17	-1.16	-0.90	-0.08	-0.04	-0.07	-0.10	-0.12	-0.14
1-1a;3-3a	Avg thrust, lb/in.	40	90	161	237	285	300	317	341	363	386
2-2a;4-4a	Avg thrust, lb/in.	70	155	233	308	413	475	512	562	590	628
	q	0.57	0.58	0.69	0.77	0.69	0.63	0.62	0.61	0.62	0.61

Table 5.4

Strain, Stress, Thrust, Moment, and Deflection; Tests B-1A, B-1B, B-2, B-3, B-4, B-5

Gage	Measurement	Overpressure, psi 50	100	150	200	250	300	315	350	400	450	500
					Test B-1A (Z = 0 in.)							
1	Strain, μin./in.	177	322	257	144	16	-80					
	Stress, psi	1770	3220	2570	1440	160	-800					
1a	Strain, μin./in.	138	276	497	814	1173	1422					
	Stress, psi	1380	2760	4970	8140	11187	11861					
1-1a	Thrust, lb/in.	102	194	245	311	385	420					
	Moment, in.-lb/in.	-0.14	-0.16	0.84	2.36	4.04	4.83					
3	Strain, μin./in.	-49	-81	-65	-65	-32	-16					
	Stress, psi	-490	-810	-650	-650	-320	-160					
3a	Strain, μin./in.	106	185	278	385	491	544					
	Stress, psi	1060	1850	2780	3850	4910	5440					
3-3a	Thrust, lb/in.	19	34	69	104	149	172					
	Moment, in.-lb/in.	0.55	0.94	1.21	1.58	1.84	1.97					
2	Strain, μin./in.	112	205	280	410	560	672					
	Stress, psi	1120	2050	2800	4100	5600	6720					
2a	Strain, μin./in.	105	134	239	314	388	448					
	Stress, psi	1050	1340	2390	3140	3880	4480					
2-2a	Thrust, lb/in.	71	110	169	235	308	364					
	Moment, in.-lb/in.	-0.02	-0.25	-0.14	-0.34	-0.61	-0.79					
4	Strain, μin./in.	172	310	449	587	742	846					
	Stress, psi	1720	3100	4490	5870	7420	8460					
4a	Strain, μin./in.	40	79	158	211	264	290					
	Stress, psi	400	790	1580	2110	2640	2900					
4-4a	Thrust, lb/in.	69	126	197	259	327	369					
	Moment, in.-lb/in.	-0.46	-0.81	-1.02	-1.32	-1.68	-1.96					
DC1	Deflection, in.	0.013	0.019	0.022	0.028	0.035	0.035					
DC2	Deflection, in.	0	0.003	0.006	0.006	0.009	0.009					
1-1a:3-3a	Avg thrust, lb/in.	61	114	157	208	267	296					
2-2a:4-4a	Avg thrust, lb/in.	70	118	183	247	318	367					
	q	0.87	0.97	0.86	0.84	0.84	0.81					
					Test B-1B (Z = 0 in.)							
1	Strain, μin./in.	-76	-152	-281	-434	-628	-810	-945				
	Stress, psi	-760	-1520	-2810	-4340	-6280	-8100	-9450				
1a	Strain, μin./in.	243	527	889	1256	1705	--	--				
	Stress, psi	2430	5270	8890	11402	12049	--	--				
1-1a	Thrust, lb/in.	54	122	198	264	311	--	--				
	Moment, in.-lb/in.	1.12	2.39	4.12	5.84	7.15	--	--				
3	Strain, μin./in.	-35	-42	-49	-69	-97	-124	-131				
	Stress, psi	-350	-420	-490	-690	-970	-1240	-1310				
3a	Strain, μin./in.	109	212	316	453	515	611	625				
	Stress, psi	1090	2120	3160	4530	5150	6110	6250				
3-3a	Thrust, lb/in.	24	55	87	125	136	158	161				
	Moment, in.-lb/in.	0.51	0.89	1.29	1.84	2.15	2.59	2.66				
2	Strain, μin./in.	100	207	331	446	577	700	708				
	Stress, psi	1000	2070	3310	4460	5770	7000	7080				
2a	Strain, μin./in.	65	123	212	294	388	465	482				
	Stress, psi	650	1230	2120	2940	3880	4650	4820				
2-2a	Thrust, lb/in.	54	107	176	240	314	379	387				
	Moment, in.-lb/in.	-0.12	-0.30	-0.42	-0.54	-0.67	-0.83	-0.80				
4	Strain, μin./in.	115	257	379	494	629	744	751				
	Stress, psi	1150	2570	3790	4940	6290	7440	7510				
4a	Strain, μin./in.	41	116	185	247	316	384	391				
	Stress, psi	410	1160	1850	2470	3160	3840	3910				
4-4a	Thrust, lb/in.	51	121	183	241	307	367	371				
	Moment, in.-lb/in.	-0.26	-0.50	-0.68	-0.87	-1.10	-1.27	-1.27				
DC1	Deflection, in.	0.007	0.017	0.023	0.027	0.033	0.044	0.047				
DC2	Deflection, in.	0.003	0.004	0.007	0.013	0.016	0.016	0.016				
1-1a:3-3a	Avg thrust, lb/in.	39	89	143	195	224	--	--				
2-2a:4-4a	Avg thrust, lb/in.	53	114	180	241	311	373	379				
	q	0.74	0.78	0.79	0.81	0.72	--	--				
					Test B-5 (Z = 7/16 in.)							
1	Strain, μin./in.	150	326	421	434	365	258		129	0	-141	-369
	Stress, psi	1500	3260	4210	4340	3650	2580		1290	0	-1410	-3690
1a	Strain, μin./in.	72	--	--	--	--	--		--	--	--	--
	Stress, psi	720	--	--	--	--	--		--	--	--	--
1-1a	Thrust, lb/in.	72	--	--	--	--	--		--	--	--	--
	Moment, in.-lb/in.	-0.27	--	--	--	--	--		--	--	--	--
3	Strain, μin./in.	-67	-108	-83	-67	-62	-71		-71	-79	-79	-117
	Stress, psi	-670	-1080	-830	-670	-620	-710		-710	-790	-790	-1170
3a	Strain, μin./in.	212	299	414	503	585	673		789	908	1019	1129
	Stress, psi	2120	2990	4140	5030	5850	6730		7890	9080	10190	11074
3-3a	Thrust, lb/in.	47	62	108	142	170	196		233	269	305	329
	Moment, in.-lb/in.	0.98	1.43	1.75	2.01	2.28	2.62		3.03	3.48	3.87	4.38
2	Strain, μin./in.	118	190	262	338	445	545		658	777	894	1040
	Stress, psi	1180	1900	2620	3380	4450	5450		6580	7770	8940	10400
2a	Strain, μin./in.	36	98	166	232	323	417		515	684	736	1011
	Stress, psi	360	980	1660	2320	3230	4170		5150	6840	7360	10110
2-2a	Thrust, lb/in.	50	94	139	185	250	313		381	455	530	667
	Moment, in.-lb/in.	-0.29	-0.32	-0.34	-0.37	-0.43	-0.45		-0.50	-0.54	-0.56	-0.10
4	Strain, μin./in.	99	165	264	343	475	587		734	861	1082	1663
	Stress, psi	990	1650	2640	3430	4750	5870		7340	8610	10820	12031
4a	Strain, μin./in.	68	103	176	239	380	397		483	569	699	1066
	Stress, psi	680	1030	1760	2390	3800	3970		4830	5690	6990	10660
4-4a	Thrust, lb/in.	54	87	143	189	258	380		396	465	546	755
	Moment, in.-lb/in.	-0.11	-0.22	-0.31	-0.37	-0.55	-0.67		-0.88	-1.03	-1.28	-0.44
DC1	Deflection, in.	0.004	0.006	0.008	0.011	0.015	0.019		0.024	0.029	0.036	0.051
DC2	Deflection, in.	0.001	0.002	0.003	0.004	0.006	0.008		0.010	0.013	0.015	0.018
1-1a:3-3a	Avg thrust, lb/in.	60	--	--	--	--	--		--	--	--	--
2-2a:4-4a	Avg thrust, lb/in.	52	91	141	187	254	317		389	460	538	711
	q	1.15	--	--	--	--	--		--	--	--	--

(Continued)

Table 5.4 (Concluded)

Gage	Measurement	50	100	150	200	250	300	315	350	400	450	500
						Overpressure, psi						
					Test B-2 (Z = 7/8 in.)							
1	Strain, μin./in.	65	158	201	208	201	187		158	129	100	43
	Stress, psi	650	1580	2010	2080	2010	1870		1580	1290	1000	430
1a	Strain, μin./in.	22	111	244	377	544	710		899	1071	1270	1457
	Stress, psi	220	1110	2440	3770	5440	7100		8990	10710	11440	11941
1-1a	Thrust, lb/in.	28	87	145	190	242	292		344	390	439	466
	Moment, in.-lb/in.	-0.15	-0.17	0.15	0.60	1.21	1.84		2.61	3.32	3.94	4.40
3	Strain, μin./in.	-51	-32	-6	6	13	6		0	-12	-32	-45
	Stress, psi	-510	-320	-60	60	130	60		0	-120	-320	-450
3a	Strain, μin./in.	164	272	369	451	563	653		787	910	1040	1158
	Stress, psi	1640	2720	3690	4510	5630	6530		7870	9100	10400	11149
3-3a	Thrust, lb/in.	37	78	118	149	187	214		256	292	328	361
	Moment, in.-lb/in.	0.76	1.07	1.32	1.57	1.94	2.28		2.77	3.25	3.77	4.21
2	Strain, μin./in.	187	315	460	581	737	862		1008	1152	1321	1923
	Stress, psi	1870	3150	4600	5810	7370	8620		10080	11133	11581	12145
2a	Strain, μin./in.	14	75	136	186	254	308		351	455	573	1070
	Stress, psi	140	750	1360	1860	2540	3080		3510	4550	5730	10700
2-2a	Thrust, lb/in.	65	127	194	249	322	380		442	521	600	764
	Moment, in.-lb/in.	-0.61	-0.84	-1.14	-1.39	-1.70	-1.95		-2.31	-2.43	-2.22	-0.43
4	Strain, μin./in.	101	191	303	397	529	633		759	880	1044	1764
	Stress, psi	1010	1910	3030	3970	5290	6330		7590	8800	10440	12075
4a	Strain, μin./in.	34	103	168	229	306	367		443	516	611	928
	Stress, psi	340	1030	1680	2290	3060	3670		4430	5160	6110	9280
4-4a	Thrust, lb/in.	44	96	153	203	271	325		391	454	538	741
	Moment, in.-lb/in.	-0.24	-0.31	-0.48	-0.59	-0.79	-0.94		-1.11	-1.28	-1.52	-0.82
DC1	Deflection, in.	0.007	0.009	0.011	0.014	0.019	0.023		0.026	0.030	0.035	0.043
DC2	Deflection, in.	0.001	0.001	0.002	0.004	0.007	0.009		0.013	0.015	0.017	0.019
1-1a:3-3a	Avg thrust, lb/in.	33	83	132	170	215	253		300	341	384	414
2-2a:4-4a	Avg thrust, lb/in.	55	112	174	226	297	353		417	488	569	753
	q	0.60	0.74	0.76	0.75	0.72	0.72		0.72	0.70	0.67	0.55
					Test B-3 (Z = 1-3/4 in.)							
1	Strain, μin./in.	7	48	75	82	82	75		65	61	41	27
	Stress, psi	70	480	750	820	820	750		650	610	410	270
1a	Strain, μin./in.	103	192	274	378	494	603		722	819	944	1055
	Stress, psi	1030	1920	2740	3780	4940	6030		7220	8190	9440	10550
1-1a	Thrust, lb/in.	36	78	113	149	187	220		256	286	320	352
	Moment, in.-lb/in.	0.34	0.51	0.70	1.04	1.45	1.86		2.31	2.67	3.18	3.62
3	Strain, μin./in.	-44	-44	-35	-35	-41	-61		-83	-104	-130	-148
	Stress, psi	-440	-440	-350	-350	-410	-610		-830	-1040	-1300	-1480
3a	Strain, μin./in.	153	270	364	452	561	670		773	899	1033	1156
	Stress, psi	1530	2700	3640	4520	5610	6700		7730	8990	10330	11144
3-3a	Thrust, lb/in.	35	73	107	136	169	198		224	258	293	327
	Moment, in.-lb/in.	0.69	1.11	1.40	1.71	2.12	2.57		3.01	3.53	4.09	4.57
2	Strain, μin./in.	158	268	365	461	574	671		768	877	992	1183
	Stress, psi	1580	2680	3650	4610	5740	6710		7680	8770	9920	11213
2a	Strain, μin./in.	10	69	121	178	243	302		374	446	515	679
	Stress, psi	100	690	1210	1780	2430	3020		3740	4460	5150	6790
2-2a	Thrust, lb/in.	55	110	158	208	266	316		371	430	490	602
	Moment, in.-lb/in.	-0.52	-0.70	-0.86	-1.00	-1.17	-1.30		-1.39	-1.52	-1.68	-1.68
4	Strain, μin./in.	218	371	502	625	775	897		1040	1153	1209	1179
	Stress, psi	2180	3710	5020	6250	7750	8970		10400	11136	11280	11203
4a	Strain, μin./in.	-32	-8	18	58	100	142		187	261	409	736
	Stress, psi	-320	-80	180	580	1000	1420		1870	2610	4090	7360
4-4a	Thrust, lb/in.	60	118	169	222	284	338		399	459	522	619
	Moment, in.-lb/in.	-0.88	-1.33	-1.70	-2.00	-2.38	-2.66		-3.00	-3.12	-2.71	-1.46
DC1	Deflection, in.	0.005	0.008	0.010	0.013	0.016	0.019		0.023	0.026	0.030	0.035
DC2	Deflection, in.	0.004	0.007	0.010	0.011	0.012	0.014		0.016	0.019	0.021	0.024
1-1a:3-3a	Avg thrust, lb/in.	36	76	110	143	178	209		240	272	307	340
2-2a:4-4a	Avg thrust, lb/in.	58	114	164	215	275	327		385	445	506	611
	q	0.62	0.67	0.67	0.67	0.65	0.64		0.62	0.61	0.61	0.56
					Test B-4 (Z = 2-5/8 in.)							
1	Strain, μin./in.	-49	-36	-4	29	60	78		98	111	122	111
	Stress, psi	-490	-360	-40	290	600	780		980	1110	1220	1110
1a	Strain, μin./in.	129	215	305	399	506	610		735	854	988	1111
	Stress, psi	1290	2150	3050	3990	5060	6100		7350	8540	9880	11028
1-1a	Thrust, lb/in.	26	58	98	139	184	224		271	314	361	407
	Moment, in.-lb/in.	0.63	0.88	1.09	1.30	1.57	1.87		2.24	2.62	3.05	3.52
3	Strain, μin./in.	-130	-177	-194	-203	-212	-227		-252	-279	-303	-325
	Stress, psi	-1300	-1770	-1940	-2030	-2120	-2270		-2520	-2790	-3030	-3250
3a	Strain, μin./in.	191	300	391	468	552	631		736	846	970	1054
	Stress, psi	1910	3000	3910	4680	5520	6310		7360	8460	9700	10540
3-3a	Thrust, lb/in.	20	40	64	86	110	131		157	184	217	237
	Moment, in.-lb/in.	1.13	1.68	2.06	2.36	2.69	3.02		3.48	3.96	4.48	4.86
2	Strain, μin./in.	174	278	370	453	555	651		765	873	1008	1108
	Stress, psi	1740	2780	3700	4530	5550	6510		7650	8730	10080	11021
2a	Strain, μin./in.	-22	26	97	178	265	344		440	537	645	946
	Stress, psi	-220	260	970	1780	2650	3440		4400	5370	6450	9460
2-2a	Thrust, lb/in.	49	99	152	205	266	323		392	458	537	607
	Moment, in.-lb/in.	-0.69	-0.89	-0.96	-0.97	-1.02	-1.08		-1.14	-1.18	-1.28	-0.57
4	Strain, μin./in.	219	361	494	617	761	890		1042	1189	1337	1480
	Stress, psi	2190	3610	4940	6170	7610	8900		10420	11228	11686	11951
4a	Strain, μin./in.	-50	-43	-17	15	54	93		137	193	283	422
	Stress, psi	-500	-430	-170	150	540	930		1370	1930	2830	4220
4-4a	Thrust, lb/in.	55	103	155	205	265	319		383	447	514	585
	Moment, in.-lb/in.	-0.95	-1.42	-1.80	-2.12	-2.49	-2.81		-3.19	-3.45	-3.36	-2.98
DC1	Deflection, in.	0.009	0.014	0.017	0.020	0.023	0.026		0.030	0.034	0.039	0.044
DC2	Deflection, in.	0.006	0.008	0.010	0.012	0.014	0.016		0.018	0.020	0.021	0.023
1-1a:3-3a	Avg thrust, lb/in.	23	49	[illegible]	113	147	178		214	249	289	317
2-2a:4-4a	Avg thrust, lb/in.	52	101	154	205	266	321		388	453	526	626
	q	0.44	0.49	0.53	0.55	0.55	0.55		0.55	0.55	0.55	0.51

Table 5.5

Strain, Stress, Thrust, and Moment; Tests B-6, B-7, B-8, B-9, B-10

Gage	Measurement	Overpressure, psi 50	100	150	200	250	300	350	400	450	500
					Test B-6 (Z = 0 in.)						
1	Strain, μin./in.	-239	207	414	233	-65	-174	-498	--		
	Stress, psi	-2390	2070	4140	2330	-650	-1740	-4980	--		
1a	Strain, μin./in.	349	244	232	791	1385	1699	2665	6471		
	Stress, psi	3490	[illegible]	2320	7910	11758	12047	12069	13050		
1-1a	Thrust, lb/in	36	[illegible]	210	333	416	448	486	--		
	Moment, in.-lb/in.	2.07	0.13	-0.64	1.96	4.73	5.36	6.30	--		
3	Strain, μin./in.	-54	123	208	216	189	185	162	131		
	Stress, psi	-540	1230	2080	2160	1890	1850	1620	1310		
3a	Strain, μin./in.	144	220	275	372	508	613	723	785		
	Stress, psi	1440	2200	2750	3720	5080	6130	7230	7850		
3-3a	Thrust, lb/in.	29	111	157	191	225	259	288	298		
	Moment, in.-lb/in.	0.70	0.34	0.24	0.55	1.10	1.51	1.98	2.30		
2	Strain, μin./in.	257	383	494	646	877	998	1167	1230		
	Stress, psi	2570	3830	4940	6460	8770	9980	11172	11334		
2a	Strain, μin./in.	-45	13	108	240	336	399	463	527		
	Stress, psi	-450	130	1080	2400	3360	3990	4630	5270		
2-2a	Thrust, lb/in.	69	129	196	288	394	454	528	565		
	Moment, in.-lb/in.	-1.06	-1.30	-1.36	-1.43	-1.90	-2.11	-2.43	-2.31		
4	Strain, μin./in.	239	301	371	446	597	729	823	880		
	Stress, psi	2390	3010	3710	4460	5970	7290	8230	8800		
4a	Strain, μin./in.	-16	63	158	222	285	364	459	523		
	Stress, psi	-160	630	1580	2220	2850	3640	4590	5230		
4-4a	Thrust, lb/in.	72	118	172	217	287	355	417	496		
	Moment, in.-lb/in.	-0.90	-0.84	-0.75	-0.79	-1.10	-1.29	-1.28	-1.26		
1-1a;3-3a	Avg thrust, lb/in.	33	129	184	262	321	354	387	--		
2-2a;4-4a	Avg thrust, lb/in.	71	124	184	253	341	405	473	511		
	q	0.46	1.04	1.00	1.04	0.94	0.87	0.82	--		
					Test B-7 (Z = 7/16 in.)						
1	Strain, μin./in.	-145	294	641	716	641	558	484	448	388	277
	Stress, psi	-1450	2940	6410	7160	6410	5580	4840	4480	3880	2770
1a	Strain, μin./in.	247	175	111	247	455	671	878	1062	1342	1605
	Stress, psi	2470	1750	1110	2470	4550	6710	8780	10620	11639	12006
1-1a	Thrust, lb/in.	33	152	244	313	356	399	443	491	547	564
	Moment, in.-lb/in.	1.38	-0.42	-1.87	-1.65	-0.65	0.40	1.39	2.61	2.96	3.53
3	Strain, μin./in.	21	218	367	449	502	530	590	606	652	700
	Stress, psi	210	2180	3670	4490	5020	5300	5900	6060	6520	7000
3a	Strain, μin./in.	145	154	179	218	273	350	393	466	539	599
	Stress, psi	1450	1540	1790	2180	2730	3500	3930	4660	5390	5990
3-3a	Thrust, lb/in.	54	121	177	217	252	286	319	348	387	422
	Moment, in.-lb/in.	0.44	-0.25	-0.66	-0.81	-0.81	-0.63	-0.69	-0.49	-0.40	-0.36
2	Strain, μin./in.	259	338	413	562	702	911	996	1128	1303	1410
	Stress, psi	2590	3380	4130	5620	7020	9110	9960	11072	11532	11827
2a	Strain, μin./in.	-8	50	128	211	294	394	444	531	614	701
	Stress, psi	-80	500	1280	2110	2940	3940	4440	5310	6140	7010
2-2a	Thrust, lb/in.	82	124	176	251	324	424	468	539	609	654
	Moment, in.-lb/in.	-0.94	-0.99	-1.00	-1.24	-1.44	-1.82	-1.94	-2.09	-2.05	-1.75
4	Strain, μin./in.	298	310	423	586	695	893	1007	1168	1338	1444
	Stress, psi	2980	3100	4230	5860	6950	8930	10070	11175	11612	11944
4a	Strain, μin./in.	10	103	186	270	354	437	566	605	709	904
	Stress, psi	100	1030	1860	2700	3540	4370	5660	6050	7090	9040
4-4a	Thrust, lb/in.	87	134	198	259	341	432	498	574	641	717
	Moment, in.-lb/in.	-0.87	-0.73	-0.83	-0.90	-1.20	-1.61	-1.69	-0.92	-1.71	-0.85
1-1a;3-3a	Avg thrust, lb/in.	44	137	211	265	304	343	381	420	467	493
2-2a;4-4a	Avg thrust, lb/in.	85	129	187	255	333	428	483	557	625	686
	q	0.52	1.06	1.13	1.04	0.91	0.80	0.79	0.75	0.75	0.72
					Test B-8 (Z = 7/8 in.)						
1	Strain, μin./in.	-97	137	292	369	366	362	356	349	319	[illegible]
	Stress, psi	-970	1370	2920	3690	3660	3620	3560	3490	3190	[illegible]
1a	Strain, μin./in.	261	251	348	449	683	784	968	--	--	--
	Stress, psi	2610	2510	3480	4490	6830	7840	9680	--	--	--
1-1a	Thrust, lb/in.	53	186	208	265	381	378	484	--	--	--
	Moment, in.-lb/in.	1.36	0.40	0.30	0.27	0.90	1.49	2.98	--	--	--
3	Strain, μin./in.	283	995	979	1172	1364	--	--	--	--	--
	Stress, psi	2830	9950	9790	11185	11700	--	--	--	--	--
3a	Strain, μin./in.	-66	-287	-417	-474	--	--	--	--	--	-684
	Strain, psi	-660	-2870	-4170	-4740	--	--	--	--	--	-6840
3-3a	Thrust, lb/in.	51	107	183	286	--	--	--	--	--	--
	Moment, in.-lb/in.	-1.08	-2.75	-4.32	-5.77	--	--	--	--	--	--
2	Strain, μin./in.	218	385	468	539	700	824	997	1159	1289	1395
	Stress, psi	2180	3850	4680	5390	7000	8240	9970	11151	11432	[illegible]
2a	Strain, μin./in.	16	80	209	297	373	459	546	659	685	908
	Stress, psi	160	800	2090	2970	3730	4590	5460	6590	6850	9080
2-2a	Thrust, lb/in.	76	132	206	272	349	420	501	389	614	783
	Moment, in.-lb/in.	-0.71	-0.86	-0.79	-0.85	-1.15	-1.38	-1.39	-1.71	-1.86	-0.93
4	Strain, μin./in.	173	259	330	416	398	607	778	988	1014	1173
	Stress, psi	1730	2590	3300	4160	3980	6070	7780	9880	10140	11449
4a	Strain, μin./in.	17	106	199	271	351	415	479	363	589	716
	Stress, psi	170	1060	1990	2710	3510	4150	4790	3630	5890	7160
4-4a	Thrust, lb/in.	62	119	178	223	306	360	409	465	521	633
	Moment, in.-lb/in.	-0.96	-0.94	-0.46	-0.51	-0.65	-0.85	-1.09	-1.29	-1.30	-1.63
1-1a;3-3a	Avg thrust, lb/in.	52	117	196	246	--	--	--	--	--	--
2-2a;4-4a	Avg thrust, lb/in.	69	186	189	248	328	384	495	537	568	688
	q	0.75	0.98	1.04	0.99	--	--	--	--	--	--

(Continued)

Table 5.5 (Concluded)

Gage	Measurement	Overpressure, psi 50	100	150	200	250	300	350	400	450	500
					Test B-9 (Z = 1-3/4 in.)						
1	Strain, µin./in.	-89	14	107	160	189	192	204	249	289	253
	Stress, psi	-890	140	1070	1640	1890	1920	2040	2490	2890	2530
1a	Strain, µin./in.	261	483	495	681	711	808	936	1068	1188	1287
	Stress, psi	2610	4830	4950	6810	7110	8080	9360	10680	11886	11470
1-1a	Thrust, lb/in.	56	142	196	255	292	331	377	426	478	493
	Moment, in.-lb/in.	1.83	1.44	1.37	1.61	1.84	2.24	2.51	2.86	3.10	3.41
3	Strain, µin./in.	-69	-9	58	180	172	180	215	258	283	292
	Stress, psi	-690	-90	580	1800	1720	1800	2150	2580	2830	2920
3a	Strain, µin./in.	208	330	380	466	531	617	696	789	890	980
	Stress, psi	2080	3300	3800	4660	5310	6170	6960	7890	8900	9800
3-3a	Thrust, lb/in.	45	104	140	190	228	259	296	340	381	413
	Moment, in.-lb/in.	0.98	1.19	1.15	1.22	1.26	1.54	1.69	1.87	2.14	2.42
2	Strain, µin./in.	209	379	486	608	770	876	1091	1163	1328	1485
	Stress, psi	2090	3790	4860	6080	7700	8760	10910	11168	11601	11953
2a	Strain, µin./in.	63	198	288	379	459	519	607	713	806	911
	Stress, psi	630	1980	2880	3790	4590	5190	6070	7130	8060	9110
2-2a	Thrust, lb/in.	88	188	250	327	399	453	552	608	670	717
	Moment, in.-lb/in.	-0.52	-0.64	-0.72	-0.88	-1.09	-1.26	-1.70	-1.52	-1.29	-0.91
4	Strain, µin./in.	211	384	487	648	776	885	1049	1163	1334	1436
	Stress, psi	2110	3840	4870	6480	7760	8890	10490	11168	11617	11899
4a	Strain, µin./in.	41	149	235	307	397	461	551	683	723	949
	Stress, psi	410	1490	2350	3070	3970	4610	5510	6830	7230	9490
4-4a	Thrust, lb/in.	82	173	228	310	381	437	520	579	647	720
	Moment, in.-lb/in.	-0.60	-0.83	-0.82	-1.20	-1.33	-1.49	-1.75	-1.85	-1.63	-0.74
1-1a&3-3a	Avg thrust, lb/in.	51	123	168	223	260	295	337	383	430	453
2-2a&4-4a	Avg thrust, lb/in.	85	181	239	319	390	445	536	594	659	719
	q	0.60	0.68	0.70	0.70	0.67	0.66	0.63	0.57	0.65	0.63
					Test B-10 (Z = 2-5/8 in.)						
1	Strain, µin./in.	-113	-87	35	89	116	134	148	169	184	177
	Stress, psi	-1130	-870	350	890	1160	1340	1480	1690	1840	1770
1a	Strain, µin./in.	199	351	442	548	648	748	837	950	1065	1178
	Stress, psi	1990	3510	4420	5480	6480	7480	8370	9500	10650	11200
1-1a	Thrust, lb/in.	28	98	155	205	246	285	320	364	406	439
	Moment, in.-lb/in.	1.10	1.47	1.43	1.59	1.85	2.14	2.43	2.75	3.10	3.48
3	Strain, µin./in.	-67	-86	-45	-4	88	30	37	56	67	82
	Stress, psi	-670	-860	-450	-40	880	300	370	560	670	820
3a	Strain, µin./in.	186	344	397	450	541	638	708	814	989	1080
	Stress, psi	1860	3440	3970	4500	5410	6380	7080	8140	9890	10800
3-3a	Thrust, lb/in.	39	84	114	145	183	215	242	283	324	358
	Moment, in.-lb/in.	0.85	1.51	1.56	1.60	1.88	2.12	2.36	2.67	3.08	3.30
2	Strain, µin./in.	214	411	546	636	764	913	1078	1200	1349	1488
	Stress, psi	2140	4110	5460	6360	7640	9130	10780	11257	11659	11955
2a	Strain, µin./in.	4	114	218	290	376	468	527	689	719	830
	Stress, psi	40	1140	2180	2900	3760	4680	5270	6890	7190	8300
2-2a	Thrust, lb/in.	71	171	248	321	370	447	580	590	648	698
	Moment, in.-lb/in.	-0.74	-1.05	-1.15	-1.22	-1.37	-1.59	-1.58	-1.89	-1.65	-1.34
4	Strain, µin./in.	204	438	573	687	858	979	1086	1285	1412	1537
	Stress, psi	2040	4380	5730	6870	8580	9790	10860	12480	11833	11976
4a	Strain, µin./in.	-13	96	138	198	276	334	410	488	570	643
	Stress, psi	-130	960	1380	1980	2760	3340	4100	4880	5700	6430
4-4a	Thrust, lb/in.	62	161	231	281	360	427	486	566	616	687
	Moment, in.-lb/in.	-0.76	-1.34	-1.53	-1.68	-1.96	-2.26	-2.38	-2.58	-2.29	-2.01
1-1a&3-3a	Avg thrust, lb/in.	34	91	135	175	215	250	281	324	365	399
2-2a&4-4a	Avg thrust, lb/in.	67	166	240	291	365	437	509	578	632	693
	q	0.51	0.53	0.56	0.60	0.59	0.57	0.56	0.56	0.58	0.59

Table 5.6

Strain, Stress, Thrust, Moment, and Deflection; Tests C-1, C-2, C-3, C-4, C-5

Gage	Measurement	Overpressure, psi													
		25	50	75	95	100	150	195	200	250	300	350	400	450	500
						Test C-1 (Z = 0 in.)									
1	Strain, μin./in.	159	634	--	--										
	Stress, psi	1590	6340	--	--										
1a	Strain, μin./in.	170	156	71	-453										
	Stress, psi	1700	1560	710	-4530										
1-1a	Thrust, lb/in.	36	87	--	--										
	Moment, in.-lb/in.	0.00	-0.19	--	--										
3	Strain, μin./in.	268	470	616	739										
	Stress, psi	2680	4700	6160	7390										
3a	Strain, μin./in.	-69	-106	-119	-125										
	Strain, psi	-690	-1060	-1190	-1250										
3-3a	Thrust, lb/in.	21	40	55	68										
	Moment, in.-lb/in.	-0.13	-0.23	-0.30	-0.35										
2	Strain, μin./in.	125	234	334	450										
	Stress, psi	1250	2340	3340	4500										
2a	Strain, μin./in.	48	121	205	320										
	Stress, psi	480	1210	2050	3200										
2-2a	Thrust, lb/in.	19	39	59	85										
	Moment, in.-lb/in.	-0.03	-0.05	-0.05	-0.05										
4	Strain, μin./in.	159	273	387	470										
	Stress, psi	1590	2730	3870	4700										
4a	Strain, μin./in.	24	62	110	153										
	Stress, psi	240	620	1100	1530										
4-4a	Thrust, lb/in.	20	37	55	69										
	Moment, in.-lb/in.	-0.05	-0.09	-0.11	-0.13										
DC1	Deflection, in.	0.003	-0.003	-0.008	-0.015										
DC2	Deflection, in.	0.003	0.003	0.003	0.009										
1-1a:3-3a	Avg thrust, lb/in.	29	64	--	--										
2-2a:4-4a	Avg thrust, lb/in.	20	38	57	77										
	q	1.45	1.68	--	--										
						Test C-4 (Z = 3/16 in.)									
1	Strain, μin./in.		491			1087	1604	1909							
	Stress, psi		4910			10870	16040	19090							
1a	Strain, μin./in.		185			308	493	822							
	Stress, psi		1850			3080	4930	8220							
1-1a	Thrust, lb/in.		74			[illegible]	231	300							
	Moment, in.-lb/in.		-0.12			-0.31	-0.45	-0.44							
3	Strain, μin./in.		352			519	686	760							
	Stress, psi		3520			5190	6860	7600							
3a	Strain, μin./in.		-179			-159	-80	20							
	Stress, psi		-1790			-1590	-800	200							
3-3a	Thrust, lb/in.		19			40	67	86							
	Moment, in.-lb/in.		-0.21			-0.27	-0.31	-0.30							
2	Strain, μin./in.		155			311	486	668							
	Stress, psi		1550			3110	4860	6680							
2a	Strain, μin./in.		263			326	790	1044							
	Stress, psi		2630			3260	7900	10440							
2-2a	Thrust, lb/in.		64			92	140	186							
	Moment, in.-lb/in.		0.04			0.09	0.12	0.14							
4	Strain, μin./in.		283			542	817	1085							
	Stress, psi		2830			5420	8170	10850							
4a	Strain, μin./in.		284			483	750	1084							
	Stress, psi		2840			4830	7500	10840							
4-4a	Thrust, lb/in.		56			113	172	232							
	Moment, in.-lb/in.		-0.08			-0.08	-0.03	-0.08							
DC1	Deflection, in.		0.004			0.006	0.008	0.013							
DC2	Deflection, in.		0.000			-0.001	-0.001	-0.001							
1-1a:3-3a	Avg thrust, lb/in.		47			97	148	193							
2-2a:4-4a	Avg thrust, lb/in.		51			103	156	209							
	q		0.92			0.94	0.94	0.92							
						Test C-5 (Z = 5/16 in.)									
1	Strain, μin./in.		483			981	1344		1639	1893	2104	2390	2485	2535	2977
	Stress, psi		4830			9810	13440		16390	18930	21040	23900	24850	25350	29770
1a	Strain, μin./in.		115			186	394		601	987	1319	1704	2210	2700	--
	Stress, psi		1150			1860	3940		6010	9870	13190	17040	22100	27000	--
1-1a	Thrust, lb/in.		59			122	167		246	311	377	446	510	376	--
	Moment, in.-lb/in.		-0.12			-0.30	-0.40		-0.42	-0.39	-0.38	-0.21	-0.09	0.07	--
3	Strain, μin./in.		184			349	477		751	661	789	973	1102	1282	1359
	Stress, psi		1840			3490	4770		7510	6610	7890	9730	11020	12820	13590
3a	Strain, μin./in.		97			235	380		323	682	898	996	1190	1356	1582
	Stress, psi		970			2350	3800		3230	6820	8980	9960	11900	13560	15820
3-3a	Thrust, lb/in.		31			64	92		119	151	181	217	232	256	317
	Moment, in.-lb/in.		-0.04			-0.05	-0.05		-0.01	0.01	0.05	0.01	0.14	0.06	0.07
2	Strain, μin./in.		258			514	771		1046	1388	1487	1949	2231	2569	--
	Stress, psi		2580			5140	7710		10460	13880	14870	19490	22310	25690	--
2a	Strain, μin./in.		185			309	330		776	1094	1331	1494	1994	2247	--
	Stress, psi		1850			3090	3300		7760	10940	13310	14940	19940	22470	--
2-2a	Thrust, lb/in.		62			91	143		220	282	329	394	477	507	--
	Moment, in.-lb/in.		-0.09			-0.08	-0.10		-0.11	-0.11	-0.12	-0.13	-0.12	-0.12	--
4	Strain, μin./in.		119			279	456		693	880	1137	1482	1692	1977	2264
	Stress, psi		1190			2790	4560		6930	8800	11370	14820	16920	19770	22640
4a	Strain, μin./in.		96			206	351		515	697	889	1105	1302	1593	1733
	Stress, psi		960			2060	3510		5150	6970	8890	11050	13020	15930	17330
4-4a	Thrust, lb/in.		25			53	89		129	174	223	278	329	385	445
	Moment, in.-lb/in.		-0.01			-0.03	-0.04		-0.06	-0.07	-0.10	-0.13	-0.16	-0.18	-0.22
DC1	Deflection, in.		0.000			0.000	0.001		0.004	0.008	0.013	0.019	0.025	0.031	0.038
DC2	Deflection, in.		0.001			0.000	-0.001		0.000	0.002	0.006	0.008	0.010	0.013	0.015
1-1a:3-3a	Avg thrust, lb/in.		45			92	140		182	231	279	331	381	431	--
2-2a:4-4a	Avg thrust, lb/in.		33			72	116		165	218	274	336	393	446	--
	q		1.39			1.28	1.20		1.11	1.06	1.02	0.99	0.97	0.95	--

(Continued)

Table 5.6 (Concluded)

Gage	Measurement	25	50	75	95	100	150	195	200	250	300	350	400	450	500
							Overpressure, psi								
	Test C-2 (Z = 7/16 in.)														
1	Strain, μin./in.		426			694	888		1034	1120	1180	1193	1217	1266	1290
	Stress, psi		4260			6940	8880		10340	11200	11800	11930	12170	12660	12900
1a	Strain, μin./in.		14			98	265		460	711	1018	1408	1798	2245	2717
	Stress, psi		140			980	2650		4600	7110	10180	14080	17980	22450	27170
1-1a	Thrust, lb/in.		46			87	127		164	201	242	286	332	386	441
	Moment, in.-lb/in.		-0.17			-0.24	-0.25		-0.23	-0.16	-0.07	0.09	0.23	0.39	0.58
3	Strain, μin./in.		31			107	176		267	351	443	550	642	779	909
	Stress, psi		310			1070	1760		2670	3510	4430	5500	6420	7790	9090
3a	Strain, μin./in.		302			480	647		801	964	1154	1369	1566	1811	2032
	Stress, psi		3020			4800	6470		8010	9640	11540	13690	15660	18110	20320
3-3a	Thrust, lb/in.		37			65	91		117	145	176	211	243	285	324
	Moment, in.-lb/in.		0.11			0.15	0.19		0.22	0.25	0.29	0.33	0.37	0.42	0.45
2	Strain, μin./in.		83			158	253		372	515	669	847	1052	1332	1640
	Stress, psi		830			1580	2530		3720	5150	6690	8470	10520	13320	16400
2a	Strain, μin./in.		75			133	195		270	373	489	616	763	982	1200
	Stress, psi		750			1330	1950		2700	3730	4890	6160	7630	9820	12000
2-2a	Thrust, lb/in.		17			32	49		71	98	127	161	200	255	312
	Moment, in.-lb/in.		0.0			-0.01	-0.02		-0.04	-0.06	-0.07	-0.09	-0.12	-0.14	-0.18
4	Strain, μin./in.		100			177	269		380	507	645	799	971	1207	1444
	Stress, psi		1000			1770	2690		3800	5070	6450	7990	9710	12070	14440
4a	Strain, μin./in.		118			243	390		544	726	909	1104	1312	1581	1840
	Stress, psi		1180			2430	3900		5440	7260	9090	11040	13120	15810	18400
4-4a	Thrust, lb/in.		24			46	72		102	136	171	209	251	307	361
	Moment, in.-lb/in.		0.01			0.03	0.05		0.07	0.09	0.11	0.12	0.14	0.15	0.16
DC1	Deflection, in.		0.002			0.003	0.006		0.011	0.015	0.021	0.027	0.031	0.037	0.044
DC2	Deflection, in.		0.001			0.001	0.001		0.003	0.005	0.007	0.010	0.011	0.013	0.015
1-1a;3-3a	Avg thrust, lb/in.		42			76	109		141	173	209	249	288	336	383
2-2a;4-4a	Avg thrust, lb/in.		21			39	61		87	117	149	185	226	281	337
	q		2.00			2.00	1.79		1.62	1.48	1.40	1.35	1.27	1.20	1.14
	Test C-3 (Z = 7/8 in.)														
1	Strain, μin./in.		243			503	694		902	1058	1180	1388	1562	1701	1857
	Stress, psi		2430			5030	6940		9020	10580	11800	13880	15620	17010	18570
1a	Strain, μin./in.		196			413	708		925	1181	1457	1673	1915	2209	2404
	Stress, psi		1960			4130	7080		9250	11810	14570	16730	19150	22090	24040
1-1a	Thrust, lb/in.		48			101	154		201	246	290	337	382	430	469
	Moment, in.-lb/in.		-0.02			-0.04	0.01		0.01	0.05	0.11	0.11	0.14	0.20	0.22
3	Strain, μin./in.		863			1654	2257		--	--	--	--	--	--	--
	Stress, psi		8630			16540	22570		--	--	--	--	--	--	--
3a	Strain, μin./in.		-445			-891	-1270		-1644	-1987	-2317	--	--	--	--
	Stress, psi		-4450			-8910	-12700		-16440	-19870	-23170	--	--	--	--
3-3a	Thrust, lb/in.		46			84	109		--	--	--	--	--	--	--
	Moment, in.-lb/in.		-0.53			-1.03	-1.42		--	--	--	--	--	--	--
2	Strain, μin./in.		223			416	616		880	1046	1298	1582	1839	--	--
	Stress, psi		2230			4160	6160		8800	10460	12980	15820	18390	--	--
2a	Strain, μin./in.		57			188	352		584	733	969	1237	1479	1771	2034
	Stress, psi		570			1880	[illegible]		5840	7330	9690	12370	14790	17710	20340
2-2a	Thrust, lb/in.		31			66	106		148	196	249	310	365	--	--
	Moment, in.-lb/in.		-0.07			-0.09	-0.11		-0.12	-0.13	-0.13	-0.14	-0.15	--	--
4	Strain, μin./in.		239			433	611		801	1019	1237	1493	1723	1976	2217
	Stress, psi		2390			4330	6110		8010	10190	12370	14930	17230	19760	22170
4a	Strain, μin./in.		4			96	286		377	561	754	984	1190	1437	1667
	Stress, psi		40			960	2860		3770	5610	7540	9840	11900	14370	16670
4-4a	Thrust, lb/in.		27			58	98		130	174	219	272	320	375	427
	Moment, in.-lb/in.		-0.09			-0.14	-0.16		-0.17	-0.18	-0.19	-0.21	-0.21	-0.22	-0.22
DC1	Deflection, in.		-0.005			-0.011	-0.016		-0.017	-0.019	-0.017	-0.015	-0.013	-0.010	-0.006
DC2	Deflection, in.		0.003			0.003	0.003		0.004	0.006	0.008	0.010	0.012	0.014	0.017
1-1a;3-3a	Avg thrust, lb/in.		47			92	131		--	--	--	--	--	--	--
2-2a;4-4a	Avg thrust, lb/in.		29			62	99		139	185	234	291	343	--	--
	q		1.64			1.48	1.32		--	--	--	--	--	--	--

Table 5.7

Strain, Stress, Thrust, and Moment; Tests C-6, C-7, C-8, C-9, C-10

Gage	Measurement	Overpressure, psi 25	50	75	100	125	150	175	200	250	300	350	400	450	500
	Test C-6 (Z = 0 in.)														
1	Strain, µin./in.	-508	-836	-312	555	1443	2033	2459							
	Stress, psi	-5080	-8360	-3120	5550	14430	20330	24590							
1a	Strain, µin./in.	709	876	1312	1106	1010	718	332							
	Stress, psi	7090	8760	13120	11060	10100	7180	3320							
1-1a	Thrust, lb/in.	22	4	110	183	270	303	307							
	Moment, in.-lb/in.	0.49	0.69	0.66	0.22	-0.17	-0.53	-0.86							
3	Strain, µin./in.	9	74	259	435	602	741	815							
	Stress, psi	90	740	2590	4350	6020	7410	8150							
3a	Strain, µin./in.	143	338	523	718	887	980	1017							
	Stress, psi	1430	3380	5230	7180	8870	9800	10170							
3-3a	Thrust, lb/in.	17	45	86	127	164	189	202							
	Moment, in.-lb/in.	0.05	0.11	0.11	0.11	0.11	0.10	0.08							
2	Strain, µin./in.	297	451	613	809	943	1184	1249							
	Stress, psi	2970	4510	6130	8090	9430	11840	12490							
2a	Strain, µin./in.	127	264	396	515	673	792	873							
	Stress, psi	1270	2640	3960	5150	6730	7920	8730							
2-2a	Thrust, lb/in.	47	79	111	146	178	217	233							
	Moment, in-lb/in.	-0.07	-0.08	-0.09	-0.12	-0.11	-0.16	-0.15							
4	Strain, µin./in.	208	333	448	567	672	781	838							
	Stress, psi	2080	3330	4480	5670	6720	7810	8380							
4a	Strain, µin./in.	136	293	430	518	660	787	850							
	Stress, psi	1360	2930	4300	5180	6600	7870	8500							
4-4a	Thrust, lb/in.	38	69	97	119	147	172	186							
	Moment, in.-lb/in.	-0.03	-0.02	-0.01	-0.02	0.00	0.00	0.00							
1-1a;3-3a	Avg thrust, lb/in.	20	25	98	155	217	246	255							
2-2a;4-4a	Avg thrust, lb/in.	43	74	104	133	163	195	210							
	q	0.47	0.34	0.94	1.17	1.33	1.26	1.21							
	Test C-7 (Z = 3/16 in.)														
1	Strain, µin./in.		-218		1037		2202		3240	3549	3767	4204			
	Stress, psi		-2180		10370		22020		32400	35490	37554	39935			
1a	Strain, µin./in.		738		237		-223		-251	167	530	599			
	Stress, psi		7380		2370		-2230		-2510	1670	5300	5990			
1-1a	Thrust, lb/in.		57		140		218		329	409	473	524			
	Moment, in.-lb/in.		0.39		-0.32		-0.98		-1.41	-1.36	-1.31	-1.41			
3	Strain, µin./in.		809		1518		2090		2520	2849	3022	--			
	Stress, psi		8090		15180		20900		25200	28490	30220	--			
3a	Strain, µin./in.		-419		-723		-1113		-1417	-1633	-1735	-1908			
	Stress, psi		-4190		-7230		-11130		-14170	-16330	-17350	-19080			
3-3a	Thrust, lb/in.		43		87		107		121	134	142	--			
	Moment, in.-lb/in.		-0.50		-0.90		-1.29		-1.59	-1.81	-1.92	--			
2	Strain, µin./in.		303		440		620		868	1185	1371	1686			
	Stress, psi		3030		4400		6200		8680	11850	13710	16860			
2a	Strain, µin./in.		281		484		730		983	1337	1547	1814			
	Stress, psi		2810		4840		7300		9830	13370	15470	18140			
2-2a	Thrust, lb/in.		64		102		148		204	277	321	376			
	Moment, in.-lb/in.		-0.01		0.02		0.04		0.05	[illegible]	0.07	[illegible]			
4	Strain, µin./in.		306		559		774		1073	1449	1689	[illegible]			
	Stress, psi		3060		5590		7740		10730	14490	16890	[illegible]			
4a	Strain, µin./in.		284		495		736		1064	1385	1574	1873			
	Stress, psi		2840		4950		7360		10640	13850	15740	18730			
4-4a	Thrust, lb/in.		65		116		166		233	312	359	448			
	Moment, in.-lb/in.		-0.01		-0.03		-0.08		0.00	-0.03	-0.05	-0.06			
1-1a;3-3a	Avg thrust, lb/in.		50		114		163		[illegible]	[illegible]	--	--			
2-2a;4-4a	Avg thrust, lb/in.		65		109		157		[illegible]	295	340	403			
	q		0.77		1.05		1.04		[illegible]	[illegible]	--	--			
	Test C-8 (Z = 5/16 in.)														
1	Strain, µin./in.		-33		979		1543		[illegible]	[illegible]	2105	[illegible]	[illegible]	[illegible]	[illegible]
	Stress, psi		-330		9790		15430		[illegible]	[illegible]	21050	[illegible]	[illegible]	[illegible]	[illegible]
1a	Strain, µin./in.		970		998		641		[illegible]	[illegible]	1719	2039	[illegible]	[illegible]	[illegible]
	Stress, psi		9700		9980		6410		[illegible]	[illegible]	17190	20390	[illegible]	[illegible]	[illegible]
1-1a	Thrust, lb/in.		39		173		[illegible]		303	[illegible]	[illegible]	[illegible]	[illegible]	[illegible]	[illegible]
	Moment, in.-lb/in.		0.24		-0.15		-0.36		-0.40	[illegible]	-0.16	[illegible]	[illegible]	[illegible]	[illegible]
3	Strain, µin./in.		57		359		[illegible]		[illegible]	[illegible]	1005	1134	1263	[illegible]	[illegible]
	Stress, psi		570		3590		[illegible]		[illegible]	[illegible]	10050	11340	[illegible]	[illegible]	[illegible]
3a	Strain, µin./in.		310		636		814		[illegible]	1095	1263	1376	[illegible]	[illegible]	[illegible]
	Stress, psi		3100		6360		8140		[illegible]	[illegible]	[illegible]	[illegible]	[illegible]	[illegible]	[illegible]
3-3a	Thrust, lb/in.		40		109		154		[illegible]	[illegible]	247	[illegible]	310	[illegible]	[illegible]
	Moment, in.-lb/in.		0.16		0.11		0.09		0.07	[illegible]	0.10	0.10	0.12	0.15	0.12
2	Strain, µin./in.		[illegible]		[illegible]		[illegible]		1051	[illegible]	[illegible]	1931	[illegible]	[illegible]	[illegible]
	Stress, psi		[illegible]		[illegible]		[illegible]		10510	[illegible]	[illegible]	[illegible]	[illegible]	[illegible]	[illegible]
2a	Strain, µin./in.		313		997		[illegible]		1093	[illegible]	[illegible]	[illegible]	2113	[illegible]	[illegible]
	Stress, psi		[illegible]		9970		[illegible]		10930	[illegible]	[illegible]	[illegible]	21130	[illegible]	[illegible]
2-2a	Thrust, lb/in.		70		189		[illegible]		236	304	[illegible]	[illegible]	[illegible]	[illegible]	[illegible]
	Moment, in.-lb/in.		0.00		[illegible]		0.01		[illegible]	[illegible]	[illegible]	[illegible]	[illegible]	[illegible]	[illegible]
4	Strain, µin./in.		[illegible]		697		951		[illegible]	[illegible]	[illegible]	[illegible]	[illegible]	[illegible]	[illegible]
	Stress, psi		[illegible]		6970		9510		[illegible]	[illegible]	[illegible]	[illegible]	[illegible]	[illegible]	[illegible]
4a	Strain, µin./in.		440		[illegible]		1113		[illegible]	[illegible]	2141	[illegible]	[illegible]	[illegible]	[illegible]
	Stress, psi		4400		[illegible]		11130		[illegible]	17940	[illegible]	[illegible]	[illegible]	[illegible]	[illegible]
4-4a	Thrust, lb/in.		91		165		[illegible]		[illegible]	[illegible]	[illegible]	[illegible]	[illegible]	[illegible]	[illegible]
	Moment, in.-lb/in.		0.02		0.04		0.07		[illegible]	[illegible]	[illegible]	[illegible]	[illegible]	[illegible]	[illegible]
1-1a;3-3a	Avg thrust, lb/in.		50		141		197		[illegible]	[illegible]	[illegible]	[illegible]	[illegible]	[illegible]	[illegible]
2-2a;4-4a	Avg thrust, lb/in.		81		145		[illegible]		[illegible]	[illegible]	411	[illegible]	[illegible]	[illegible]	[illegible]
	q		[illegible]		0.97		0.97		[illegible]	[illegible]	[illegible]	[illegible]	[illegible]	0.77	[illegible]

(Continued)

Table 5.7 (Concluded)

Gage	Measurement	Overpressure, psi 25	50	75	100	125	150	175	200	250	300	350	400	450	500
							Test C-[illegible] (X = 7/16 in.)								
1	Strain, μin./in.		84		738		1268		1603	1854	2019	2187	2382	2549	2674
	Stress, psi		840		7380		12680		16030	18540	20190	21870	23820	[illegible]	26740
1a	Strain, μin./in.		565		863		1046		1286	1527	1998	2314	2679	[illegible]	3184
	Stress, psi		5650		8630		10460		12860	15270	19980	23140	26790	29180	31840
1-1a	Thrust, lb/in.		71		176		295		318	372	441	495	557	601	644
	Moment, in.-lb/in.		0.19		0.05		-0.09		-0.13	-0.13	-0.01	0.05	0.12	0.15	0.21
3	Strain, μin./in.		144		462		780		983	1127	1272	1388	1532	1691	1807
	Stress, psi		1440		4620		7800		9830	11270	12720	13880	15320	16910	18070
3a	Strain, μin./in.		294		484		734		896	1013	1219	1410	1601	1718	1880
	Stress, psi		2940		4840		7340		8960	10130	12190	14100	16010	17180	18800
3-3a	Thrust, lb/in.		45		104		167		207	235	274	308	345	375	406
	Moment, in.-lb/in.		0.09		0.01		-0.02		-0.04	-0.05	-0.02	0.01	0.03	0.01	0.03
2	Strain, μin./in.		401		780		1082		1360	1708	2098	2509	2941	3342	3759
	Stress, psi		4010		7800		10820		13600	17080	20980	25090	29410	33420	37320
2a	Strain, μin./in.		473		718		1041		1378	1637	2066	2412	2808	3168	3564
	Stress, psi		4730		7180		10410		[illegible]	16370	20660	24120	28080	31680	35640
2-2a	Thrust, lb/in.		90		165		234		[illegible]	358	457	541	632	716	805
	Moment, in.-lb/in.		0.03		-0.03		[illegible]		[illegible]	-0.03	-0.01	-0.04	-0.05	-0.07	[illegible]
4	Strain, μin./in.		398		667		943		1181	1449	1833	2116	[illegible]	2685	[illegible]
	Stress, psi		3980		6670		[illegible]		11810	[illegible]	18330	21160	[illegible]	26850	[illegible]
4a	Strain, μin./in.		216		527		830		1012	1754	1619	1879	2185	2407	2488
	Stress, psi		2160		[illegible]		8300		10120	17540	16190	18790	21850	[illegible]	24880
4-4a	Thrust, lb/in.		68		[illegible]		196		261	298	380	439	506	561	595
	Moment, in.-lb/in.		-0.07		-0.06		-0.06		-0.07	-0.08	-0.09	-0.10	-0.09	-0.11	-0.09
1-1a,3-3a	Avg thrust, lb/in.		58		140		231		263	304	358	[illegible]	451	488	527
2-2a,4-4a	Avg thrust, lb/in.		82		146		245		269	333	419	490	569	639	701
	q		0.71		0.95		0.98		0.98	0.91	0.85	0.82	0.79	0.76	0.75
							Test C-[illegible] (X = 7/8 in.)								
1	Strain, μin./in.		30		530		968		1151	1378	1540	1757	1969	2181	2287
	Stress, psi		300		[illegible]		[illegible]		11510	13780	15400	17570	19690	21810	22870
1a	Strain, μin./in.		508		[illegible]		1432		1555	[illegible]	2014	2319	2563	2777	3021
	Stress, psi		[illegible]		[illegible]		13380		15550	18580	20140	23190	25630	27770	30210
1-1a	Thrust, lb/in.		59		143		[illegible]		[illegible]	[illegible]	[illegible]	[illegible]	[illegible]	[illegible]	[illegible]
	Moment, in.-lb/in.		[illegible]		0.17		[illegible]		[illegible]	[illegible]	[illegible]	[illegible]	[illegible]	[illegible]	[illegible]
3	Strain, μin./in.		104		[illegible]		[illegible]		[illegible]	[illegible]	[illegible]	[illegible]	[illegible]	[illegible]	[illegible]
	Stress, psi		[illegible]		[illegible]		[illegible]		[illegible]	[illegible]	[illegible]	[illegible]	[illegible]	[illegible]	[illegible]
3a	Strain, μin./in.		[illegible]		[illegible]		[illegible]		[illegible]	[illegible]	[illegible]	1611	[illegible]	[illegible]	[illegible]
	Stress, psi		[illegible]		[illegible]		[illegible]		[illegible]	[illegible]	[illegible]	16110	[illegible]	[illegible]	[illegible]
3-3a	Thrust, lb/in.		[illegible]		108		157		[illegible]	[illegible]	[illegible]	[illegible]	[illegible]	371	[illegible]
	Moment, in.-lb/in.		[illegible]		[illegible]		0.13		[illegible]	0.17	0.17	0.19	[illegible]	[illegible]	[illegible]
2	Strain, μin./in.		[illegible]		[illegible]		[illegible]		[illegible]	1701	[illegible]	[illegible]	[illegible]	[illegible]	[illegible]
	Stress, psi		[illegible]		7100		[illegible]		[illegible]	[illegible]	[illegible]	[illegible]	27150	[illegible]	[illegible]
2a	Strain, μin./in.		[illegible]		377		[illegible]		[illegible]	[illegible]	[illegible]	[illegible]	[illegible]	[illegible]	[illegible]
	Stress, psi		[illegible]		[illegible]		[illegible]		[illegible]	[illegible]	[illegible]	[illegible]	[illegible]	[illegible]	[illegible]
2-2a	Thrust, lb/in.		[illegible]		[illegible]		[illegible]		[illegible]	[illegible]	[illegible]	[illegible]	[illegible]	[illegible]	[illegible]
	Moment, in.-lb/in.		[illegible]		[illegible]		[illegible]		[illegible]	[illegible]	[illegible]	[illegible]	[illegible]	[illegible]	[illegible]
4	Strain, μin./in.		[illegible]		[illegible]		[illegible]		[illegible]	[illegible]	[illegible]	[illegible]	[illegible]	[illegible]	[illegible]
	Stress, psi		[illegible]		[illegible]		[illegible]		[illegible]	[illegible]	[illegible]	[illegible]	[illegible]	[illegible]	[illegible]
4a	Strain, μin./in.		[illegible]		[illegible]		[illegible]		[illegible]	[illegible]	[illegible]	[illegible]	[illegible]	[illegible]	[illegible]
	Stress, psi		[illegible]		[illegible]		[illegible]		[illegible]	[illegible]	[illegible]	[illegible]	[illegible]	[illegible]	[illegible]
4-4a	Thrust, lb/in.		[illegible]		[illegible]		[illegible]		[illegible]	[illegible]	[illegible]	[illegible]	[illegible]	[illegible]	[illegible]
	Moment, in.-lb/in.		[illegible]		[illegible]		[illegible]		[illegible]	[illegible]	-0.13	[illegible]	-0.15	-0.17	[illegible]
1-1a,3-3a	Avg thrust, lb/in.		[illegible]		[illegible]		[illegible]		[illegible]	[illegible]	[illegible]	[illegible]	[illegible]	[illegible]	[illegible]
2-2a,4-4a	Avg thrust, lb/in.		[illegible]		[illegible]		[illegible]		[illegible]	[illegible]	[illegible]	[illegible]	[illegible]	[illegible]	[illegible]
	q		[illegible]		[illegible]		[illegible]		[illegible]	[illegible]	[illegible]	[illegible]	[illegible]	[illegible]	[illegible]

Table 5.8

Strain, Stress, Thrust, Moment, and Deflection; Tests E-1, E-2, E-3

Gage	Measurement	Overpress ure, psi 50	100	150	175	200	20[illegible]	[illegible]	300	350	400	450
					Test E-3 (E = 0 in.)							
1	Strain, μin./in.	606	1361	2995	4193		11000					
	Stress, psi	4903	6308	7527	8111		10760					
2	Strain, μin./in.	-397	-620	[illegible]	-1179		--					
	Stress, psi	-3970	-4965	-5767	-6123		--					
1-2	Thrust, lb/in.	62	140	[illegible]	266		--					
	Moment, in.-lb/in.	3.36	4.50	4.8	5.05		--					
3	Strain, μin./in.	-96	-169	[illegible]	-288		-480					
	Stress, psi	-960	-1690	-1980	-2880		-4579					
4	Strain, μin./in.	310	761	1536	--		--					
	Stress, psi	3100	5314	6487	--		--					
3-4	Thrust, lb/in.	70	167	263	--		--					
	Moment, in.-lb/in.	-1.42	-2.64	-2.79	--		--					
5	Strain, μin./in.	-47	70	239	320		560					
	Stress, psi	-470	700	2390	3200		4738					
6	Strain, μin./in.	264	346	445	522		691					
	Stress, psi	2640	3460	4450	4689		5131					
5-6	Thrust, lb/in.	71	135	222	267		322					
	Moment, in.-lb/in.	-1.09	-0.77	-0.73	-0.56		-0.12					
7	Strain, μin./in.	51	139	221	370		444					
	Stress, psi	510	1390	2210	3700		4440					
8	Strain, μin./in.	97	156	209	228		258					
	Stress, psi	970	1560	2090	2280		2580					
7-8	Thrust, lb/in.	48	96	140	194		229					
	Moment, in.-lb/in.	-0.16	[illegible].06	0.04	0.50		0.65					
9	Strain, μin./in.	280	401	491	600		660					
	Stress, psi	2800	4010	4607	4893		5056					
10	Strain, μin./in.	-206	-220	-202	-189		-176					
	Stress, psi	-2060	-2200	-2020	-1890		-1760					
9-10	Thrust, lb/in.	26	59	93	127		[illegible]					
	Moment, in.-lb/in.	1.71	2.19	2.42	2.58		2.60					
11	Strain, μin./in.	120	271	399	517		[illegible]					
	Stress, psi	1200	2710	3990	4675		4869					
12	Strain, μin./in.	36	50	59	64		68					
	Stress, psi	360	500	590	640		680					
11-12	Thrust, lb/in.	[illegible]	[illegible]	[illegible]	186		205					
	Moment, in.-lb/in.	[illegible]	[illegible]	1.20	1.53		1.60					
13	Strain, μin./in.	[illegible]	[illegible]	271	472		766					
	Stress, psi	[illegible]	[illegible]	2710	[illegible]		[illegible]					
14	Strain, μin./in.	[illegible]	[illegible]	[illegible]	[illegible]		[illegible]					
	Stress, psi	[illegible]	[illegible]	[illegible]	[illegible]		[illegible]					
13-14	Thrust, lb/in.	[illegible]	[illegible]	[illegible]	[illegible]		[illegible]					
	Moment, in.-lb/in.	[illegible]	[illegible]	[illegible]	[illegible]		[illegible]					
15	Strain, μin./in.	[illegible]	[illegible]	[illegible]	[illegible]		[illegible]					
	Stress, psi	[illegible]	[illegible]	[illegible]	[illegible]		[illegible]					
16	Strain, μin./in.	[illegible]	[illegible]	[illegible]	[illegible]		[illegible]					
	Stress, psi	[illegible]	[illegible]	[illegible]	[illegible]		[illegible]					
15-16	Thrust, lb/in.	[illegible]	[illegible]	[illegible]	[illegible]		[illegible]					
	Moment, in.-lb/in.	[illegible]	[illegible]	[illegible]	[illegible]		[illegible]					
DC1	Deflection, in.	[illegible]	[illegible]	[illegible]	[illegible]		[illegible]					
DC2	Deflection, in.	[illegible]	[illegible]	[illegible]	--		--					
[illegible]	Avg thrust	[illegible]	[illegible]	[illegible]	[illegible]		--					
[illegible]	Avg moment	[illegible]	[illegible]	[illegible]	[illegible]		[illegible]					
	[illegible]	[illegible]	[illegible]	[illegible]	[illegible]		--					
					Test E-[illegible] ([illegible])							
1	Strain, μin./in.	[illegible]	[illegible]	[illegible]		[illegible]		[illegible]	[illegible]	[illegible]	[illegible]	
	Stress, psi	[illegible]	[illegible]	[illegible]		[illegible]		[illegible]	[illegible]	[illegible]	[illegible]	
2	Strain, μin./in.	[illegible]	[illegible]	[illegible]		-417		[illegible]	[illegible]	[illegible]	[illegible]	
	Stress, psi	[illegible]	[illegible]	[illegible]		[illegible]		[illegible]	[illegible]	[illegible]	[illegible]	
1-2	Thrust, lb/in.	[illegible]	[illegible]	[illegible]		[illegible]		[illegible]	[illegible]	[illegible]	[illegible]	
	Moment, in.-lb/in.	[illegible]	[illegible]	[illegible]		[illegible]		[illegible]	[illegible]	[illegible]	[illegible]	
3	Strain, μin./in.	[illegible]	[illegible]	[illegible]		[illegible]		[illegible]	[illegible]	[illegible]	[illegible]	
	Stress, psi	[illegible]	[illegible]	[illegible]		[illegible]		[illegible]	[illegible]	[illegible]	[illegible]	
4	Strain, μin./in.	[illegible]	[illegible]	[illegible]		[illegible]		[illegible]	[illegible]	[illegible]	[illegible]	
	Stress, psi	[illegible]	[illegible]	[illegible]		[illegible]		[illegible]	[illegible]	[illegible]	[illegible]	
3-4	Thrust, lb/in.	[illegible]	[illegible]	[illegible]		[illegible]		[illegible]	[illegible]	[illegible]	[illegible]	
	Moment, in.-lb/in.	[illegible]	[illegible]	[illegible]		[illegible]		[illegible]	[illegible]	[illegible]	[illegible]	
5	Strain, μin./in.	[illegible]	[illegible]	[illegible]		[illegible]		[illegible]	[illegible]	[illegible]	[illegible]	
	Stress, psi	[illegible]	[illegible]	[illegible]		[illegible]		[illegible]	[illegible]	[illegible]	[illegible]	
6	Strain, μin./in.	[illegible]	[illegible]	[illegible]		[illegible]		[illegible]	[illegible]	[illegible]	[illegible]	
	Stress, psi	[illegible]	[illegible]	[illegible]		[illegible]		[illegible]	[illegible]	[illegible]	[illegible]	
5-6	Thrust, lb/in.	[illegible]	[illegible]	[illegible]		[illegible]		[illegible]	[illegible]	[illegible]	[illegible]	
	Moment, in.-lb/in.	[illegible]	[illegible]	[illegible]		[illegible]		[illegible]	[illegible]	[illegible]	[illegible]	
7	Strain, μin./in.	[illegible]	[illegible]	[illegible]		[illegible]		[illegible]	[illegible]	[illegible]	[illegible]	
	Stress, psi	[illegible]	[illegible]	[illegible]		[illegible]		[illegible]	[illegible]	[illegible]	[illegible]	
8	Strain, μin./in.	[illegible]	[illegible]	[illegible]		[illegible]		[illegible]	[illegible]	[illegible]	[illegible]	
	Stress, psi	[illegible]	[illegible]	[illegible]		[illegible]		[illegible]	[illegible]	[illegible]	[illegible]	
7-8	Thrust, lb/in.	[illegible]	[illegible]	[illegible]		[illegible]		[illegible]	[illegible]	[illegible]	[illegible]	
	Moment, in.-lb/in.	[illegible]	[illegible]	[illegible]		[illegible]		[illegible]	[illegible]	[illegible]	[illegible]	
9	Strain, μin./in.	[illegible]	[illegible]	[illegible]		[illegible]		[illegible]	[illegible]	[illegible]	[illegible]	
	Stress, psi	[illegible]	[illegible]	[illegible]		[illegible]		[illegible]	[illegible]	[illegible]	[illegible]	
10	Strain, μin./in.	[illegible]	[illegible]	[illegible]		[illegible]		[illegible]	[illegible]	[illegible]	[illegible]	
	Stress, psi	[illegible]	[illegible]	[illegible]		[illegible]		[illegible]	[illegible]	[illegible]	[illegible]	
9-10	Thrust, lb/in.	[illegible]	[illegible]	[illegible]		[illegible]		[illegible]	[illegible]	[illegible]	[illegible]	
	Moment, in.-lb/in.	[illegible]	[illegible]	[illegible]		[illegible]		[illegible]	[illegible]	[illegible]	[illegible]	
11	Strain, μin./in.	[illegible]	[illegible]	[illegible]		[illegible]		[illegible]	[illegible]	[illegible]	[illegible]	
	Stress, psi	[illegible]	[illegible]	[illegible]		[illegible]		[illegible]	[illegible]	[illegible]	[illegible]	
12	Strain, μin./in.	[illegible]	[illegible]	[illegible]		[illegible]		[illegible]	[illegible]	[illegible]	[illegible]	
	Stress, psi	[illegible]	[illegible]	[illegible]		[illegible]		[illegible]	[illegible]	[illegible]	[illegible]	
11-12	Thrust, lb/in.	[illegible]	[illegible]	[illegible]		[illegible]		[illegible]	[illegible]	[illegible]	[illegible]	
	Moment, in.-lb/in.	[illegible]	[illegible]	1.40		1.63		[illegible]	[illegible]	[illegible]	[illegible]	

(Continued)

Table 5.8 (Concluded)

Gage	Measurement	50	100	150	175	200	225	250	300	350	400	440
	Test E-2 (Z = 7/16 in.) (Continued)											
13	Strain, µin./in.	-92	-12	161		518		1313	2788	4331	5668	
	Stress, psi	-920	-120	1610		4678		6259	7409	8164	8731	
14	Strain, µin./in.	327	480	716		1091		1995	3690	5209	6512	
	Stress, psi	3270	4579	5196		6033		6955	7875	8538	9082	
13-14	Thrust, lb/in.	76	152	254		352		429	497	543	579	
	Moment, in.-lb/in.	-1.48	-1.72	-1.28		-0.51		-0.24	-0.16	-0.13	-0.12	
15	Strain, µin./in.	34	69	165		434		1220	2701	3821	5385	
	Stress, psi	340	690	1650		4340		6164	7360	7940	8612	
16	Strain, µin./in.	173	302	590		1138		2318	4306	6163	7953	
	Stress, psi	1730	3020	4867		6081		7141	8159	8938	9680	
15-16	Thrust, lb/in.	67	121	234		348		436	506	549	595	
	Moment, in.-lb/in.	-0.49	-0.82	-1.22		-0.61		-0.36	-0.28	-0.35	-0.38	
DC1	Deflection, in.	0.017	0.026	0.035		0.043		0.055	0.070	0.086	0.105	
DC2	Deflection, in.	0.017	0.022	0.027		0.031		0.035	0.037	0.039	0.041	
1-2:9-10	Avg thrust	41	90	157		231		310	381	431	484	
5-6:13-14	Avg thrust	75	149	262		354		433	496	542	580	
	q	0.55	0.60	0.62		0.65		0.72	0.77	0.80	0.83	
	Test E-1 (Z = 7/8 in.)											
1	Strain, µin./in.	365	635	917		1237		1626	1989	2530	3253	3885
	Stress, psi	3650	4984	5723		6182		6579	6949	7262	7656	7972
2	Strain, µin./in.	-226	-272	-266		-214		-98	29	324	753	1268
	Stress, psi	-2260	-2720	-2660		-2140		-980	290	3240	5293	6213
1-2	Thrust, lb/in.	45	109	167		228		292	340	400	442	470
	Moment, in.-lb/in.	2.08	2.94	3.11		2.93		2.37	1.85	1.07	0.74	0.59
3	Strain, µin./in.	37	70	148		397		987	1821	2933	3828	4816
	Stress, psi	370	700	1480		3870		5906	6777	7492	7944	8373
4	Strain, µin./in.	151	307	531		937		1955	2899	4179	5528	6808
	Stress, psi	1510	3070	4712		5775		6944	7472	8105	8672	9205
3-4	Thrust, lb/in.	61	123	217		327		417	465	507	540	571
	Moment, in.-lb/in.	-0.40	-0.83	-1.23		-0.56		-0.35	-0.23	-0.22	-0.25	-0.29
5	Strain, µin./in.	-57	24	190		538		1304	2129	3236	4429	5451
	Stress, psi	-570	240	1900		4730		6250	7034	7648	8210	8639
6	Strain, µin./in.	273	439	682		1052		2028	3369	4866	6176	7392
	Stress, psi	2730	4390	5107		6033		6976	7714	8394	8943	9448
5-6	Thrust, lb/in.	70	150	257		354		430	480	522	558	588
	Moment, in.-lb/in.	-1.16	-1.46	-1.15		-0.49		-0.26	-0.24	-0.26	-0.26	-0.28
7	Strain, µin./in.	304	456	609		913		1217	1522	2282	2891	3347
	Stress, psi	3040	4516	4916		5712		6161	6472	7121	7468	7703
8	Strain, µin./in.	26	75	178		387		827	1111	2202	3370	3871
	Stress, psi	260	750	1780		3870		5487	6053	7075	7565	7966
7-8	Thrust, lb/in.	107	173	242		325		384	407	461	489	509
	Moment, in.-lb/in.	0.98	1.34	1.17		0.54		0.23	0.15	0.02	-0.03	-0.09
9	Strain, µin./in.	112	112	112		162		349	686	1129	1629	1914
	Stress, psi	1120	1120	1120		1620		3490	5118	6072	6582	6872
10	Strain, µin./in.	56	169	294		450		662	918	1238	1433	1842
	Stress, psi	560	1690	2940		4500		5055	5725	6183	6362	6799
9-10	Thrust, lb/in.	55	91	132		199		294	352	398	421	444
	Moment, in.-lb/in.	0.20	-0.20	-0.64		-1.01		-0.49	-0.21	-0.04	0.07	0.03
11	Strain, µin./in.	72	187	288		475		893	1339	2059	2808	3586
	Stress, psi	720	1870	2880		4565		5660	6286	6994	7421	7823
12	Strain, µin./in.	52	124	195		357		685	1047	1690	2390	3115
	Stress, psi	520	1240	1950		3570		5115	5988	6644	7182	7588
11-12	Thrust, lb/in.	40	101	157		269		350	399	444	475	501
	Moment, in.-lb/in.	0.07	0.22	0.33		0.38		0.19	0.10	0.13	0.08	0.08
13	Strain, µin./in.	-33	49	262		687		2021	2781	4057	5464	6528
	Stress, psi	-330	490	2620		5121		6972	7405	8054	8645	9089
14	Strain, µin./in.	281	455	718		1201		2431	3674	5088	6501	7575
	Stress, psi	2810	4513	5202		6145		7206	7867	8487	9078	9524
13-14	Thrust, lb/in.	81	164	281		372		461	497	538	576	605
	Moment, in.-lb/in.	-1.11	-1.43	-0.86		-0.38		-0.08	-0.16	-0.15	-0.15	-0.15
15	Strain, µin./in.	28	69	152		388		1053	1953	2964	4141	4972
	Stress, psi	280	690	1520		3880		5994	6912	7509	8089	8438
16	Strain, µin./in.	156	341	611		1081		2048	3114	4579	5987	7133
	Stress, psi	1560	3410	4922		6023		6987	7587	8273	8865	9340
15-16	Thrust, lb/in.	60	133	234		339		423	472	514	551	578
	Moment, in.-lb/in.	-0.45	-0.96	-1.28		-0.66		-0.36	-0.23	-0.27	-0.27	-0.32
DC1	Deflection, in.	0.014	0.021	0.027		0.033		0.042	0.050	0.060	0.070	0.079
DC2	Deflection, in.	0.013	0.017	0.020		0.023		0.025	0.026	0.027	0.029	0.030
1-2:9-10	Avg thrust	50	100	150		214		293	346	399	431	457
5-6:13-14	Avg thrust	76	157	269		363		446	489	520	567	597
	q	0.66	0.64	0.56		0.59		0.66	0.71	0.75	0.76	0.77

Table 5.9

Strain, Stress, Thrust, and Moment; Tests E-4, E-5, E-6

Gage	Measurement	Test E-6 Z = 0 in. P_{so} = 254 psi	Test E-5 Z = 7/16 in. P_{sc} = 262 psi	Test E-4 Z = 7/8 in. P_{so} = 264 psi
1	Strain, μin./in.	5841	7899	5698
	Stress, psi	8803	9658	8743
2	Strain, μin./in.	8637	4881	3849
	Stress, psi	9933	8400	7955
1-2	Thrust, lb/in.	610	587	543
	Moment, in.-lb/in.	-0.40	0.44	0.27
3	Strain, μin./in.	3207	3949	3326
	Stress, psi	7634	8004	7693
4	Strain, μin./in.	5131	6189	5344
	Stress, psi	8505	8948	8594
3-4	Thrust, lb/in.	526	551	531
	Moment, in.-lb/in.	-0.30	-0.33	-0.31
5	Strain, μin./in.	4197	5582	4802
	Stress, psi	8113	8694	8367
6	Strain, μin./in.	4654	4946	5392
	Stress, psi	8305	8427	8615
5-6	Thrust, lb/in.	534	556	552
	Moment, in.-lb/in.	-0.07	0.09	-0.09
7	Strain, μin./in.	5878	7562	6045
	Stress, psi	8819	9518	8889
8	Strain, μin./in.	3944	5904	4565
	Stress, psi	8002	8830	8267
7-8	Thrust, lb/in.	547	596	558
	Moment, in.-lb/in.	0.29	0.24	0.22
9	Strain, μin./in.	5098	6552	5300
	Stress, psi	8491	9099	8576
10	Strain, μin./in.	3622	4991	3653
	Stress, psi	7841	8446	7856
9-10	Thrust, lb/in.	532	570	535
	Moment, in.-lb/in.	0.23	0.23	0.25
11	Strain, μin./in.	4415	6537	4503
	Stress, psi	8204	9093	8241
12	Strain, μin./in.	5347	5148	4890
	Stress, psi	8596	8512	8404
11-12	Thrust, lb/in.	546	572	541
	Moment, in.-lb/in.	-0.14	0.20	-0.06
13	Strain, μin./in.	3233	5350	3757
	Stress, psi	7647	8597	7909
14	Strain, μin./in.	3949	4969	4297
	Stress, psi	8004	8437	8155
13-14	Thrust, lb/in.	509	554	522
	Moment, in.-lb/in.	-0.13	0.06	-0.09
15	Strain, μin./in.	2651	3581	3630
	Stress, psi	7331	7821	7845
16	Strain, μin./in.	4898	6172	5499
	Stress, psi	8407	8941	8660
15-16	Thrust, lb/in.	514	546	537
	Moment, in.-lb/in.	-0.38	-0.39	-0.28
1-2;9-10	Avg thrust	571	579	539
5-6:13-14	Avg thrust	521	555	537
	q	1.10	1.04	1.00

Table 5.10

Strain, Stress, Thrust, Moment, and Deflection; Tests D-1, D-2, D-3, D-4, D-5

Gage	Measurement	Overpressure, psi 25	50	75	90	95	100	130	150	175	180	190
					Test D-1 (Z = 0 in.)							
1	Strain, μin./in.	293	684	2891		16194						
	Stress, psi	2930	4249	6285		--						
2	Strain, μin./in.	-184	-434	-994		-1036						
	Stress, psi	-1840	-3677	-4888		-4927						
1-2	Thrust, lb/in.	35	58	179		--						
	Moment, in.-lb/in.	168	3.23	4.23		--						
3	Strain, μin./in.	-57	12	27		-1710						
	Stress, psi	-570	120	270		-5512						
4	Strain, μin./in.	195	224	402		7109						
	Stress, psi	1950	2240	3583		8157						
3-4	Thrust, lb/in.	45	77	137		278						
	Moment, in.-lb/in.	-0.89	-0.75	-1.25		-4.61						
5	Strain, μin./in.	190	-59	-542		-398						
	Stress, psi	1900	-590	-3957		-3571						
6	Strain, μin./in.	-54	255	1303		2142						
	Stress, psi	-540	2650	5161		5845						
5-6	Thrust, lb/in.	44	67	125		223						
	Moment, in.-lb/in.	0.86	-1.14	-3.61		-2.89						
7	Strain, μin./in.	88	-32	-12		268						
	Stress, psi	880	-320	-120		2680						
8	Strain, μin./in.	-39	112	236		81						
	Stress, psi	-390	1120	2360		810						
7-8	Thrust, lb/in.	16	26	73		113						
	Moment, in.-lb/in.	0.45	-0.51	-0.87		0.66						
9	Strain, μin./in.	-136	341	1609		3040						
	Stress, psi	-1360	3403	5424		6380						
10	Strain, μin./in.	163	-222	-1073		-1718						
	Stress, psi	1630	-2220	-4963		-5517						
9-10	Thrust, lb/in.	9	39	67		108						
	Moment, in.-lb/in.	-1.05	1.98	4.60		5.23						
11	Strain, μin./in.	60	-6	-66		90						
	Stress, psi	600	-60	-660		900						
12	Strain, μin./in.	-11	81	237		188						
	Stress, psi	-110	810	2370		1880						
11-12	Thrust, lb/in.	16	24	56		90						
	Moment, in.-lb/in.	0.25	-0.31	-1.07		-0.35						
13	Strain, μin./in.	525	389	204		642						
	Stress, psi	3922	3544	2040		4162						
14	Strain, μin./in.	--	--	--		--						
	Stress, psi	--	--	--		--						
13-14	Thrust, lb/in.	--	--	--		--						
	Moment, in.-lb/in.	--	--	--		--						
15	Strain, μin./in.	-348	-321	-417		-3980						
	Stress, psi	-3424	-3210	-3627		-6864						
16	Strain, μin./in.	799	1065	1725		9744						
	Stress, psi	4484	4956	5525		9171						
15-16	Thrust, lb/in.	102	148	191		220						
	Moment, in.-lb/in.	-2.97	-2.88	-3.08		-6.43						
DC1	Deflection, in.	0	0.018	0.078		0.165						
DC2	Deflection, in.	-0.002	0.024	0.056		0.070						
1-2:9-10	Avg thrust	22	49	123		--						
5-6:13-14	Avg thrust	--	--	--		--						
	q	0.50	0.73	0.98		--						
					Test D-2 (Z = 7/16 in.)							
1	Strain, μin./in.	-11	476	1585			4043	14400				
	Stress, psi	-110	3799	5403			6888	10634				
2	Strain, μin./in.	195	-251	-832			-1530	-9231				
	Stress, psi	1950	-2510	-4554			-5356	-8974				
1-2	Thrust, lb/in.	60	67	102			182	140				
	Moment, in.-lb/in.	-0.73	2.39	4.22			4.84	8.54				
3	Strain, μin./in.	159	235	320			353	-738				
	Stress, psi	1590	2350	3200			3438	-4360				
4	Strain, μin./in.	-26	56	82			256	4665				
	Stress, psi	-260	560	820			2560	7156				
3-4	Thrust, lb/in.	43	95	131			198	287				
	Moment, in.-lb/in.	0.65	0.63	0.84			0.33	-3.30				
5	Strain, μin./in.	24[illegible]	-78	-476			-740	-266				
	Stress, psi	2440	-780	-3799			-4364	-2660				
6	Strain, μin./in.	-147	356	1260			2035	2410				
	Stress, psi	-1470	3447	5124			5781	6606				
5-6	Thrust, lb/in.	32	90	134			158	261				
	Moment, in.-lb/in.	1.38	-1.52	-3.42			-3.92	-2.35				
7	Strain, μin./in.	--	--	--			--	--				
	Stress, psi	--	--	--			--	--				
8	Strain, μin./in.	341	407	445			428	422				
	Stress, psi	3403	3597	3708			3659	3641				
7-8	Thrust, lb/in.	--	--	--			--	--				
	Moment, in.-lb/in.	--	--	--			--	--				
9	Strain, μin./in.	74	285	618			1014	1490				
	Stress, psi	740	2850	4113			4912	5121				
10	Strain, μin./in.	42	-114	-350			-506	-[illegible]74				
	Stress, psi	420	-1140	-3429			-3882	-4022				
9-10	Thrust, lb/in.	38	56	68			96	139				
	Moment, in.-lb/in.	0.11	1.40	2.91			3.53	3.65				
11	Strain, μin./in.	13	153	392			717	1195				
	Stress, psi	130	1530	3553			4317	5068				
12	Strain, μin./in.	103	24	-108			-195	-171				
	Stress, psi	1030	240	-1080			-1950	-171[illegible]				
11-12	Thrust, lb/in.	38	58	91			132	199				
	Moment, in.-lb/in.	-0.32	0.45	1.72			2.33	2.23				

(Continued)

Table 5.10 (Continued)

Gage	Measurement	25	50	75	90	95	100	130	150	175	180	190
							Overpressure, psi					
Test D-2 (Z = 7/16 in.) (Continued)												
13	Strain, μin./in	87	-261	-639			-881	-387				
	Stress, psi	870	-2610	-4156			-4655	-3538				
14	Strain, μin./in.	21	618	1895			3023	4008				
	Stress, psi	210	4113	5670			6372	6873				
13-14	Thrust, lb/in.	35	95	163			202	306				
	Moment, in.-lb/in.	0.23	-2.56	-3.71			-3.96	-2.51				
15	Strain, μin./in.	7	106	173			233	-1091				
	Stress, psi	70	1060	1730			2330	-4978				
16	Strain, μin./in.	147	199	199			387	5444				
	Stress, psi	1470	1990	1990			3538	7491				
15-16	Thrust, lb/in.	50	99	121			198	278				
	Moment, in.-lb/in.	-0.49	-0.33	-0.09			-0.46	-3.89				
DC1	Deflection, in.	-0.005	0.017	0.054			0.100	0.167				
DC2	Deflection, in.	-0.009	0.015	0.047			0.072	0.088				
1-2:9-10	Avg thrust	44	62	85			139	140				
5-6:13-14	Avg thrust	34	93	149			180	282				
	q	1.38	0.67	0.57			0.77	0.50				
Test D-3 (Z = 7/8 in.)												
1	Strain, μin./in.	319	2376	7863	13973		--					
	Stress, psi	3190	5986	8447	10502		--					
2	Strain, μin./in.	-264	-1390	-4063	-9730		--					
	Stress, psi	-2640	-5235	-6897	-9166		--					
1-2	Thrust, lb/in.	18	96	159	115		--					
	Moment, in.-lb/in.	2.05	4.95	6.57	8.66		--					
3	Strain, μin./in.	-49	-222	-386	-1052		-9530					
	Stress, psi	-490	-2220	-3535	-4945		-9089					
4	Strain, μin./in.	167	593	1493	3068		17656					
	Stress, psi	1670	4062	5324	6395		--					
3-4	Thrust, lb/in.	38	102	178	183		--					
	Moment, in.-lb/in.	-0.76	-2.40	-3.04	-4.30		--					
5	Strain, μin./in.	30	-438	-651	-533		166					
	Stress, psi	300	-3688	-4181	-3938		1660					
6	Strain, μin./in.	118	836	1447	1554		1206					
	Stress, psi	1180	4562	5284	5376		5077					
5-6	Thrust, lb/in.	48	84	120	153		265					
	Moment, in.-lb/in.	-0.31	-3.30	-3.86	-3.52		-0.98					
7	Strain, μin./in.	-136	44	515	946		1211					
	Stress, psi	-1360	440	3901	4789		5081					
8	Strain, μin./in.	--	--	--	--		--					
	Stress, psi	--	--	--	--		--					
7-8	Thrust, lb/in.	--	--	--	--		--					
	Moment, in.-lb/in.	--	--	--	--		--					
9	Strain, μin./in.	271	527	703	802		841					
	Stress, psi	2710	3926	4288	4492		4572					
10	Strain, μin./in.	-261	-522	-657	-657		-687					
	Stress, psi	-2610	-3915	-4193	-4193		-4255					
9-10	Thrust, lb/in.	3	1	9	28		29					
	Moment, in.-lb/in.	1.87	3.26	3.69	3.77		3.84					
11	Strain, μin./in.	-161	194	871	1419		1504					
	Stress, psi	-1610	1940	4634	5260		5333					
12	Strain, μin./in.	161	-50	-448	-589		-606					
	Stress, psi	1610	-500	-3717	-4053		-4088					
11-12	Thrust, lb/in.	0	47	87	128		134					
	Moment, in.-lb/in.	-1.13	0.86	3.34	3.71		3.74					
13	Strain, μin./in.	94	-230	-325	-168		691					
	Stress, psi	940	-2300	-3250	-1680		4263					
14	Strain, μin./in.	-24	478	918	1083		762					
	Stress, psi	-240	3805	4731	4971		4410					
13-14	Thrust, lb/in.	23	74	127	188		282					
	Moment, in.-lb/in.	0.42	-2.32	-2.89	-2.24		-0.05					
15	Strain, μin./in.	-154	-308	-411	-1101		-7581					
	Stress, psi	-1540	-3080	-3609	-4987		-8339					
16	Strain, μin./in.	295	707	1521	3278		14530					
	Stress, psi	2950	4296	5348	6502		10674					
15-16	Thrust, lb/in.	46	98	175	188		195					
	Moment, in.-lb/in.	-1.58	-2.79	-3.12	-4.34		-8.03					
DC1	Deflection, in.	0.013	0.058	0.142	0.171		0.186					
DC2	Deflection, in.	0.007	0.040	0.073	0.088		0.093					
1-2:9-10	Avg thrust	11	49	84	72		--					
5-6:13-14	Avg thrust	36	79	124	171		274					
	q	0.31	0.62	0.68	0.42		--					
Test D-4 (Z = 1-3/4 in.)												
1	Strain, μin./in.		561				2896		5370			9051
	Stress, psi		3996				6298		7459			8905
2	Strain, μin./in.		-348				-1201		-1584			-1966
	Stress, psi		-3423				-5073		-5402			-5731
1-2	Thrust, lb/in.		57				154		232			312
	Moment, in.-lb/in.		2.86				4.60		4.68			4.74
3	Strain, μin./in.		143				211		737			756
	Stress, psi		1430				2110		4358			4397
4	Strain, μin./in.		132				448		1453			5082
	Stress, psi		1320				3717		5290			7335
3-4	Thrust, lb/in.		89				203		320			403
	Moment, in.-lb/in.		0.04				-0.58		-0.3[illegible]			-0.93
5	Strain, μin./in.		-185				-1826		-2434			-2383
	Stress, psi		-1850				-5610		-6020			-5990
6	Strain, μin./in.		431				3553		6360			8480
	Stress, psi		3667				6642		7869			8685
5-6	Thrust, lb/in.		77				189		203			272
	Moment, in.-lb/in.		-2.08				-5.27		-5.51			-5.24

(Continued)

Table 5.10 (Concluded)

Gage	Measurement	25	50	75	90	95	100	130	150	175	180	190
						Overpressure, psi						
Test D-4 (Z = 1-3/4 in.) (Continued)												
7	Strain, μin./in.		-253				250		826			1505
	Stress, psi		-2530				2500		4542			5334
8	Strain, μin./in.		354				127		236			761
	Stress, psi		3441				1270		2360			4408
7-8	Thrust, lb/in.		33				123		248			323
	Moment, in.-lb/in.		-2.13				0.43		0.63			0.30
9	Strain, μin./in.		318				1346		2366			3155
	Stress, psi		3180				5198		5980			6439
10	Strain, μin./in.		-263				-665		-673			-459
	Stress, psi		-2630				-4210		-4226			-3750
9-10	Thrust, lb/in.		18				106		192			265
	Moment, in.-lb/in.		2.05				3.91		3.66			2.85
11	Strain, μin./in.		478				1410		2397			3120
	Stress, psi		3805				5253		5998			6421
12	Strain, μin./in.		-252				-697		-692			-468
	Stress, psi		-2520				-4276		-4266			-3776
11-12	Thrust, lb/in.		67				107		191			262
	Moment, in.-lb/in.		2.40				3.97		3.70			2.8[illegible]
13	Strain, μin./in.		-230				-1270		-1577			-1292
	Stress, psi		-2300				-5132		-5396			-5151
14	Strain, μin./in.		476				3913		6811			9347
	Stress, psi		3799				6826		8042			9019
13-14	Thrust, lb/in.		74				201		279			361
	Moment, in.-lb/in.		-2.32				[illegible]		-4.47			-3.86
15	Strain, μin./in.		-175				223		811			1121
	Stress, psi		-1750				[illegible]230		4511			5004
16	Strain, μin./in.		444				36[illegible]		985			3543
	Stress, psi		3706				3459		4869			6637
15-16	Thrust, lb/in.		83				[illegible]		305			384
	Moment, in.-lb/in.		-2.06				-0.46		-0.13			-0.57
DC1	Deflection, in.		0.026				--		--			--
DC2	Deflection, in.		0.023				0.080		0.093			0.100
1-2:9-10	Avg thrust		38				130		162			289
5-6:13-14	Avg thrust		76				165		244			317
	q		0.50				0.79		0.66			0.91
Test D-5 (Z = 2-5/8 in.)												
1	Strain, μin./in.		1591				7368		11022	--	--	
	Stress, psi		5408				8257		9587	--	--	
2	Strain, μin./in.		-871				-4137		-5661	-9906	--	
	Stress, psi		-4634				-6929		-7584	-9234	--	
1-2	Thrust, lb/in.		97				139		180	--	--	
	Moment, in.-lb/in.		4.29				6.63		7.28	--	--	
3	Strain, μin./in.		-397				-521		-715	-2740	-6975	
	Stress, psi		-3567				-3913		-4313	-6204	-8105	
4	Strain, μin./in.		972				2104		4472	10259	20912	
	Stress, psi		4842				5822		7073	9350	--	
3-4	Thrust, lb/in.		116				199		283	296	--	
	Moment, in.-lb/in.		-3.18				-3.31		-3.28	-5.45	--	
5	Strain, μin./in.		-201				-331		-77	602	878	
	Stress, psi		-2010				-3310		-770	4080	4649	
6	Strain, μin./in.		361				998		1617	1669	1408	
	Stress, psi		3462				4896		5431	5475	5251	
5-6	Thrust, lb/in.		52				137		250	320	325	
	Moment, in.-lb/in.		-1.97				-2.92		-1.79	-0.46	-0.19	
7	Strain, μin./in.		198				529		541	660	680	
	Stress, psi		1980				3930		3954	4200	4241	
8	Strain, μin./in.		-194				-289		89	194	206	
	Stress, psi		-1940				-2890		890	1940	2060	
7-8	Thrust. lb/in.		1				68		184	226	230	
	Moment, in.-lb/in.		1.38				2.60		1.12	0.71	0.67	
9	Strain, μin./in.		468				1404		2635	3160	3160	
	Stress, psi		3776				5247		6141	6442	6442	
10	Strain, μin./in.		-381				-1026		-1251	-1269	-1273	
	Stress, psi		-3520				-4922		-5116	-5131	-5135	
9-10	Thrust, lb/in.		24				51		131	162	162	
	Moment, in.-lb/in.		2.85				4.52		4.73	4.65	4.65	
11	Strain, μin./in.		-22				368		703	855	876	
	Stress, psi		-220				3482		4288	4601	4645	
12	Strain, μin./in.		127				8		208	389	408	
	Stress, psi		1270				80		2080	3544	3600	
11-12	Thrust, lb/in.		34				122		233	267	270	
	Moment, in.-lb/in.		-0.52				1.25		0.67	0.36	0.35	
13	Strain, μin./in.		-127				-233		0	710	1356	
	Stress, psi		-2170				-2330		0	4303	5206	
14	Strain, μin./in.		304				1000		1588	1795	1726	
	Stress, psi		3040				[illegible]		5406	5584	5524	
13-14	Thrust, lb/in.		58				[illegible]		261	330	349	
	Moment, in.-lb/in.		-1.52				-2.51		-1.52	-0.41	-0.11	
15	Strain, μin./in.		-228				-250		-323	-1688	-5159	
	Stress, psi		-2280				-2500		-3230	-5492	-7368	
16	Strain, μin./in.		558				1144		3173	7639	14749	
	Stress, psi		3989				5196		6448	8361	10742	
15-16	Thrust, lb/in.		93				195		285	294	287	
	Moment, in.-lb/in.		-2.40				[illegible]		-2.42	-4.52	-6.95	
DC1	Deflection, in.		0.038				0.149		0.176	0.184	0.186	
DC2	Deflection, in.		0.032				[illegible]		0.098	0.099	0.101	
1-2:9-10	Avg thrust		61				95		156	--	--	
5-6:13-14	Avg thrust		55				150		256	325	337	
	q		1.11				0.63		0.61	--	--	

Table 5.11

Strain, Stress, Thrust, and Moment; Tests D-6, D-7, D-8, D-9, D-10

Gage	Measurement	Test D-10 Z = 7/8 in. P_{so} = 97* psi	Test D-8 Z = 7/8 in. P_{so} = 116* psi	Test D-9 Z = 7/8 in. P_{so} = 148 psi	Test D-6 Z = 1-3/4 in. P_{so} = 160* psi	Test D-7 Z = 1-3/4 in. P_{so} = 180 psi
1	Strain, μin./in.	--	3361	17296	13714	19059
	Stress, psi	--	6541	--	10421	--
2	Strain, μin./in.	--	-891	-15970	-5512	-10134
	Stress, psi	--	-4675	--	-7520	-9312
1-2	Thrust, lb/in.	--	218	--	251	--
	Moment, in.-lb/in.	--	3.90	--	7.16	--
3	Strain, μin./in.	--	343	-14665	-5063	-7055
	Stress, psi	--	3409	-10716	-7327	-8136
4	Strain, μin./in.	--	--	5836	14380	19105
	Stress, psi	--	--	7659	10628	--
3-4	Thrust, lb/in.	--	--	--	283	--
	Moment, in.-lb/in.	--	--	-7.30	-6.90	--
5	Strain, μin./in.	--	1174	9087	3881	5384
	Stress, psi	--	5050	8918	6809	7465
6	Strain, μin./in.	--	550	17760	-665	-686
	Stress, psi	--	3973	--	-4210	-4253
5-6	Thrust, lb/in.	--	298	--	268	314
	Moment, in.-lb/in.	--	0.40	--	3.26	3.10
7	Strain, μin./in.	--	-53	1468	860	-2511
	Stress, psi	--	-530	5302	4612	-6067
8	Strain, μin./in.	--	1933	-411	591	6892
	Stress, psi	--	5702	-3609	4057	8073
7-8	Thrust, lb/in.	--	271	170	282	216
	Moment, in.-lb/in.	--	-1.68	3.14	0.20	-5.52
9	Strain, μin./in.	1551	3195	--	2865	-1910
	Stress, psi	5374	6459	--	6279	-5683
10	Strain, μin./in.	-1306	-576	--	720	5327
	Stress, psi	-5163	-4027	--	4323	7441
9-10	Thrust, lb/in.	29	250	--	358	204
	Moment, in.-lb/in.	4.83	3.18	--	0.62	-5.10
11	Strain, μin./in.	349	-754	--	880	508
	Stress, psi	3426	-4393	--	4653	3886
12	Strain, μin./in.	0	3827	--	3477	295
	Stress, psi	0	6782	--	6603	2950
11-12	Thrust, lb/in.	113	255	--	377	231
	Moment, in.-lb/in.	1.23	-3.49	--	-0.64	0.28
13	Strain, μin./in.	517	665	--	2079	3998
	Stress, psi	3905	4210	--	5807	6869
14	Strain, μin./in.	0	480	--	1935	206
	Stress, psi	0	3811	--	5704	2060
13-14	Thrust, lb/in.	154	261	--	374	362
	Moment, in.-lb/in.	1.47	0.14	--	0.04	1.18
15	Strain, μin./in.	-2171	823	--	-768	-11447
	Stress, psi	-5863	4535	--	-4422	-9719
16	Strain, μin./in.	8019	1105	--	5976	22539
	Stress, psi	8507	4990	--	7720	--
15-16	Thrust, lb/in.	272	312	--	323	--
	Moment, in.-lb/in.	-5.06	-0.17	--	-3.21	--
1-2:9-10	Avg thrust	--	234	--	305	--
5-6:13-14	Avg thrust	--	280	--	321	338
	q	--	0.84	--	0.95	--

* No failure.

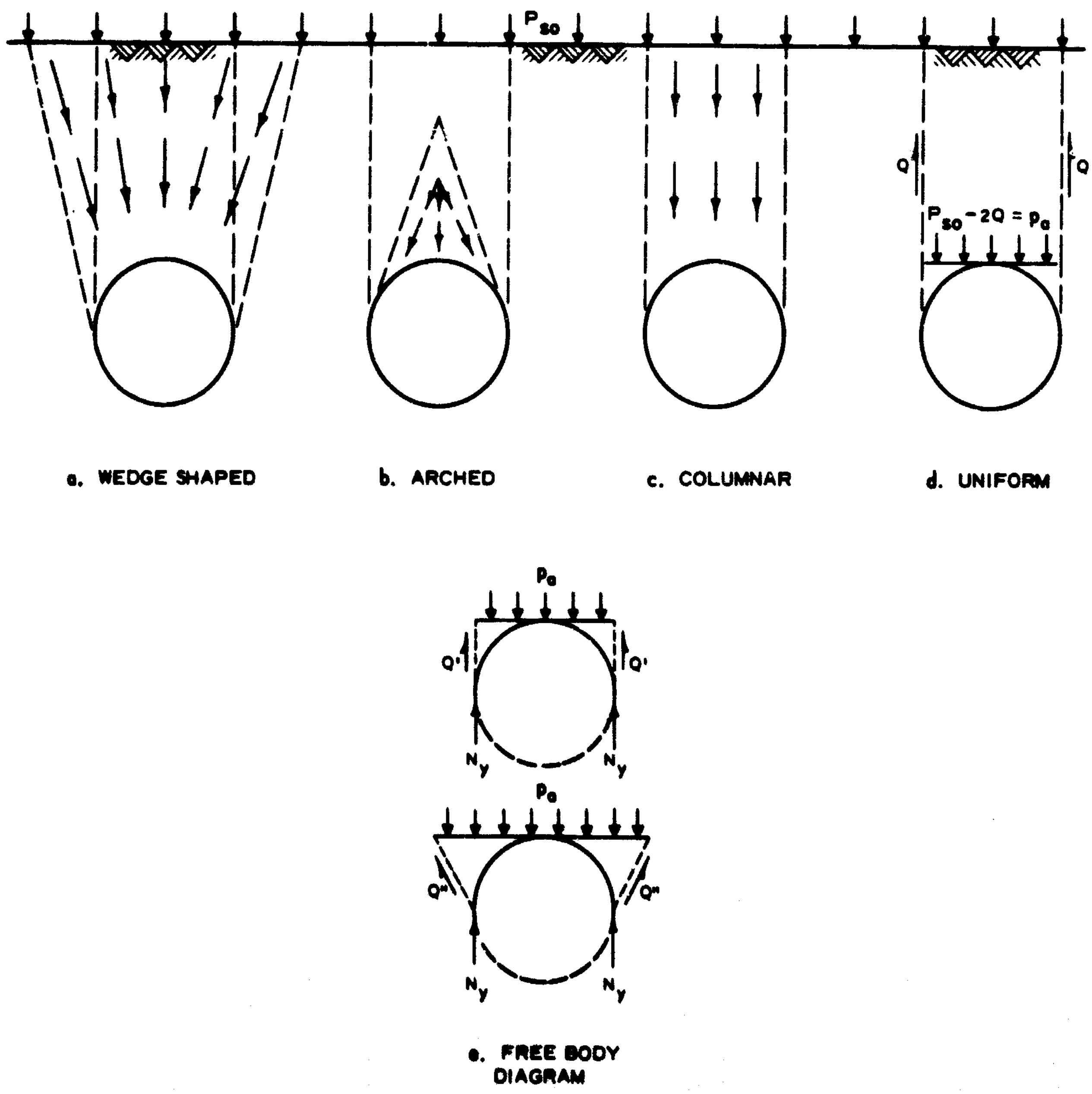

Fig. 1.1 Concepts of Load Transfer

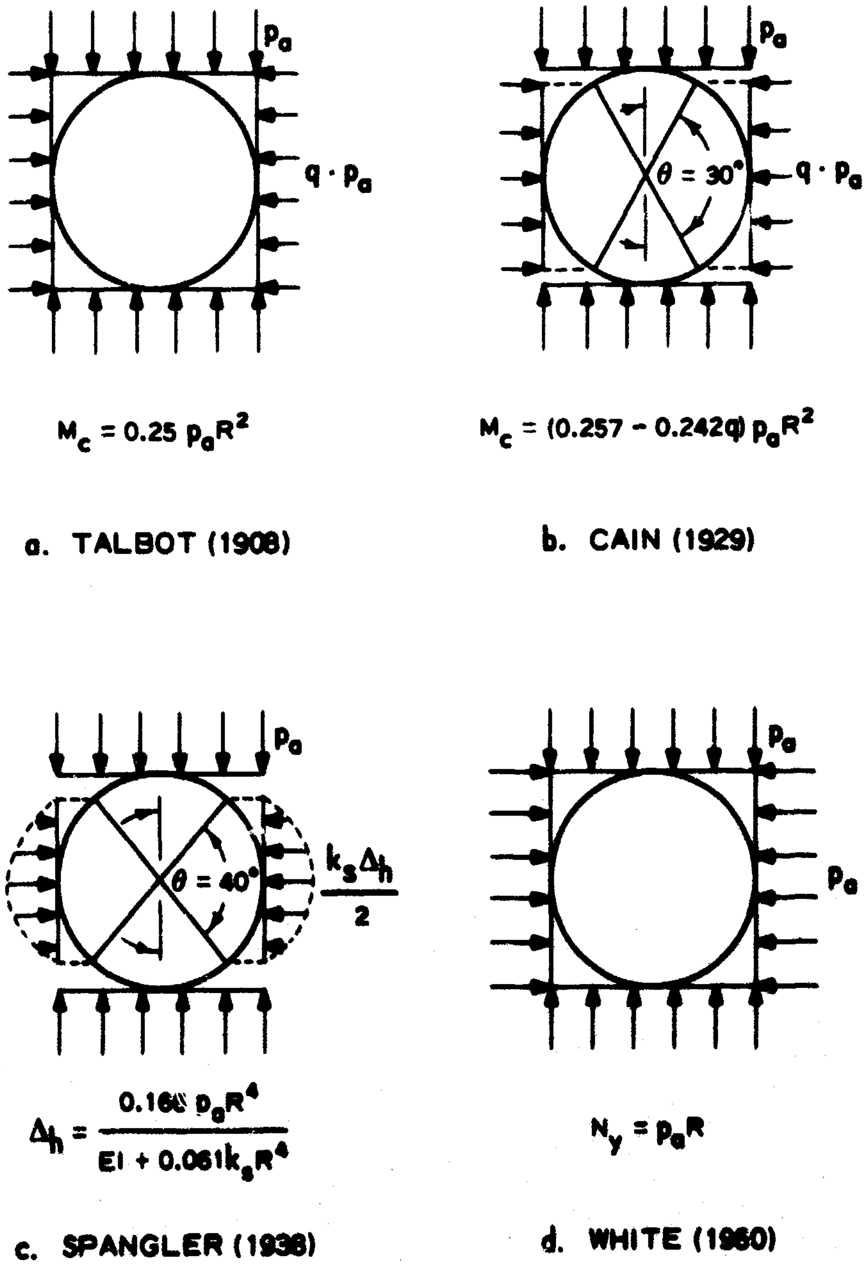

Fig. 2.1 Concepts of Load Distribution

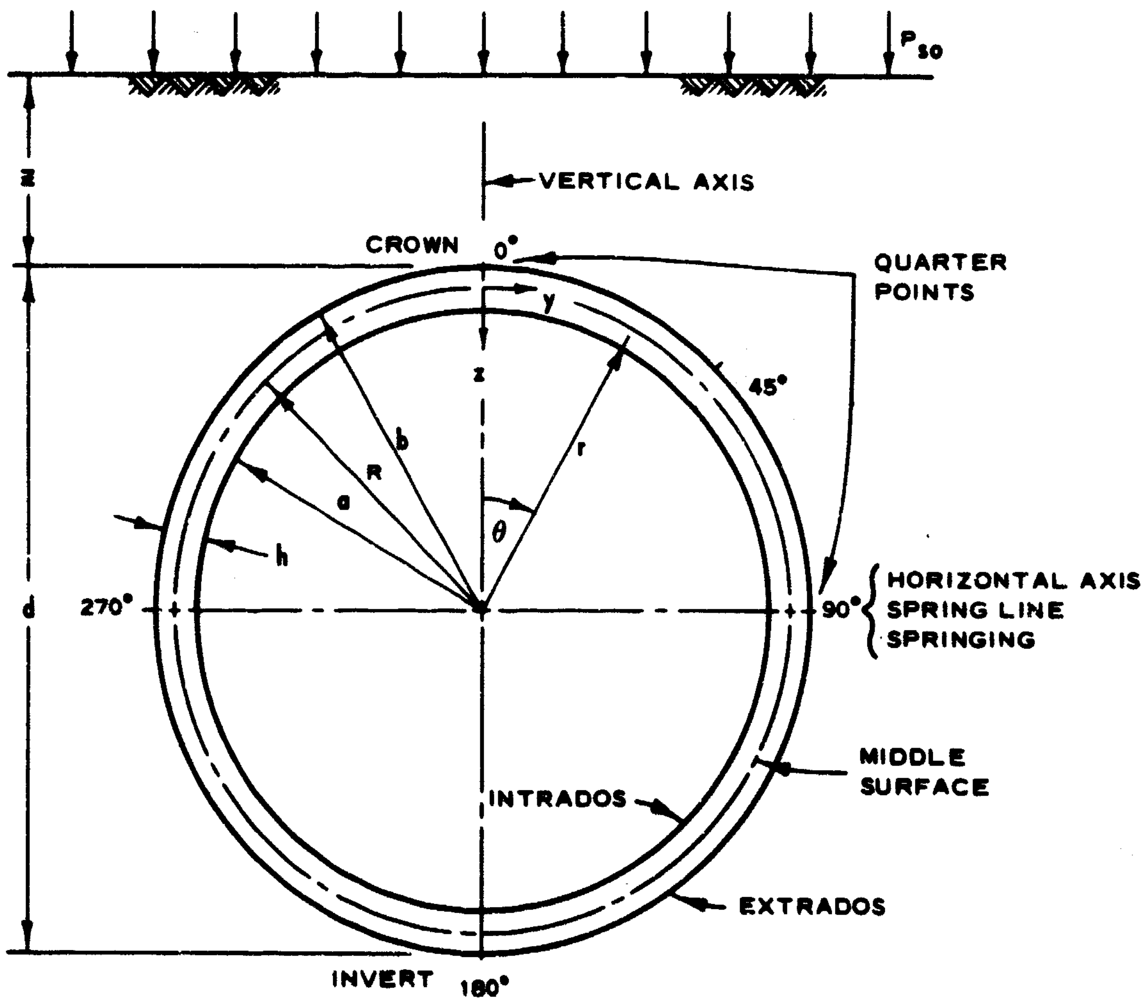

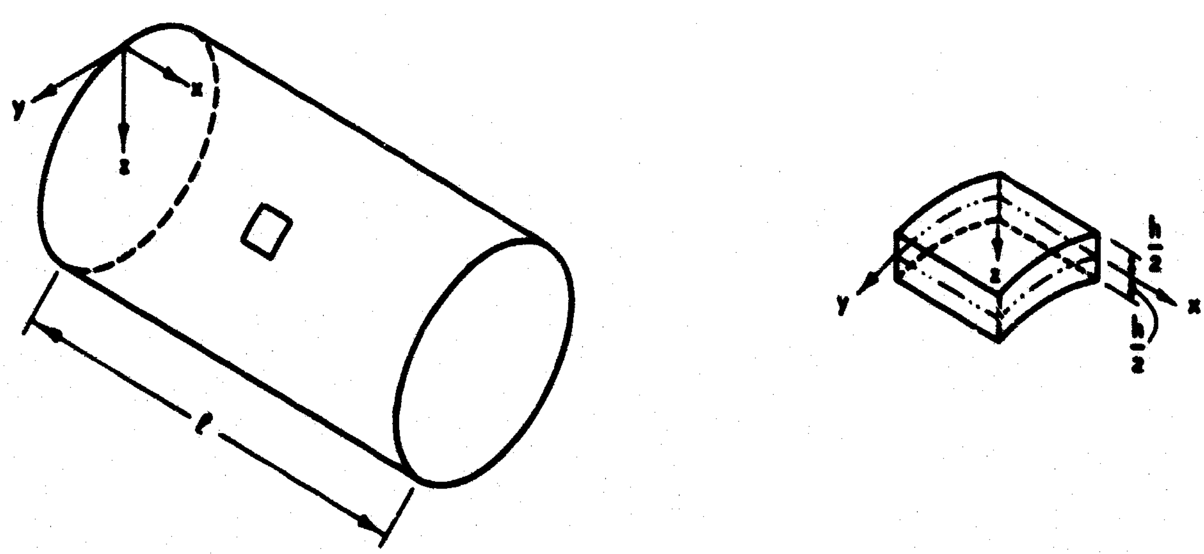

Fig. 3.1 Cylindrical Shell and Ring Notation

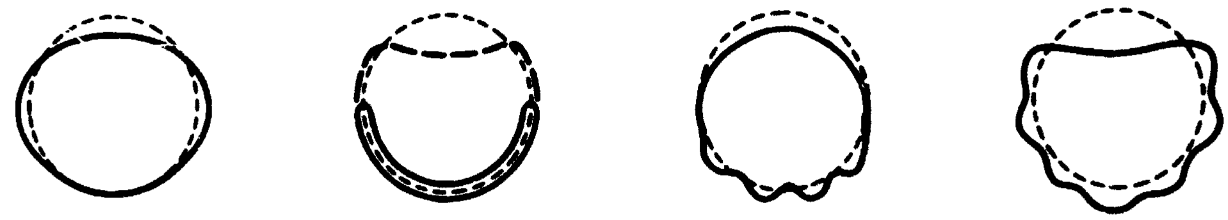

a. DEFLECTION (WATKINS) b. SNAP-THROUGH (DONNELLAN) c. RIPPLING (BULSON) d. COMBINATION (ALLGOOD)

Fig. 3.2 Actual Modes of Failure

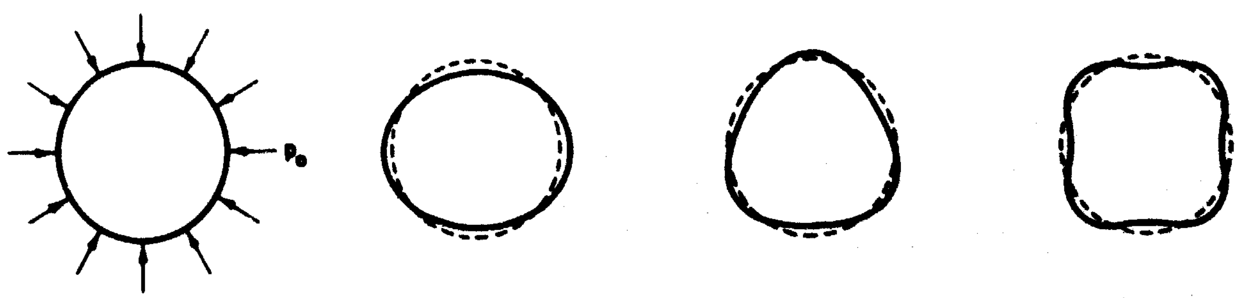

a. UNIFORM RADIAL LOAD b. MODE 2 (n = 2) c. MODE 3 (n = 3) d. MODE 4 (n = 4)

Fig. 3.3 Buckling Modes

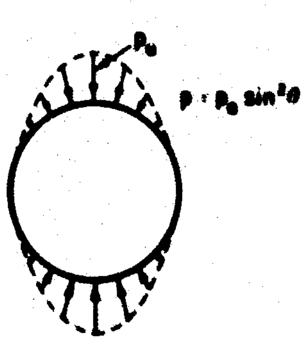

Fig. 3.4 Nonuniform Load

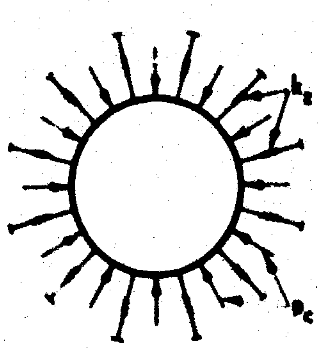

Fig. 3.5 Elastic Supports

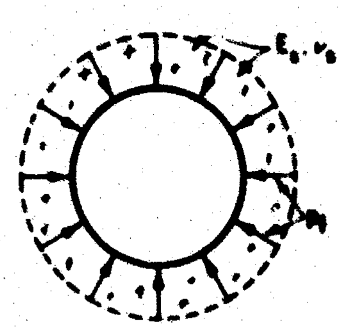

Fig. 3.6 Elastic Medium

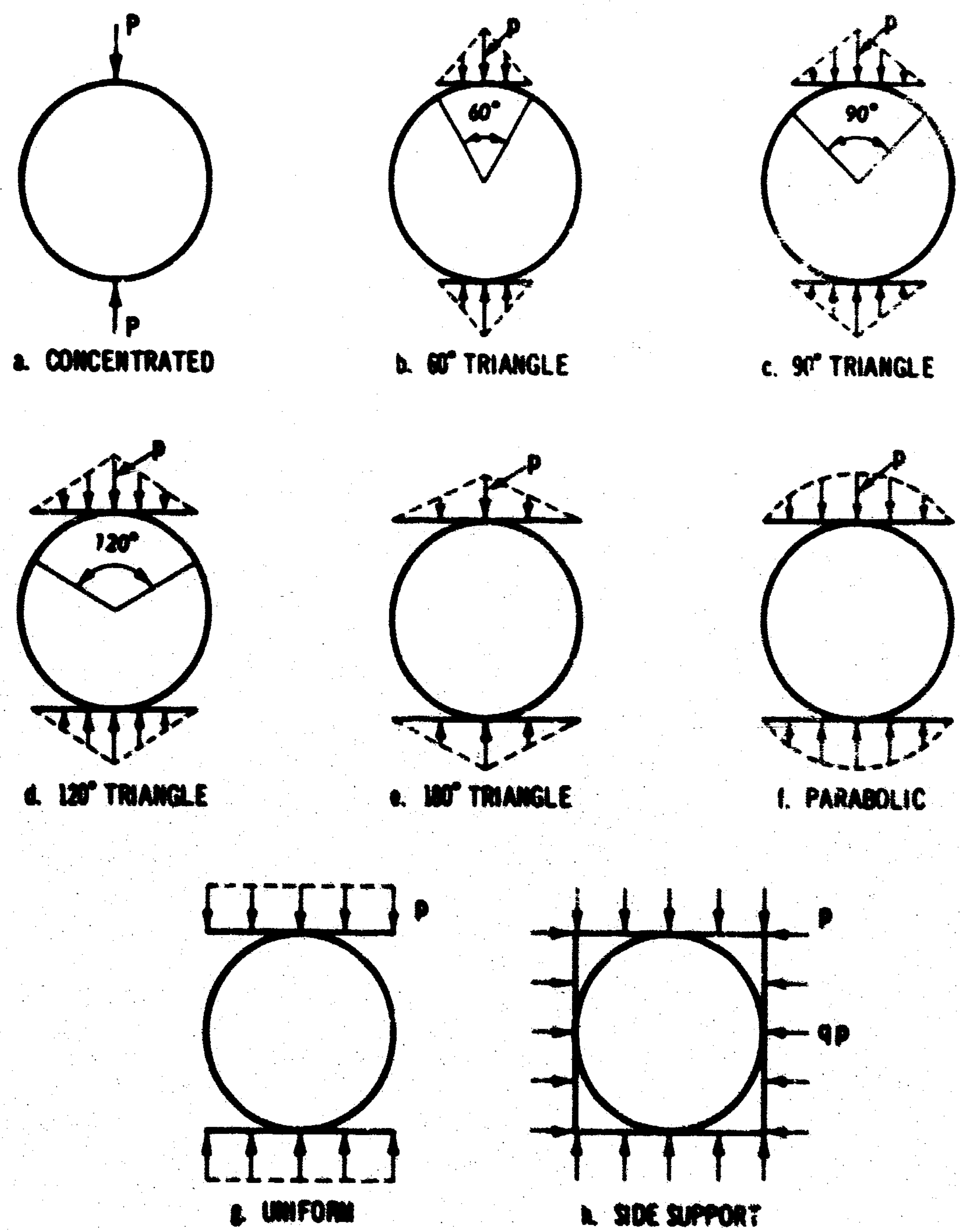

Fig. 3.7 Idealized Loading Configurations

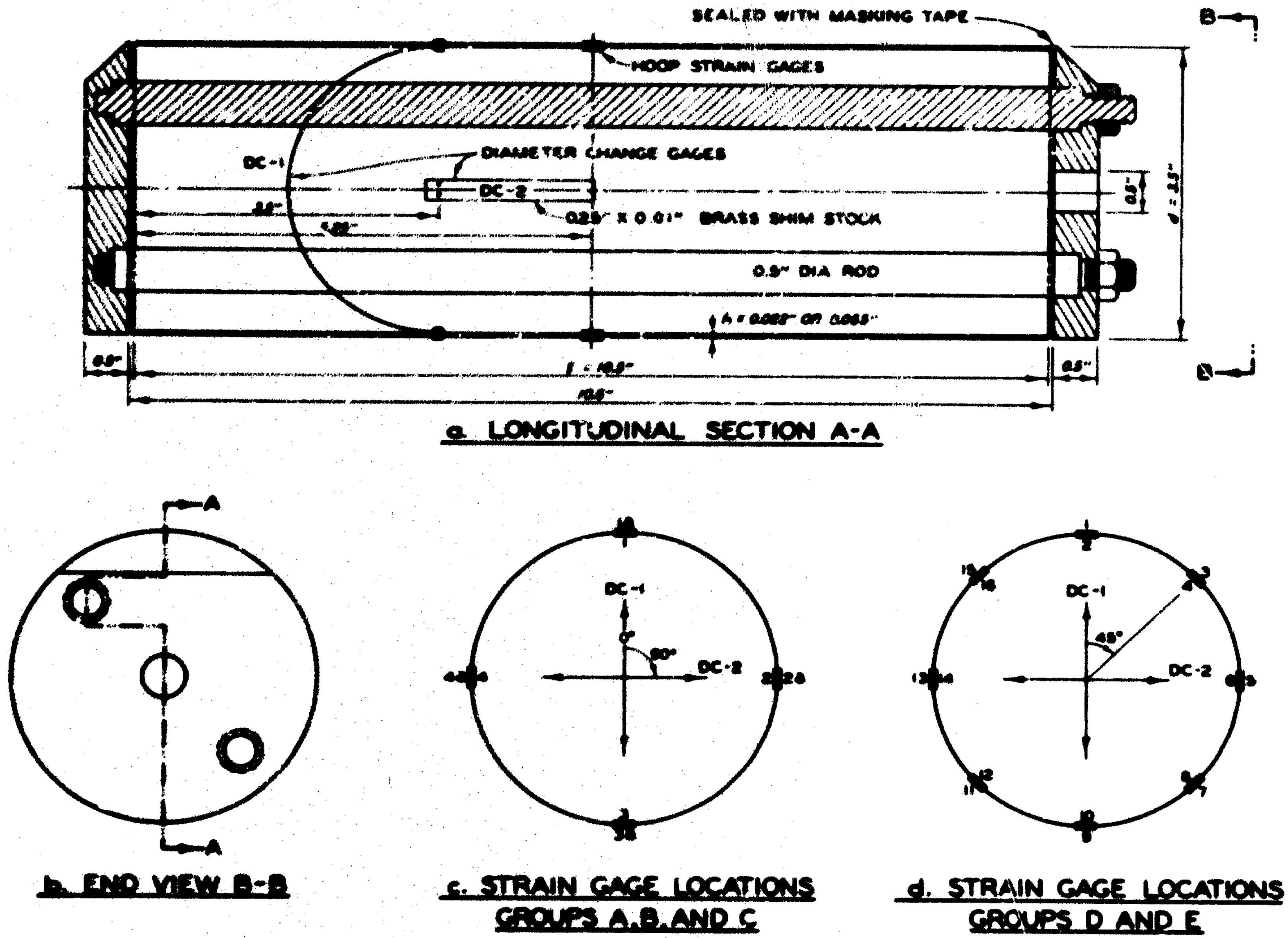

Fig. 4.1 Longitudinal Section of Cylinder and Gage Locations

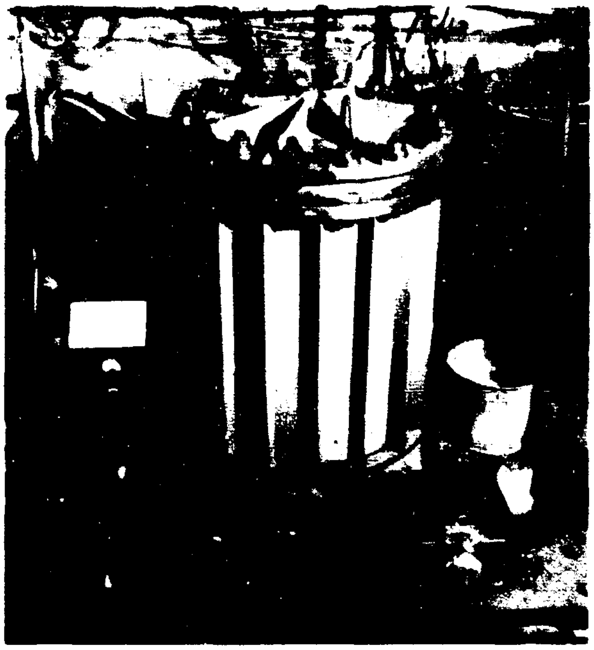

a. Static Bonnet (2-ft Diameter, 500 psi)

b. Dynamic Bonnet

c. Spacer Ring and Posttest Diaphragm Configuration

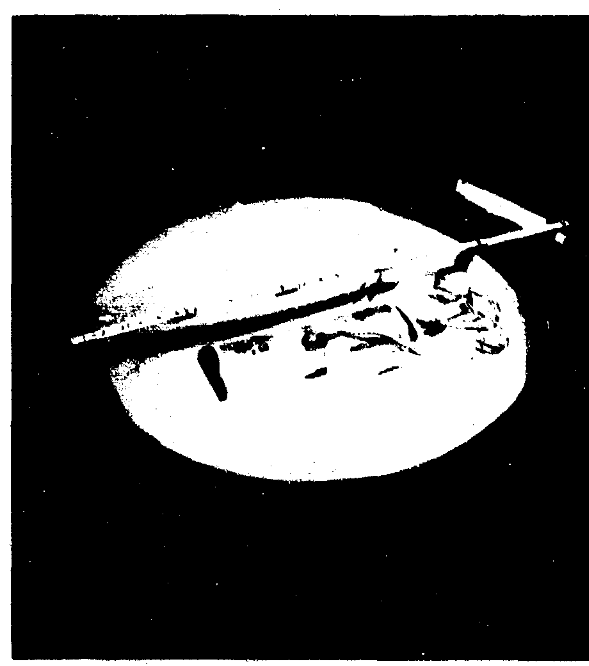

d. Cylinder in Position

Fig. 4.2 University of Illinois Blast Load Generator

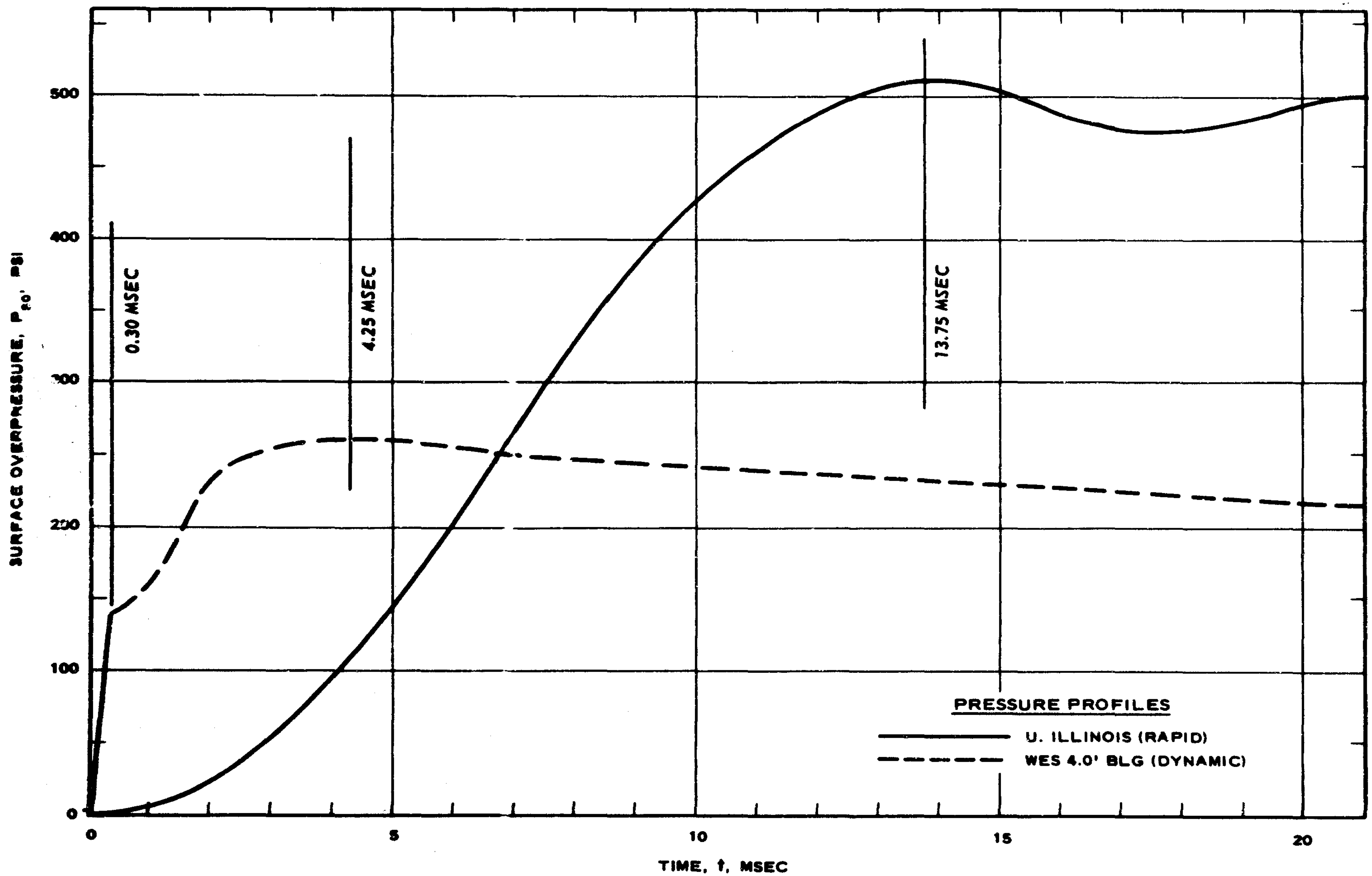

Fig. 4.3 Overpressure-Time Relation for Rapid and Dynamic Loading

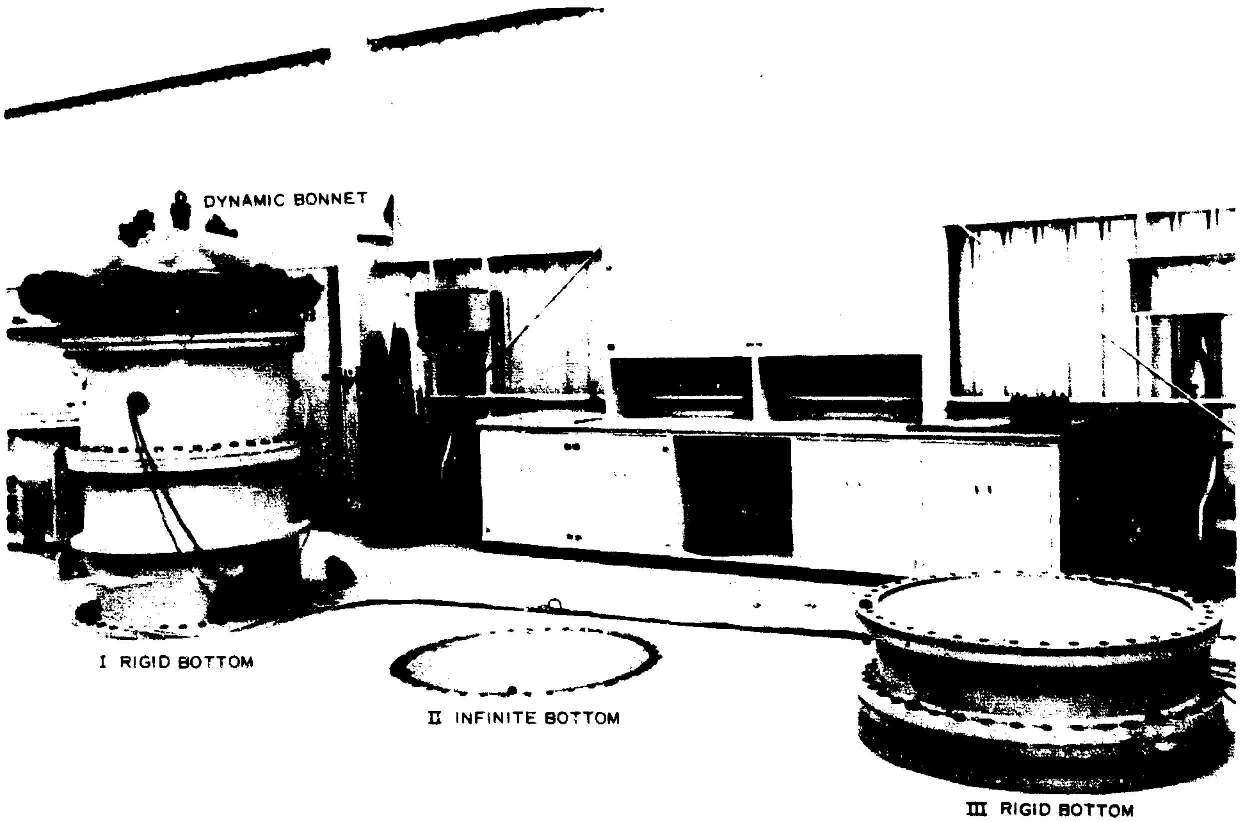

Fig. 4.4 WES Small Blast Load Generator (SBLG) Facility

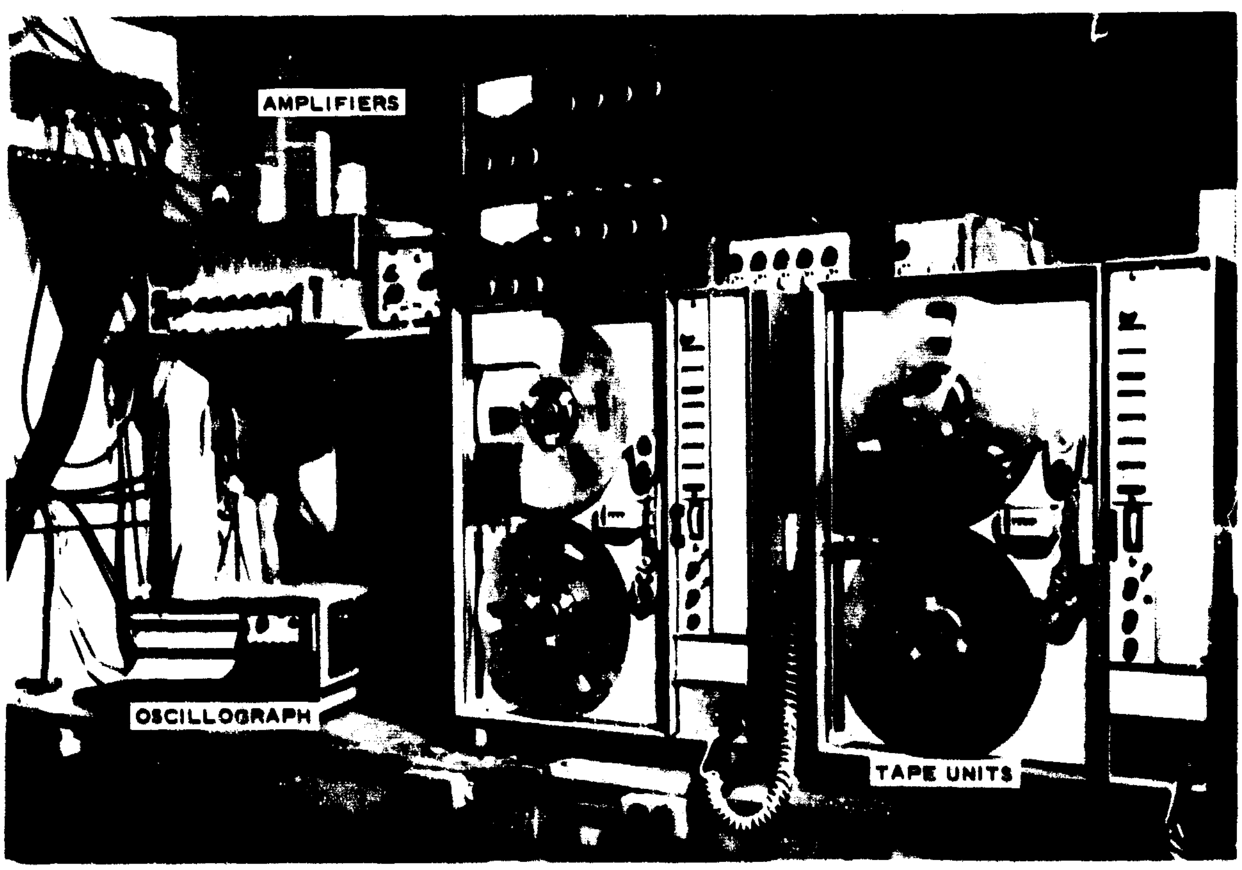

Fig. 4.5 Illinois Instru ntation Equipment

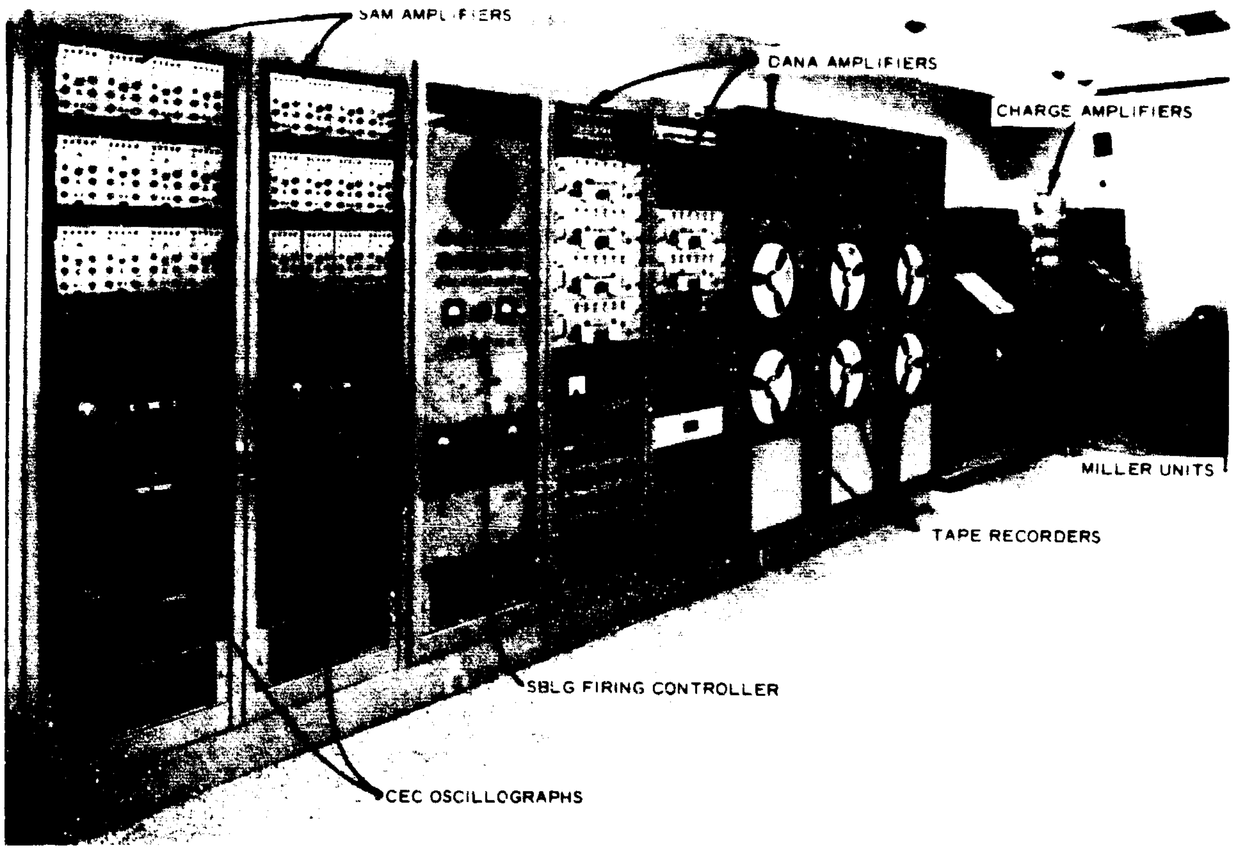

Fig. 4.6 WES Large Instrumentation Room

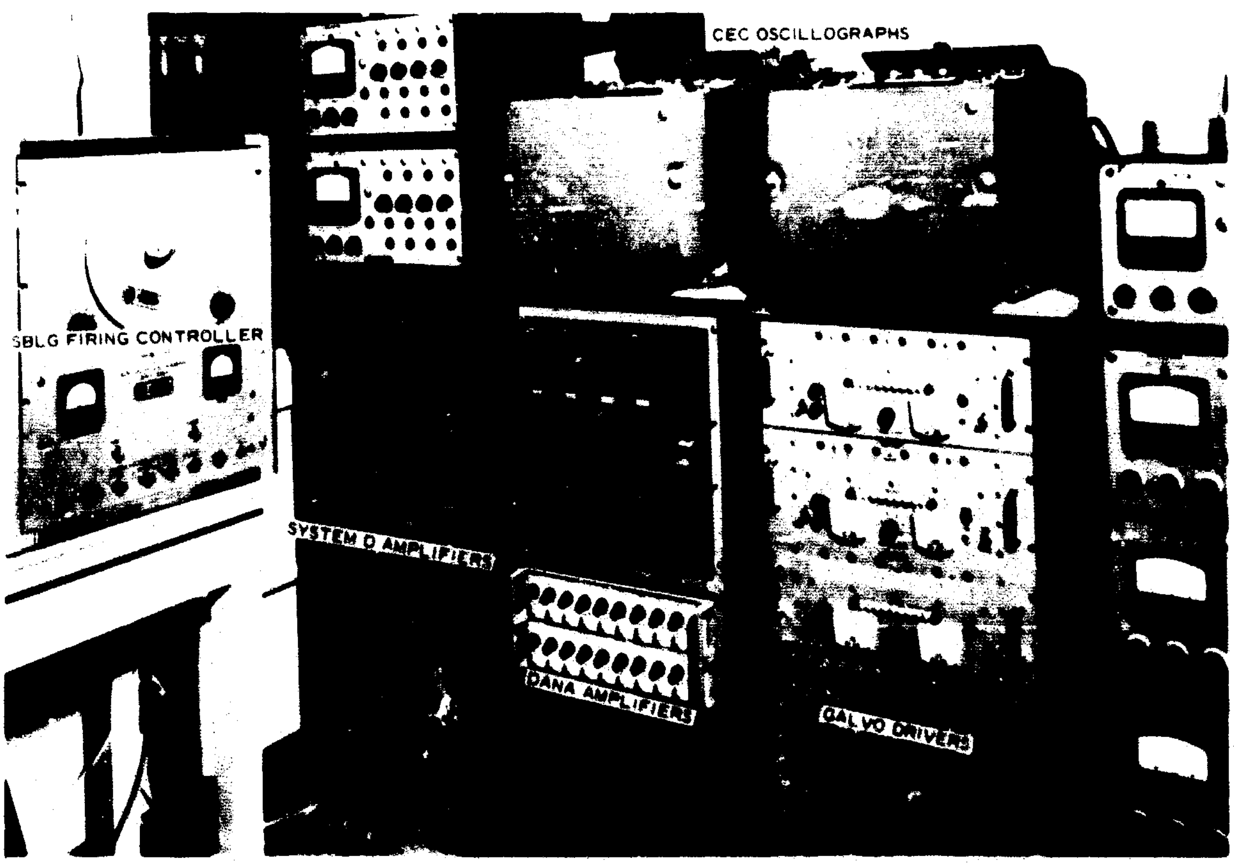

Fig. 4.7 WES Small Blast Load Generator (SBLG) Instrumentation

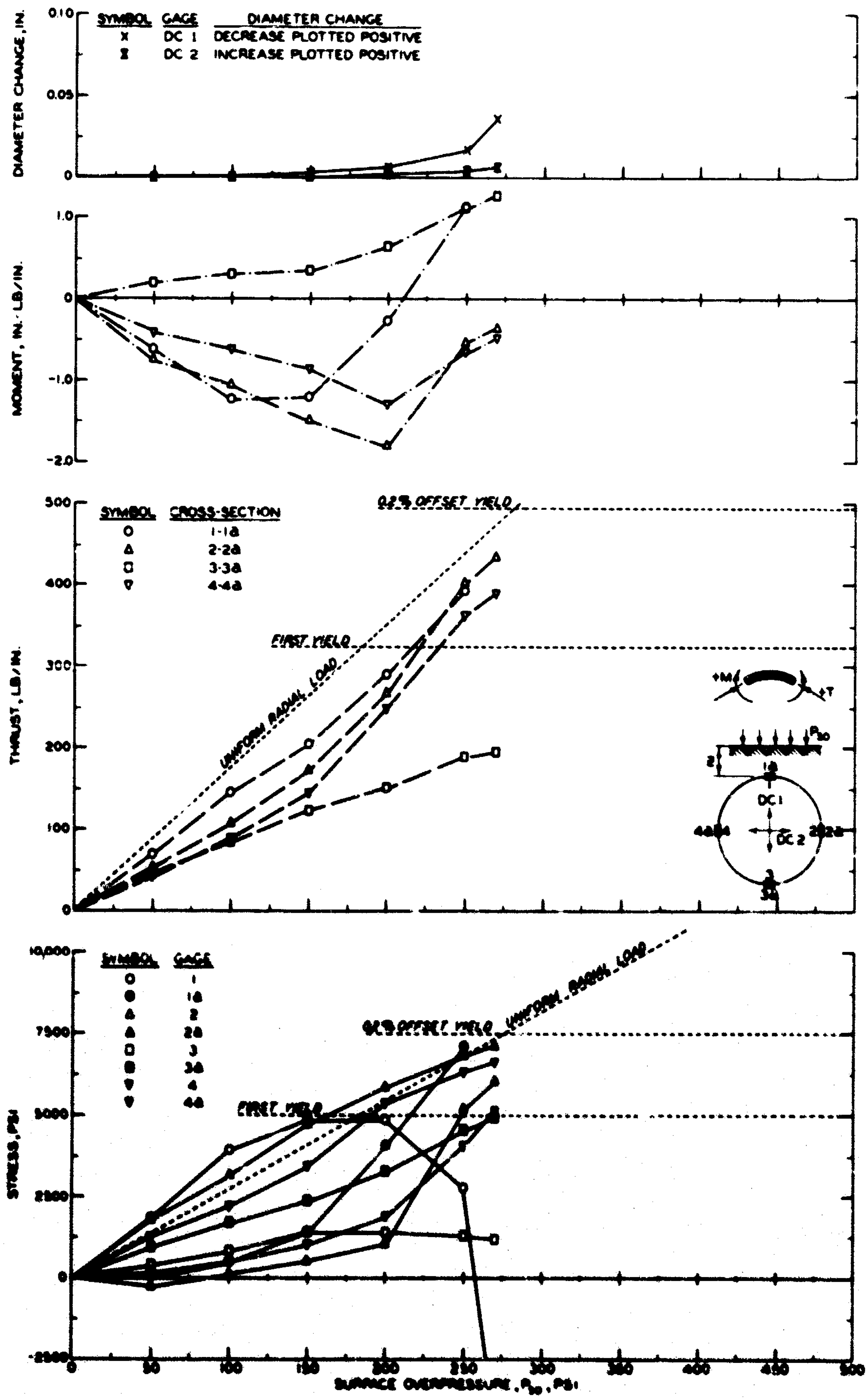

Fig. 5.1 Stress, Thrust, Moment, and Deflection, Test A-1 (Z = 0 in.)

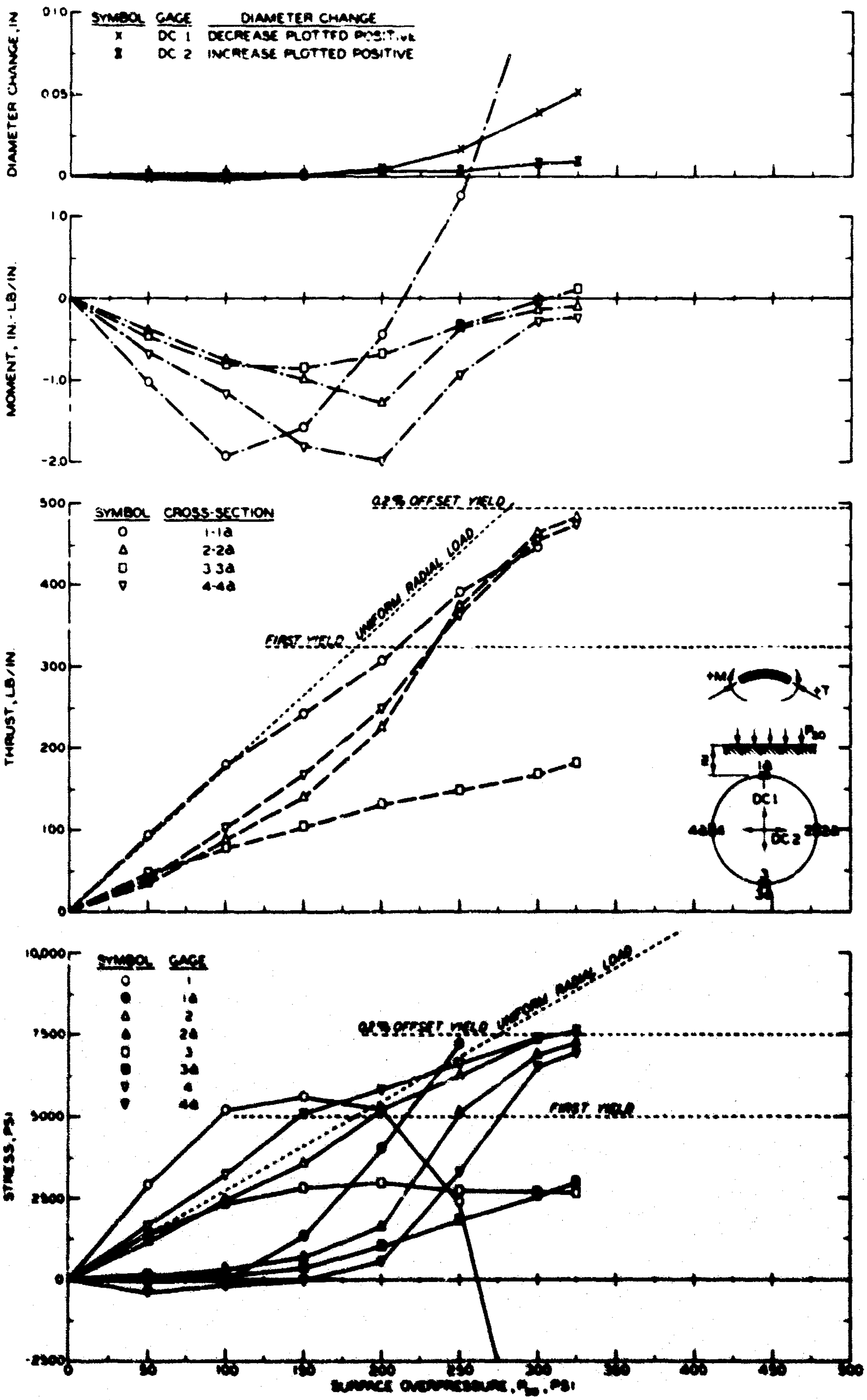

Fig. 5.2 Stress, Thrust, Moment, and Deflection, Test A-5 (Z = 3/16 in.)

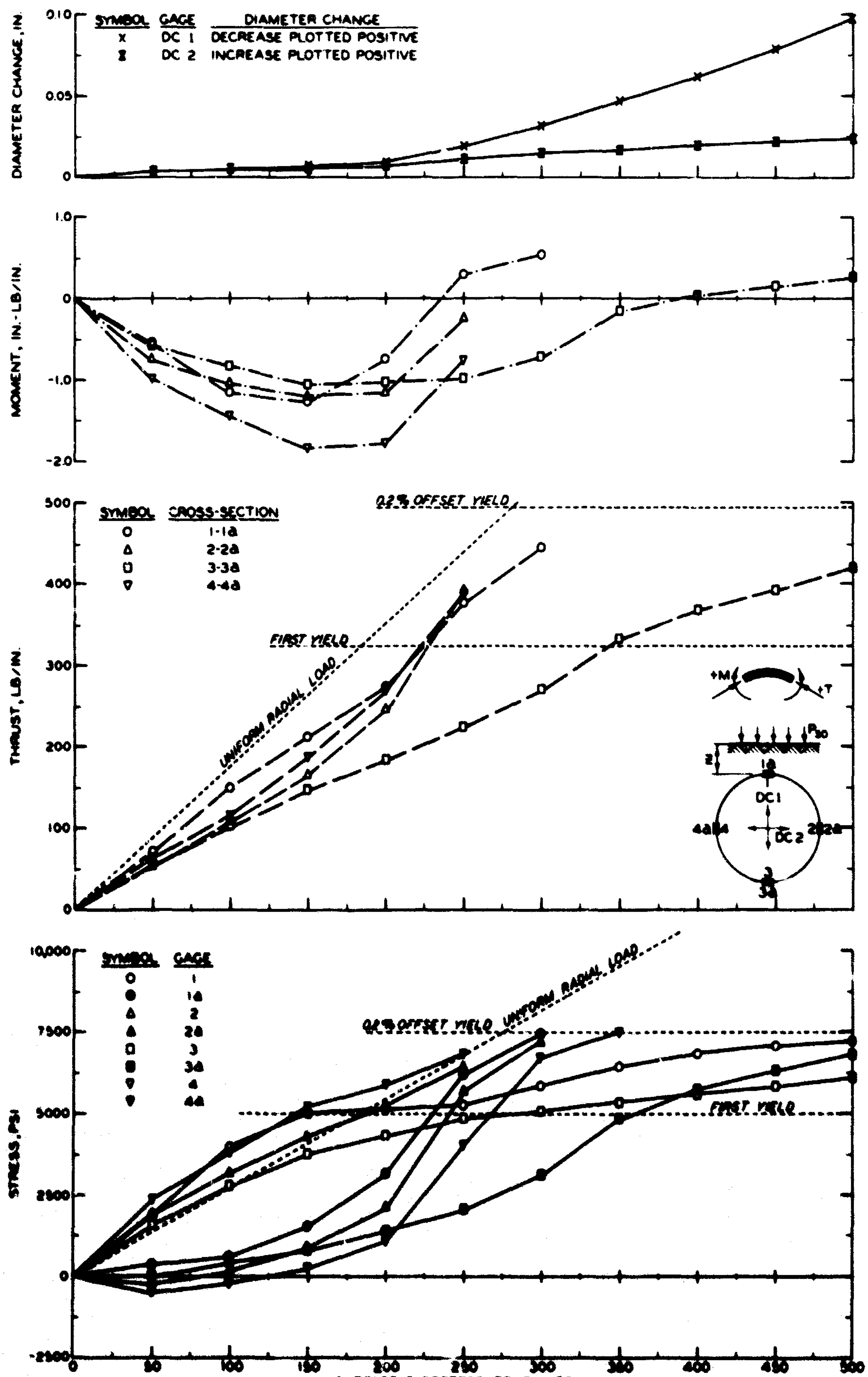

Fig. 5.3 Stress, Thrust, Moment, and Deflection, Test A-2 (Z = 7/16 in.)

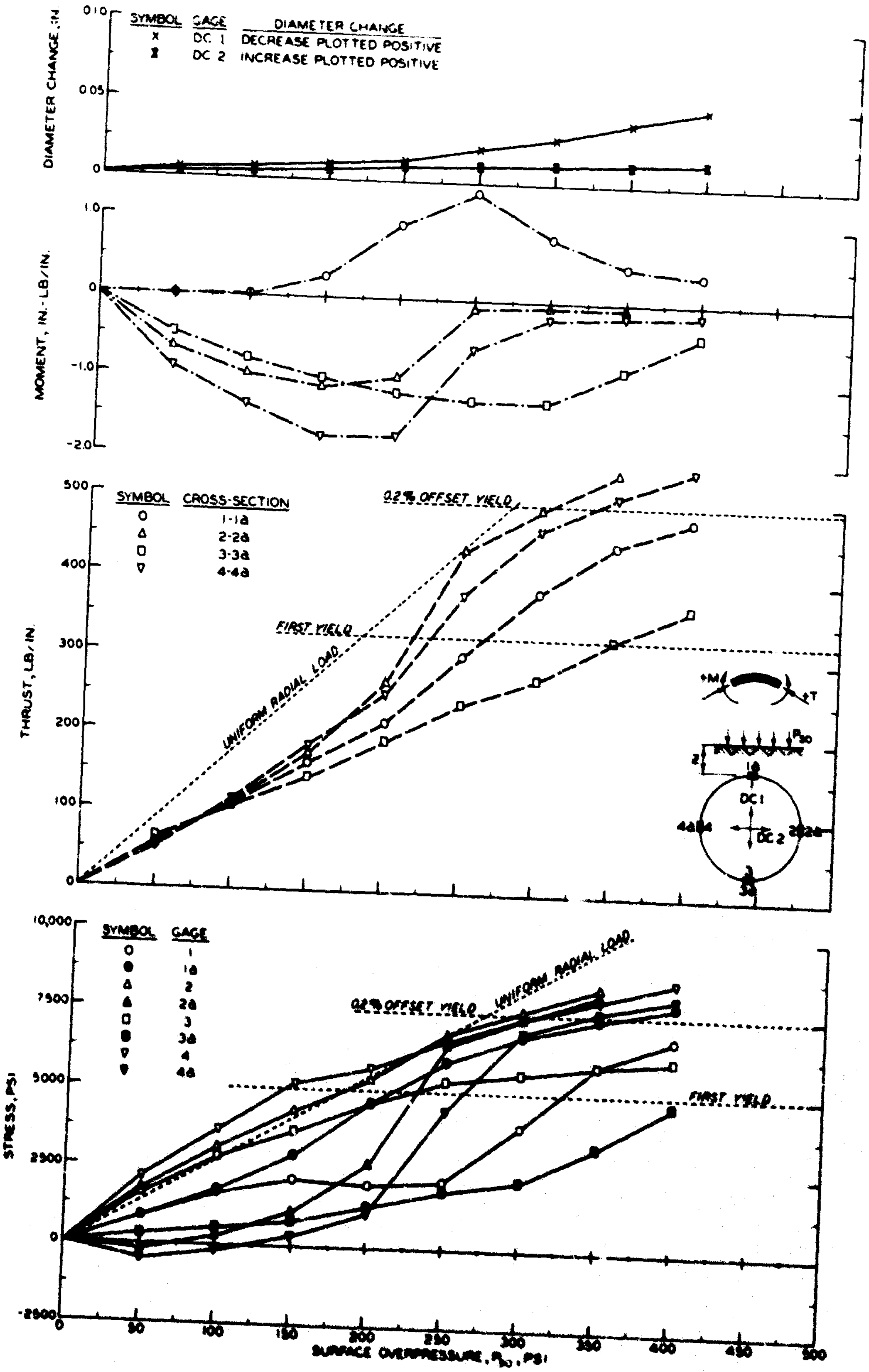

Fig. 5.4 Stress, Thrust, Moment, and Deflection, Test A-3A (Z = 7/8 in.)

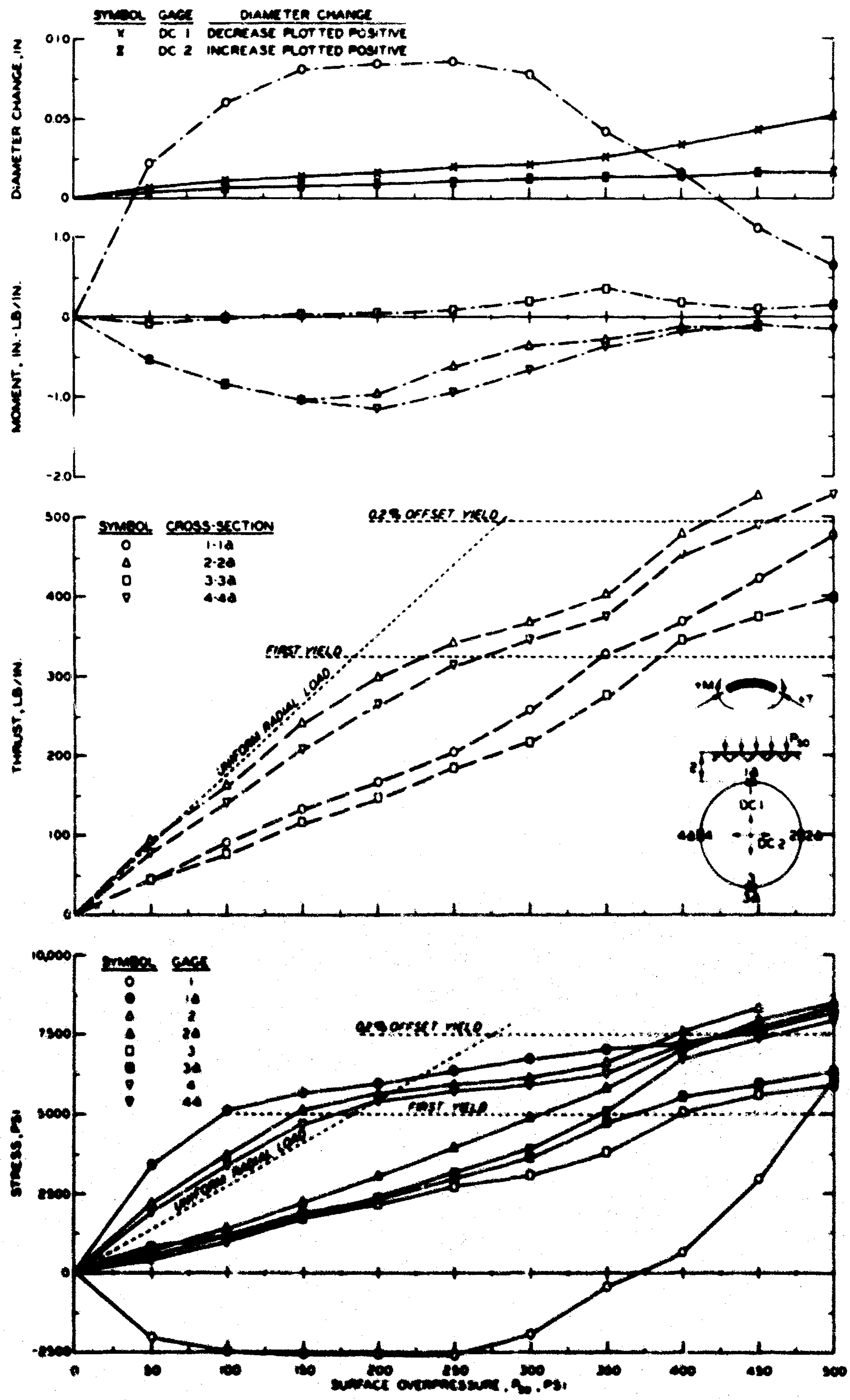

Fig. 5.5 Stress, Thrust, Moment, and Deflection, Test A-3B (Z = 7/8 in.)

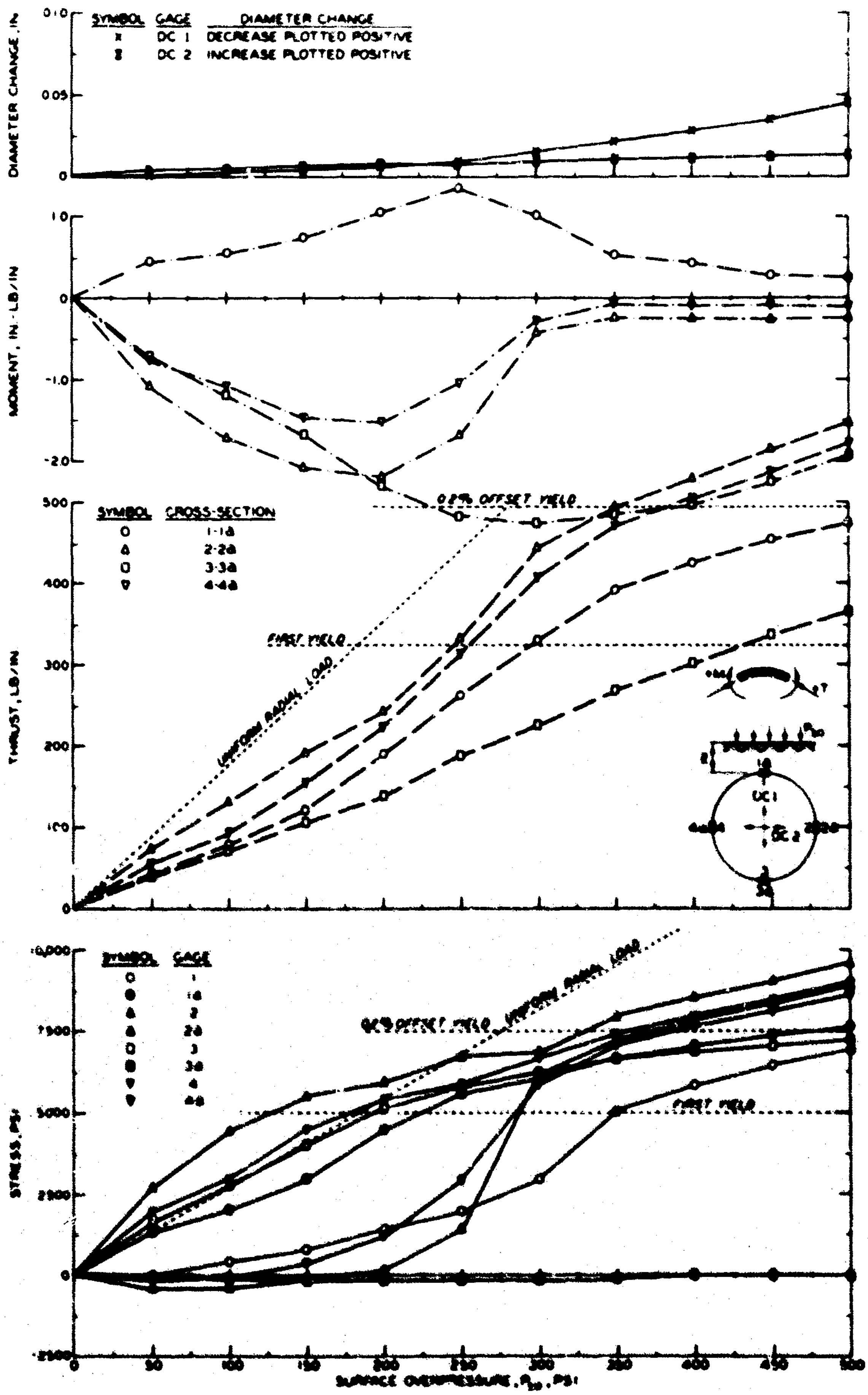

Fig. 5.6 Stress, Thrust, Moment, and Deflection, Test A-4 (Z = 1-3/4 in.)

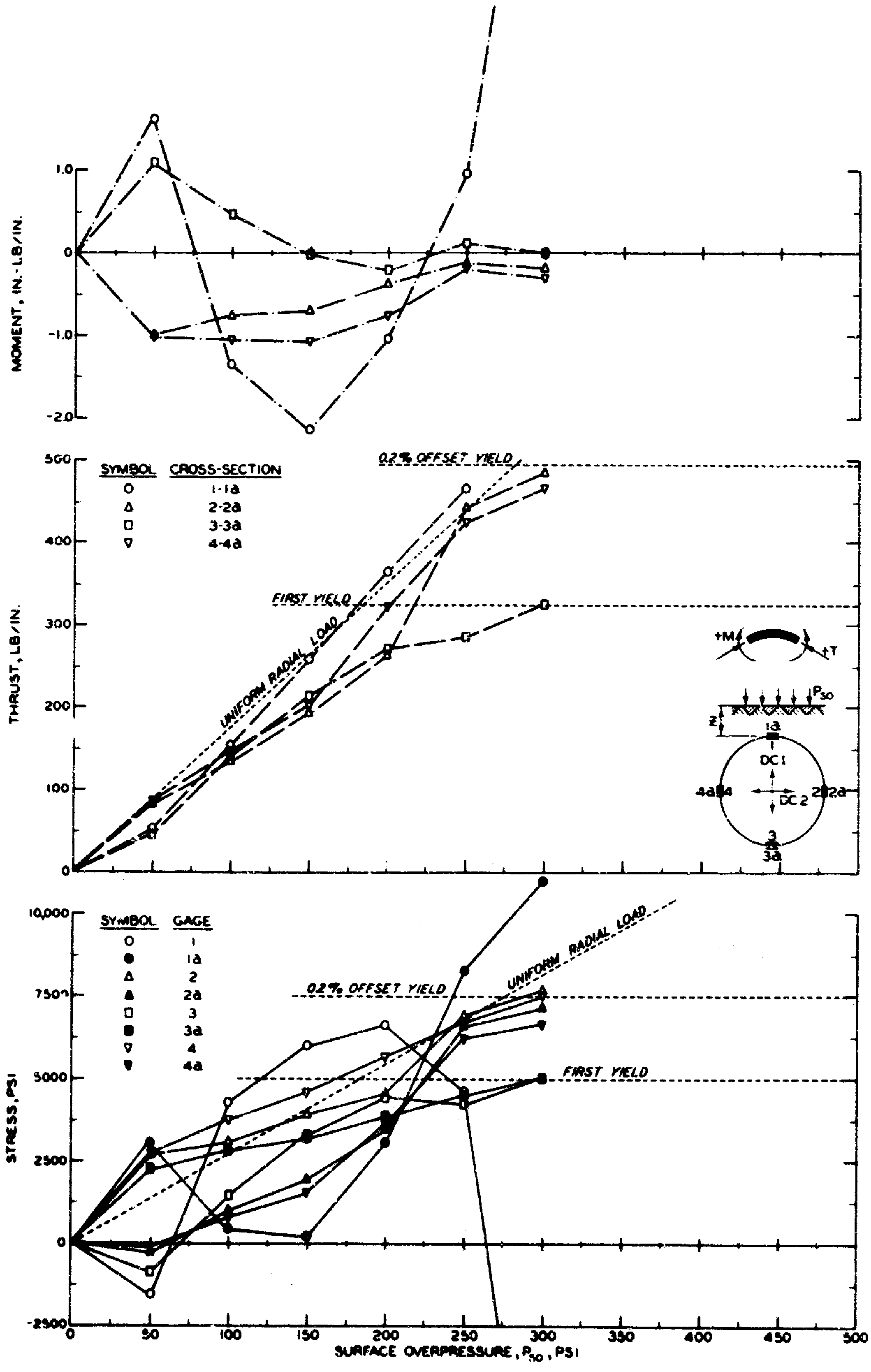

Fig. 5.7 Stress, Thrust, and Moment, Test A-10 (Z = 0 in.)

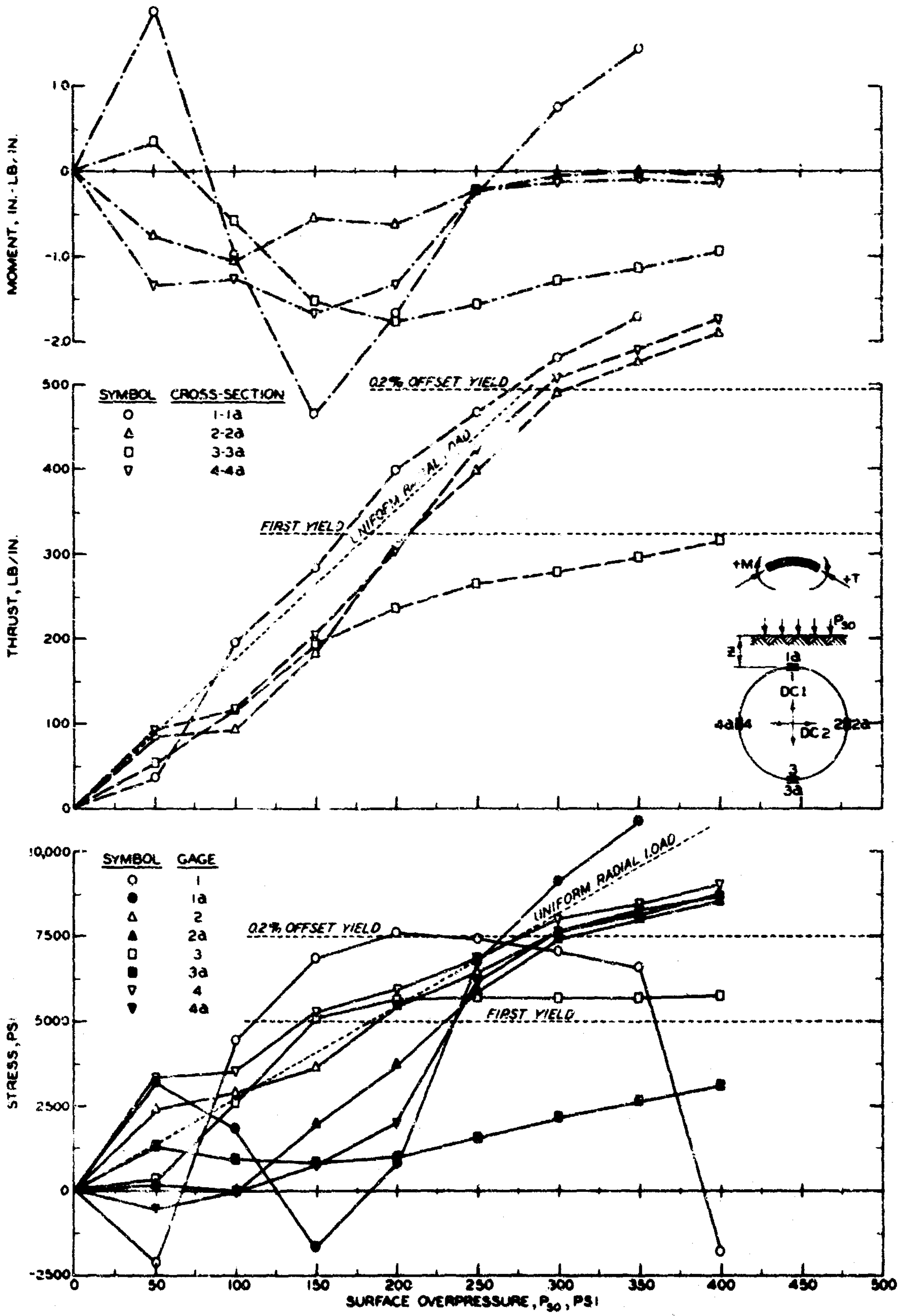

Fig. 5.8 Stress, Thrust, and Moment, Test A-9 (Z = 3/16 in.)

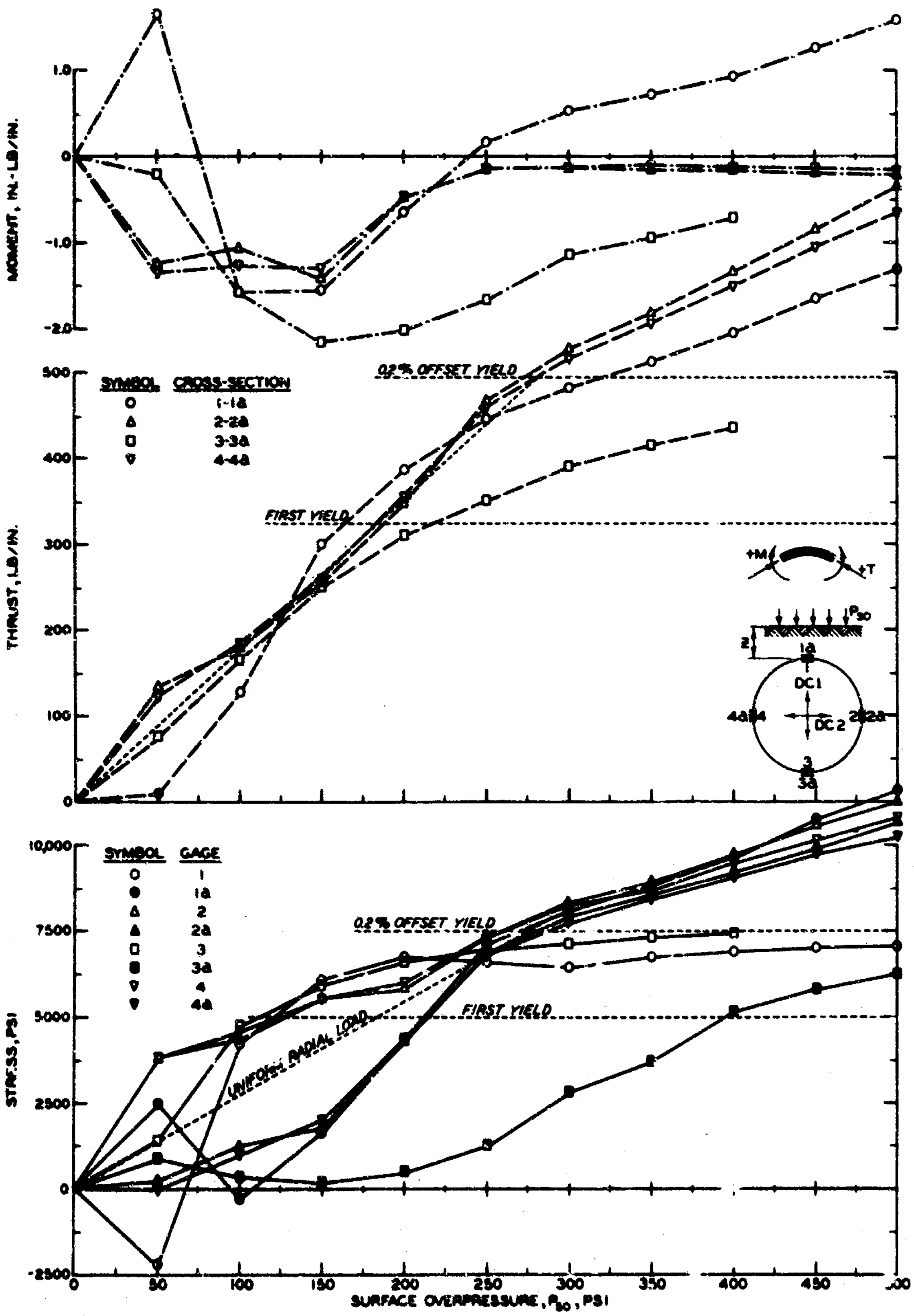

Fig. 5.9 Stress, Thrust, and Moment, Test A-8 (Z = 1/16 in.)

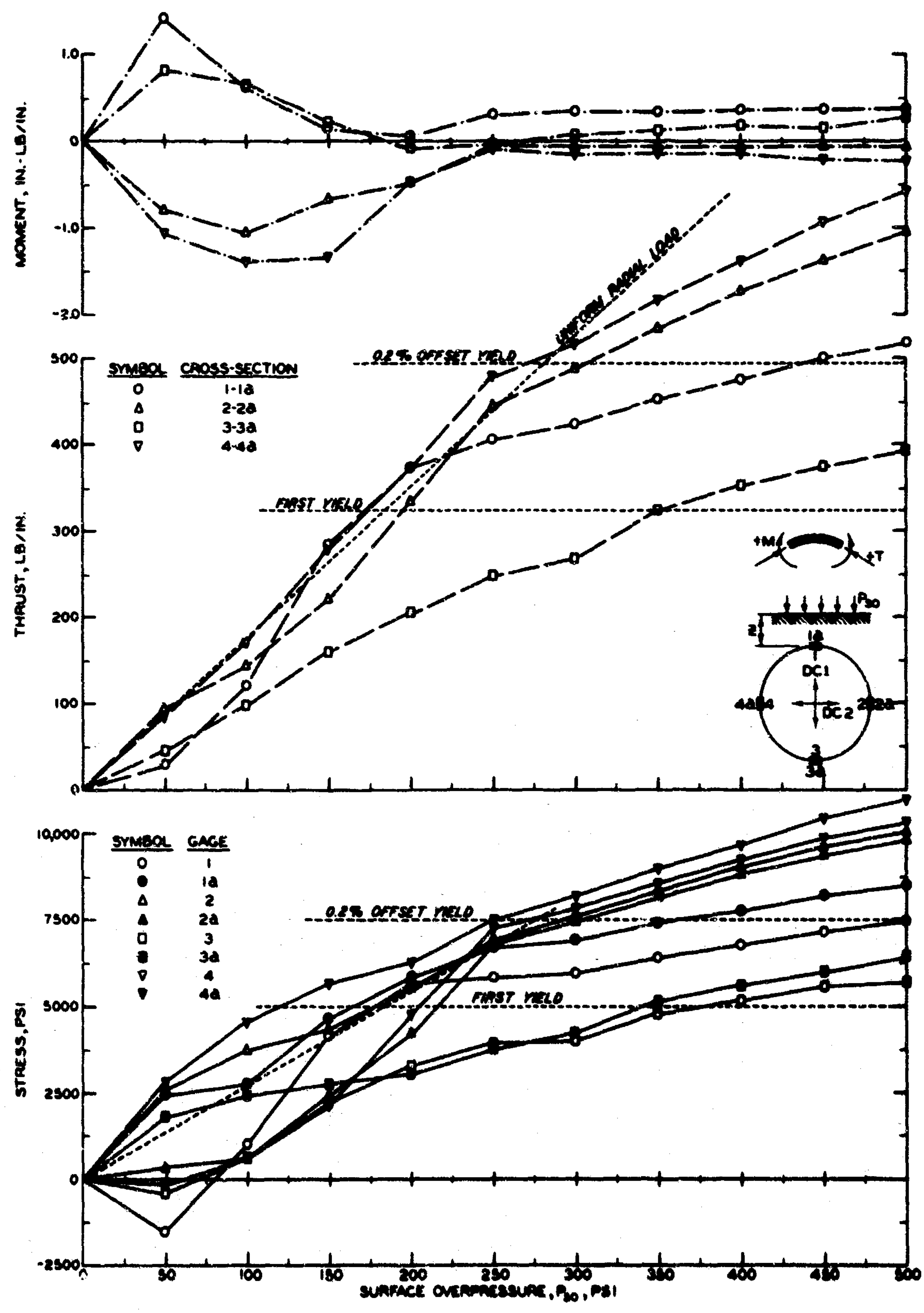

Fig. 5.10 Stress, Thrust, and Moment, Test A-7 (Z = 7/8 in.)

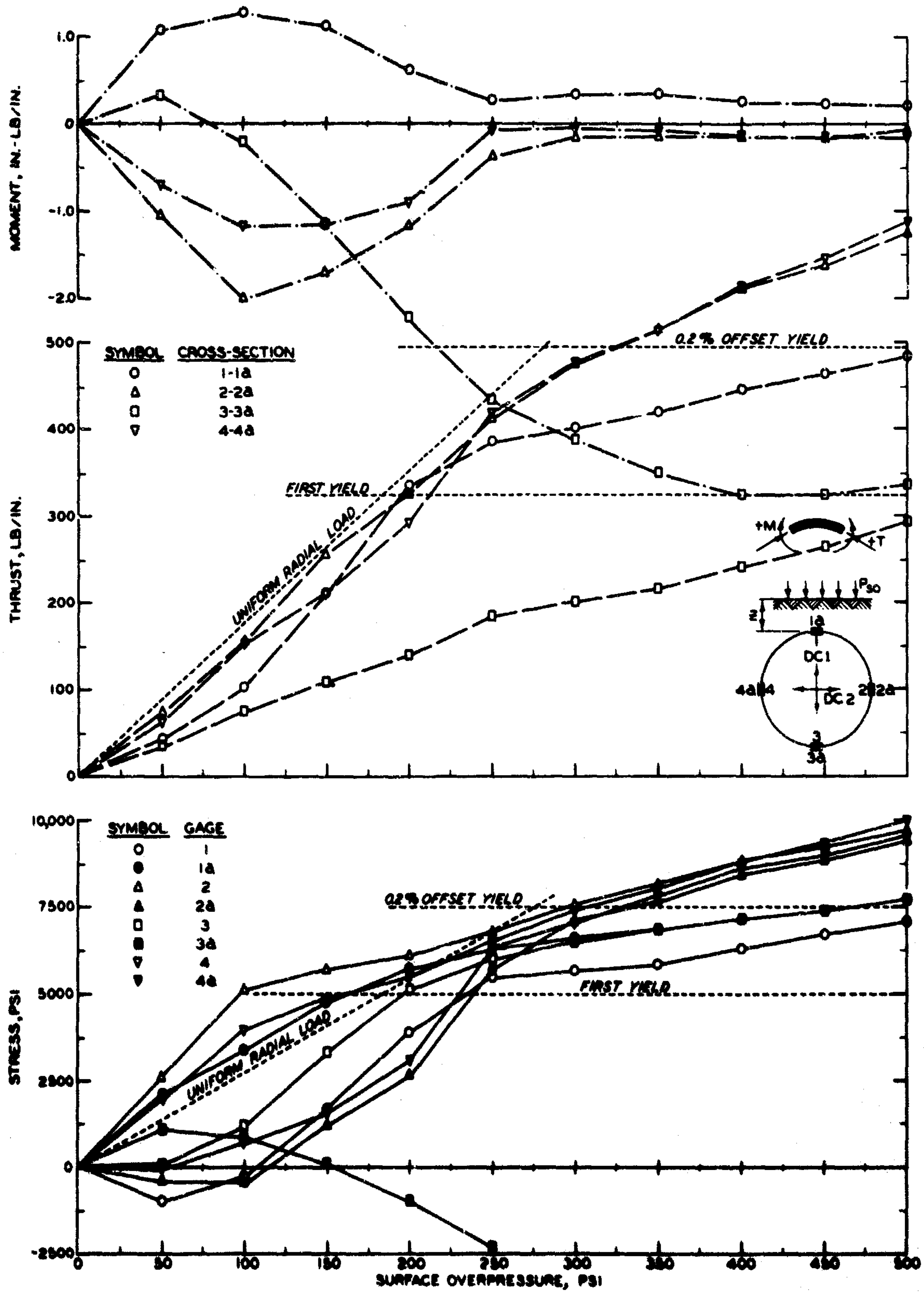

Fig. 5.11 Stress, Thrust, and Moment, Test A-6 (Z = 1-3/4 in.)

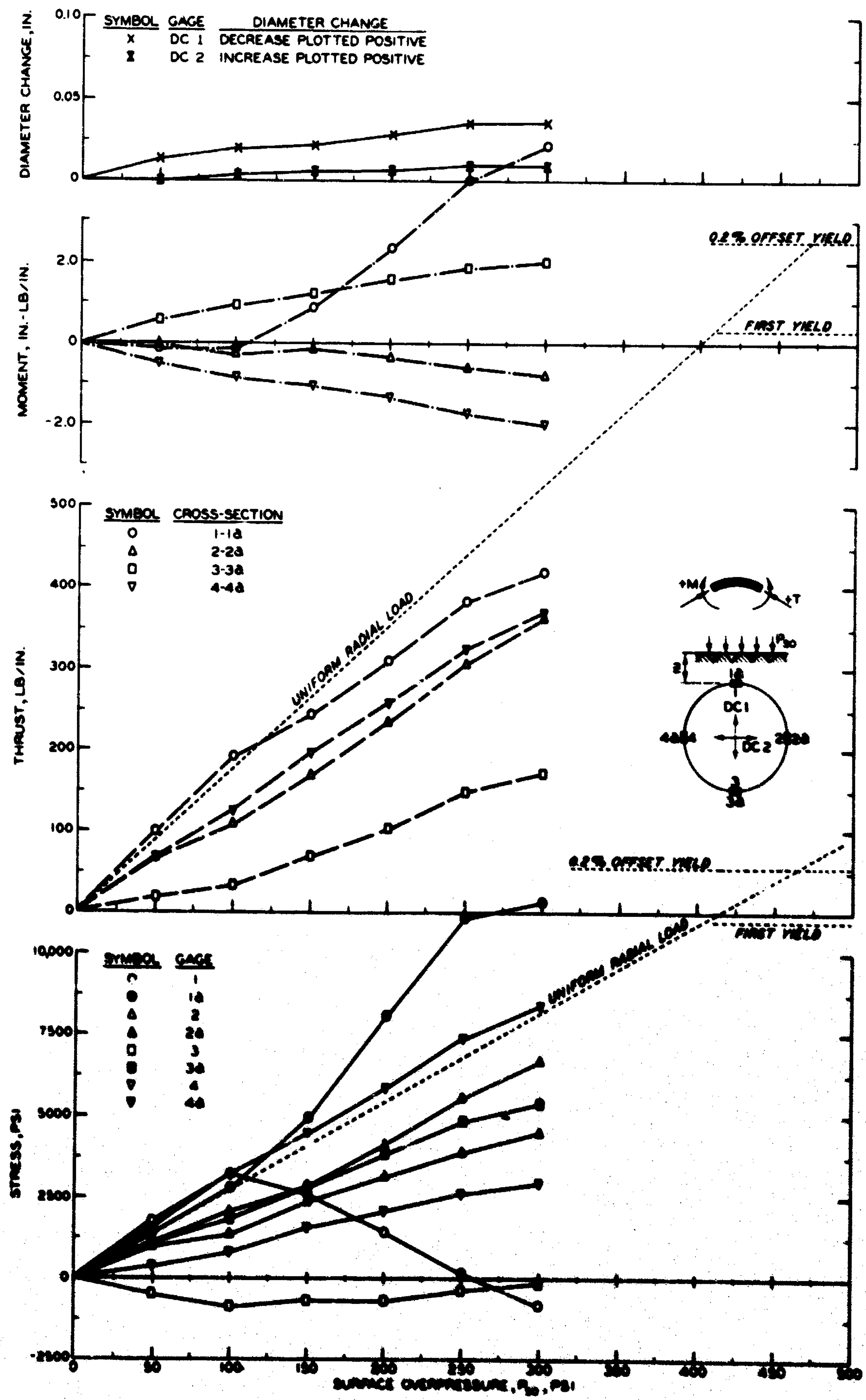

Fig. 5.12 Stress, Thrust, Moment, and Deflection, Test B-1A (Z = 0 in.)

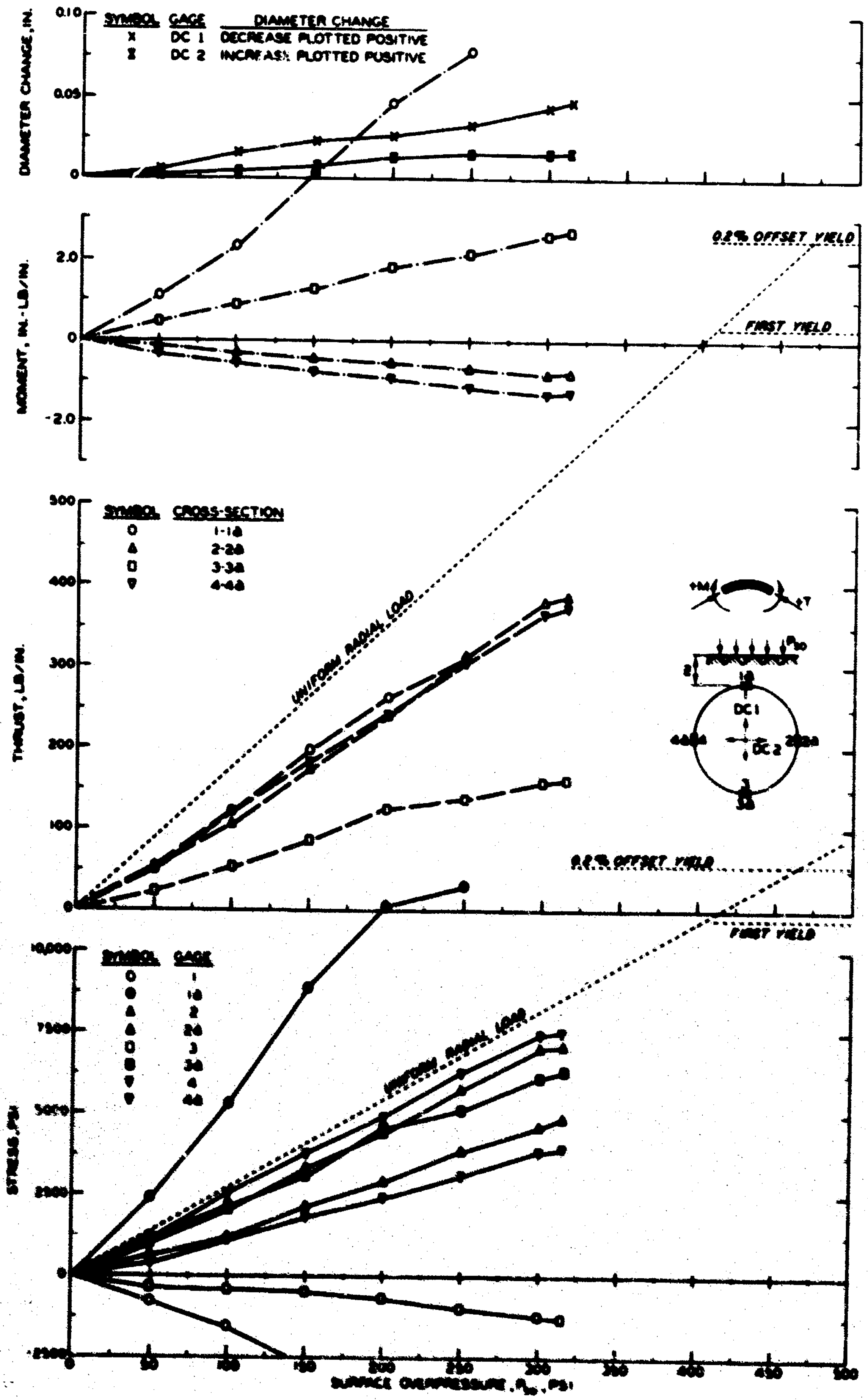

Fig. 5.13 Stress, Thrust, Moment, and Deflection, Test B-1B (Z = 0 in.)

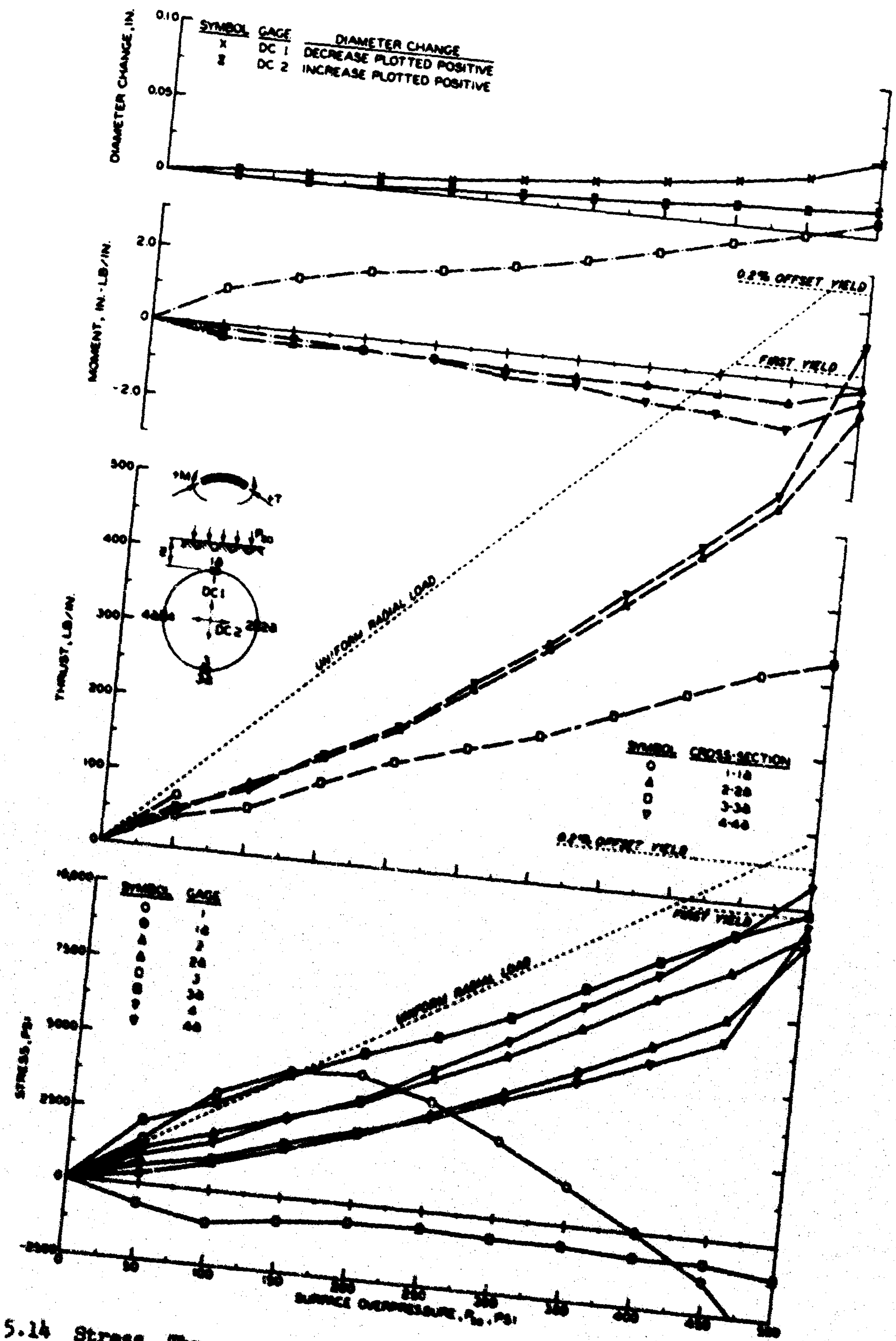

Fig. 5.14 Stress, Thrust, Moment, and Deflection, Test B-5 (Z = 7/16 in.)

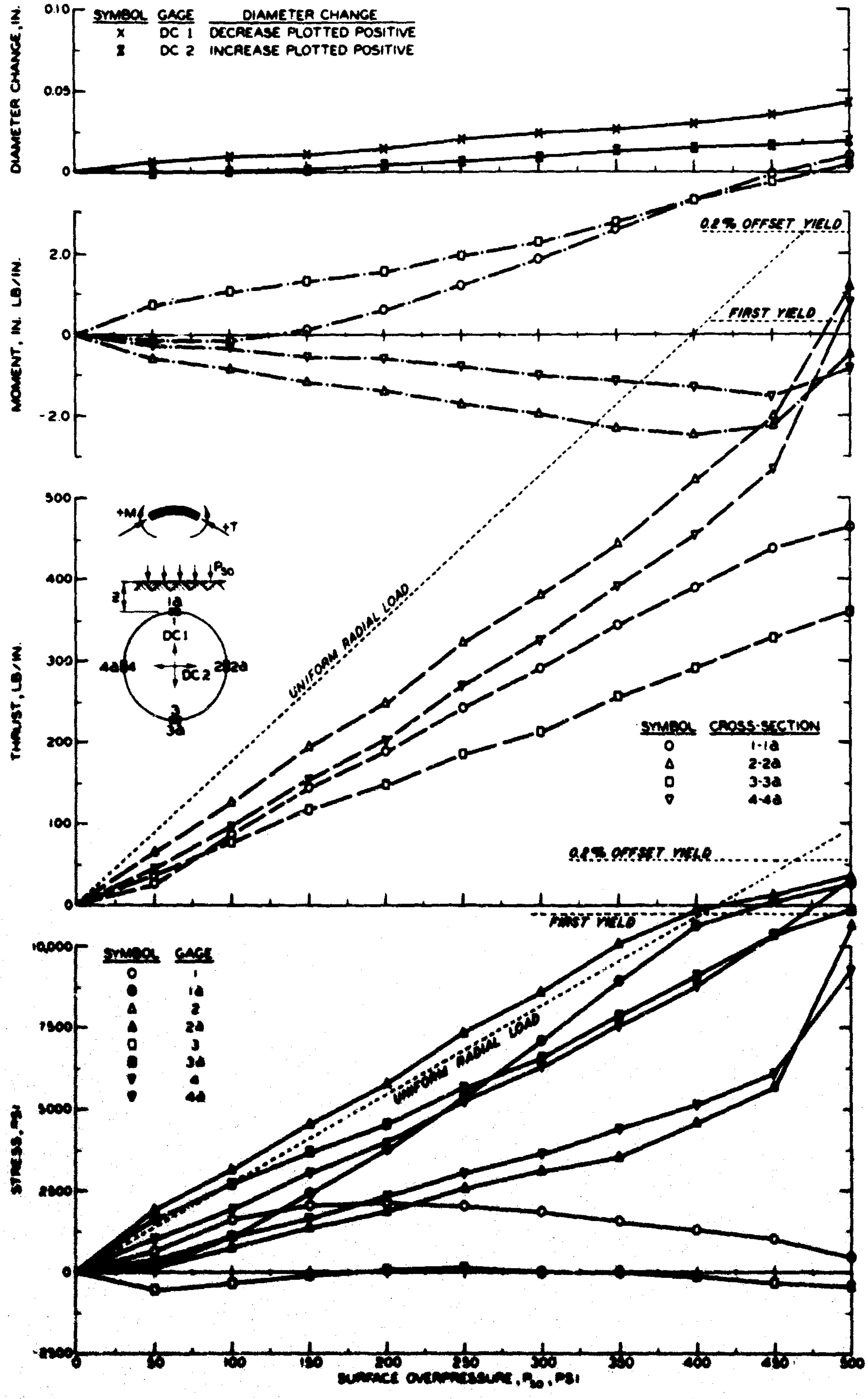

Fig. 5.15 Stress, Thrust, Moment, and Deflection, Test B-2 (Z = 7/8 in.)

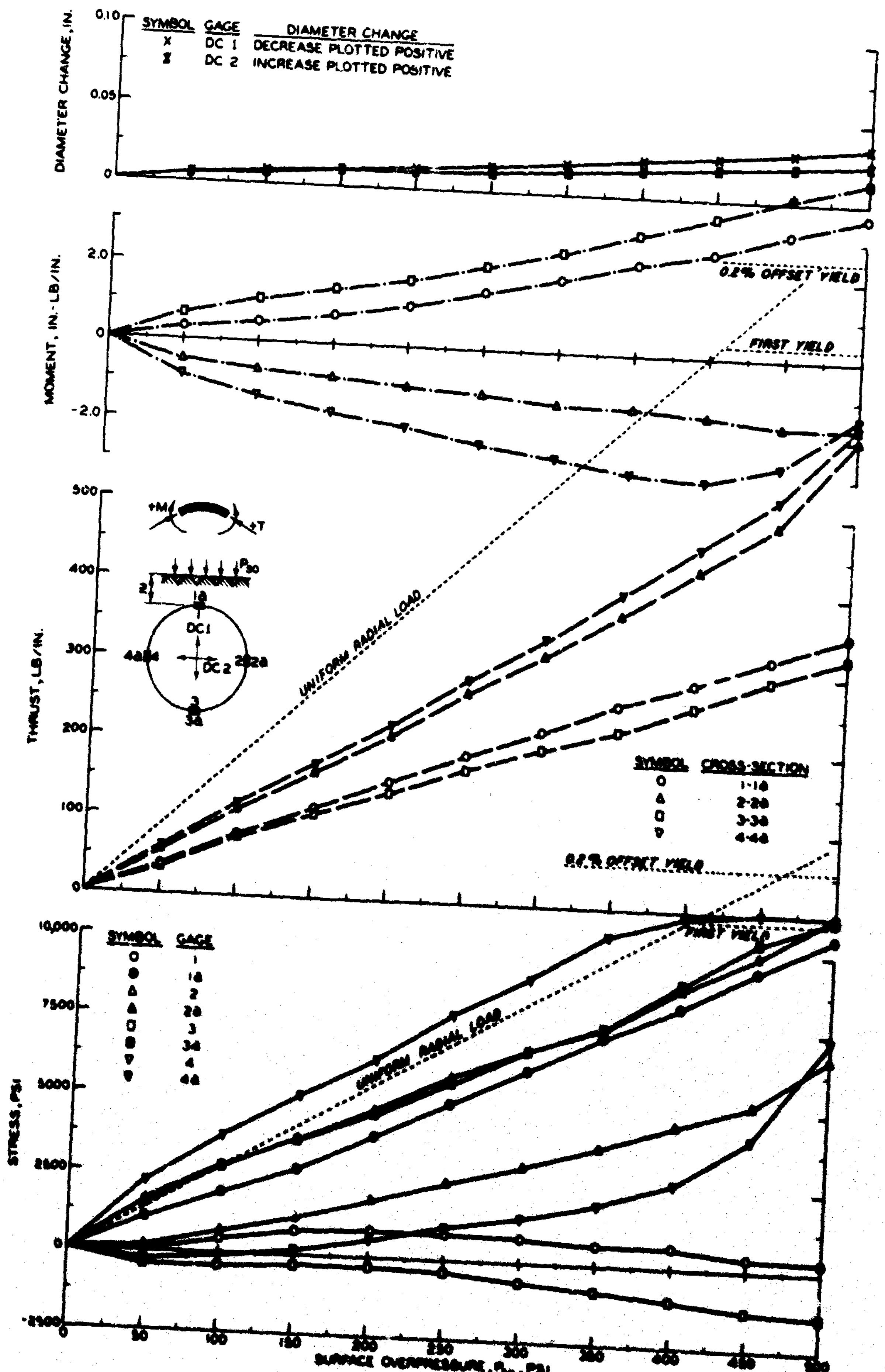

Fig. 5.16 Stress, Thrust, Moment, and Deflection, Test B-3 (Z = 1-3/4 in.)

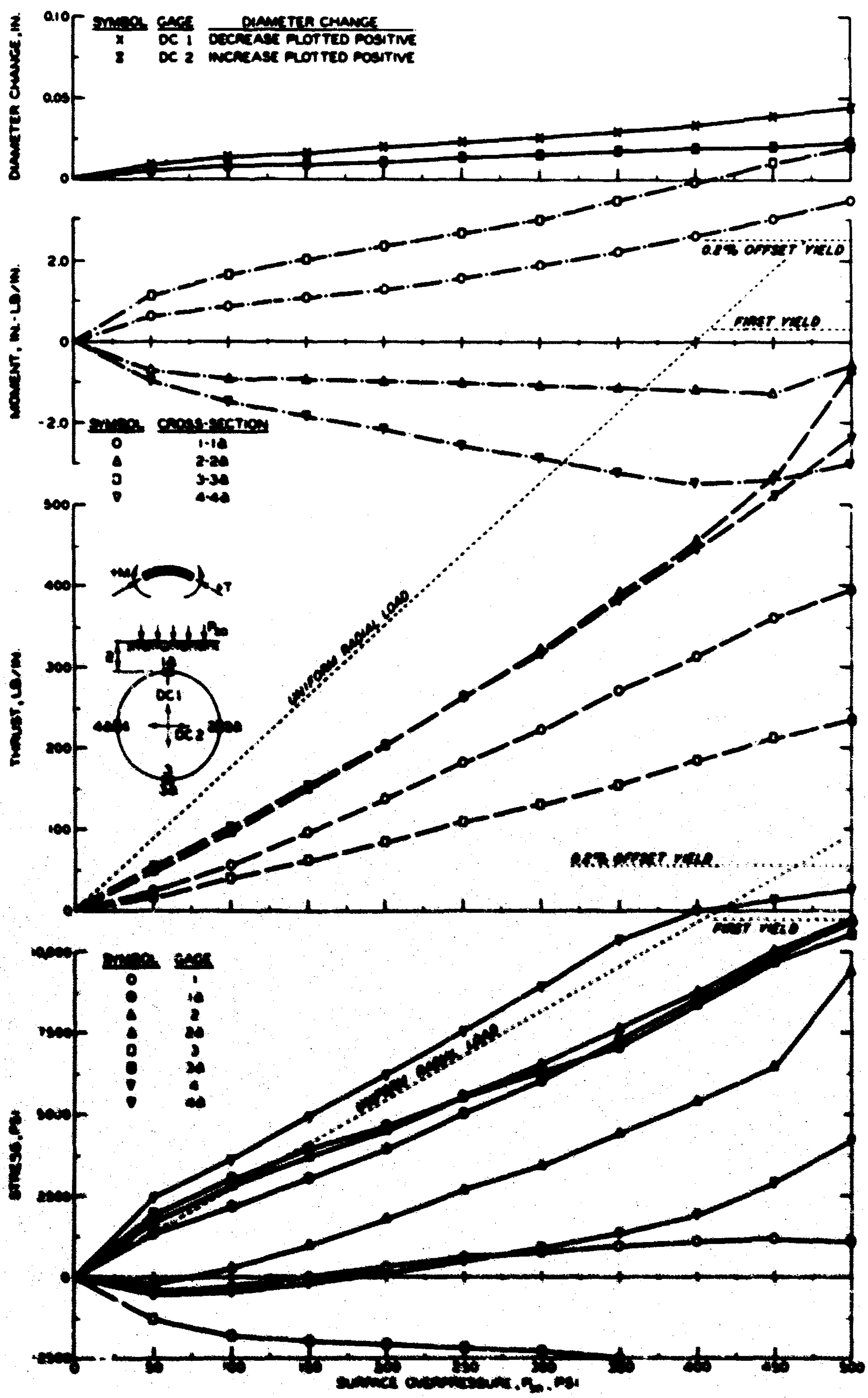

Fig. 5.17 Stress, Thrust, Moment, and Deflection, Test B-4 (Z = 2-5/8 in.)

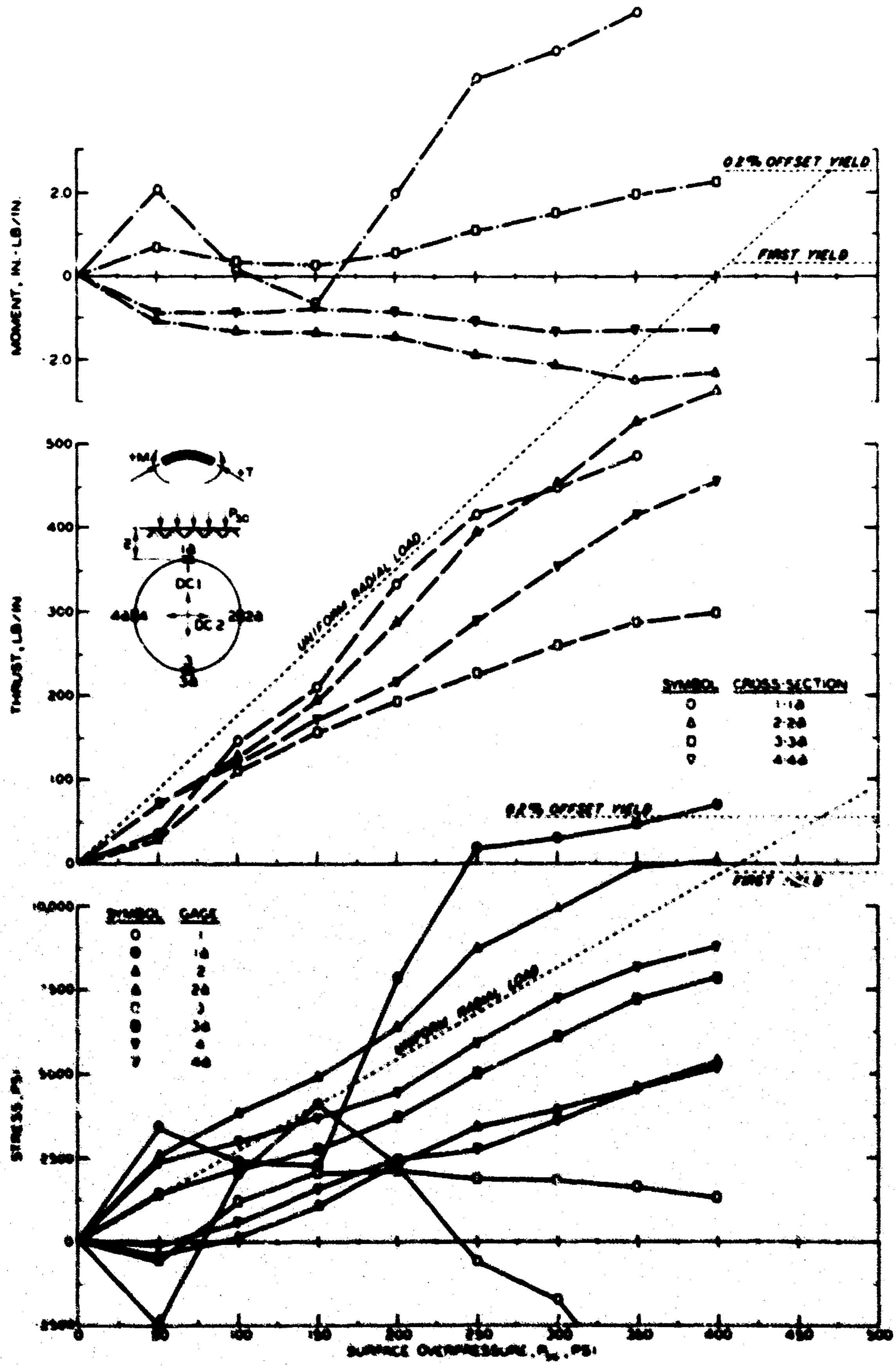

Fig. 5.18 Stress, Thrust, and Moment, Test B-6 (Z = 0 in.)

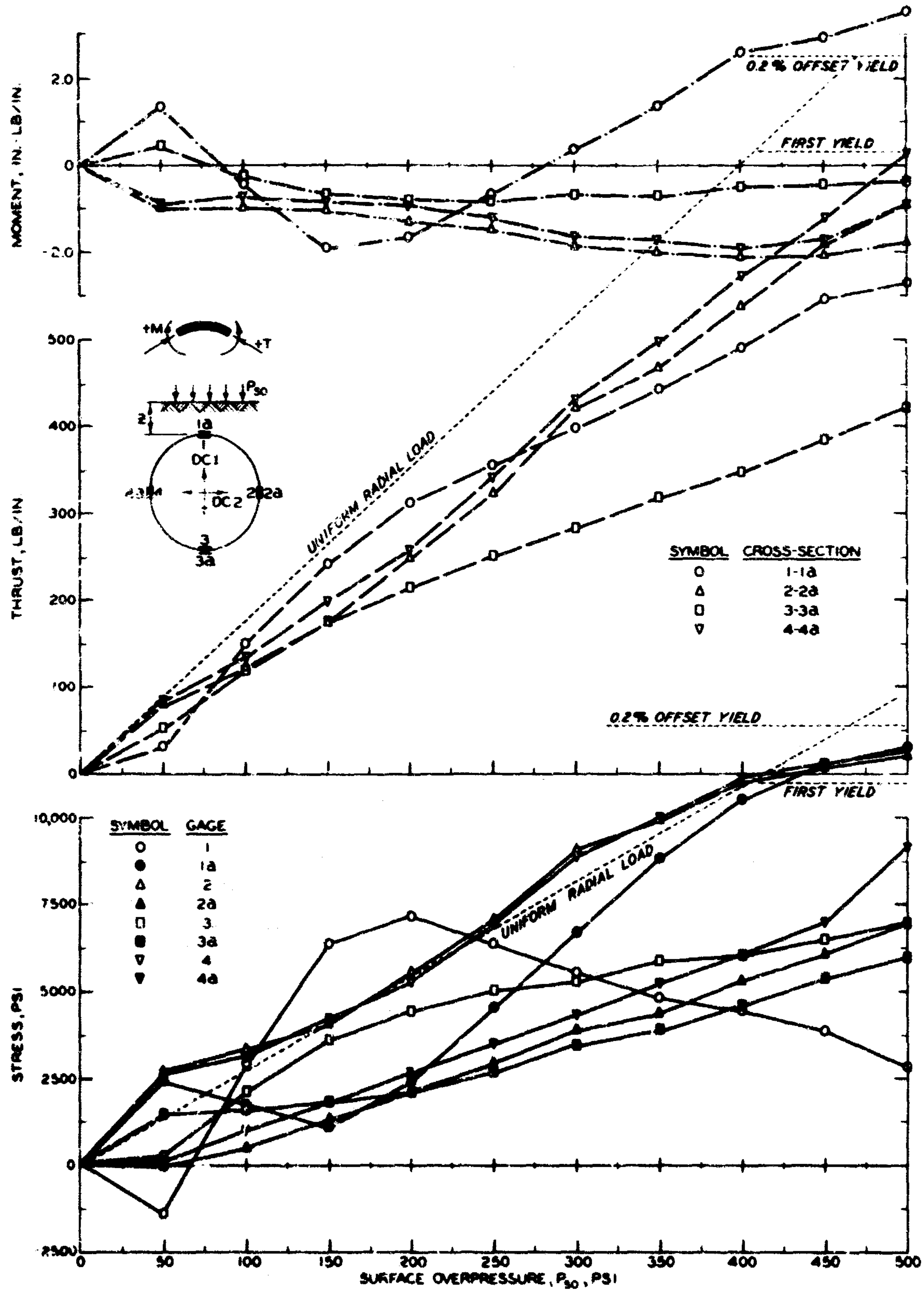

Fig. 5.19 Stress, Thrust, and Moment, Test B-7 (Z = 7/16 in.)

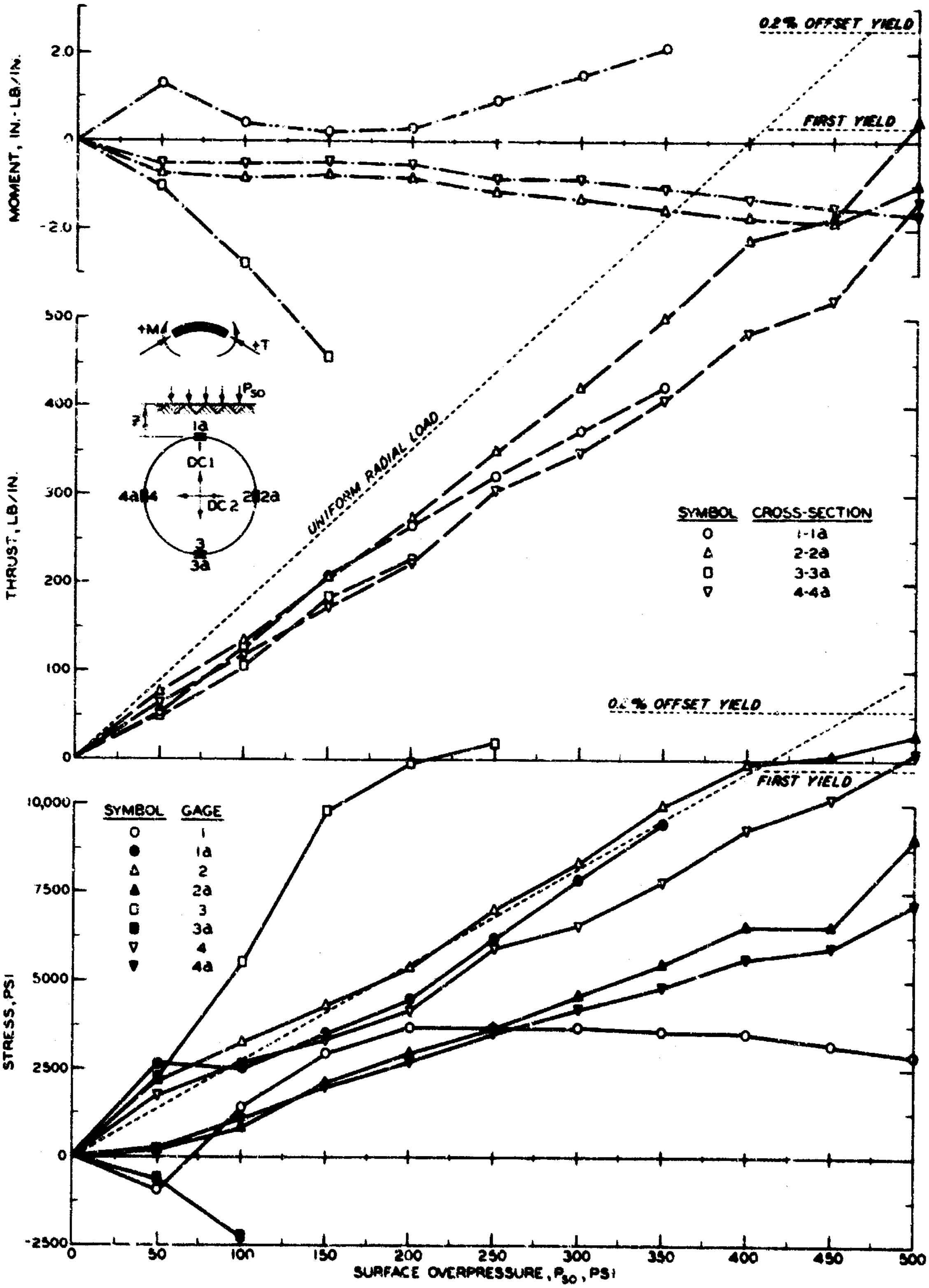

Fig. 5.20 Stress, Thrust, and Moment, Test B-8 (Z = 7/8 in.)

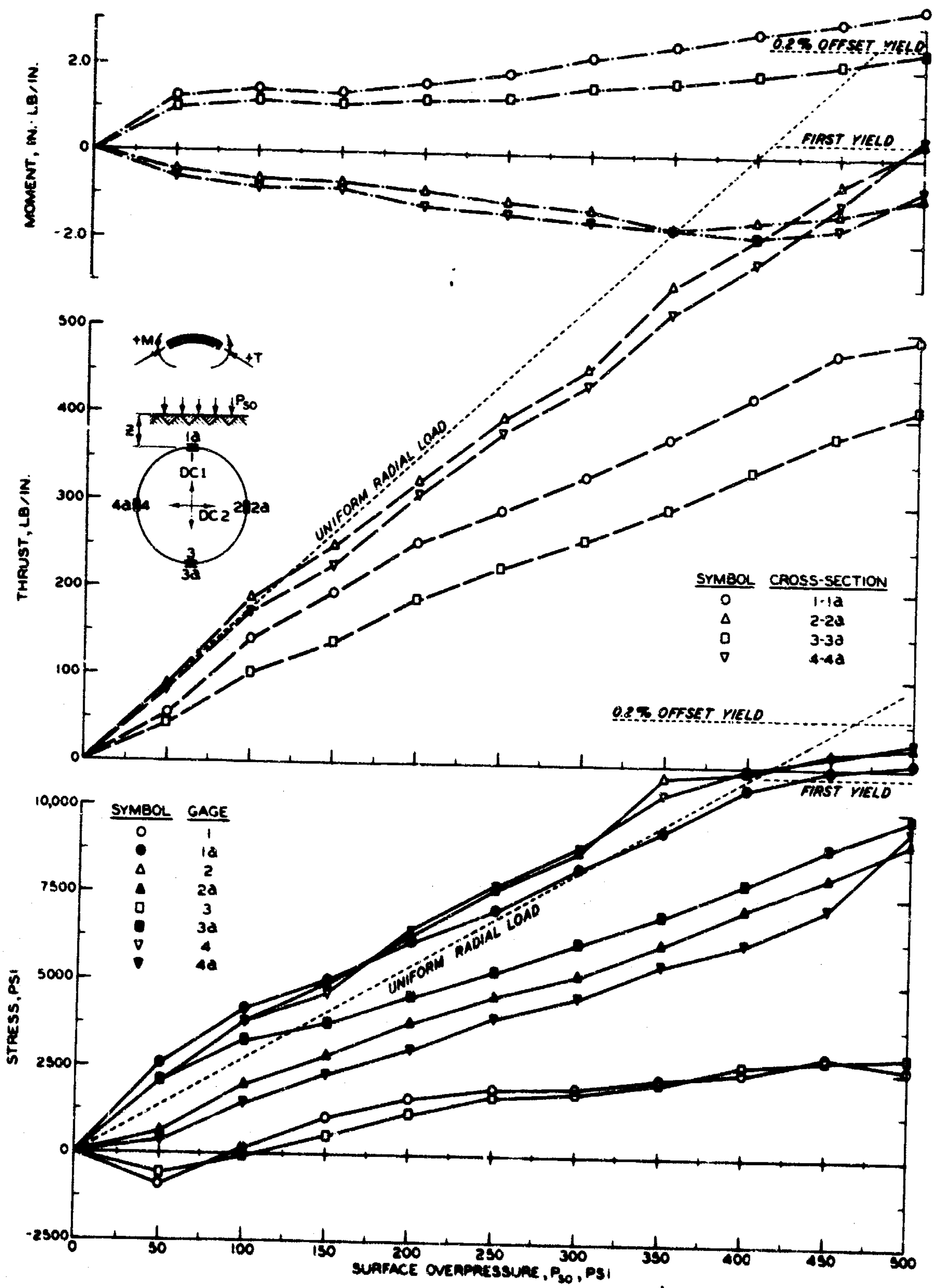

Fig. 5.21 Stress, Thrust, and Moment, Test B-9 (Z = 1-3/4 in.)

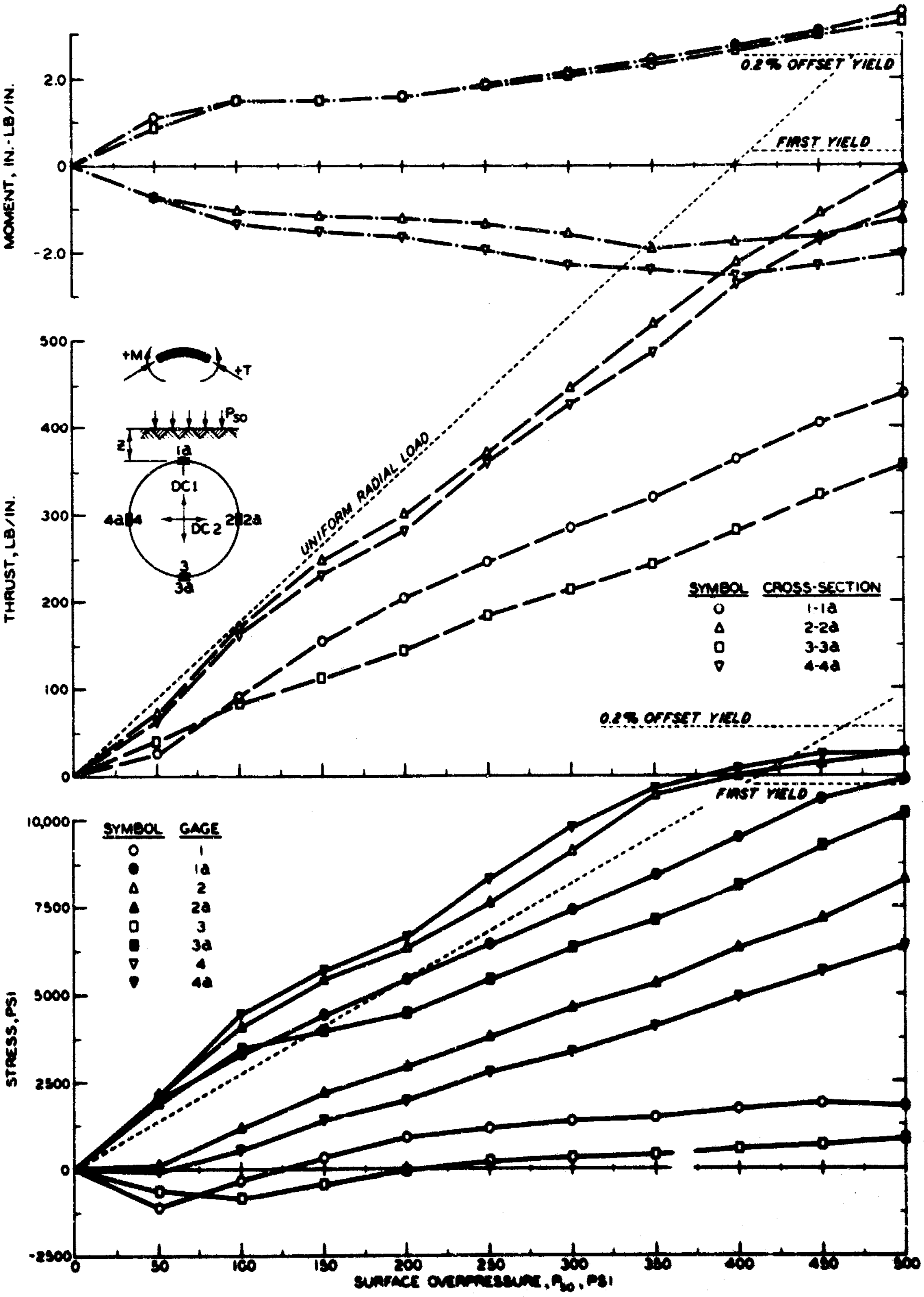

Fig. 5.22 Stress, Thrust, and Moment, Test B-10 (Z = 2-5/8 in.)

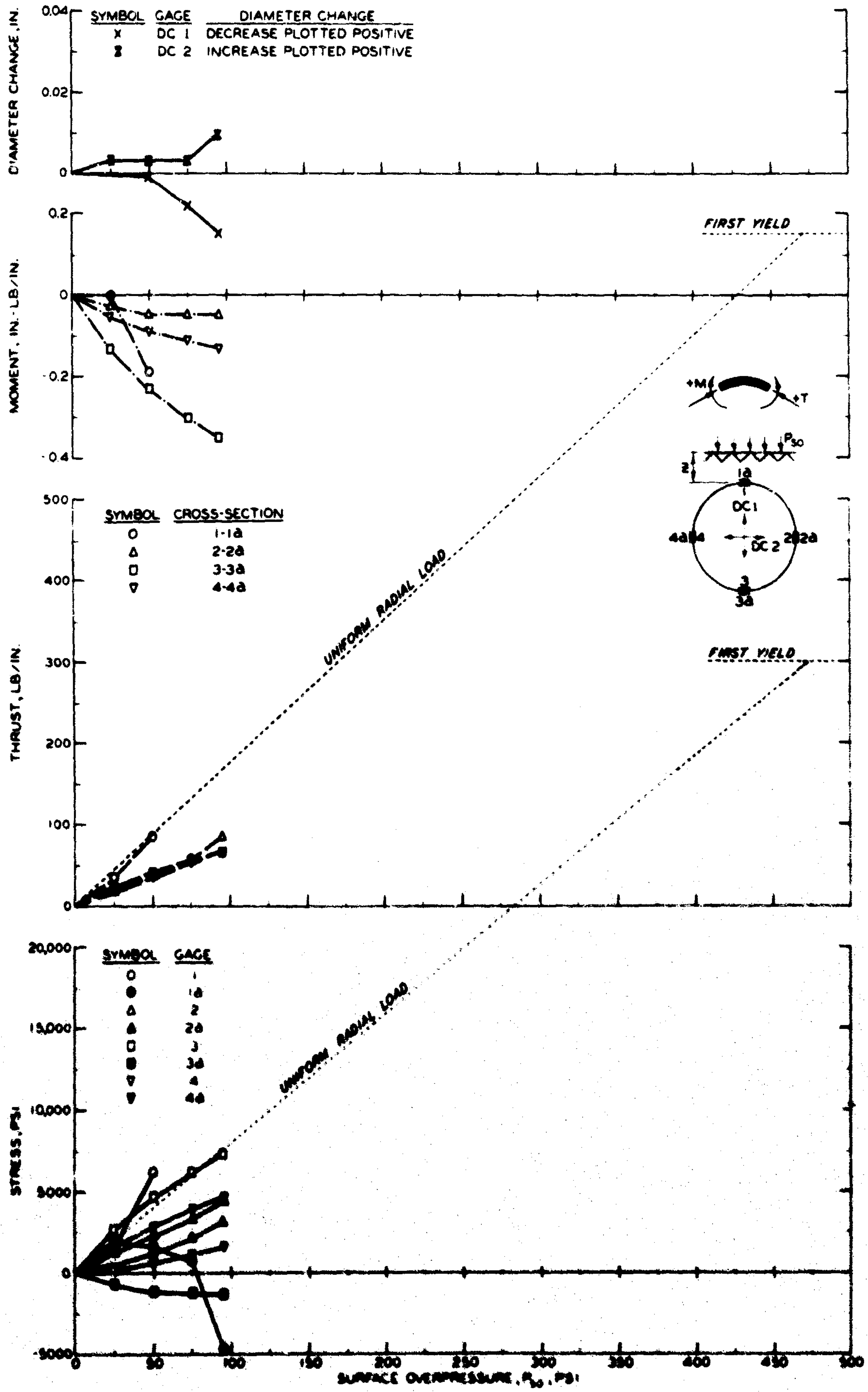

Fig. 5.23 Stress, Thrust, Moment, and Deflection, Test C-1 (Z = 0 in.)

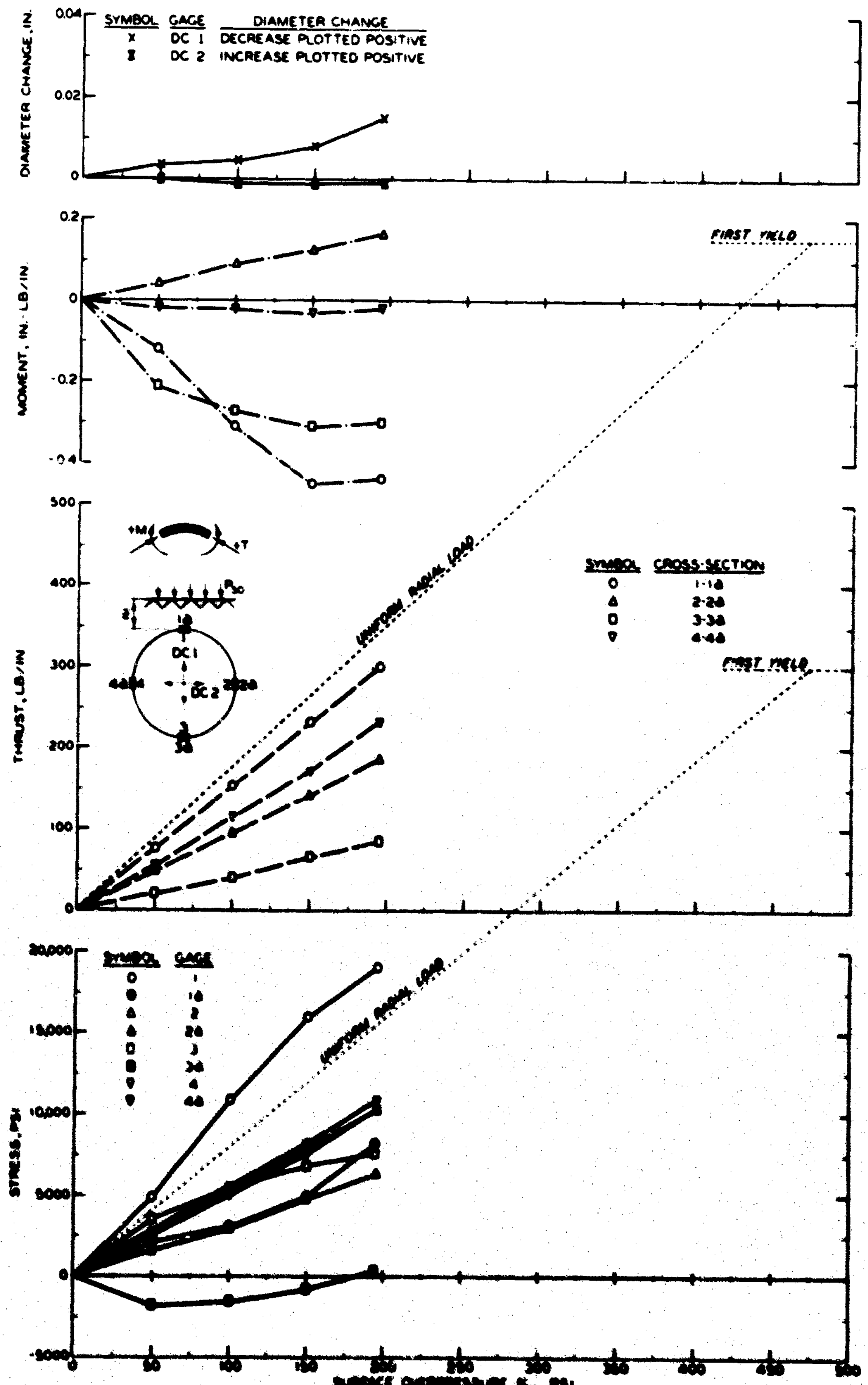

Fig. 5.24 Stress, Thrust, Moment, and Deflection, Test C-4 (Z = 3/16 in.)

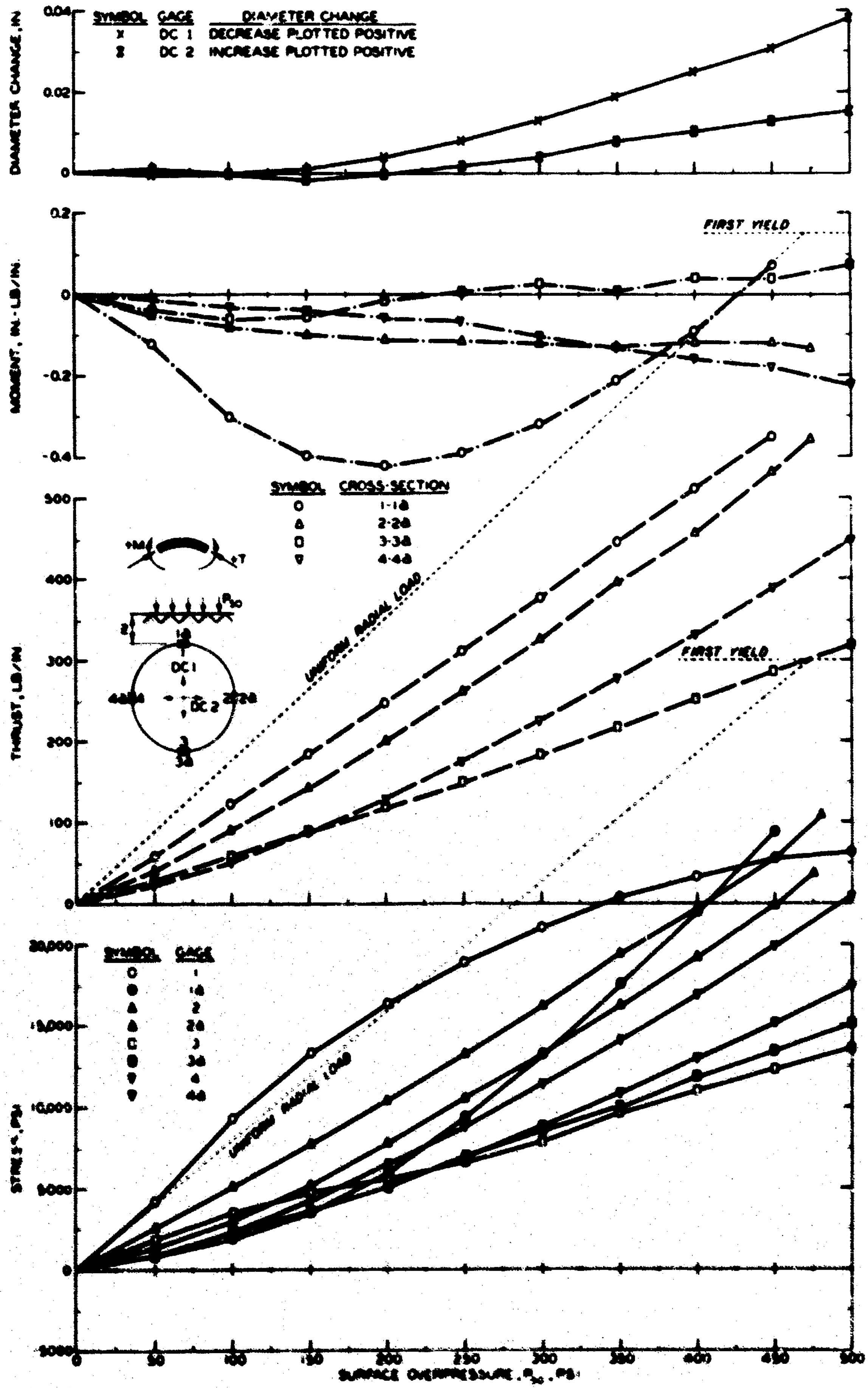

Fig. 5.25 Stress, Thrust, Moment, and Deflection, Test C-5 (Z = 5/16 in.)

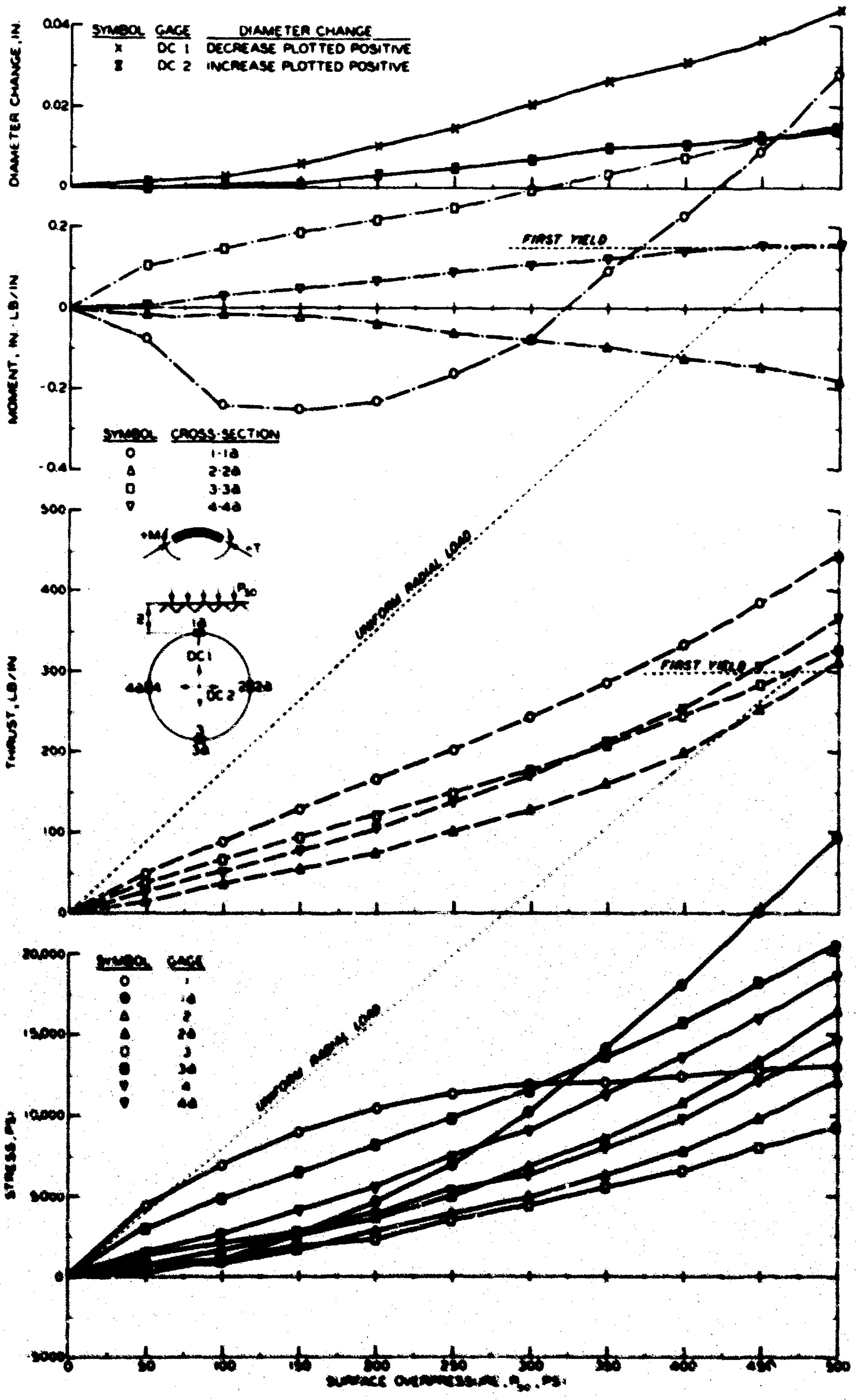

Fig. 5.26 Stress, Thrust, Moment, and Deflection, Test C-2 (Z = 7/16 in.)

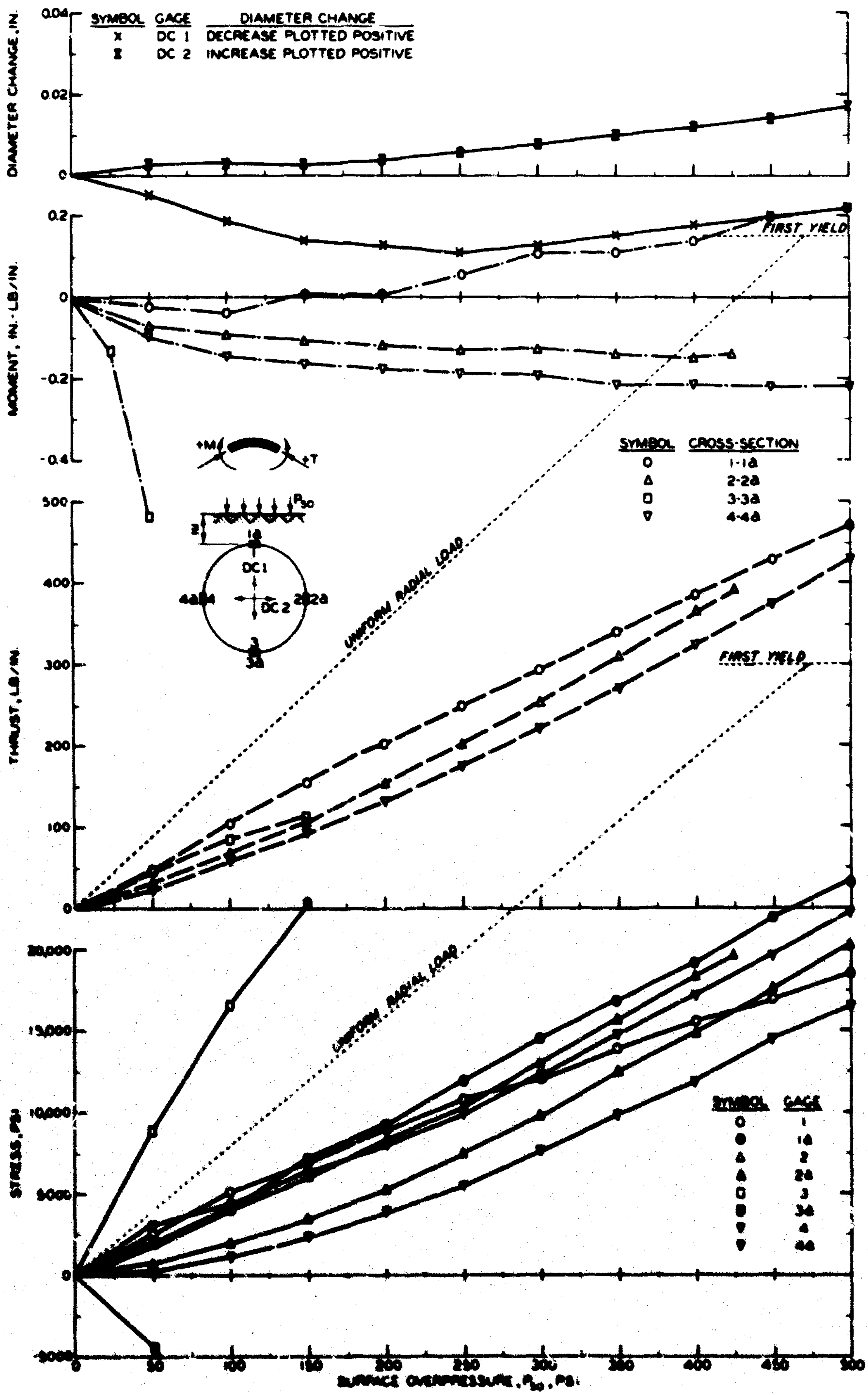

Fig. 5.27 Stress, Thrust, Moment, and Deflection, Test C-3 (Z = 7/8 in.)

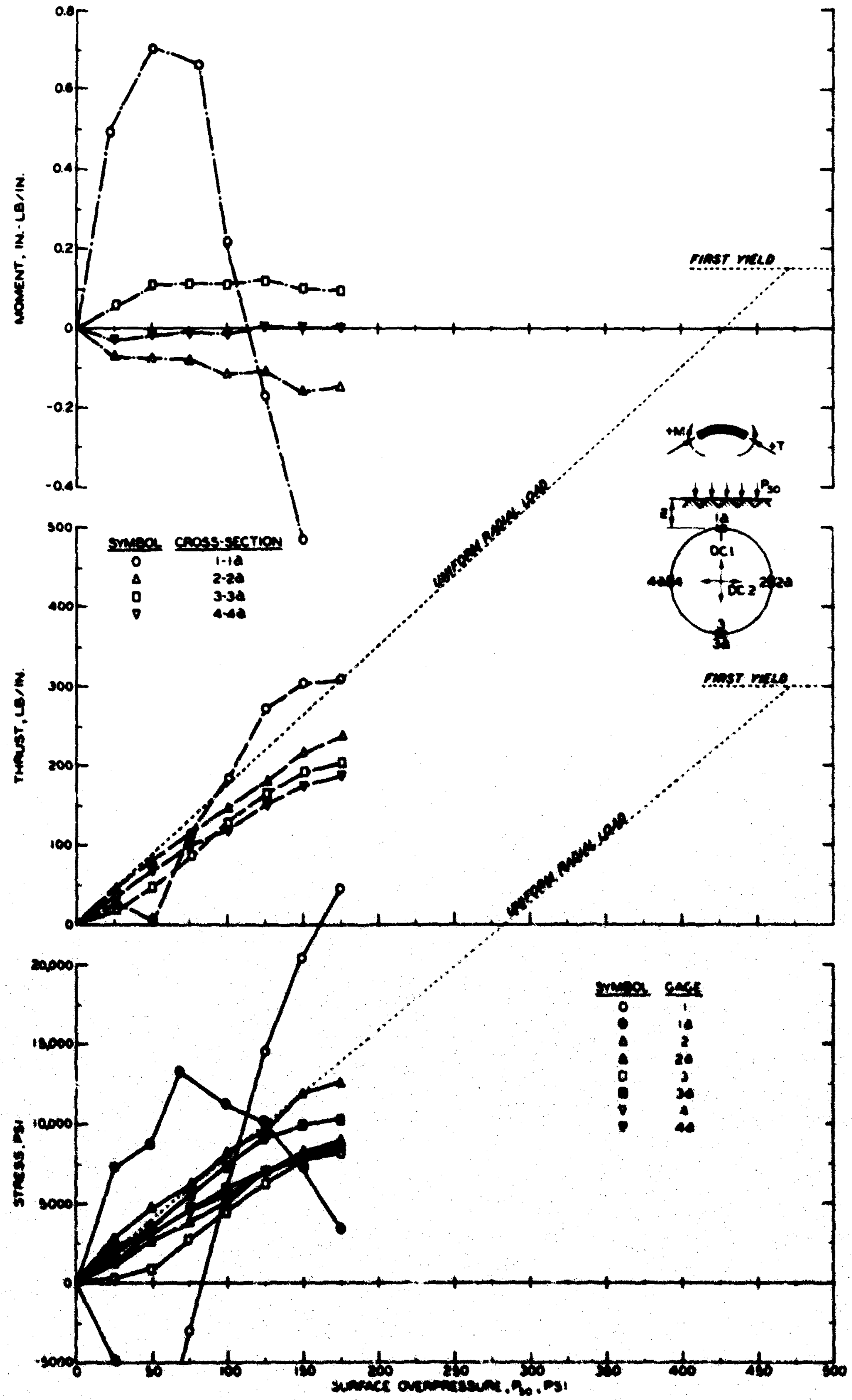

Fig. 5.28 Stress, Thrust, and Moment, Test C-6 (Z = 0 in.)

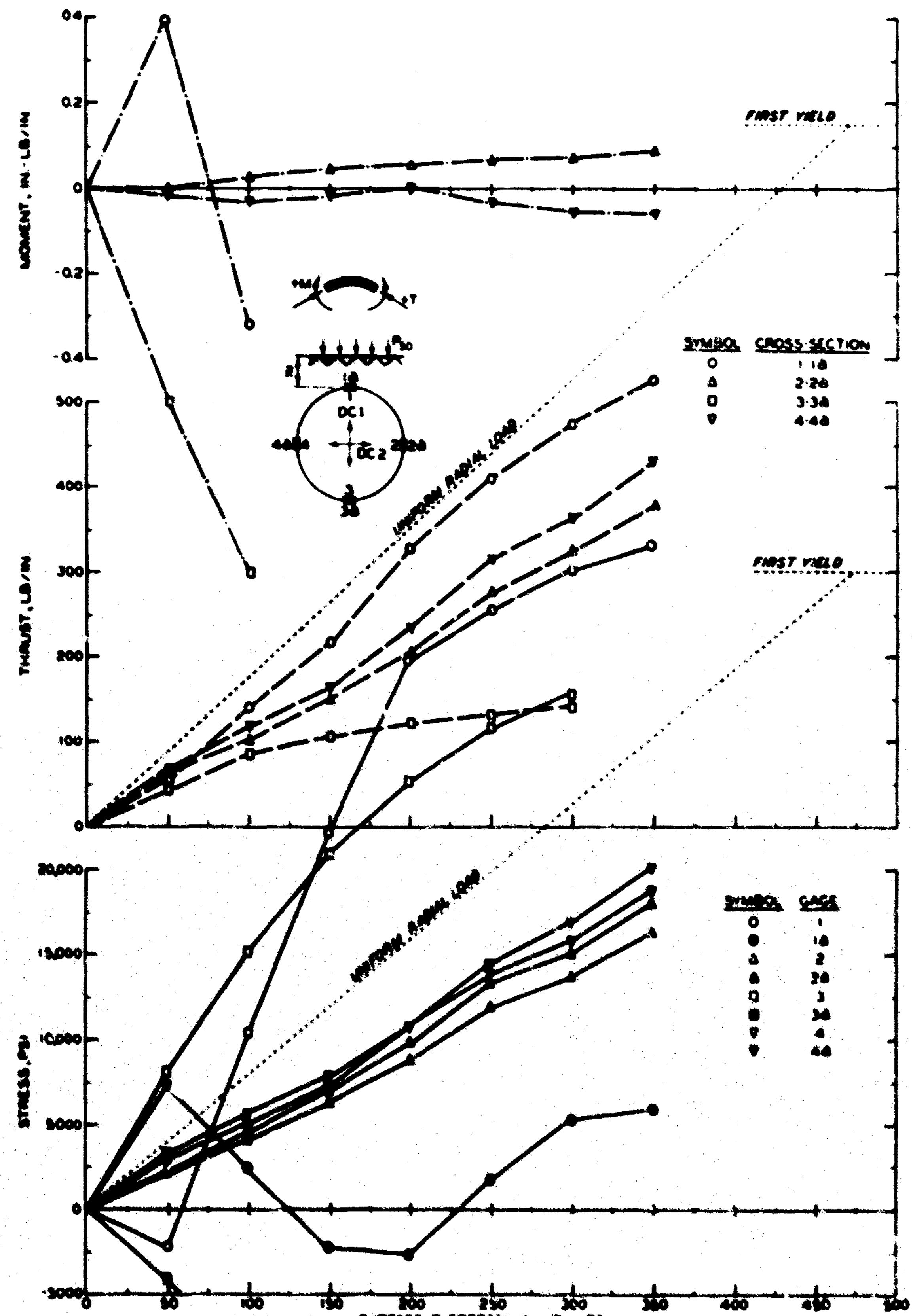

Fig. 5.29 Stress, Thrust, and Moment, Test C-7 (Z = 3/16 in.)

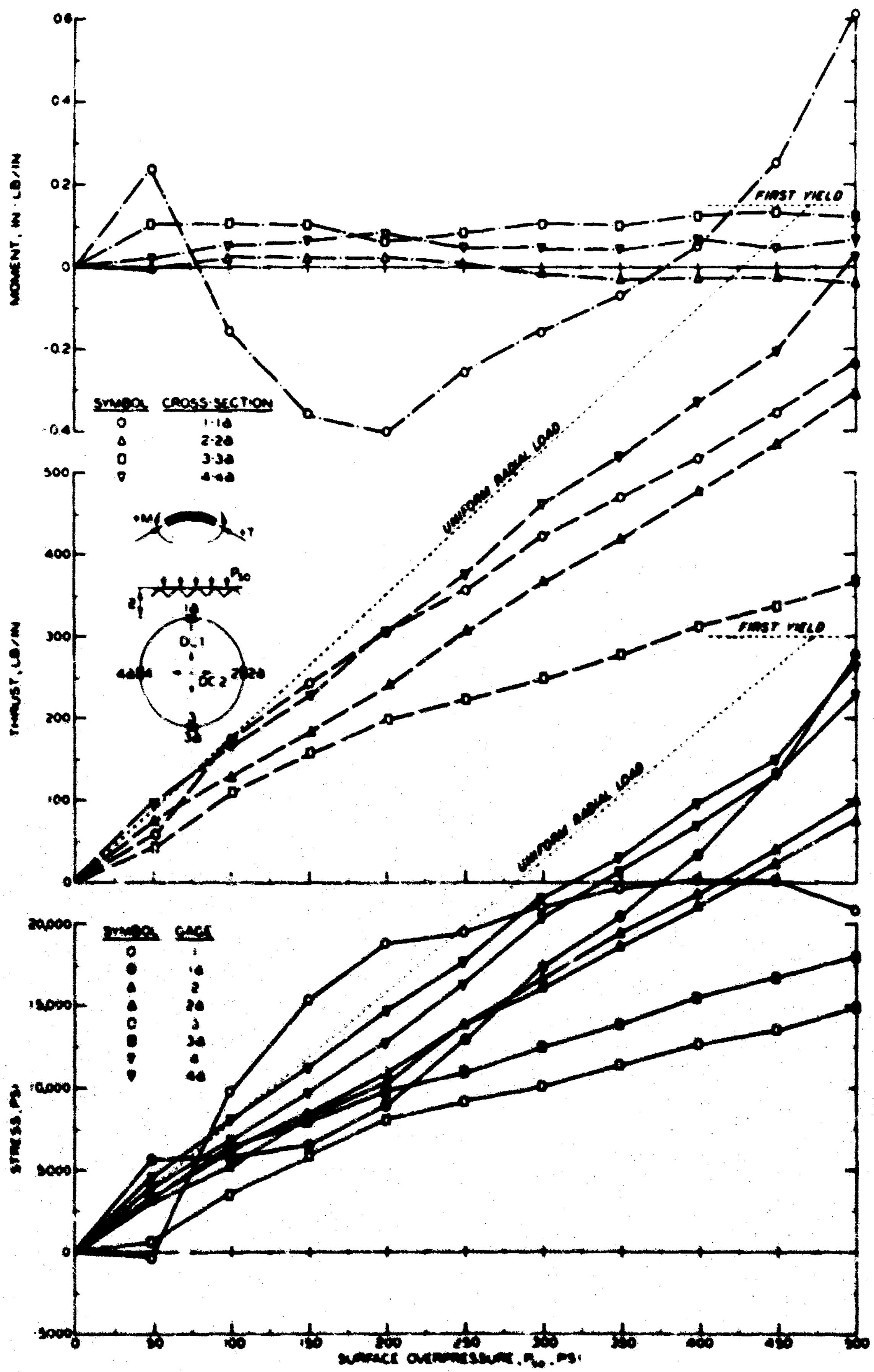

Fig. 5.30 Stress, Thrust, and Moment, Test C-8 (Z = 5/16 in.)

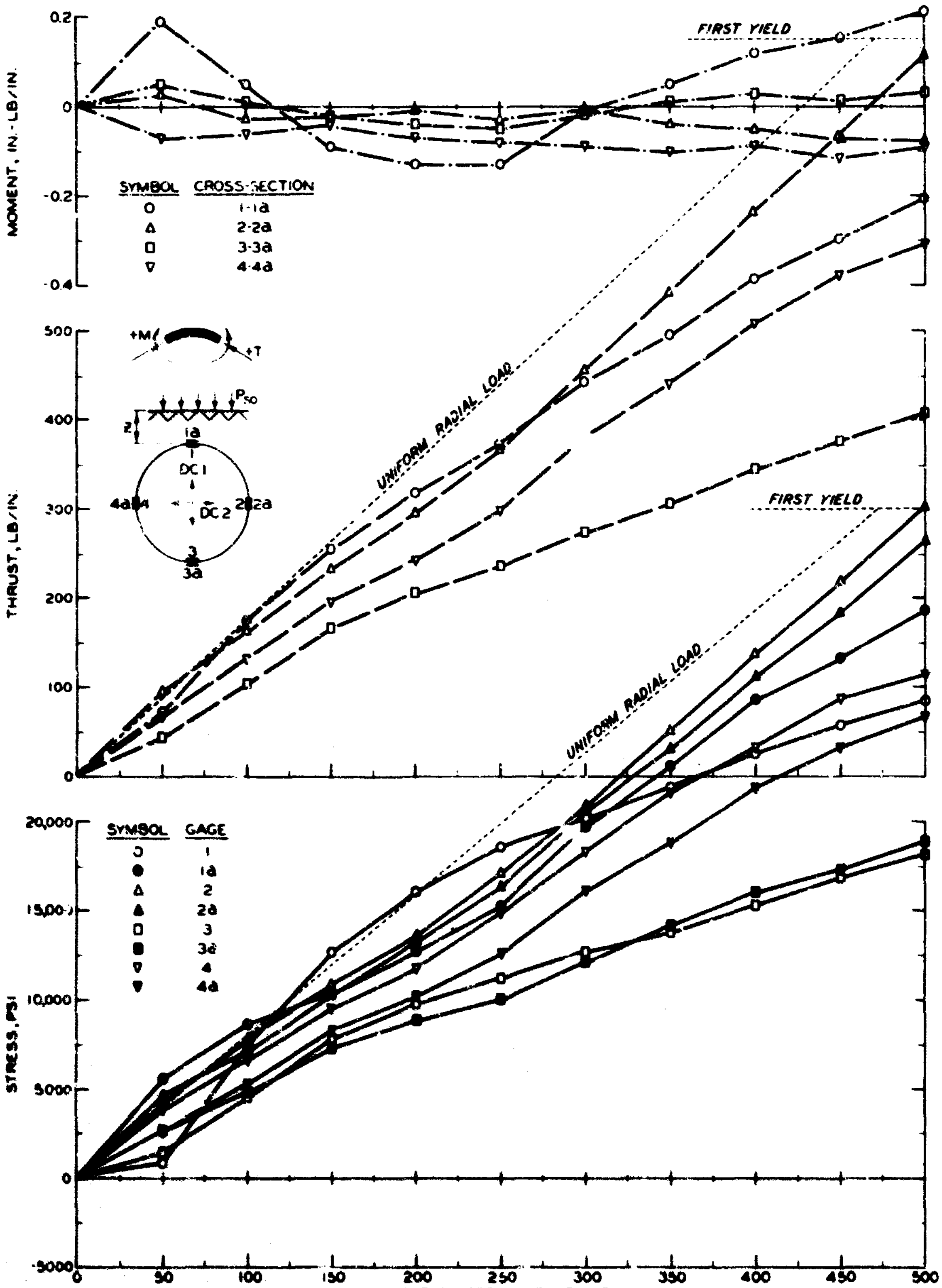

Fig. 5.31 Stress, Thrust, and Moment, Test C-9 (Z = 7/16 in.)

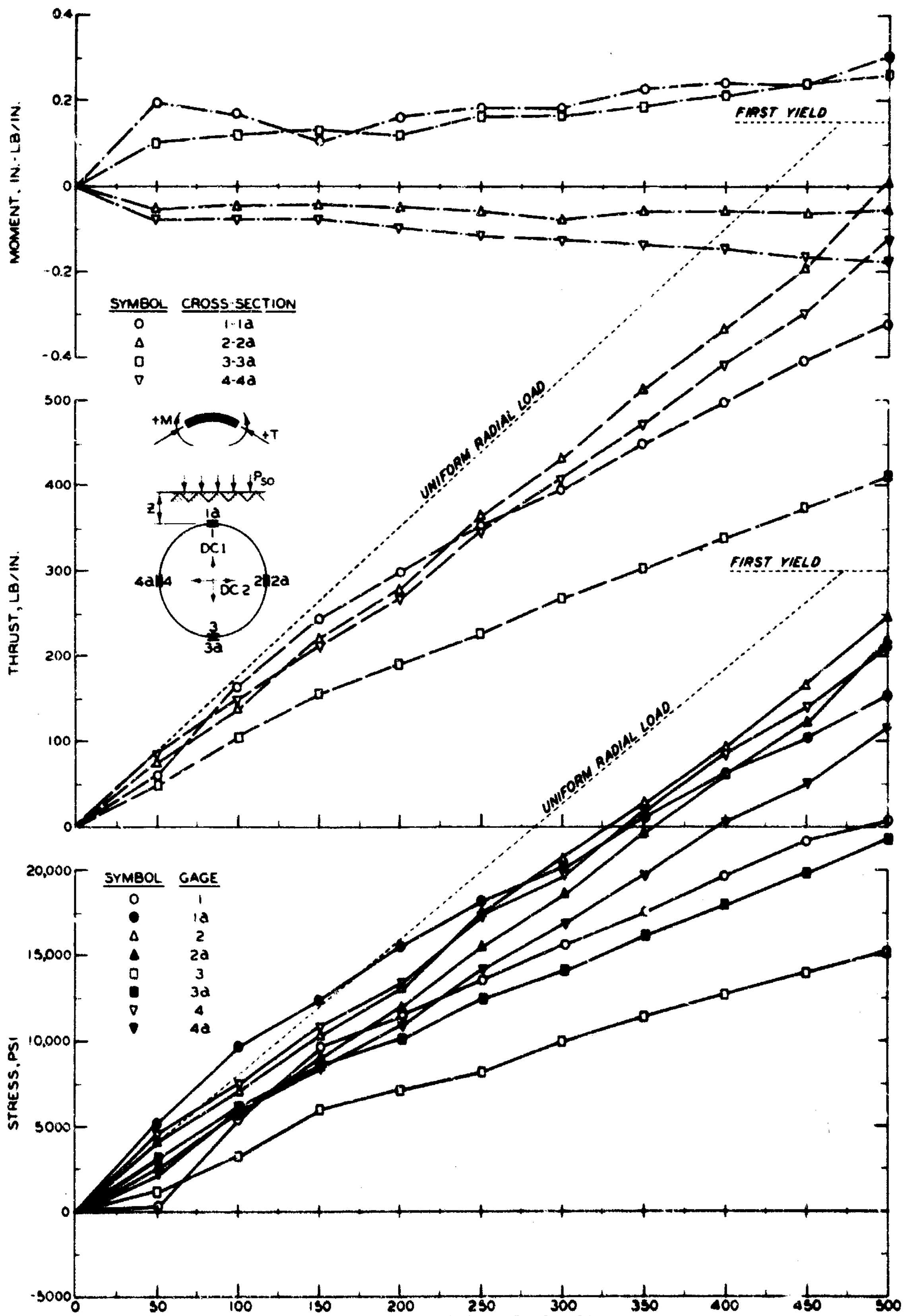

Fig. 5.32 Stress, Thrust, and Moment, Test C-10 (Z = 7/8 in.)

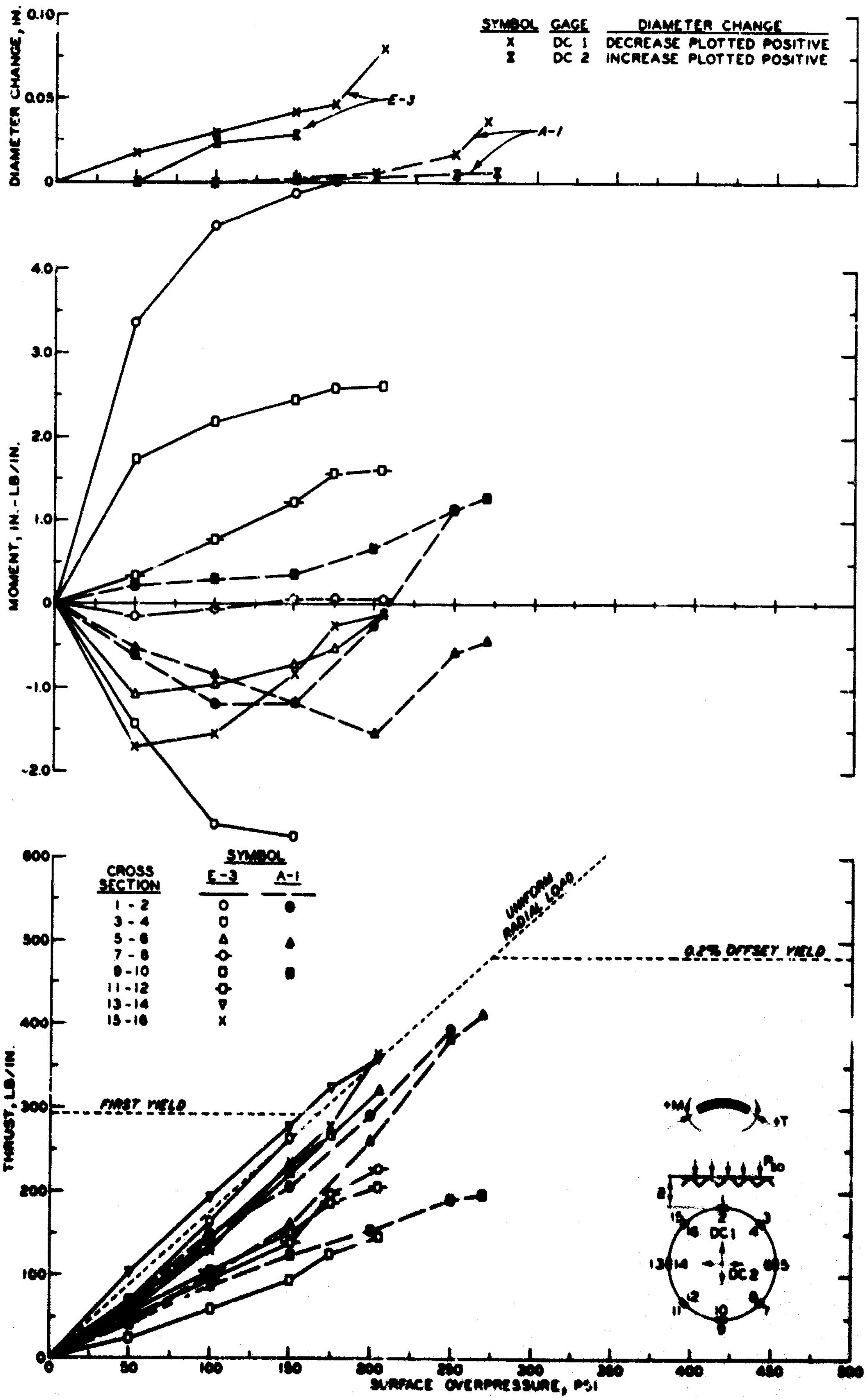

Fig. 5.33 Thrust, Moment, and Deflection, Test E-3 (Z = 0 in.)

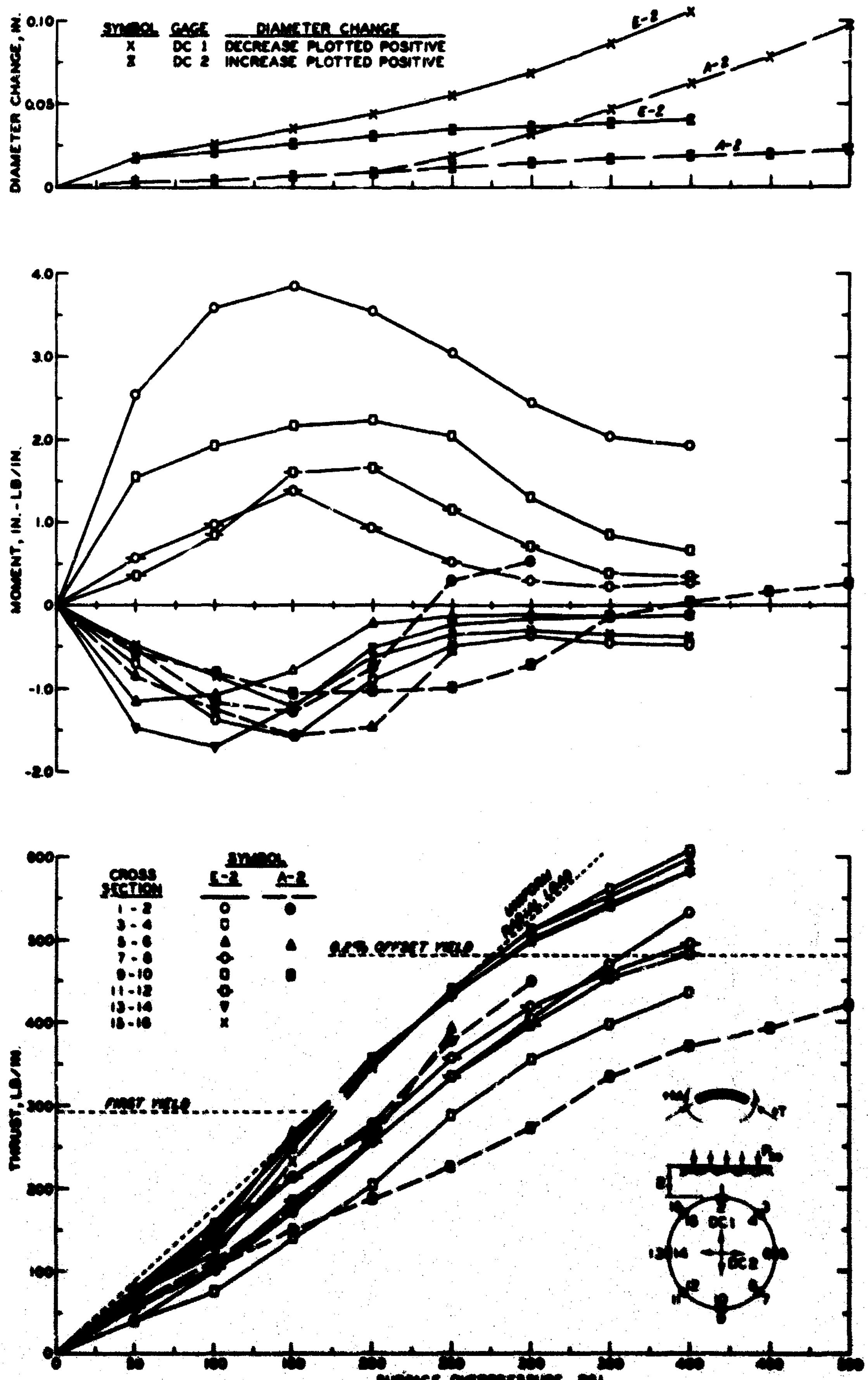

Fig. 5.34 Thrust, Moment, and Deflection, Test E-2 (Z = 7/16 in.)

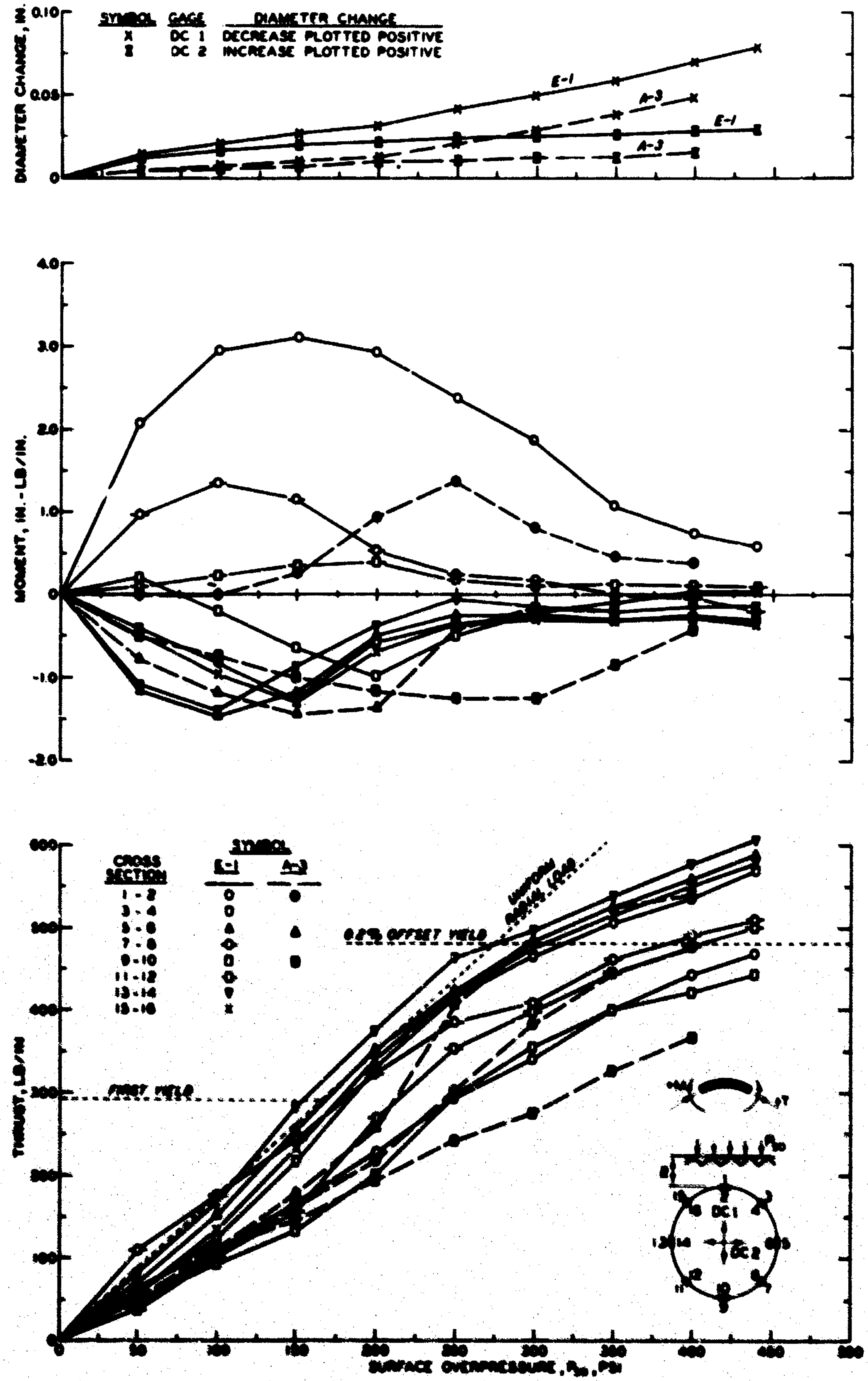

Fig. 5.35 Thrust, Moment, and Deflection, Test E-1 (Z = 7/8 in.)

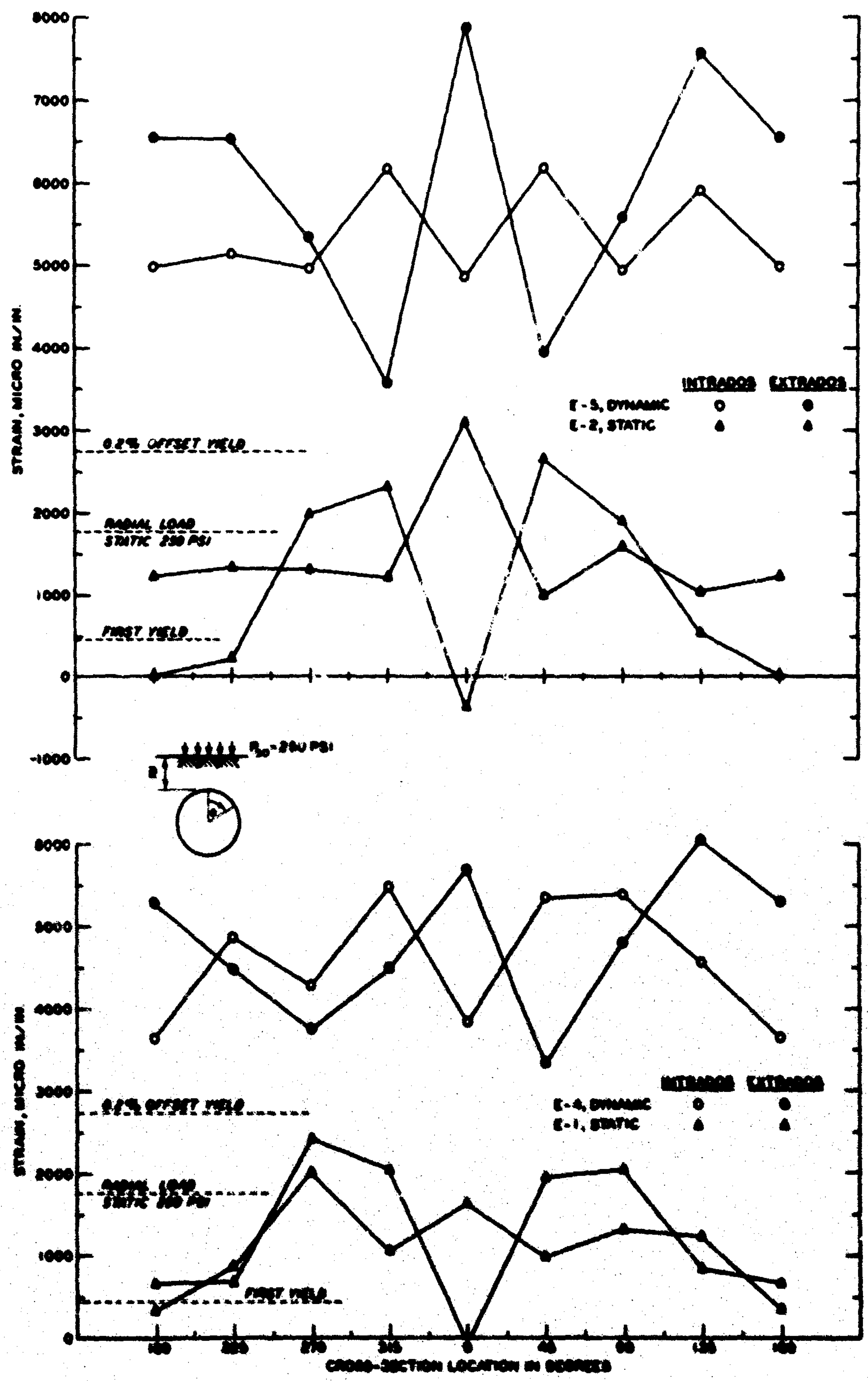

Fig. 5.36 Strain, Test E-5 (Z = 7/16 in.) and Test E-4 (Z = 7/8 in.); Surface Overpressure = 250 psi

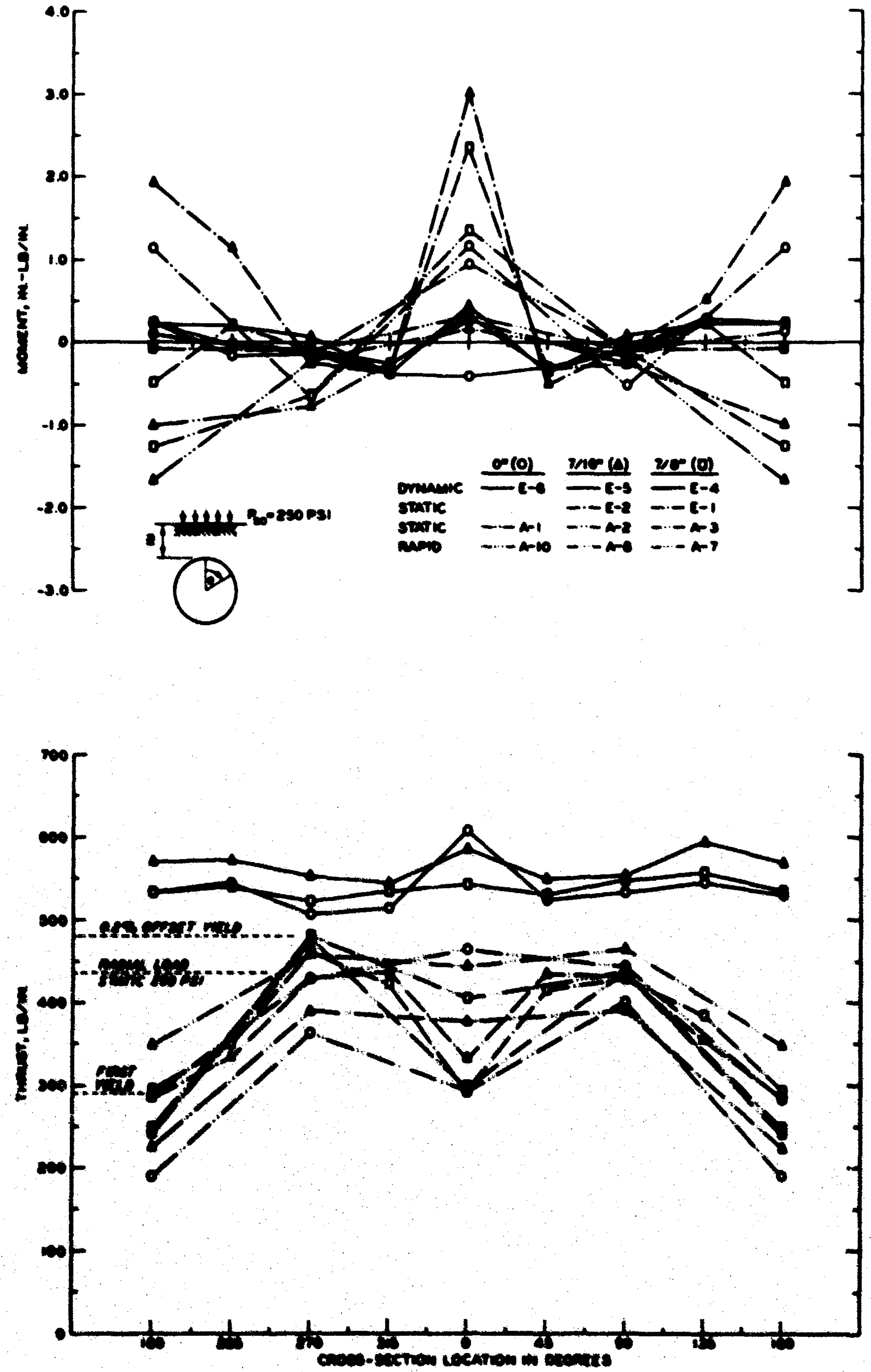

Fig. 5.37 Thrust and Moment, Tests E-6 (Z = 0 in.), E-5 (Z = 7/16 in.), and E-4 (Z = 7/8 in.); Surface Overpressure = 250 psi

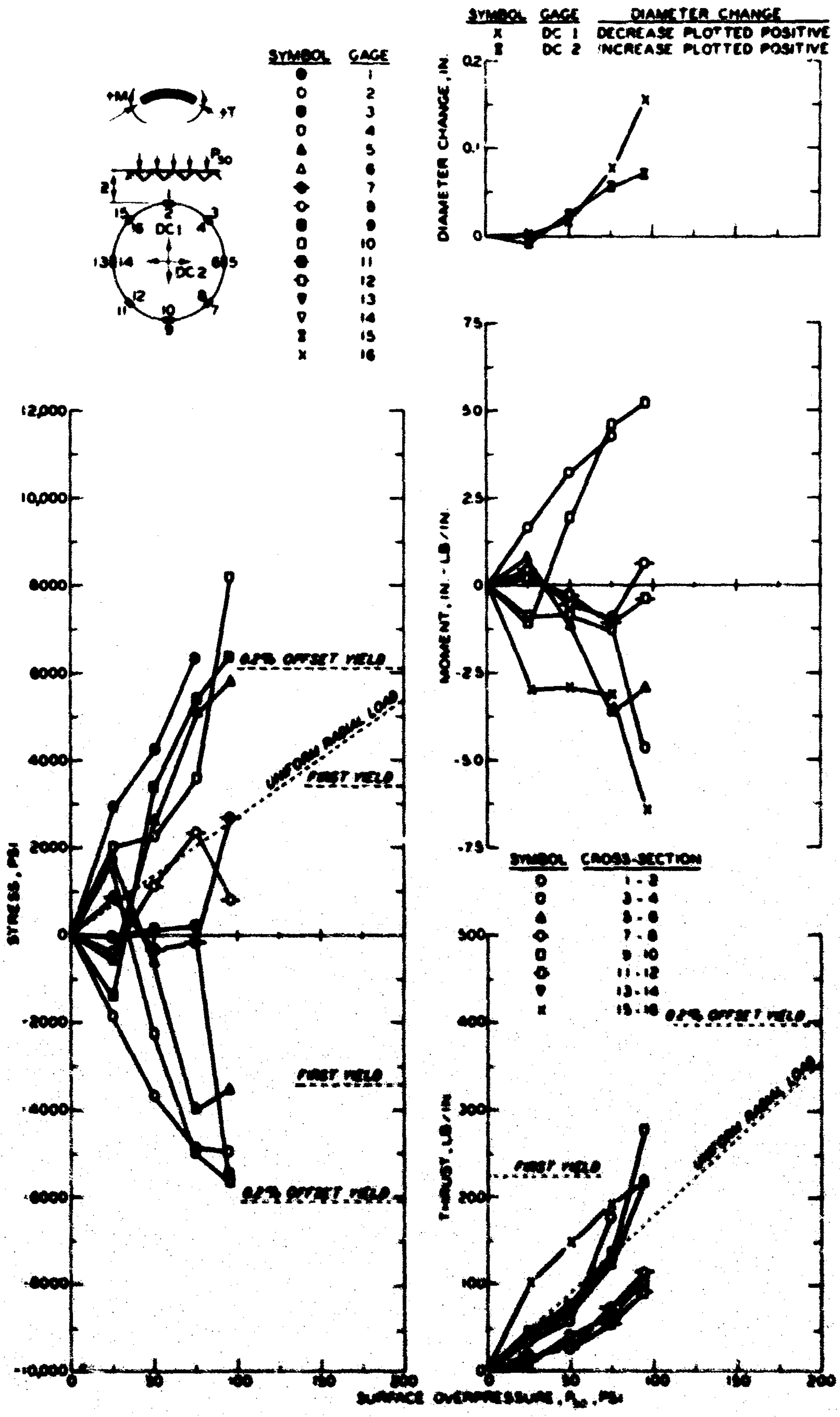

Fig. 5.38 Stress, Thrust, Moment, and Deflection, Test D-1 (Z = 0 in.)

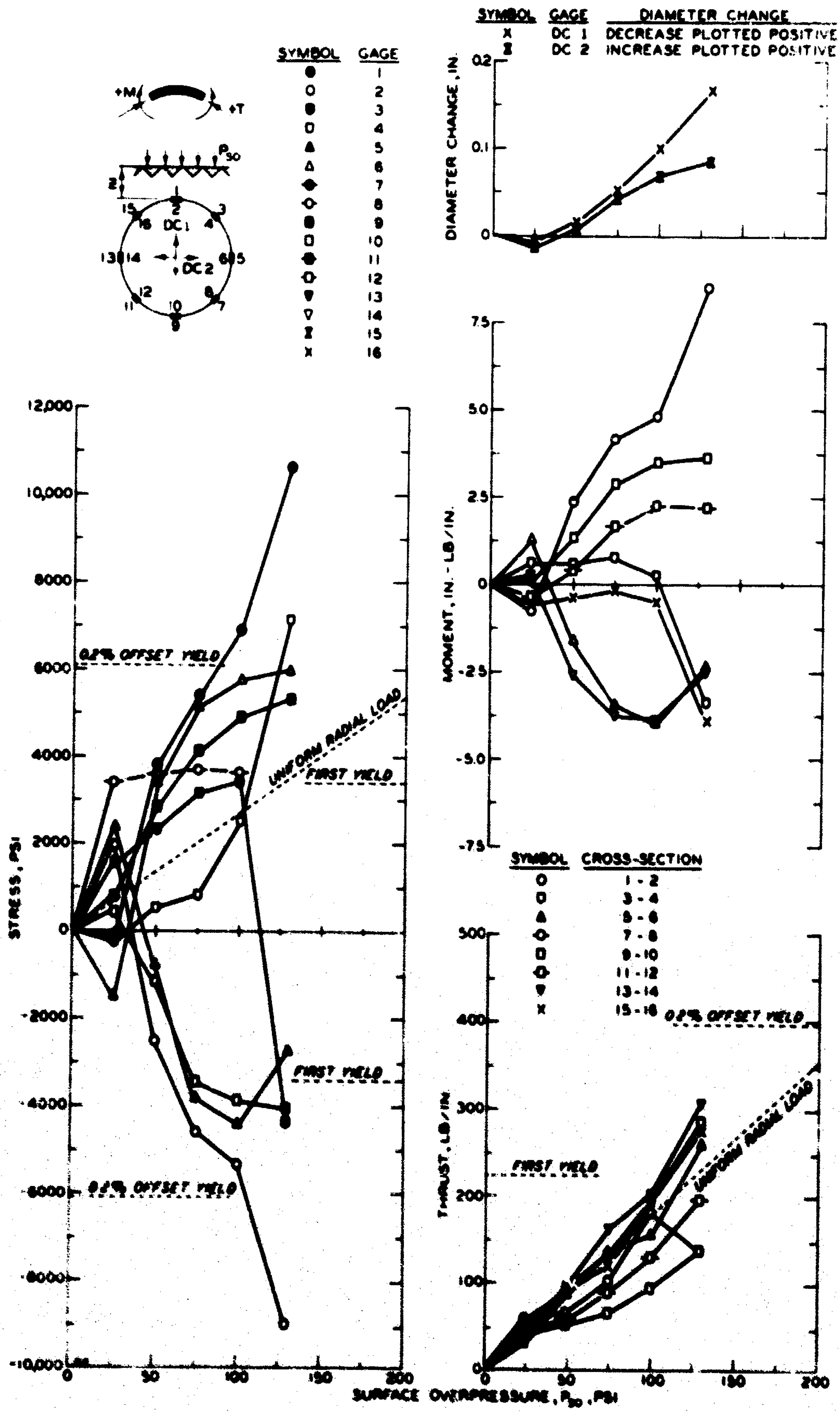

Fig. 5.39 Stress, Thrust, Moment, and Deflection, Test D-2 (Z = 7/16 in.)

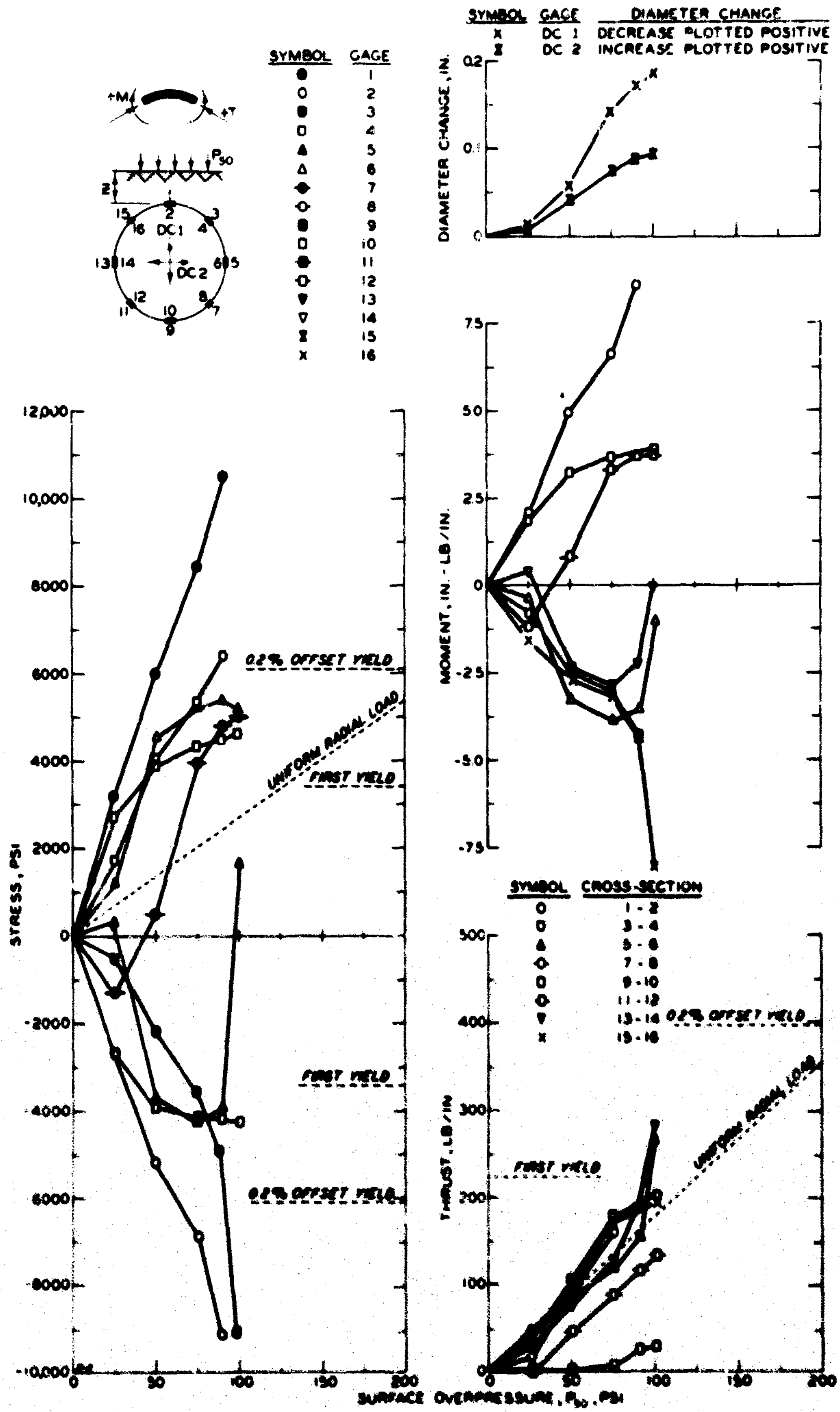

Fig. 5.40 Stress, Thrust, Moment, and Deflection, Test D-3 (Z = 7/8 in.)

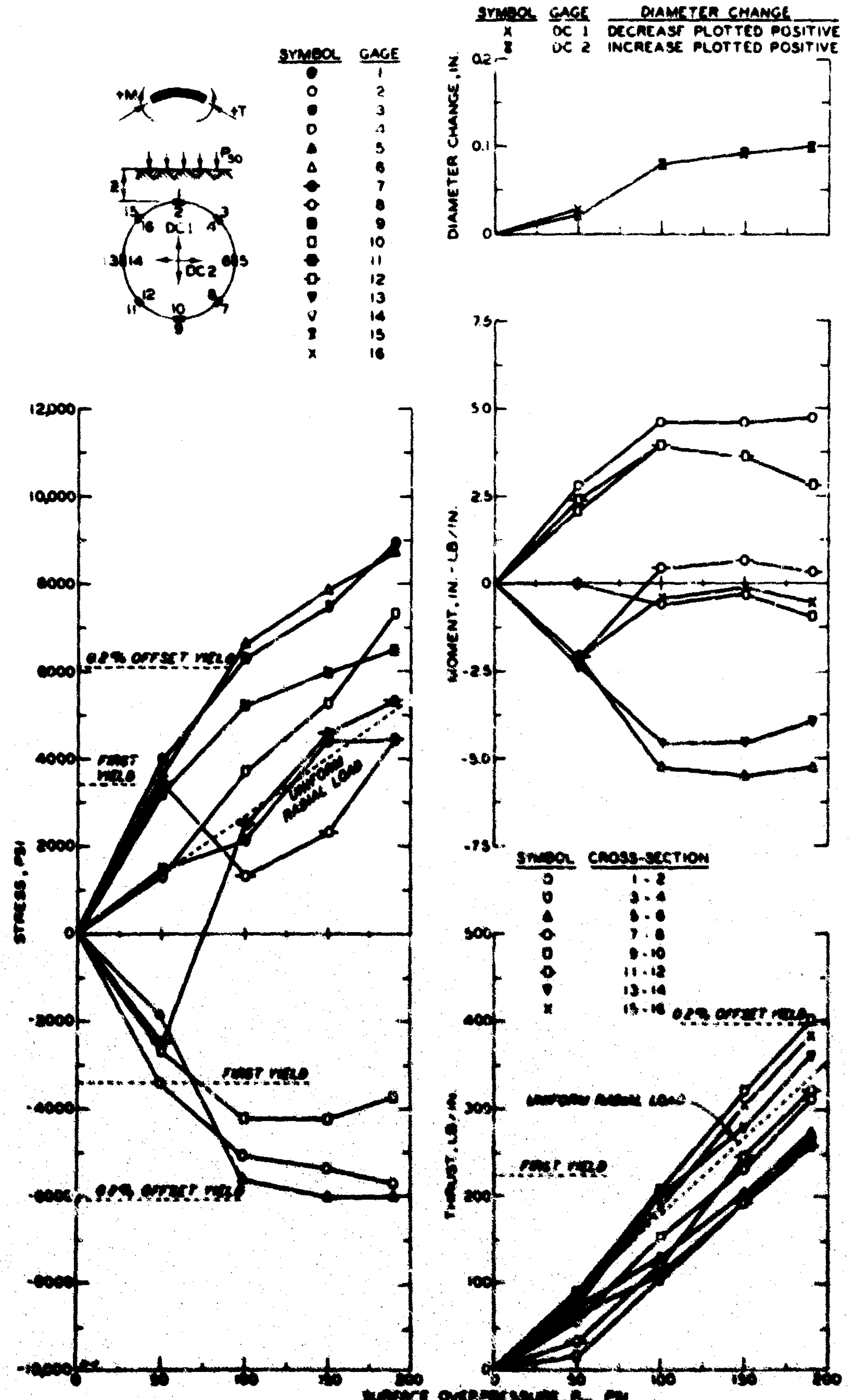

Fig. 5.41 Stress, Thrust, Moment, and Deflection, Test D-4 (Z = 1-3/4 in.)

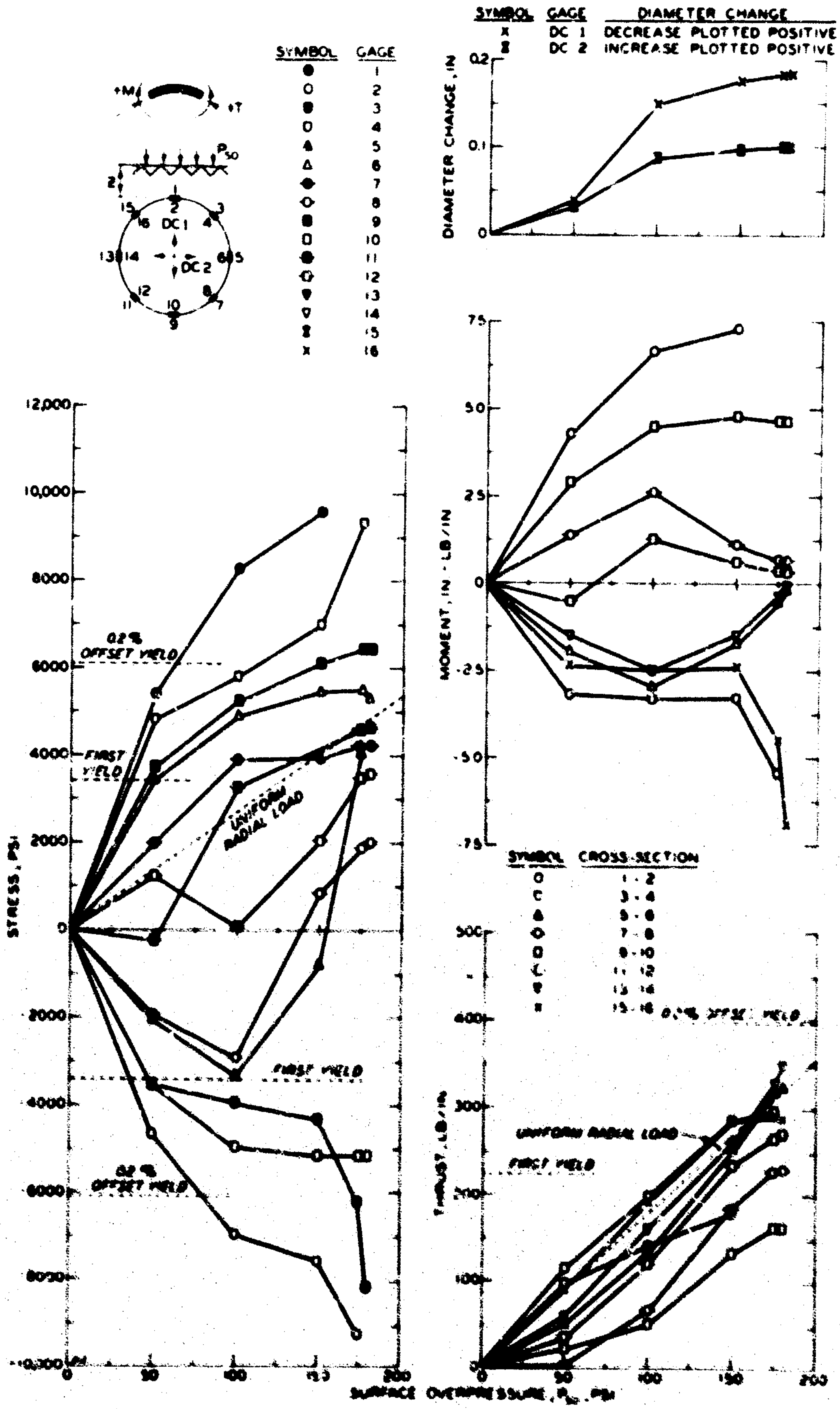

Fig. 5.42 Stress, Thrust, Moment, and Deflection, Test D-5 (Z = 2-5/8 in.)

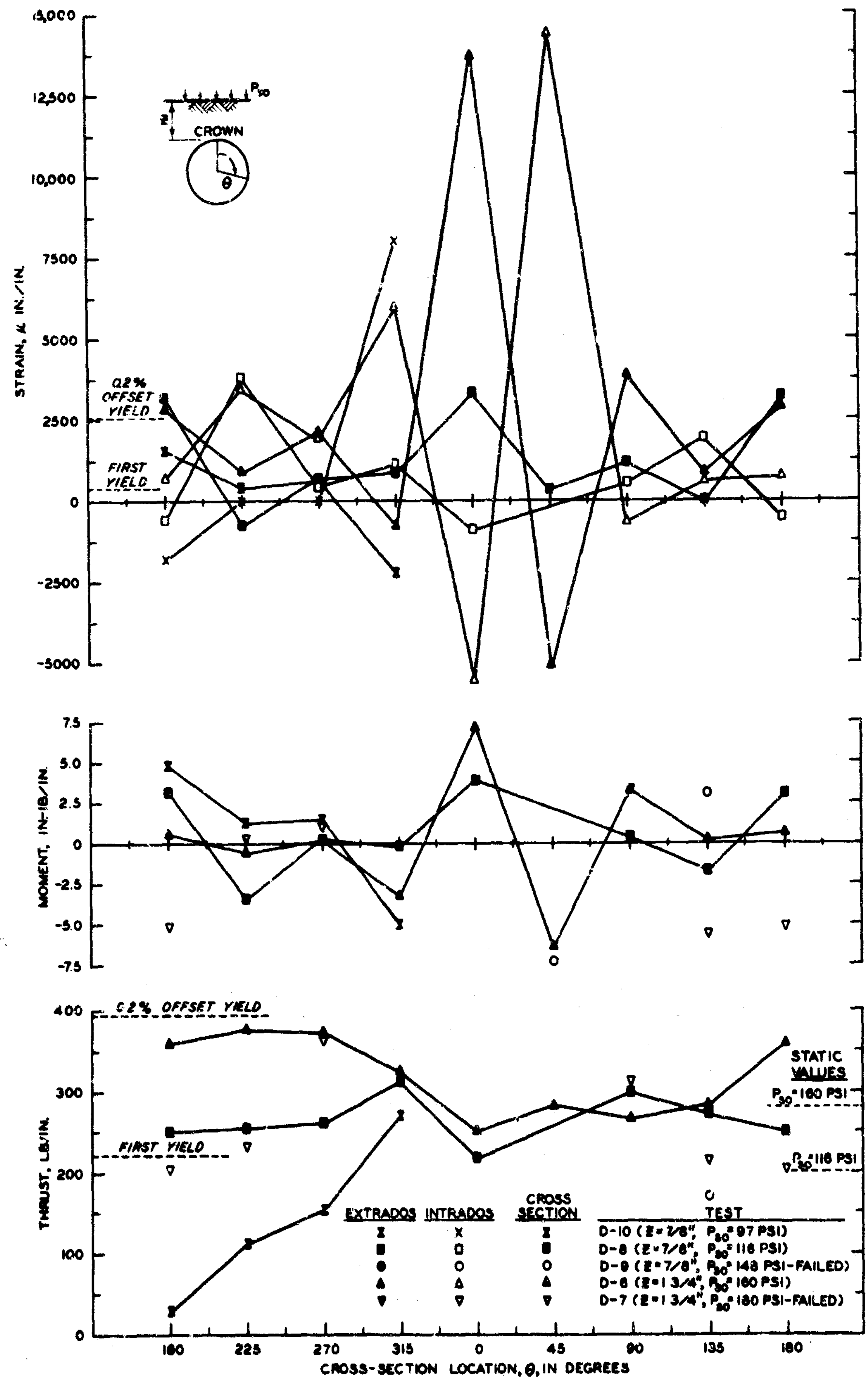

Fig. 5.43 Strain, Thrust, and Moment, Tests D-6 Through D-10

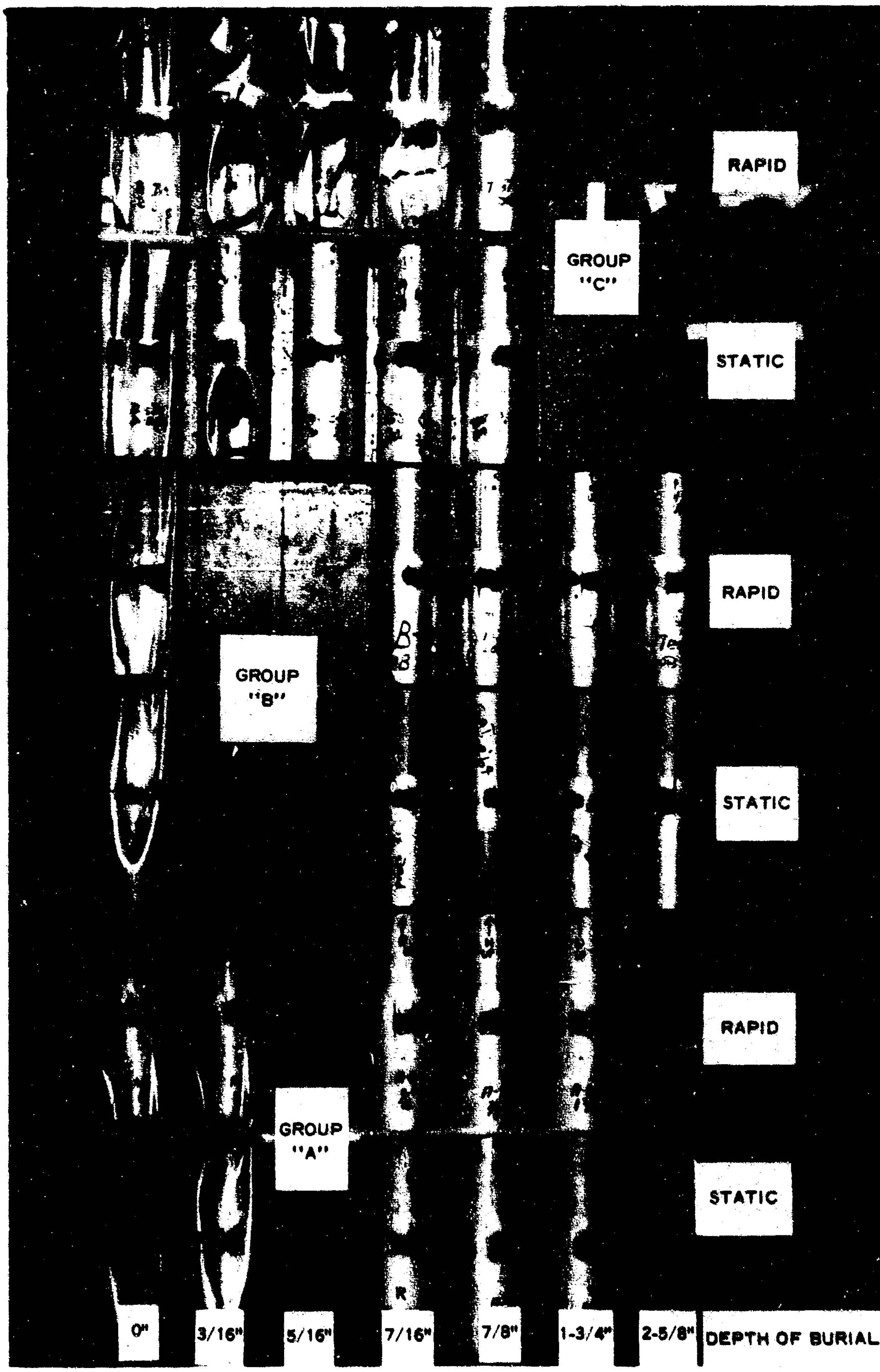

Fig. 5.44 Cylinders of Groups A, B, and C after Tests

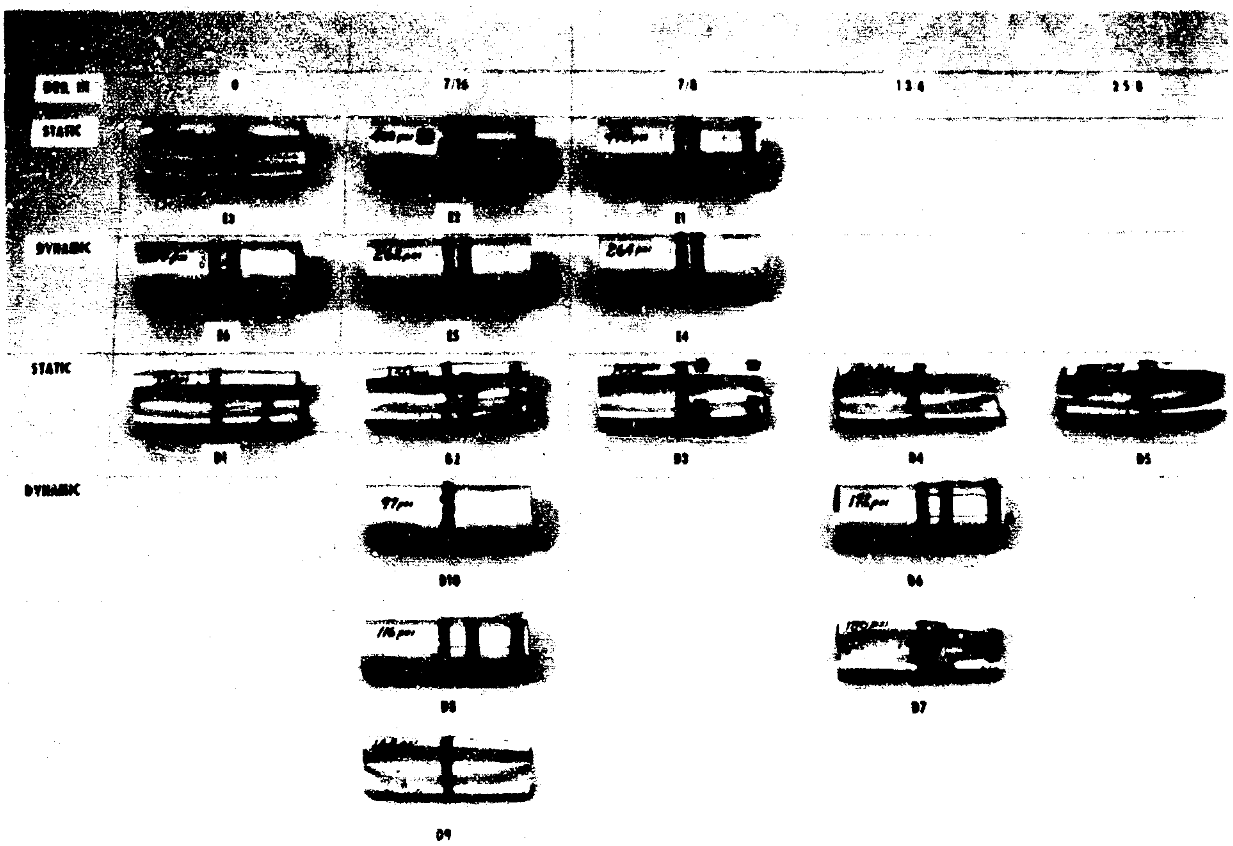

Fig. 5.45 Cylinders of Groups D and E after Tests

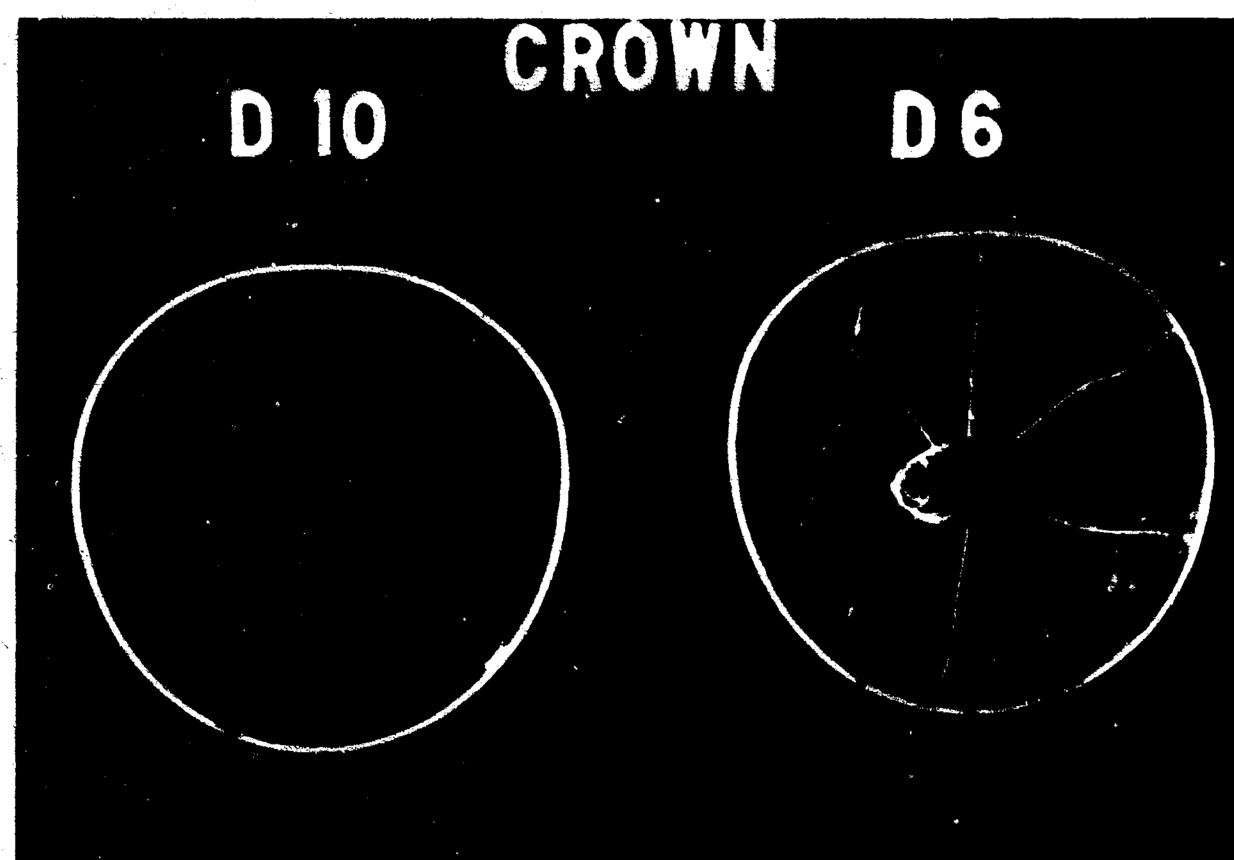

Fig. 5.46 Cylinders D-6 and D-10 after Test

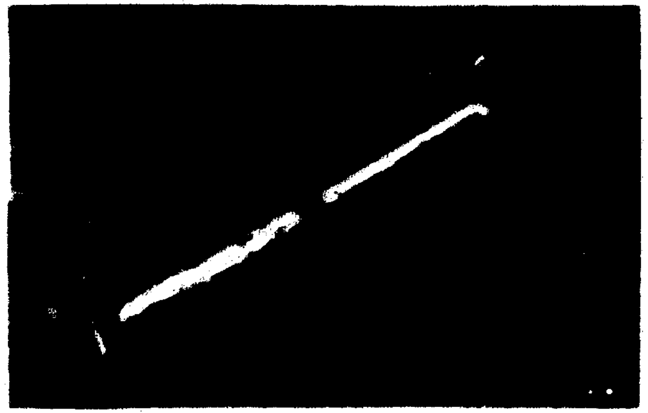

a. Cylinder Failure (Z = 0 in.)

b. End View, Failed Cylinder (Z = 0 in.)

c. Surface after Cylinder Failure (Z = 2-5/8 in.)

d. End View with End Cap (Z = 2-5/8 in.)

e. End View, End Cap Removed (Z = 2-5/8 in.)

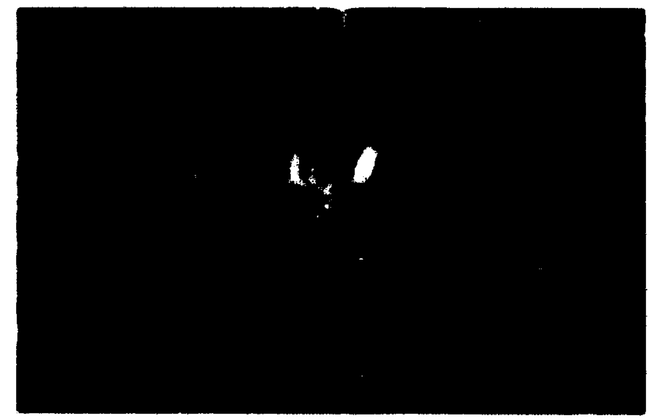

f. End View, Soil Cutback (Z = 2-5/8 in.)

Fig. 5.47 Posttest Cylinder Configuration in Clay

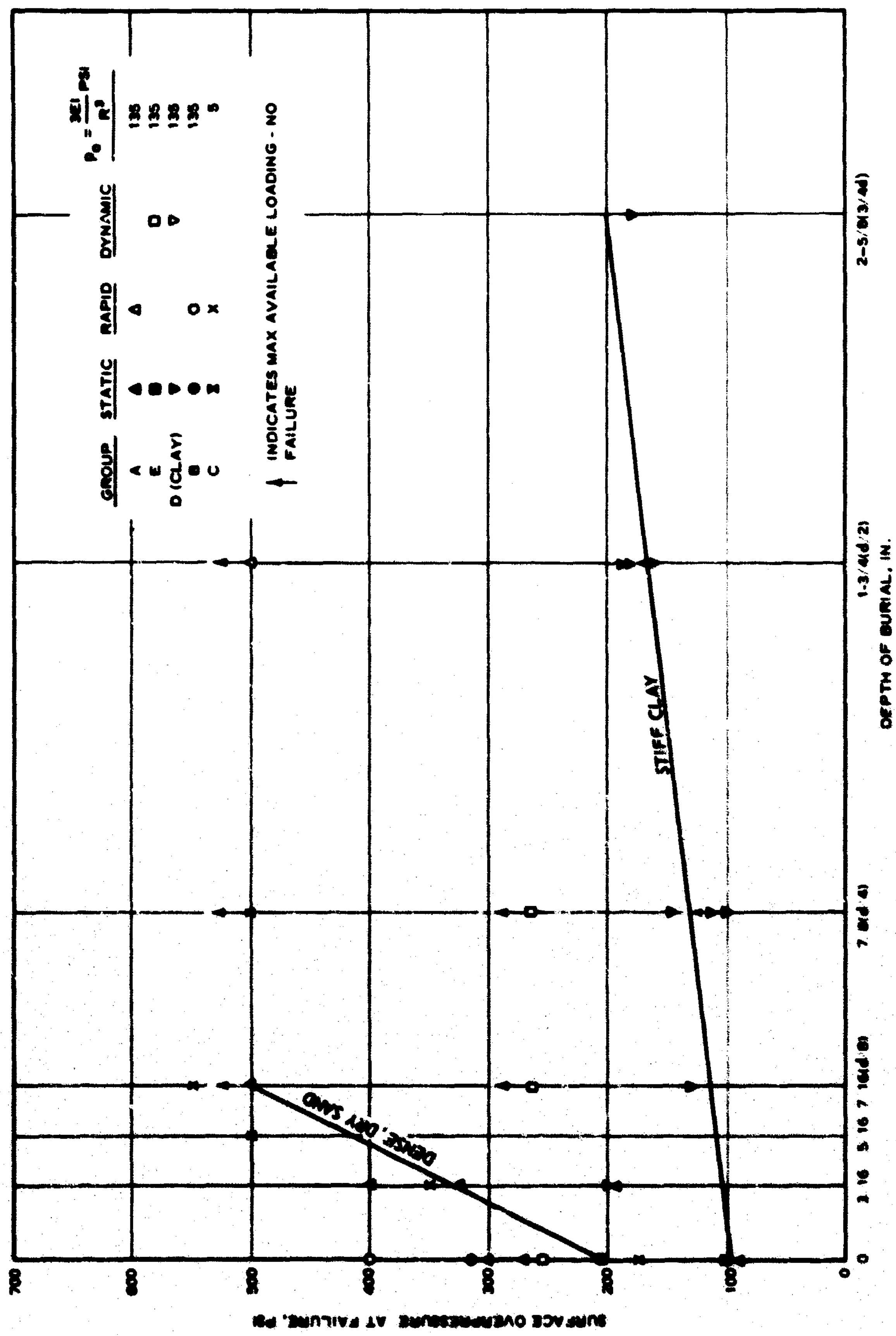

Fig. 5.48 Relation Between Failure Pressure and Depth of Burial

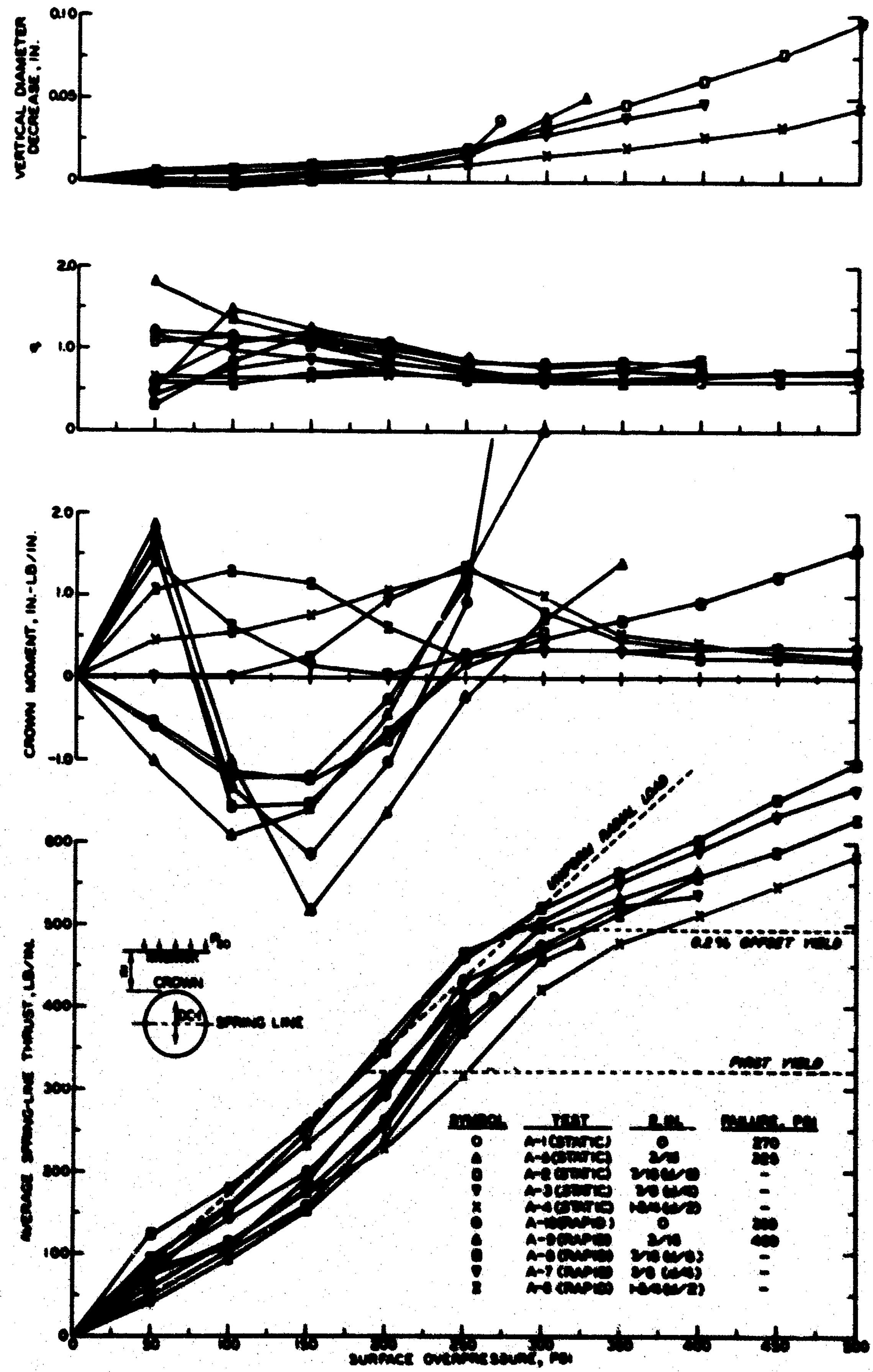

Fig. 6.1 A Group: Average Spring Line Thrusts, Crown Moments, Vertical Diameter Changes, and q Values

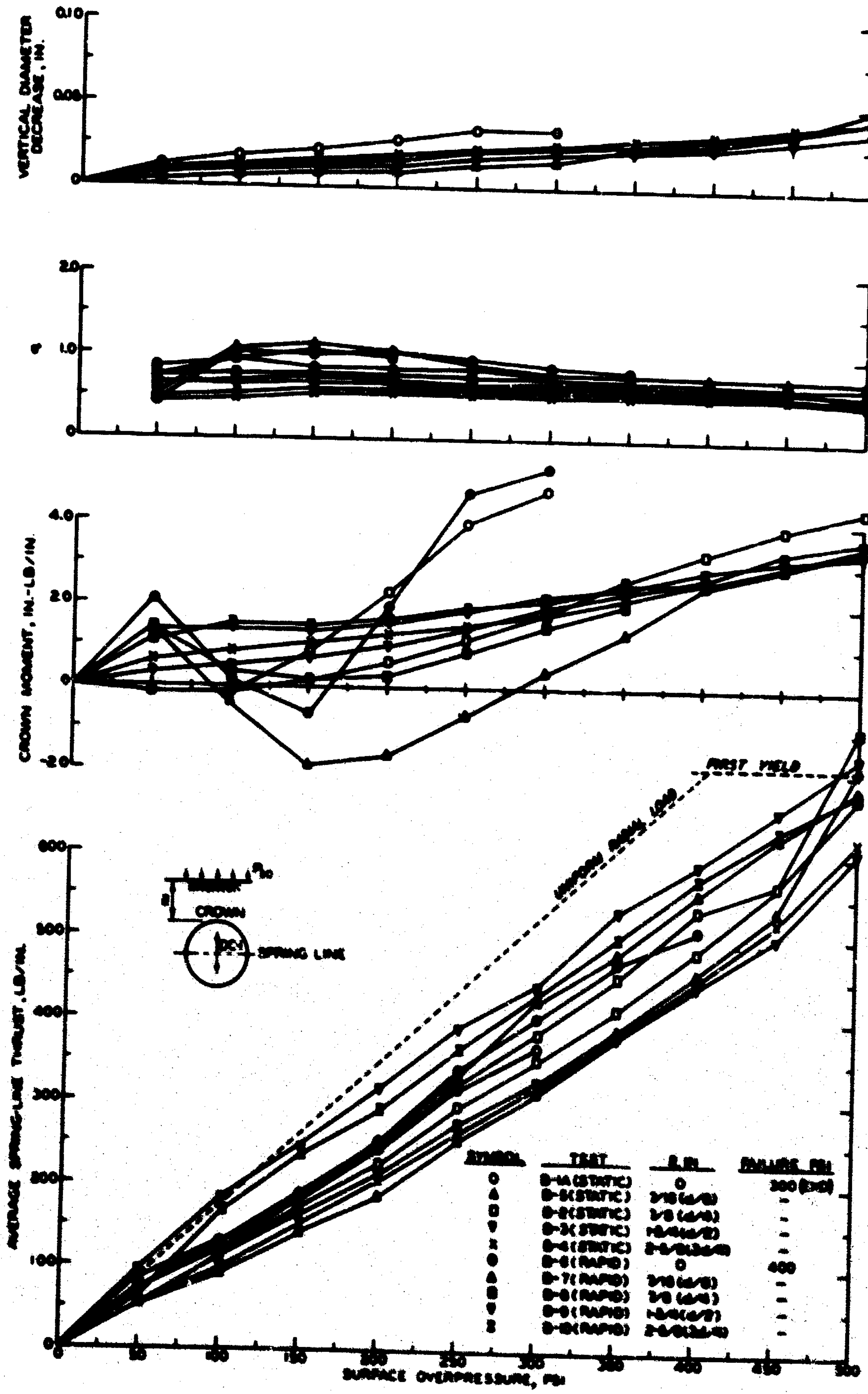

Fig. 6.2 B Group: Average Spring Line Thrusts, Crown Moments, Vertical Diameter Changes, and q Values

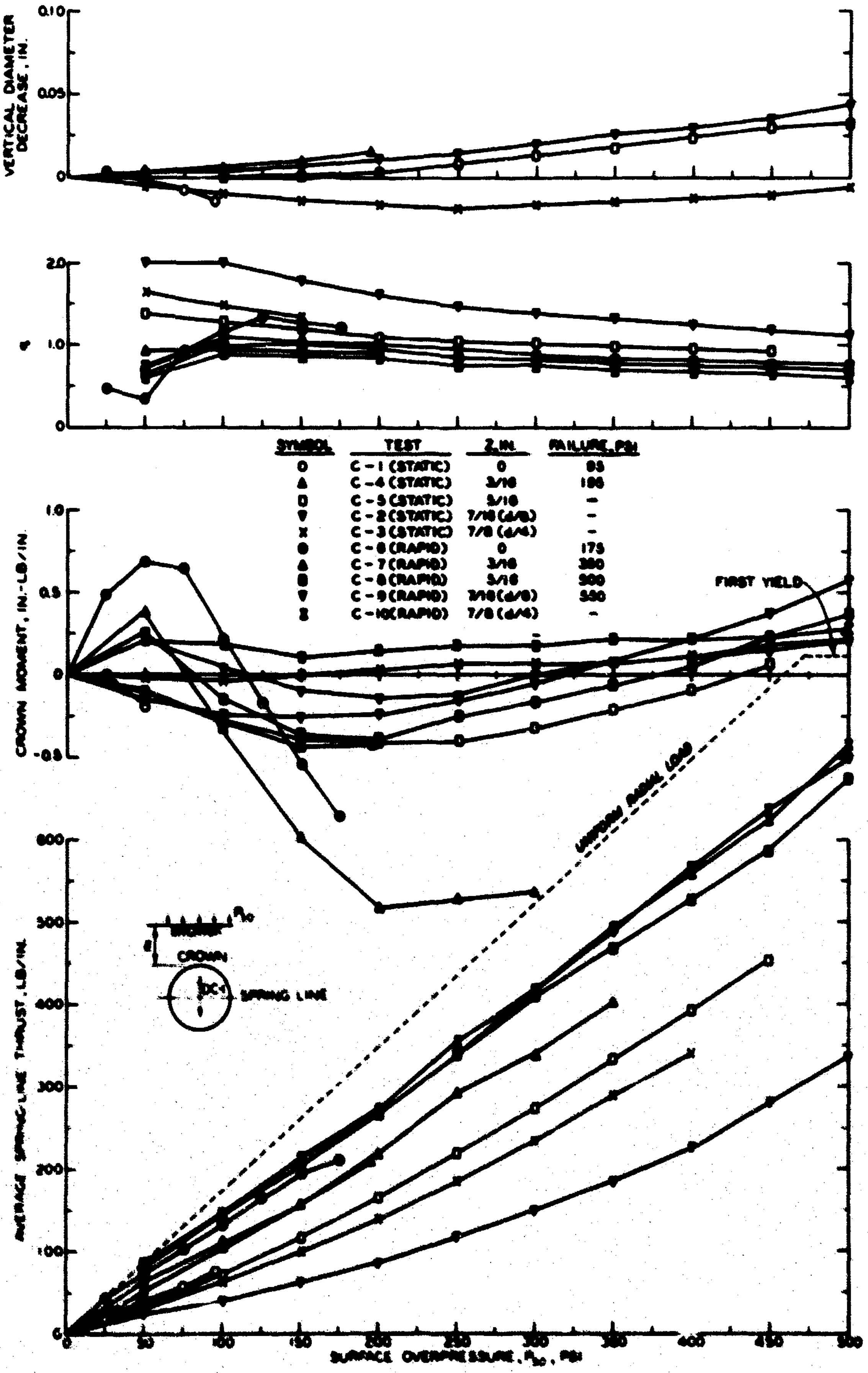

Fig. 6.3 C Group: Average Spring Line Thrusts, Crown Moments, Vertical Diameter Changes, and q Values

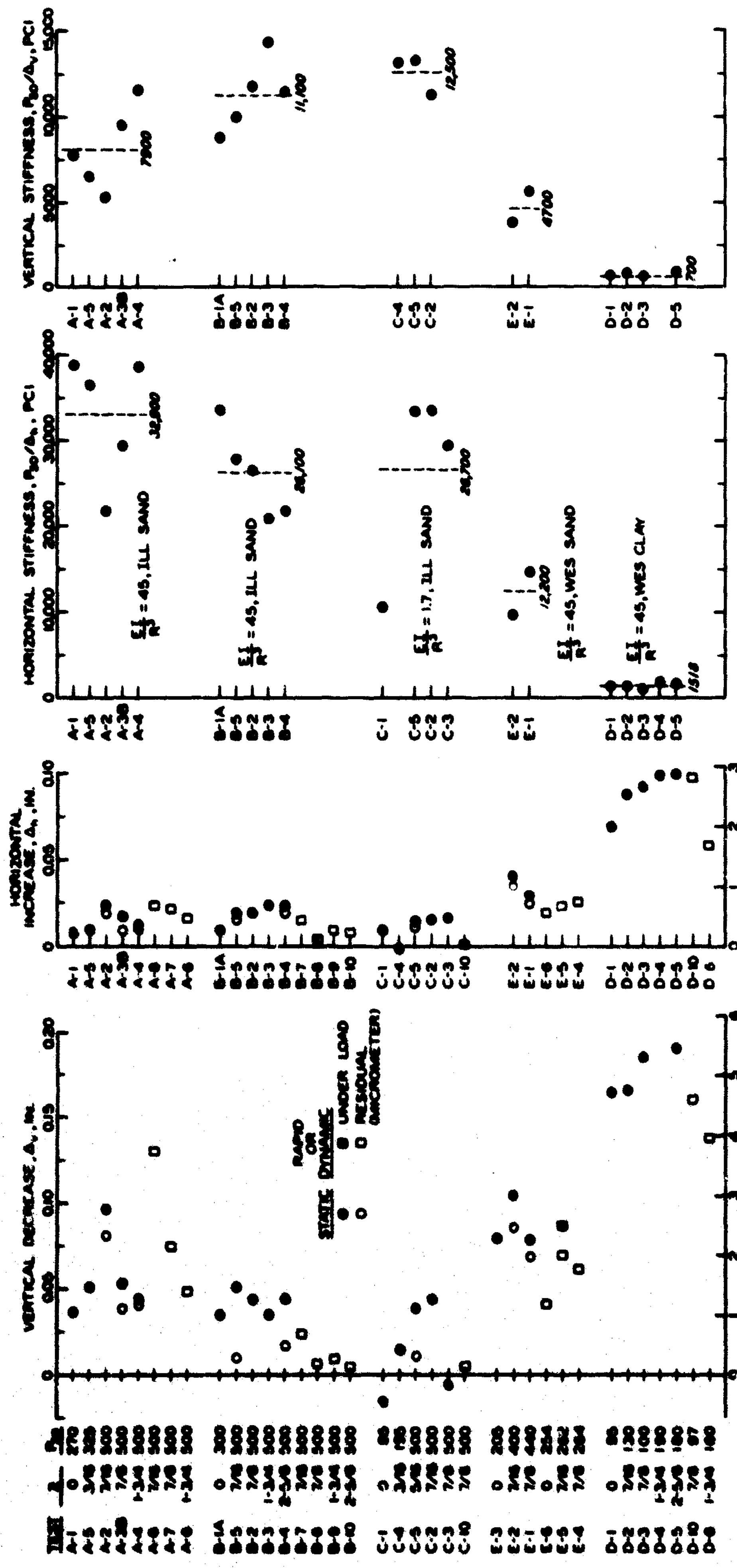

Fig. 6.4 Peak Diameter Changes and Deflection Stiffnesses

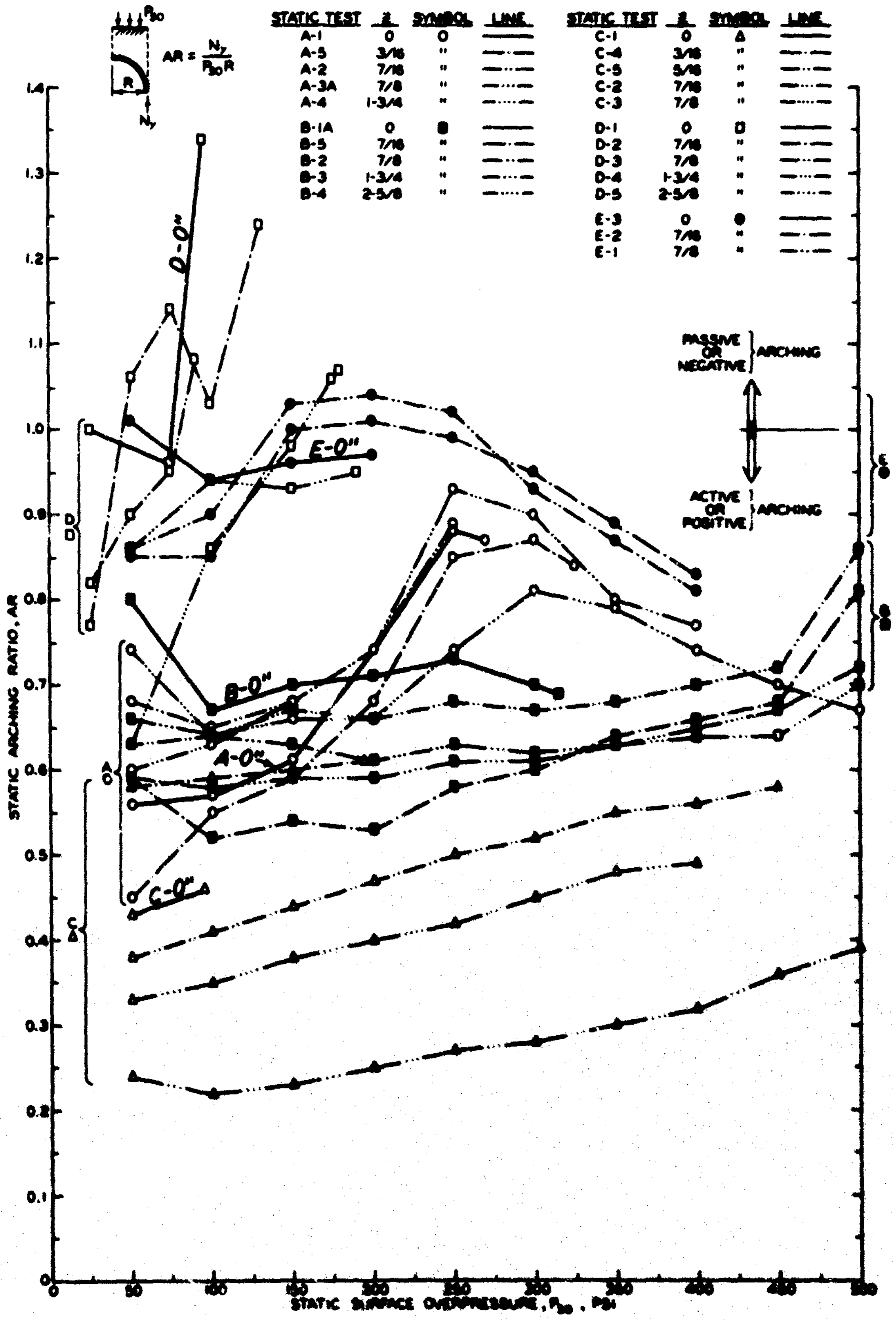

Fig. 6.5 Static Arching Ratio

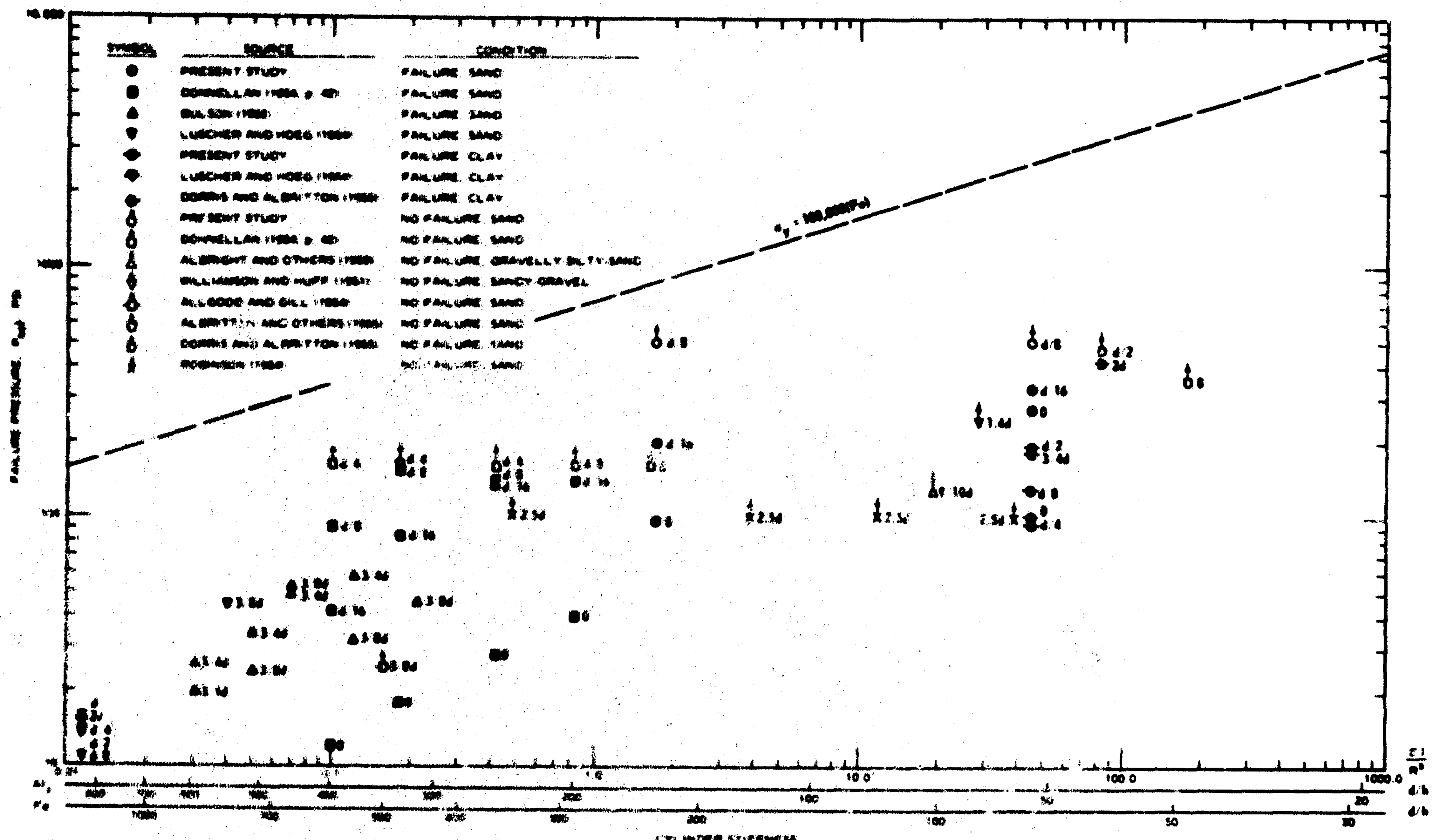

Fig. 6.6 Relation Between Failure Pressure and Cylinder Stiffness

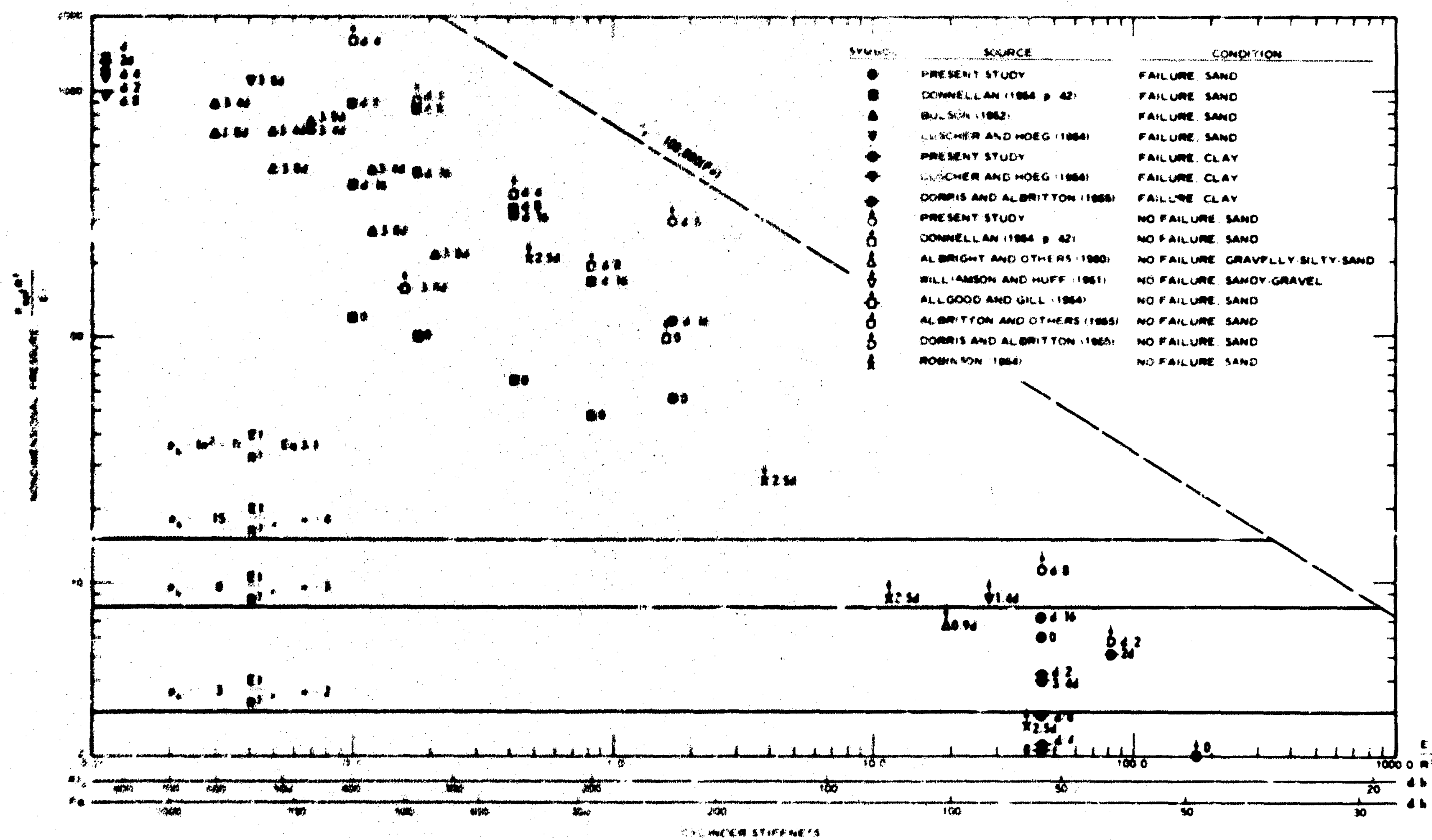

Fig. 6.7 Relation Between Nondimensional Pressure and Equation 3.1

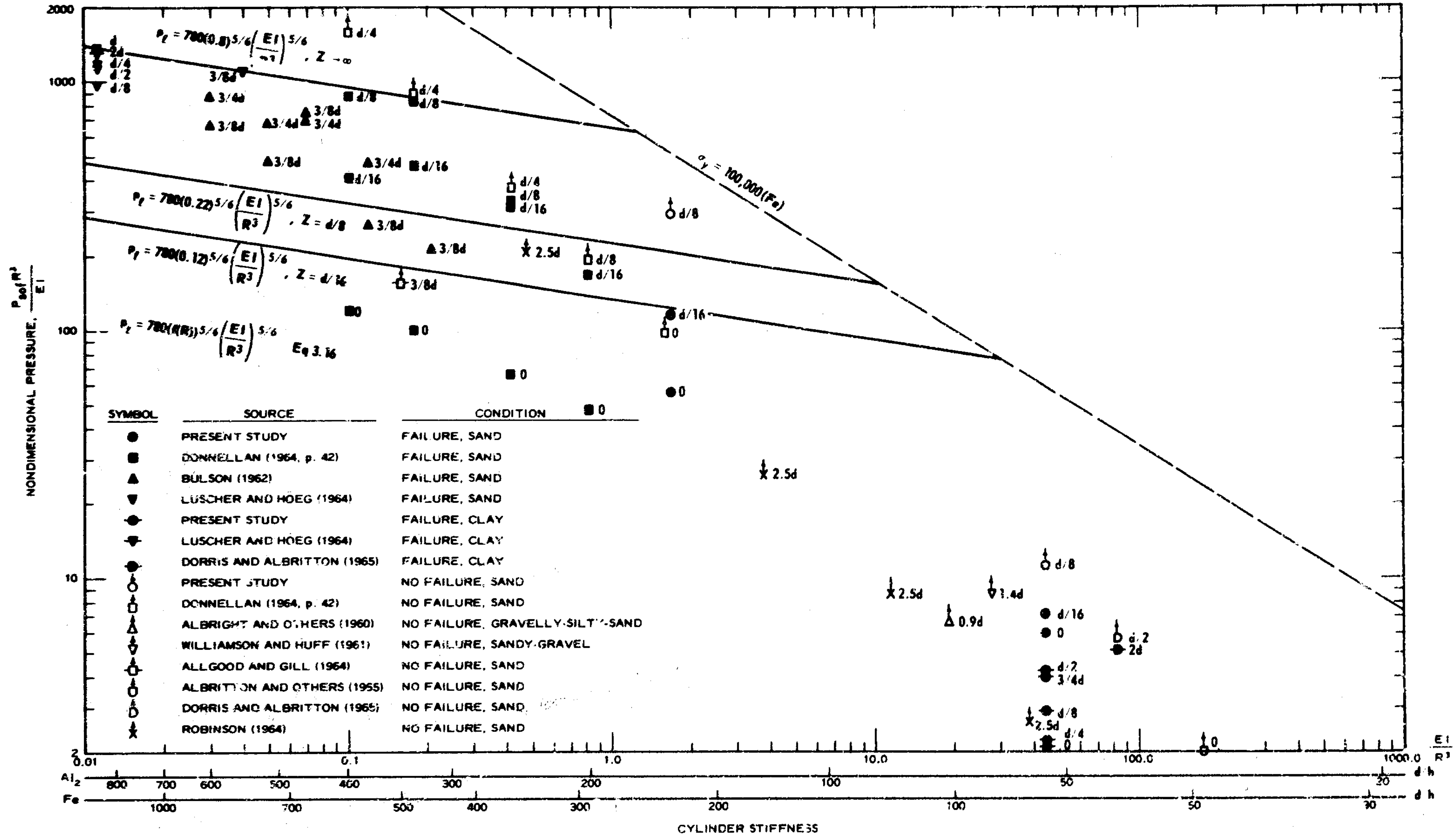

Fig. 6.8 Relation Between Nondimensional Pressure and Equation 3.16

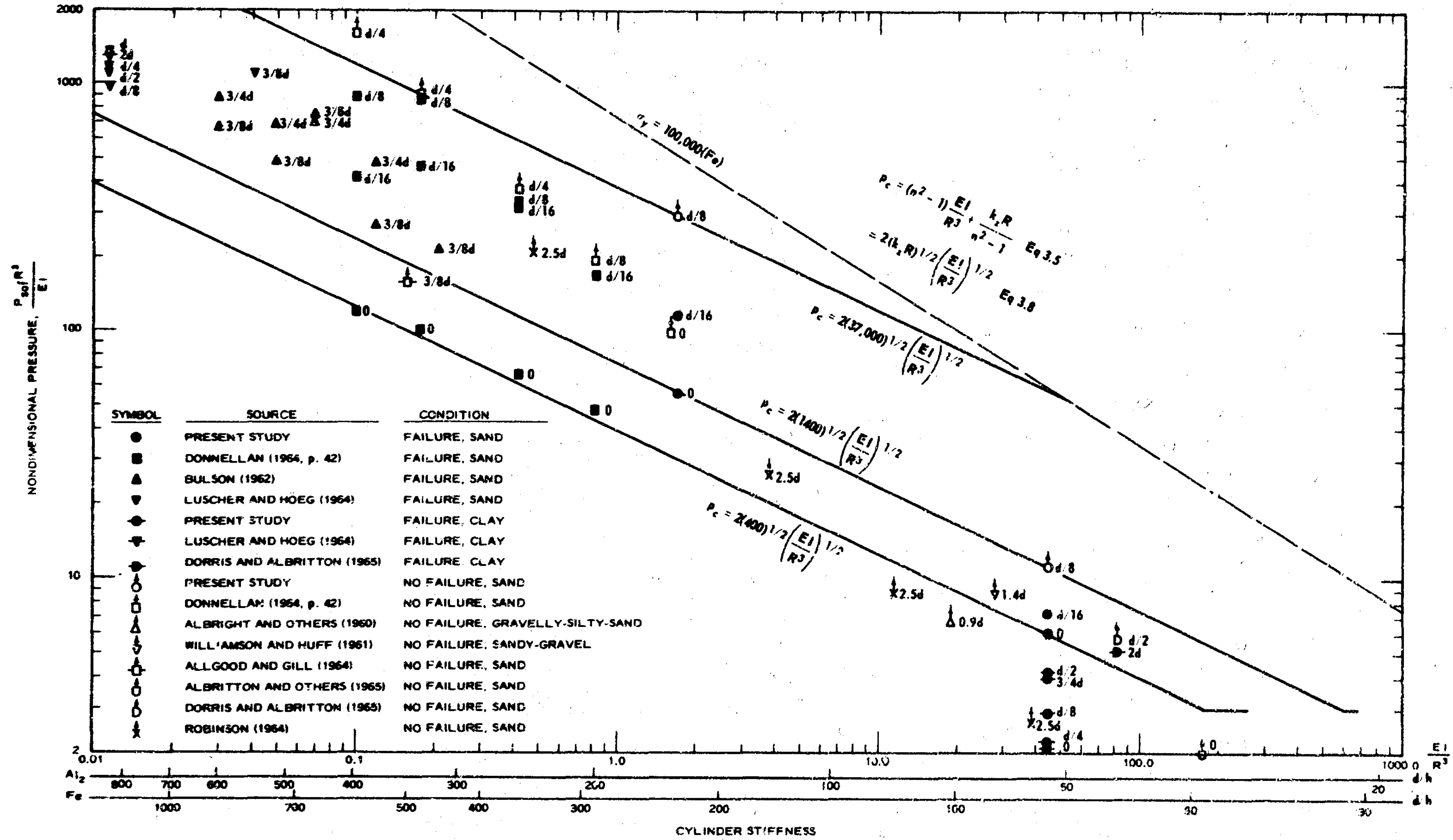

Fig. 6.9 Relation Between Nondimensional Pressure and Equation 3.8

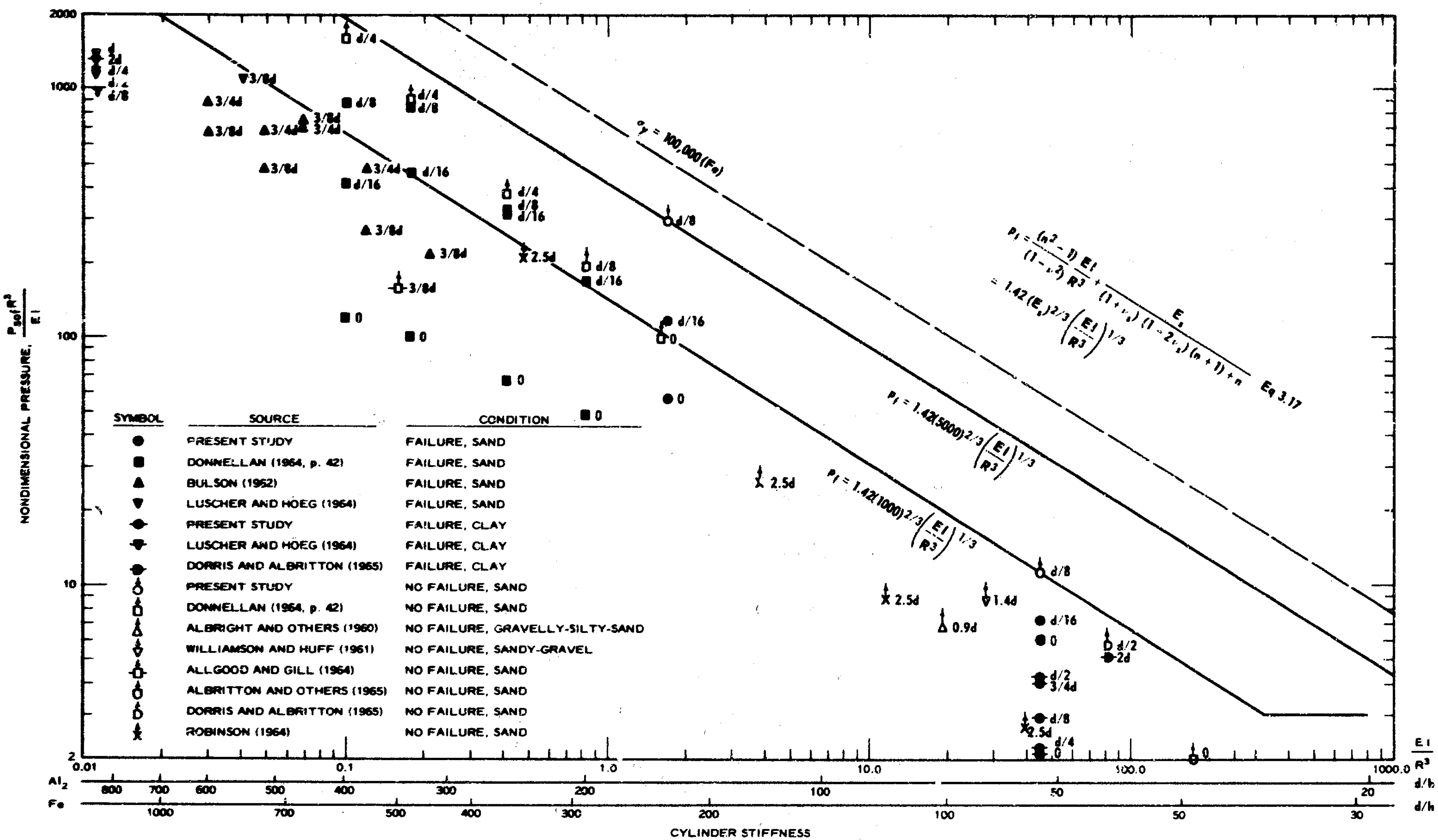

Fig. 6.10 Relation Between Nondimensional Pressure and Equation 3.17

APPENDIX A. PROPERTIES OF ALUMINUM TUBE MATERIAL

The cylindrical test specimens were cut from 12-ft lengths of Alcoa, drawn, aluminum tubing which was commercially available. Static, mechanical properties for the material are published in the manufacturer's literature, Aluminum Company of America (1960, p 59, and 1962, p 162). However, the values given are either minimum or average values, and hence do not adequately describe a given piece of tubing. Additionally, it was necessary to know the full stress-strain curve for the material up to the maximum strains experienced during the cylinder tests. In many cases, these strains far exceeded the indicated yield values.

Longitudinal tension test specimens were cut from each end and from the center section of the 12-ft lengths of tubing. The specimens averaged about 10 in. in length and were proportioned in accordance with ASTM Designation: E8-61T, ASTM STANDARDS 1961, Part 3 (pp 165-181).

The flat grips of the tension test machine proved unable to hold the slightly curved test specimen adequately once yielding commenced. Therefore, a special adapter was designed to accommodate the curvature of the specimen to the flat test grips.

Specimen from the tubes designated A, B, and C were all tested at the University of Illinois in a Tinius Olsen Testing Machine. It was used as a constant strain-rate device. An average crosshead speed of 0.05 in./min was used. It was first thought that the strain could be recorded adequately by monitoring with a manually operated Baldwin strain indicator. This proved satisfactory only for strains below first yield. The strain indicator operator was not able to keep a continuous balance above yield due to the large strain changes. Hence, the system finally established utilized a Moseley X-Y plotter to record both load and strain simultaneously.

Specimens from the tubes designated D and E were tested at WES in a 30,000-lb, Riehle universal testing machine. An X-Y plotter was again employed.

Average stress-strain curves were developed for each 12-ft tube. They are plotted in Fig. A.1 and reduced to a finite number of digitized points in the tables shown on the figure. These points were used to describe the curve for the computer program.

The tension tests revealed no systematic variation in stress-strain characteristics along the length of the 12-ft tubes. The modulus of elasticity for the material, 10×10^6 psi ($\pm 5\%$), was verified by all of the tests. However, the inelastic stress-strain curves for the 6061-0 A, D, and E material varied from the average by ± 10 percent. The overall accuracy of the measurements, procedure, and reduction of data for the 6061-T6 and 5052-0 material was within ± 5 percent of the average.

Although tubes A, D, and E were made of the same material, 6061-0, the inelastic stress-strain properties were sufficiently different from tube to tube that separate stress-strain curves were utilized in the data reduction.

Handbook yield values taken from Aluminum Company of America (1960, p 59) point up the fact that all the tubing does, in fact, exceed the manufacturer's indicated strengths. The values are indicated in Fig. A.1.

The stress-strain properties in Fig. A.1 were used in the computation of thrust and moment under both static and dynamic loading. It was assumed that the static stress-strain relation would be a good approximation of the dynamic stress-strain relation. Aluminum is not, in general, strain-rate sensitive according to Steidel and Makerov (1960) and Smith (1963).

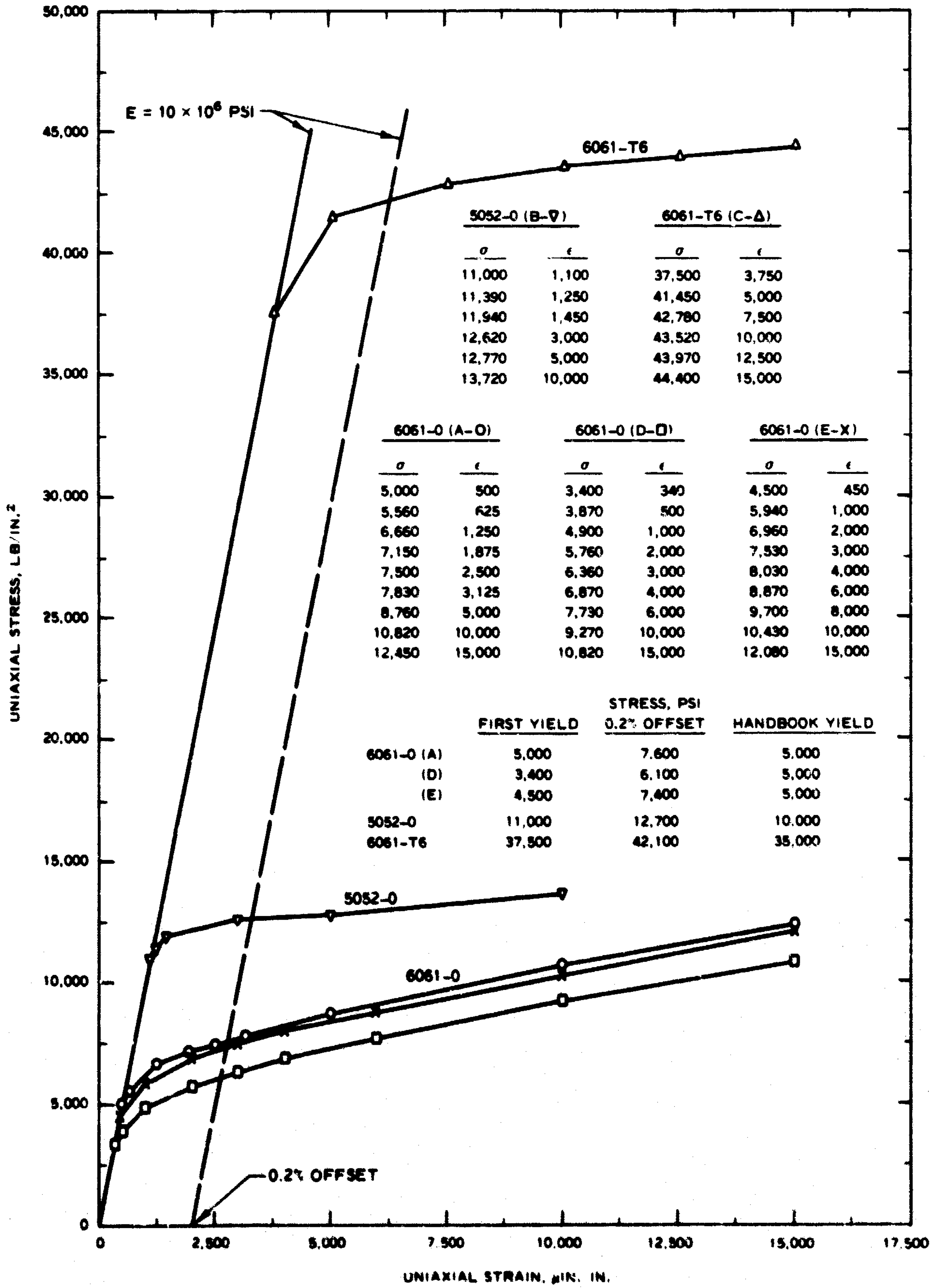

Fig. A.1 Aluminum Stress-Strain Properties

APPENDIX B. PROPERTIES OF SANGAMON RIVER AND COOK'S BAYOU SANDS

B.1 Placement Techniques

Since special effort was made to place and control the quality of the soil medium, it is probably denser and more uniform than that which could be obtained in a field installation.

B.1.1 Sangamon River Sand

This sand was stored in closed 55-gal drums near the testing device. A 2-gal water bucket was filled with sand, weighed on Toledo scales (0.1-lb graduations), carried to the test device and sprinkled into place. The sand was placed in 6-in. lifts. After 6 in. of sand had been placed, the lift was vibrated with a probe-type, concrete vibrator (Viber Co., Model II). The probe was vibrated completely through the 6-in. lift and was positioned on 2-in. centers in an ever-decreasing spiral around the center. This process was repeated until the test device was filled (four lifts) and screeded off.

A trench was then scooped out of the center of the sand and the cylinder placed at its intended depth and leveled. The sand was backfilled in the vicinity of the cylinder in 3/4-in. lifts by sprinkling the lift in and then rodding with a small ruler and tamping with a piece of wood.

The weight of sand displaced by the cylinder placement and subsequent backfilling was measured for each test. By assuming an effective volume of soil to be disturbed during placement, it was possible to calculate the average density of the sand in the immediate vicinity of the cylinders. The calculations indicated an average density of 105.4 ± 1.5 pcf. The horizontal stiffness calculations in Section 6.2 also verify the fact that the sand was very stiff. Penetration tests were not run because of the likelihood of disturbing the cylinder specimen. Additionally, recent research at WES* on the use of penetration tests in dense sand has indicated that inherent scatter in hand-operated penetration test data within a layer is so great that variations in density on the order of 1 or 2 pcf are effectively masked.

The overall density was established by dividing the measured weight of the sand placed by the known volume of the test device (less the cylinder volume). The overall density was very reproducible and averaged 104.0 pcf with a minimum of 103.5 pcf and a maximum of 104.5 pcf.

The strain gages were continuously monitored during the placement. The A and B groups of cylinders were insensitive to the placement, but great care had to be exercised in backfilling around the very thin C group. In all cases the tendency was for elongation of the vertical axis. However, impressed strains were kept below 50 µin./in.

B.1.2 Cook's Bayou Sand

This sand was stored in piles on the floor and shoveled into the hopper of a sprinkling (also known as raining or showering) device. The gross weight was measured by an electric load cell. The sprinkling device was placed over the SBLG base and maintained a known distance above the surface (24 in.); while the device was slowly turned at a constant rate, the sand dropped through the hoses, Fig. B.1. A density-height of fall study was made to determine an optimum turning rate and height of

* Private communication with J. G. Jackson, Jr., Chief of the Impulse Load Section, Soils Division, U. S. Army Engineer Waterways Experiment Station, CE, Vicksburg, Miss., April 13, 1965.

fall.* The full merits of the sprinkling technique are discussed by Whitman and others (1962, Appendix B).

The sand was placed up to the proposed level of the bottom of the cylinder. The cylinder was then positioned and sand was sprinkled in a manner intended to duplicate the free-field placement to bed the lower portion (90 degrees to 270 degrees). A piece of cardboard was used to deflect the sand beneath the spring line. The sprinkler was then repositioned and the remainder of the sand placed. The excess was screeded from the top to form a flat surface. A study** to determine the effect of sprinkling sand around a small-scale buried structure has shown that the density in the vicinity of the structure can be about 2 pcf less than the average density in the free field.

The average density was 106.6 $\pm$ 1.0 pcf. There was more scatter in average density with the sprinkling technique than with the vibration technique used for the Sangamon River sand.

B.2 Soil Strength and Deformation Characteristics

B.2.1 Sangamon River Sand

This sand was obtained from the Pontiac Stone Company, Mahomet, Illinois. It was wet and not of desired gradation when received. A system outlined by Prakash (1962, p 223) was used to obtain a uniform sand comparable to that tested by Hendron (1963). The sand was spread on the floor of

* W. J. Turnbull, Chief, Soils Division, WES, "Soil Tests on Sprinkled Cook's Bayou No. 1 Sand Small Blast Load Generator Specimens," Memorandum for: Chief, Nuclear Weapons Effects Division, July 22, 1964.

** R. W. Cunny, Chief. Soil Dynamics Branch, Soils Division, WES, "The Effect of an 8-In.-Diameter Arch on the Density Produced by Showering Placement Method," Memorandum for: Chief, Nuclear Weapons Effects Division, December 1, 1964.

the Illinois civil engineering test track and dried. Then, 8-lb batches were subjected to 5 min of sieving on a Gilson shaker (Model CL-262) that was fitted with a No. 40 and No. 60 sieve. The material retained on the No. 60 sieve was utilized for this investigation. The grain size distribution is shown in Fig. B.2.

The static, stress-deformation characteristics in triaxial and consolidometer tests are presented in Fig. B.3. These tests were run on sand having a density as close as possible to the overall average density used during the cylinder tests. The relative density, D_r , is also listed in Fig. B.3. Standard procedures were used.* Moduli and shear strength data are presented in Fig. B.5.

B.2.2 Cook's Bayou Sand

This sand is commonly used in most of the WES blast load generator experiments, e.g. Tener (1964). It was procured locally and its characteristics were originally documented (then called Bayou Pierre Sand No. 1) in a WES Soils Division Memorandum for Record.** However, recent laboratory tests performed for this investigation, Figs. B.4 and B.5, indicate that the one-dimensional stress-strain curve and angle of internal friction for a density of 106 pcf in the memorandum were in error.

It is evident that the two sands used have nearly identical laboratory properties at the densities employed because they were placed at equal relative densities. Also, the differences in the techniques used

* Described in a laboratory manual prepared by the Waterways Experiment Station for the Office, Chief of Engineers, which will be issued as a Corps of Engineers Engineer Manual.

** P. F. Hadala, Impulse Load Section, Soils Division, WES, "Soils Laboratory Tests on Bayou Pierre Sand No. 1," Memorandum for Record, 1963.

to place the sand in the vicinity of the cylinder negate any refinements in explaining differences in laboratory soil properties. The sand around the cylinder in the Cook's Bayou sand tests may have been only of medium relative density.

B.3 Elastic Properties

Hendron (1963, p 84) concluded that the coefficient of earth pressure at rest, K_o , varies inversely with the angle of internal friction, ϕ , as determined from drained triaxial tests.

$$K_o = 1 - \sin \phi \qquad \text{B.1}$$

For these sands, $\phi = 38^o$, Fig. B.5, and therefore

$$K_o = 1 - \sin 38^o = 1 - 0.6 = 0.4 \qquad \text{B.2}$$

If the soil were an elastic medium,

$$K_o = \frac{v_s}{1 - v_s} \qquad \text{B.3}$$

and hence

$$v_s = \frac{K_o}{1 + K_o} = \frac{0.4}{1.4} = 0.29 \qquad \text{B.4}$$

where v_s is Poisson's ratio for the soil.

Young's modulus of elasticity for the soil, E_s , may be expressed in terms of the constrained modulus from t e consolidation test, M_c , as

$$E_s = \frac{(1 + v_s)(1 - 2v_s)}{(1 - v_s)} \quad M_c \qquad \text{B.5}$$

$$= \frac{(1 + 0.29)(1 - 0.58)}{(1 - 0.29)} \quad M_c$$

$$= \frac{(1.29)(0.42)}{0.71} \quad M_c = 0.76 \; M_c \qquad \text{B.6}$$

Variations of the constrained secant modulus, M_{cs} , with vertical pressure are plotted in Fig. B.5. One-dimensional properties obtained at several relative densities for the Cook's Bayou No. 1 sand are reported by McNulty (1965).

Whitman and Healy (1962), discussing triaxial test results, and Davisson (1964), discussing one-dimensional test results, have indicated that essentially no dynamic strain-rate effects exist for dense, dry sands of the type used in this investigation.

Fig. B.1 Sand Placement in the SBLG

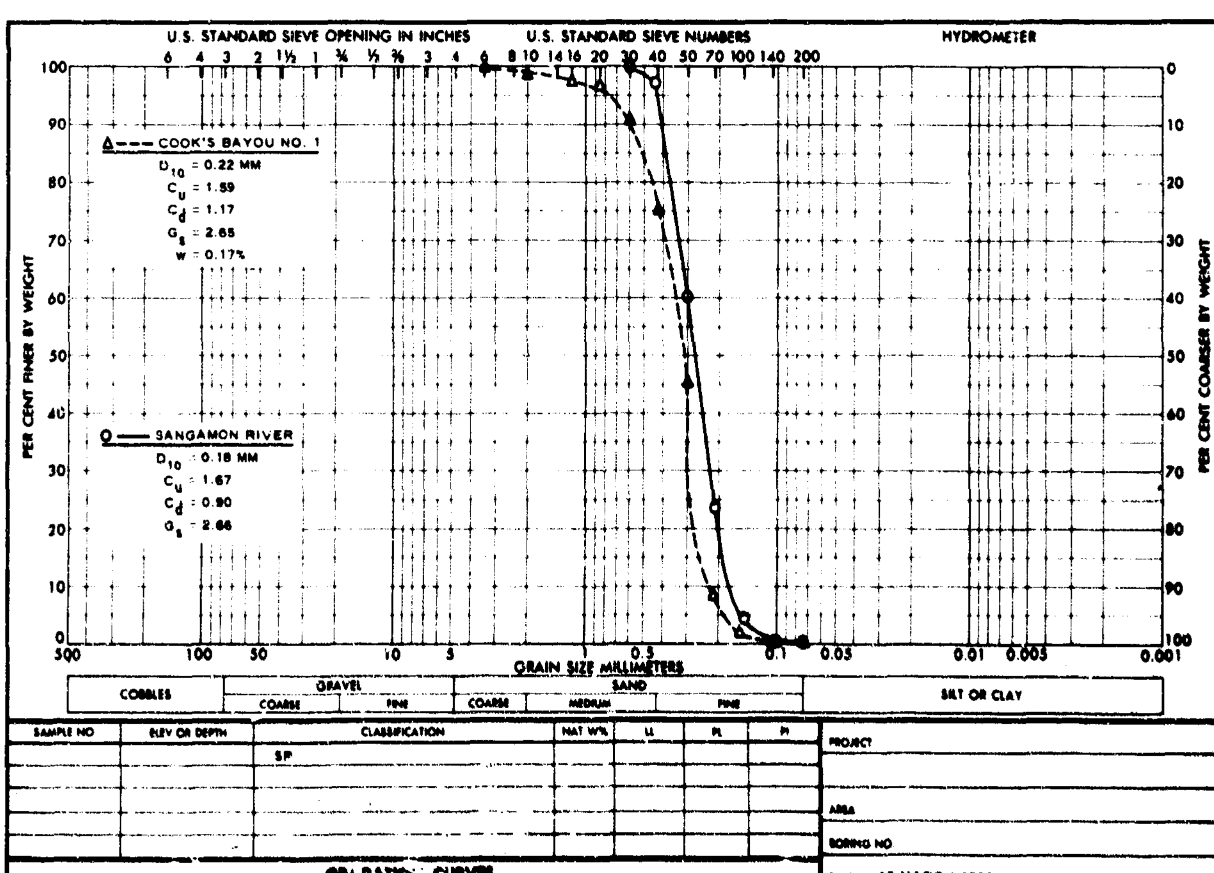

Fig. B.2 Gradation Curves for the Sands

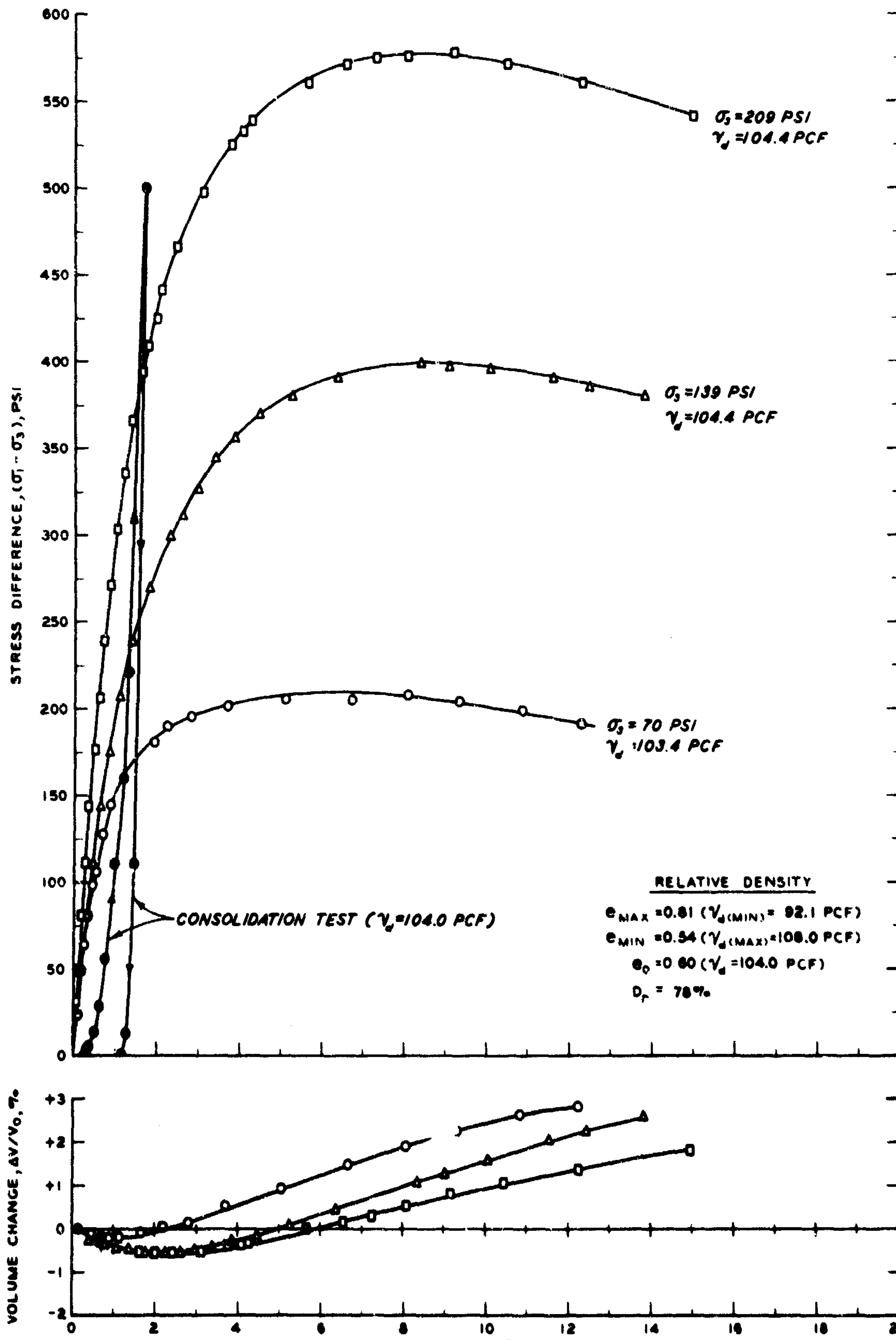

Fig. B.3 Stress-Strain Relations for Sangamon River Sand

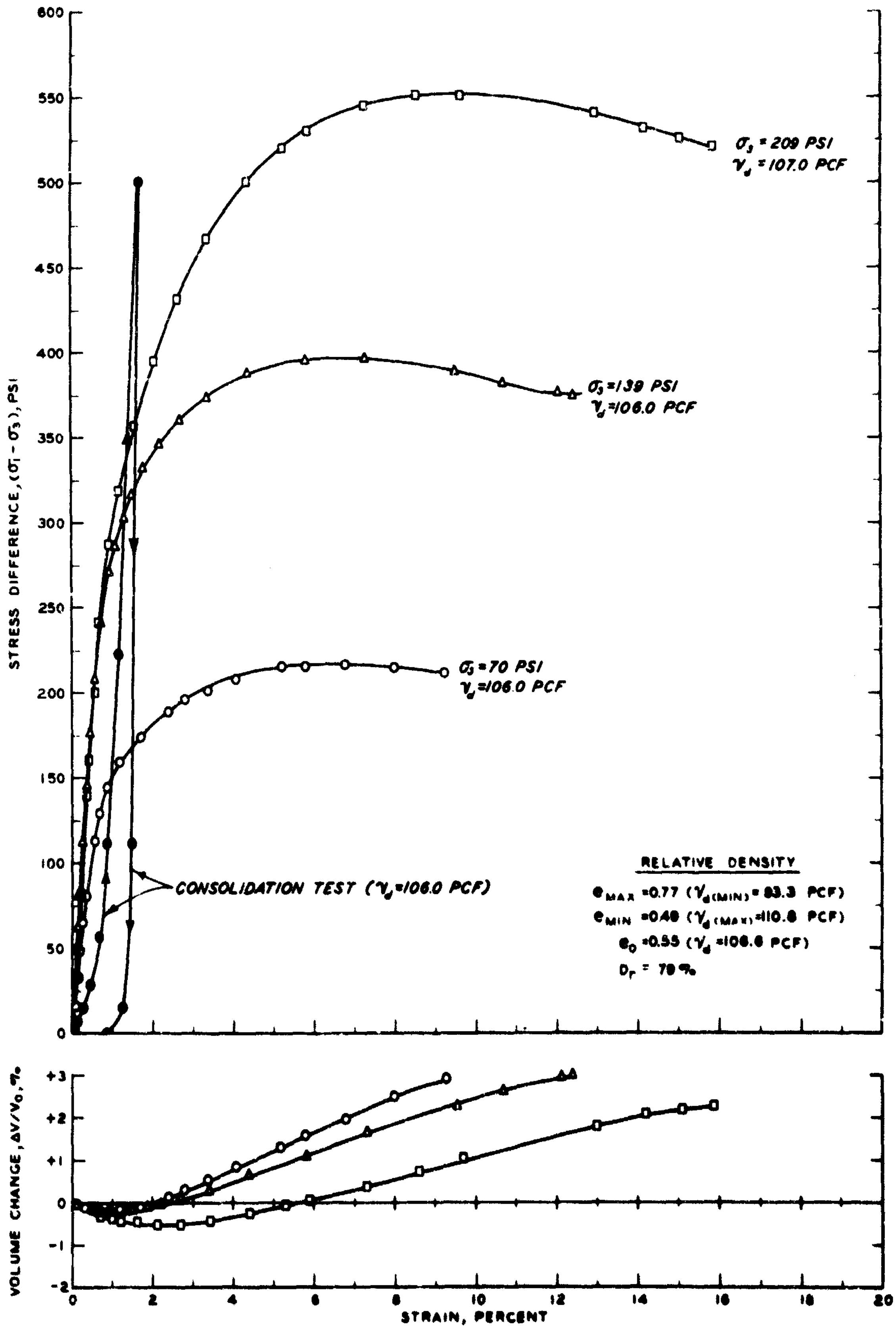

Fig. B.4 Stress-Strain Relations for Cook's Bayou No. 1 Sand

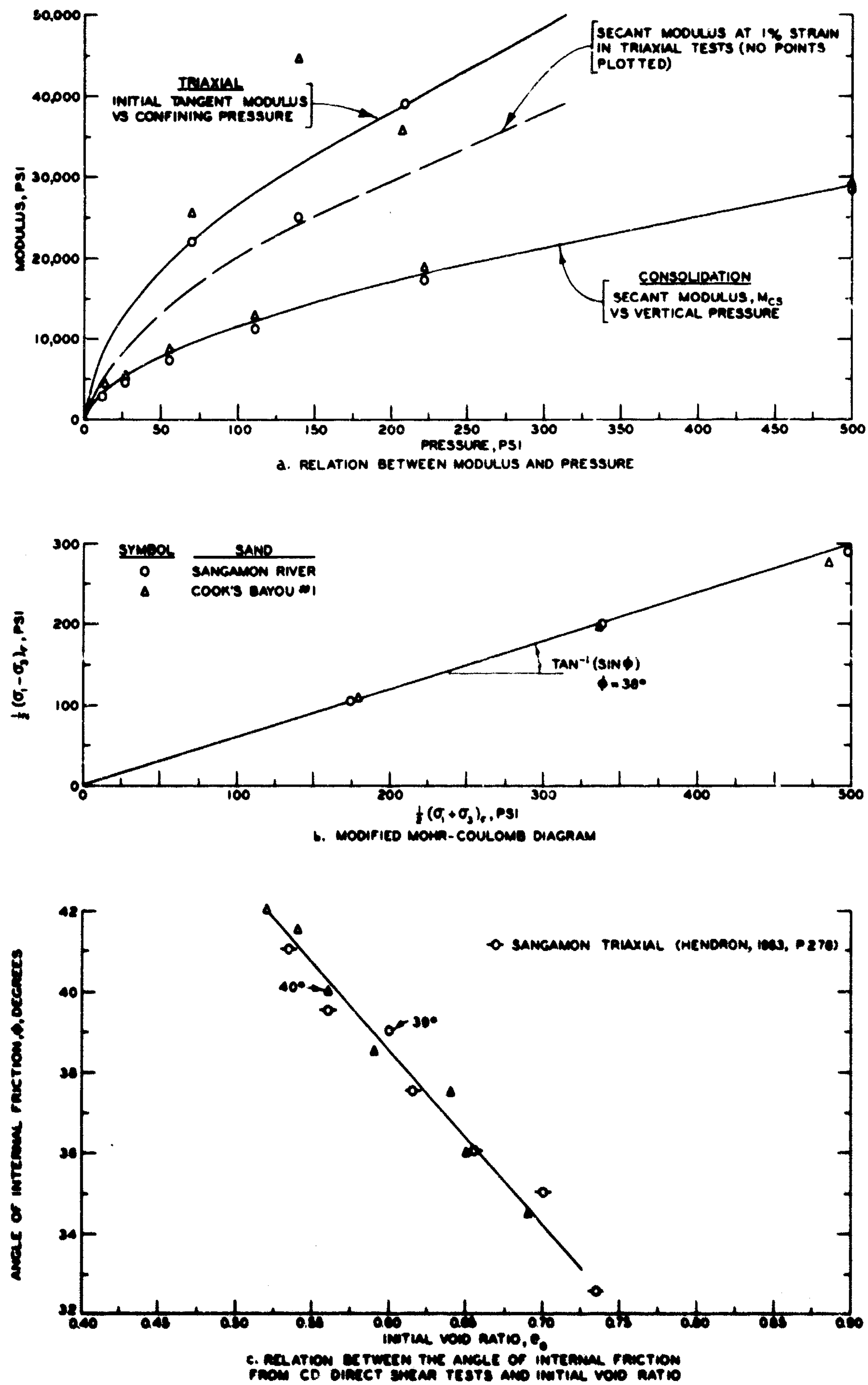

Fig. B.5 Moduli and Strength Characteristics for Sands

APPENDIX C. PROPERTIES OF BUCKSHOT CLAY

C.1 Placement Techniques

The placement of small-scale test structures in a clay soil is a new endeavor. Luscher and Höeg (1964, pp 219-225) pointed out some of the difficulties in soil control. Inherent in the WES test setup are two additional difficulties: (a) the cylinder ends are closed before burial so that strutting the diameters is impracticable; (b) the cylinder cannot be positioned vertically for soil placement and then positioned horizontally for loading because the test chamber is a complete ring and cannot be sectioned.

It was therefore decided to use a technique already developed for footing tests, Carroll (1963) and Jackson and Hadala (1964), to place and compact the clay to the top of the 2-ft-deep test device. The cylinder would then be placed in the medium by cutting out a trench of appropriate dimensions in the center of the clay specimens and carefully backfilling around the cylinder. The technique for accomplishing the latter task was determined and patterned after procedures described in a feasibility study.* Although adequate for the present investigation, the technique still has some drawbacks which will be discussed below.

The procedure followed in placing the 2-ft-thick clay specimen in the SBLG ring is shown in Fig. C.1. The clay was mixed in a pugmill and brought to the test area by truck, Fig. C.1a. When stored, the clay was kept continuously sealed in a polyethylene membrane (wrapper) except when

---

* R. W. Cunny, Chief, Soil Dynamics Branch, Soils Division, WES, "Tentative Placement Technique for Cylinders Buried in Clay Specimens," Memorandum for: Chief, Nuclear Weapons Effects Division, 1965 (in preparation).

soil was removed. The soil was processed on Fridays and allowed to cure over a weekend. The soil was weighed so that each loose lift, Fig. C.1b, would produce a 2-in. compacted lift. The loose soil was first hand-tamped, Fig. C.1c, and then compacted by three passes of a pneumatic tamper, Fig. C.1d. The soil surface was scarified, Fig. C.1e, between lifts. The quality of the placement was controlled and checked primarily through the use of density samples, Fig. C.1f. Vane-shear tests, Fig. C.1g, were made for certain specimens. Unconfined and confined compressive tests were performed on soil cubes that were taken from the top 8 in. of the specimen before and after each test. The pretest cube was taken at a distance of 1 ft from the cylinder and the hole was filled in a manner to duplicate the free-field placement. These results, as well as water content and density determinations,are given in Table C.1.

The cylinder was placed by cutting out an area in the center of the 2-ft-thick clay specimen, Fig. C.2a. The length and width of the cavity were the same for all tests and only the depth was varied. A template was used to size the excavation, Fig. C.2b, and it also served as a guide for the scooping operations, Fig. C.2c, which cut out a seat for the bottom half of the cylinder. The half-cylindrical cavity was formed exactly to the cylinder dimensions, and areas were carved out to accommodate the strain gages and end nuts, Fig. C.2d. The cylinder was then placed in the carved-out area, Fig. C.2e. The backfill was placed in loose, 3/4-in. lifts, Fig. C.2f, and compacted by three passes of a Harvard miniature compactor, Fig. C.2g. A lift is shown in place in Fig. C.2h. It is believed that very close contact was achieved between the clay and the cylinder.

All 16 hoop strain gages were monitored during the placement operation. Some strain was impressed into the cylinder during each phase of the placement. Although several remedial methods (such as imposing a small vertical load on the cylinder through a saddle adapter) were tried to eliminate the strains, it was only possible to minimize them. About 40 percent of the total strain caused by placement occurred during the first seating phase, Fig. C.2e. Much of the remainder came during the first and second backfilling lifts; very little disturbance was noted in the cylinder due to lifts placed after the crown was covered.

The strains were primarily bending in nature and were most severe at the quarter points. The strains indicated that the cylinders assumed a slight vertical-elliptical shape. They probably did not significantly influence the failure pressure or mode of failure.

The average impressed strain resulting from the placement is shown in Fig. C.3. It is apparent that this placement technique must be improved before it can be applied to more flexible cylinders. Dorris and Albritton (1965) had very satisfactory results with this technique on a stiffer cylinder ($EI/R^3 = 82$).

The placement technique was tedious and required a considerable amount of time. So much hand labor is involved that each of the ten tests required an average of one week in the testing device. Great care had to be taken to keep the clay sealed to avoid moisture loss. The water content determination from the cube tests indicates that this was successful (Table C.1).

The placement technique in the WES laboratory is probably better than that which could be achieved in a field installation.

C.2 Soil Strength and Deformation Characteristics

The gradation curve and specific gravity, G_s , are shown in Fig. C.4. The clay is classified as a CH , and the results of several Atterberg limits tests are shown in Fig. C.5. The static, unconfined compressive strengths, q_u , were determined in the laboratory from samples taken from 8-in. cubes cut from the in-place clay specimens (the hole was refilled to the same density). The results are plotted in Fig. C.6. Average values are listed for each test in Table C.1.

In order to establish the quality of the backfill, specimens of clay were compacted in a mold in as nearly the same manner as the backfill was compacted. Unconfined specimens were cut from the mold and tested. The results are plotted in Fig. C.6. Those, coupled with the information from the vane-shear tests, indicate that the backfill was about 25 percent weaker than the compacted soil in the free field. Some of the weaker mold specimens were honeycombed (visual inspection) and this resulted in the lower values plotted in Fig. C.6 and the lower density values plotted in Fig. C.9. These molds were made during the early weeks of the investigation, and they may not have been truly representative of the compacted backfill.

Static triaxial (UU) test results are plotted in Fig. C.7. The degree of saturation, S_r , was about 90 percent and an apparent friction angle, ϕ , equal to 1.7 degrees was deduced.

In order to establish an approximation to the one-dimensional stress-strain relation, three consolidation tests were run in which the vertical stress was applied and the deformation recorded as a function of time, Fig. C.7.

Moduli from the triaxial (UU) tests are plotted against confining pressure, σ_3 , in Fig. C.8. These moduli exhibited a negligible increase with confining pressure and a line representing the average value is shown. Also in Fig. C.8, the secant modulus from the consolidation test at 6 sec elapsed time (after load application) is plotted with respect to vertical pressure.

The dry density, γ_d , is shown in Fig. C.9 with respect to water content. It can be seen that the in-place soil is very similar to that used by Jackson and Hadala (1964).

Carroll (1963) conducted dynamic triaxial tests on buckshot clay (w = 27.1%) and indicated that the clay is strain-rate sensitive. However, the dynamic cylinder tests of this investigation either masked the effect or did not benefit from it. Kane and others (1964) discussed the behavior of clay under rapid and dynamic loading.

Table C.1

Pretest Properties of Clay Specimens

	Order of Construction		Average Water Content, w, Percent					Cube Tests, Degree of Satura-tion, S_r %	Average Dry Unit Weights, pcf		Average UC Compres-sive Strength tons/sq ft		Average Vane Strength tons/sq ft		Pressure Applied During Cyl. Test psi	Average Posttest UC Com-pressive Strength tons/sq ft
Test	Ring	Date	Requested from Pug Mill	At Pug Mill	In Truck	From Top 8 in. Density Samples	From Soil Cube Tests		Top 8 in. of Ring γ_d	Soil Cube Tests γ_d	Soil Cube	Mold	Soil Field	Backfill		
D-1	1	11/16/64	26	25.2	24.9	24.9	25.2	89.9	96.3	96.0	2.90	1.65	3.97	--	300	3.8
D-2	2	11/30/64	25	24.7	24.7	24.1	24.2	91.3	97.3	98.1	3.16	--	--	--	130	3.6
D-3	3	12/7/64	25	24.7	24.7	23.8	23.9	87.2	97.8	96.9	2.83	--	--	--	100	4.8
D-4	4	12/14/64	25	25.2	25.4	24.5	24.4	88.9	96.5	96.7	2.72	2.22	--	--	190	3.9
D-5	5	12/21/64	25	25.2	25.4	24.3	24.3	90.2	96.6	97.5	3.38	1.89	--	--	180	4.4
D-10	6	1/11/65	25	25.5	24.4	24.1	24.0	88.5	98.1	97.3	3.05	--	--	--	97	3.4
D-9	7	1/18/65	25	25.5	24.4	23.7	23.7	89.1	8.6	98.1	3.35	1.91	5.28	4.22	148	3.6
D-8	8	1/25/65	25	27.0	25.0	25.6	25.0	88.2	95.3	95.4	2.52	3.10	4.20	4.06	116	2.9
D-7	9	2/1/65	25	27.0	25.0	26.1	26.7	90.7	95.0	93.8	1.90	2.18	--	--	180	2.1
D-6	10	2/8/65	25	--	--	24.6	24.3	89.0	96.9	96.9	3.06	2.76	--	--	160	3.1
				Average			24.6	89.3	96.8	96.7	2.89	2.24	4.48	4.14		

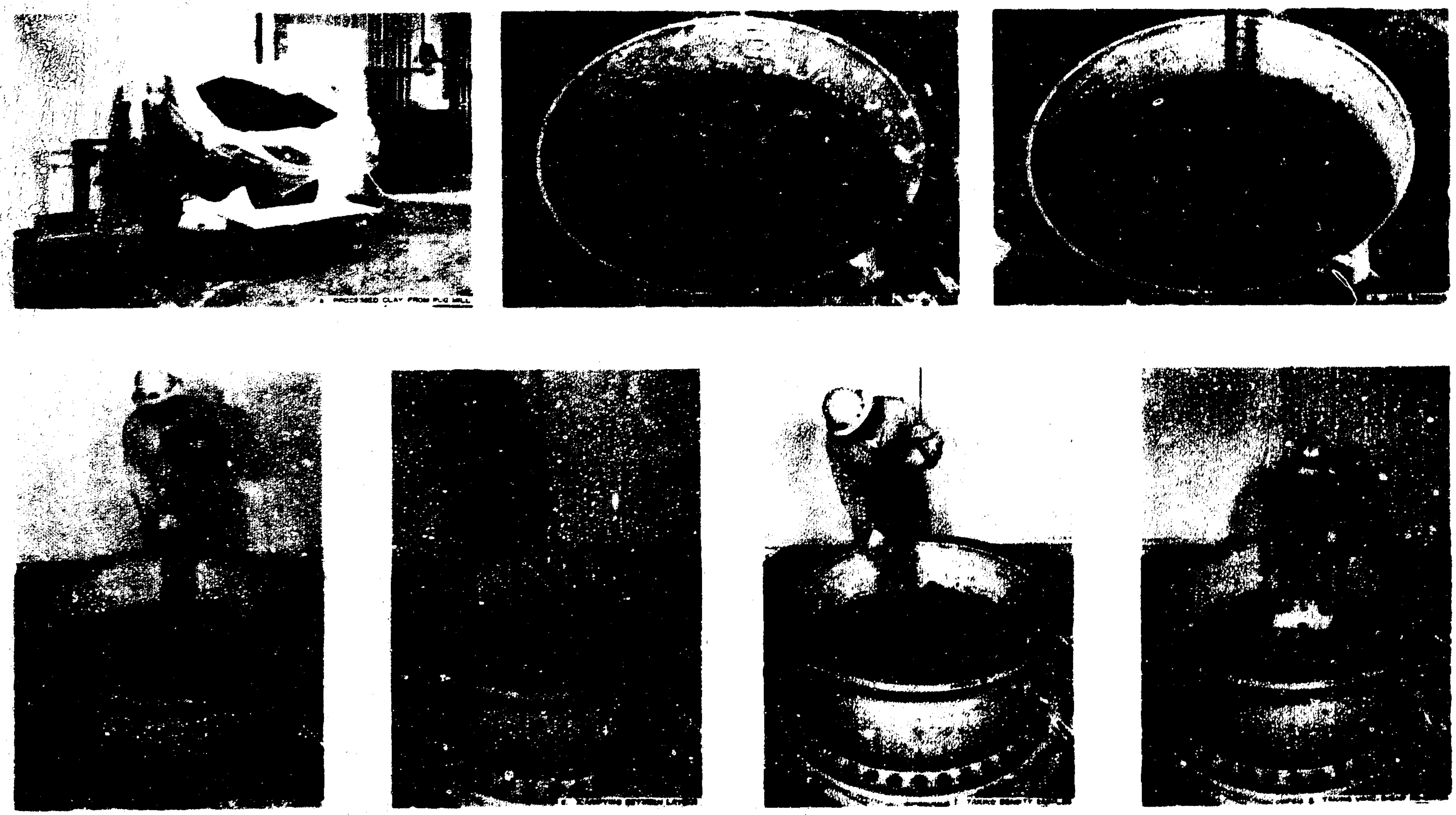

Fig. C.1 Placement of Buckshot Clay in WES Small Blast Load Generator

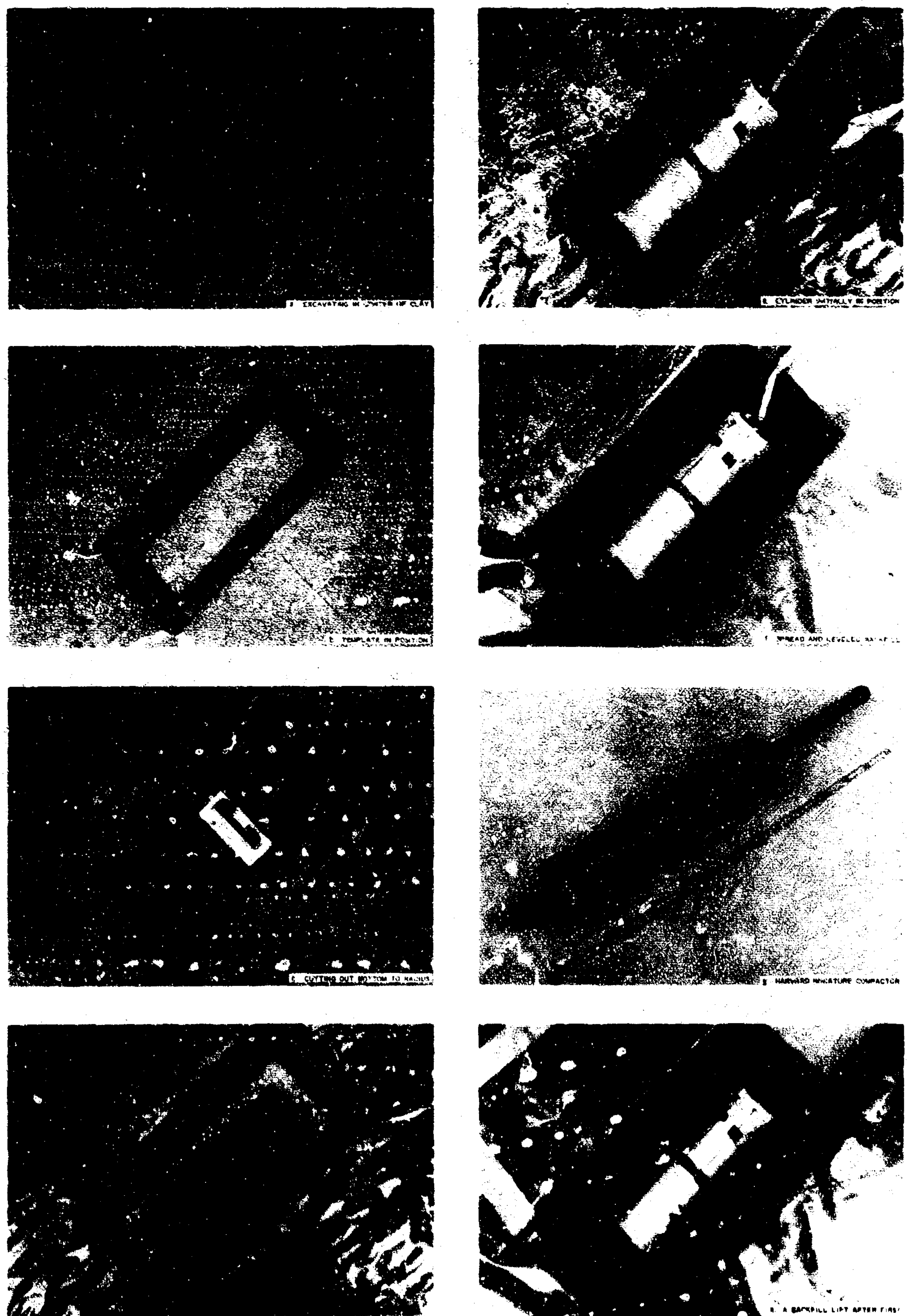

Fig. C.2 Placement of Cylinder in Buckshot Clay and Subsequent Backfilling

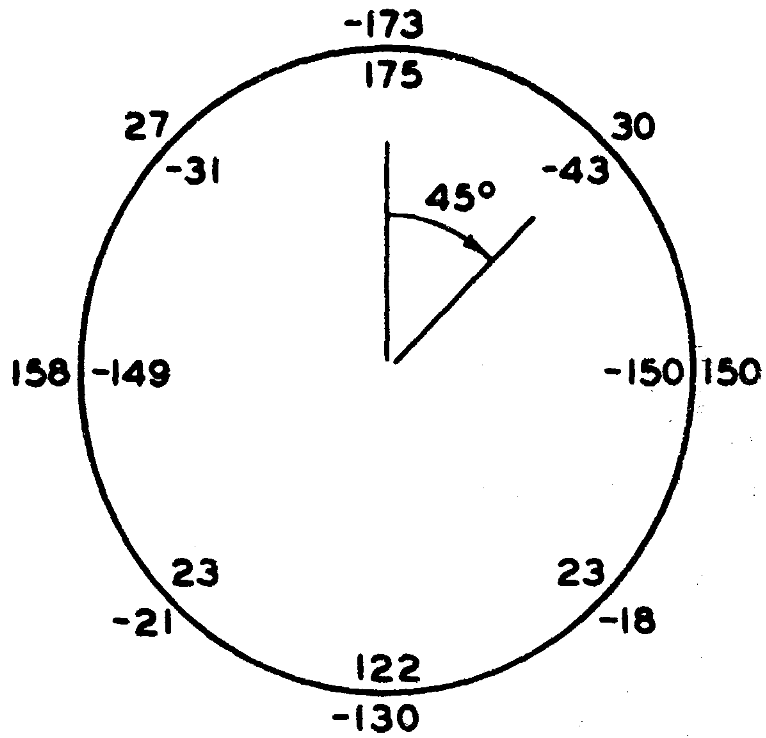

Fig. C.3 Average Placement Strains

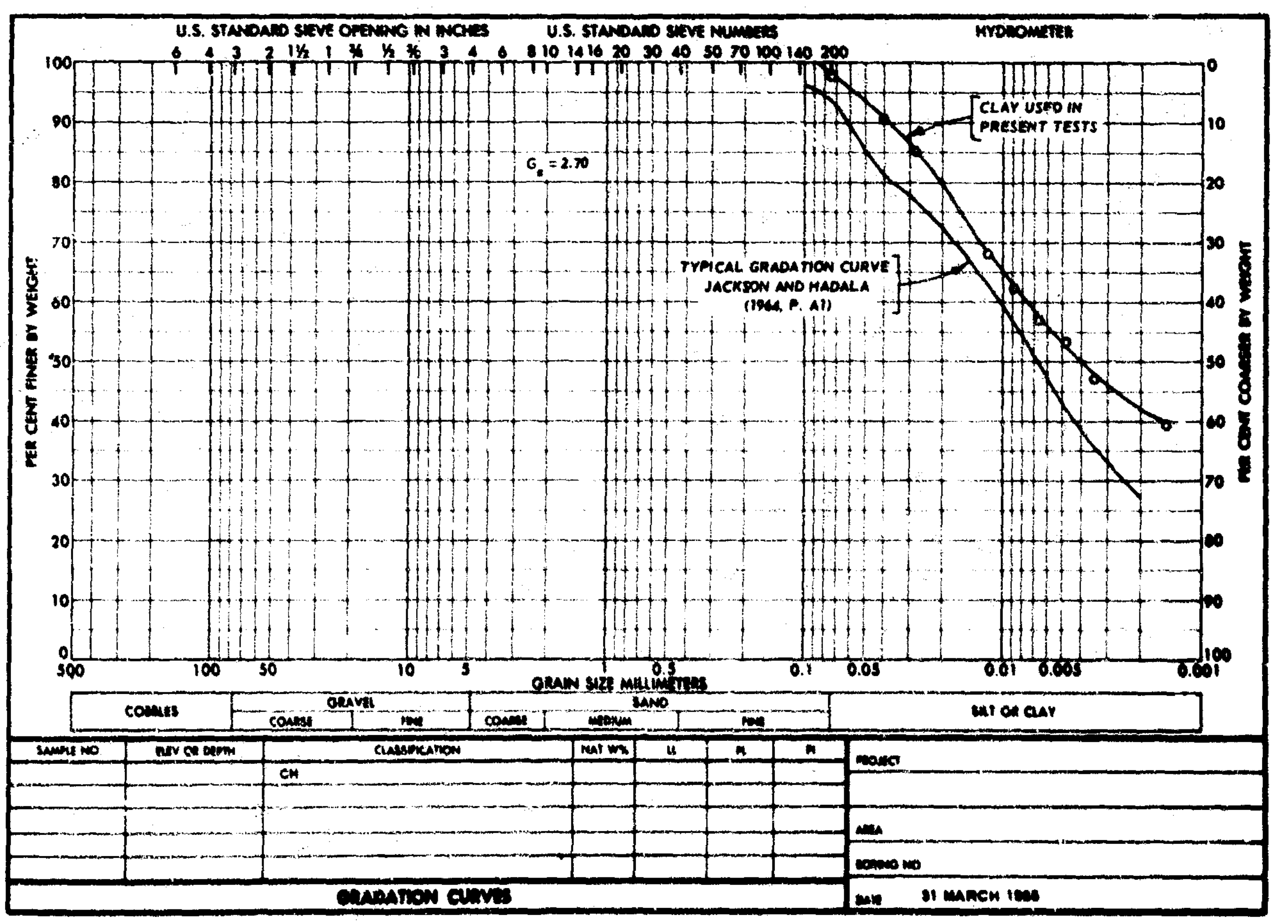

Fig. C.4 Gradation Curve for Buckshot Clay

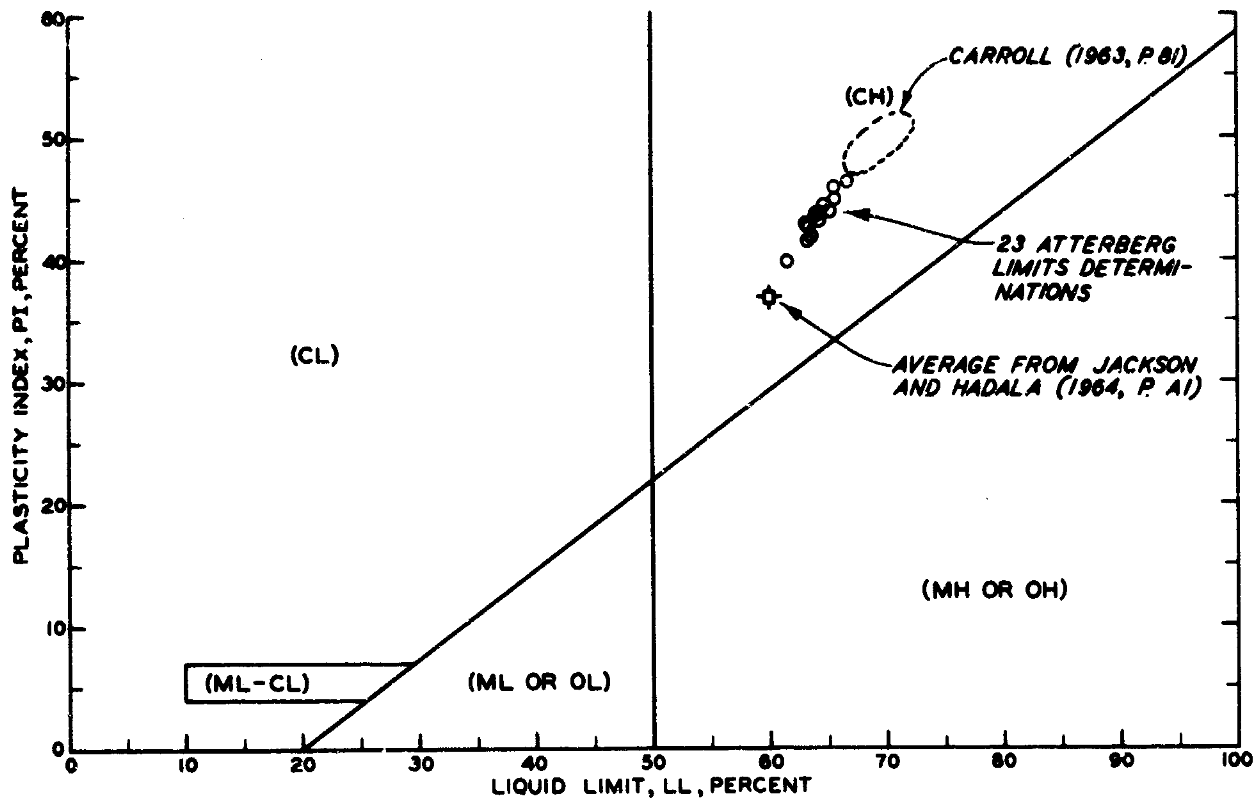

Fig. C.5 Atterberg Limits

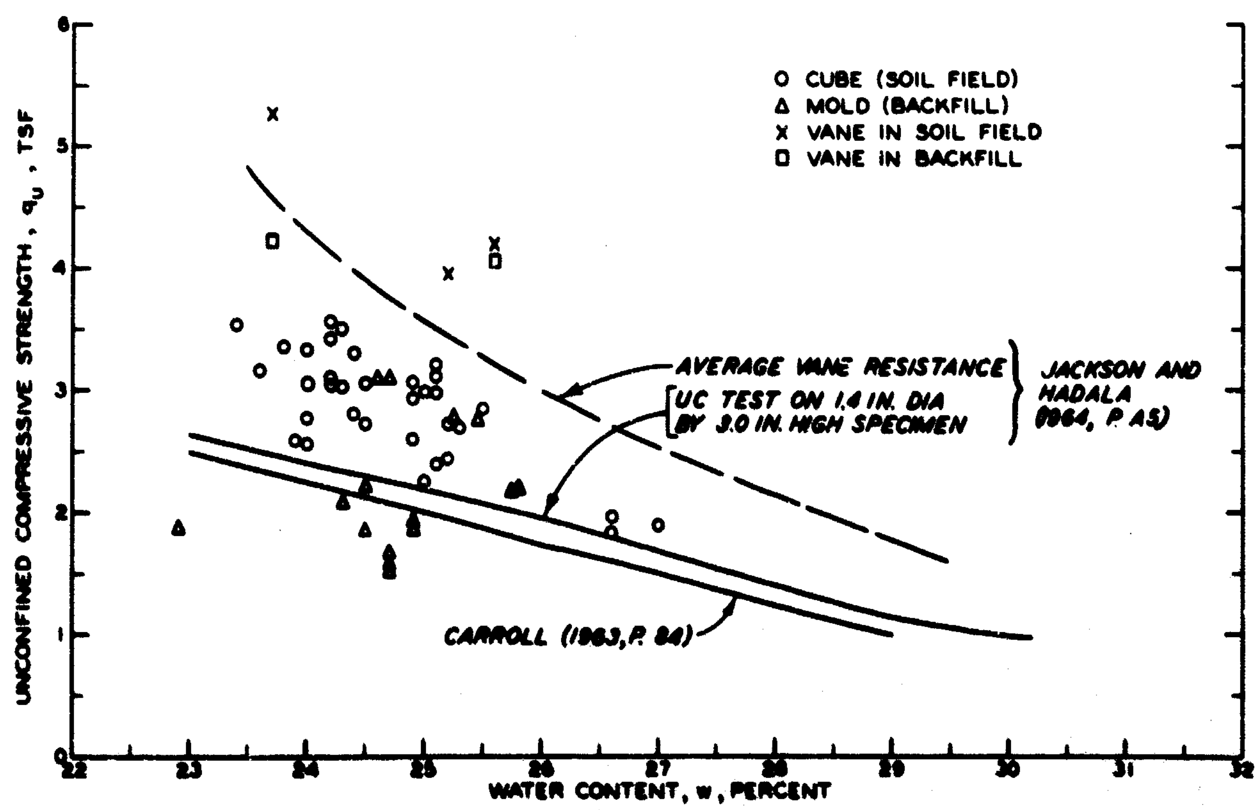

Fig. C.6 Unconfined Compressive Strength-Water Content Relation

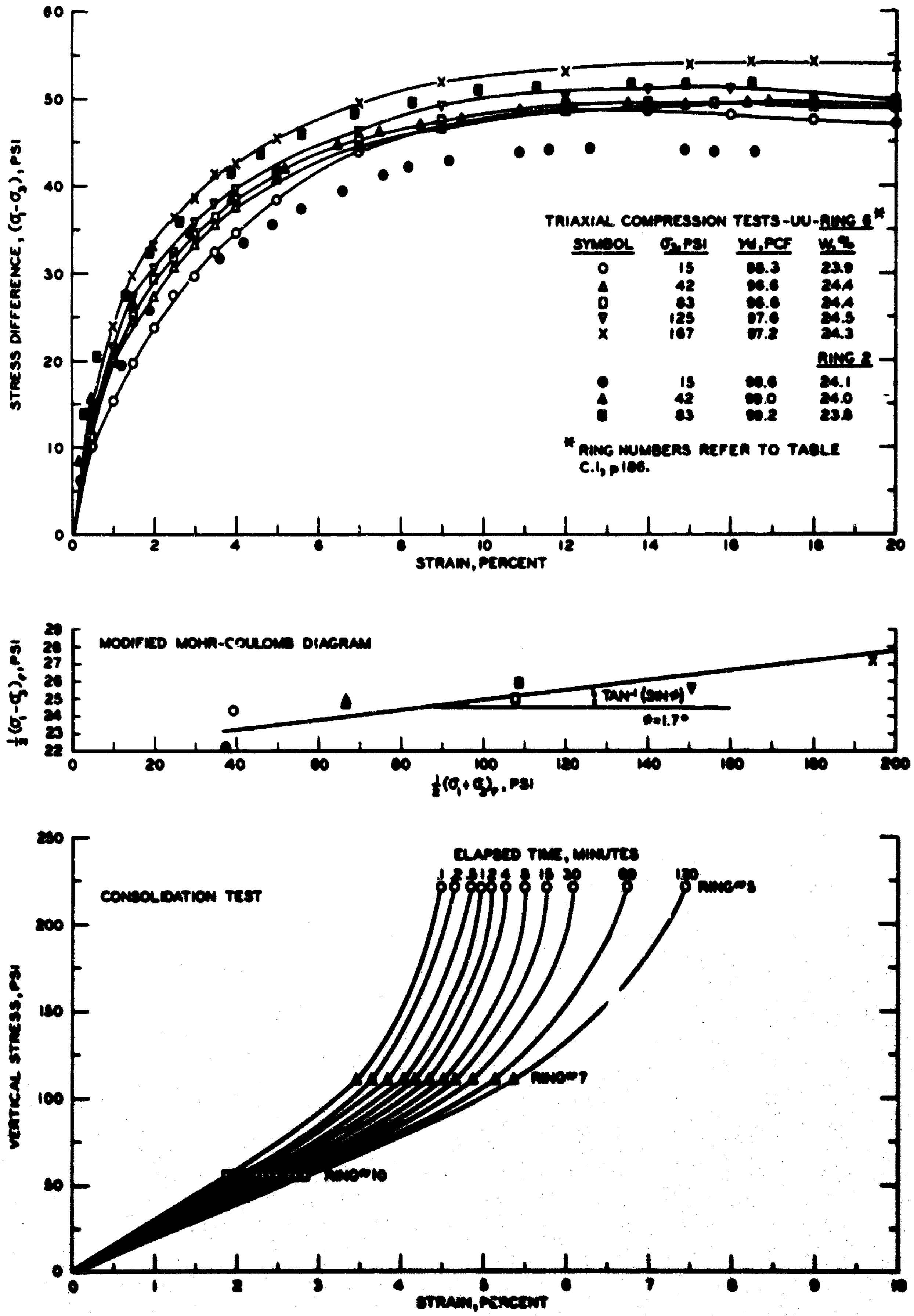

Fig. C.7 Stress-Strain Relations for Buckshot Clay

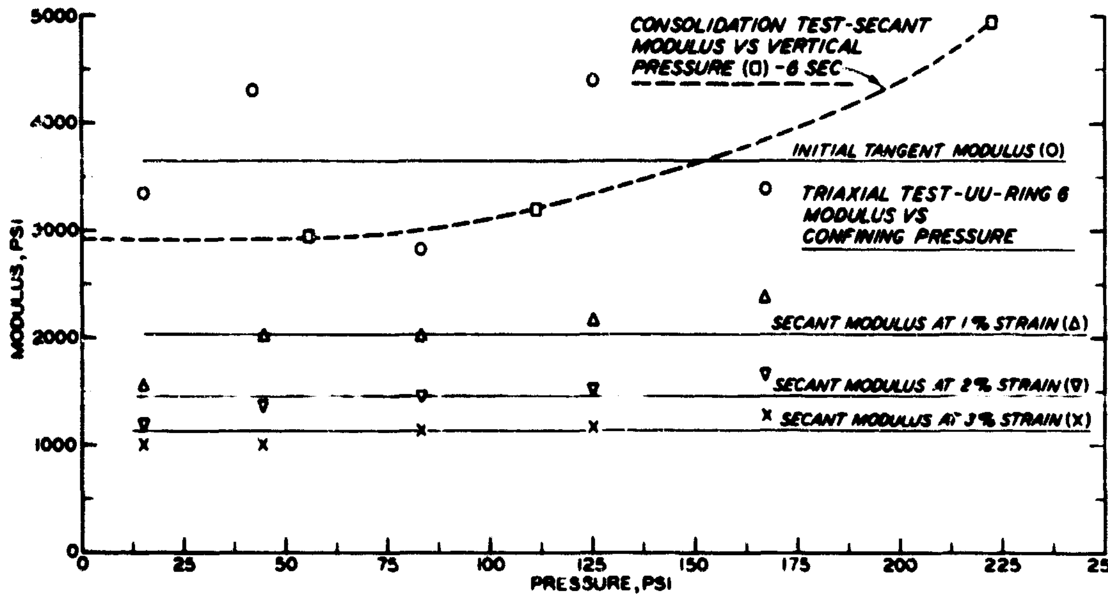

Fig. C.8 Relation Between Moduli and Pressure for Buckshot Clay

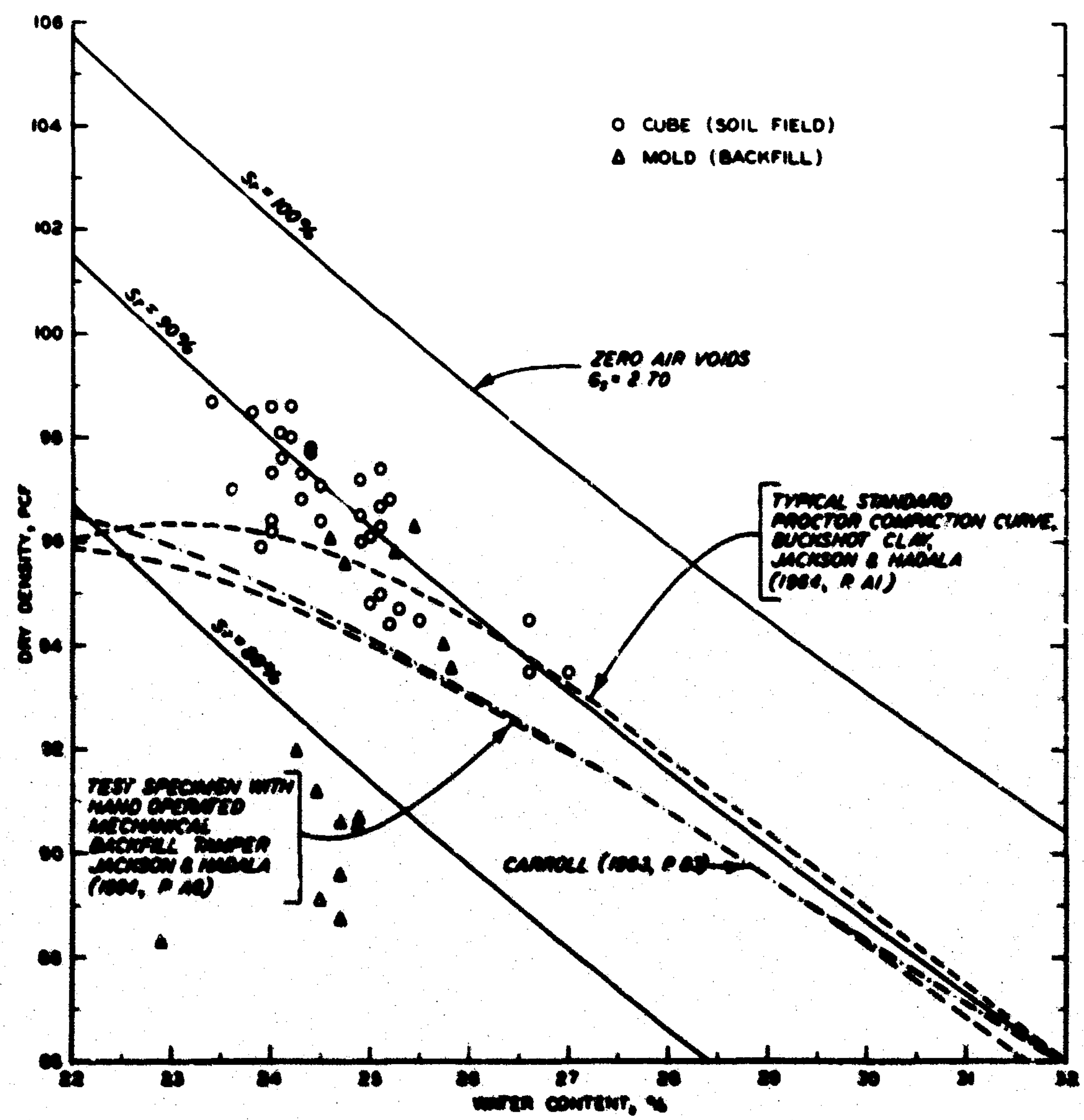

Fig. C.9 Density-Moisture Content Relation for Buckshot Clay

APPENDIX D. TRANSDUCERS

D.1 Strain Gages

Gages 3/8 in. long were used because gages long enough to give reasonable average strains but short enough to eliminate the necessity of making curvature corrections were desired.

However, to initiate the investigation while the 3/8-in. gages were being procured, cylinders B-1 through B-5 were instrumented with 1/4-in.-long gages. They were Budd Metalfilm strain gages, Type C12 141B, 1/4 in. by 1/8 in. The remainder of the B group and all of the A and C groups were instrumented with Type C12 161. These gages were all temperature-compensated for aluminum. They are not classified as post-yield strain gages but are capable of measuring strains accurately to 4-5 percent, according to the manufacturer. The gages functioned satisfactorily on tension test specimens (Appendix A) in that they measured strains accurately to values greater than 2 percent, and appeared to perform satisfactorily for the cylinder measurements.

Procurement complications prevented the acquisition of identical gages for cylinder groups D and E. Instead, Baldwin-Lima-Hamilton gages, Type FA-37-12-S13, were used. These are also 3/8-in. gages which are temperature-compensated for aluminum. The manufacturer indicates that these are accurate to 2 percent strain and they performed satisfactorily on tension test specimens strained beyond 1-5/10 percent.

Eastman 910 cement was tried as a gage adhesive on several tension test specimens, but was found to be unsatisfactory for strain levels beyond 0.5 percent. Armstrong adhesive C-2 was used to bond all of the strain gages to the cylinders.

The inside gages were waterproofed by an application of Gagekote No. 1 (a solvent-thinned synthetic resin compound) while the outside gages were covered with Gagekote No. 5 (a two-compound, rubber-like epoxy resin) followed by Gagekote No. 2 (a solvent-thinned nitrile rubber) to isolate them further from the soil media.

A limited study was made to determine the potential influence of the soil pressure (acting as a normal force) on the outside strain gages. Four gages were mounted on a piece of 1/2-in.-thick aluminum plate and covered with various protective coatings, Fig. D.1. Gage 1 had a metal cover so that no soil pressure could reach the gage, and hence it served as a control on the response of the other three gages. All gages were waterproofed. Gage 2 was covered with a 0.015-in.-thick strip of fish-paper, gage 3 with Gagekote No. 5, and gage 4 with a piece of electrical, rubber tape. The plate was horizontally buried in sand and loaded statically to 300 psi. Negligible differences were noted in the response of the four gages, and the technique used for gage 3 was selected for its ease of use.

D.2 Diameter Change Gages

A diameter change gage was required which would be expendable since the cylinder collapse would destroy anything inside. The transducer used was recommended by Professor V. J. McDonald of the University of Illinois. It consisted of a curved strip of 0.01-in.-thick brass shim stock 1/4 in. by 6 in., Fig. D.2. Budd Metalfilm, Type C12 141B, strain gages were mounted on each side of the strip's center with Eastman 910 cement. The gages were joined electrically to indicate only the bending strains. Two 1/32-in.-diameter holes were drilled in each end of the strip and in the cylinder. The same nut and bolt arrangement was used for mounting the strip in the cylinder, Fig. 4.1a, as was used in calibration.

Each diameter change gage was calibrated in extension and compression in a Pratt and Whitney Super Micrometer. The apparent strain gage output was a linear function of displacement, and amounted to 5 μin./in. per 0.001 in. of diameter change.

The gage could not be used for rapid or dynamic testing because it experienced excessive ringing under these loadings. Gages were coated with petroelastic to dampen the spurious vibrations but no improvement resulted.

D.3 Overpressure Gages

For the tests conducted at the University of Illinois, Bourdon gages were used to measure the static overpressure. Their accuracy was verified relative to other available gages.

The rapid pressure tests were monitored by a Kistler piezoelectric pressure transducer Model 601. The transducer was calibrated prior to testing and its output was a linear function of overpressure, 0.41 picocoulombs per psi or about 125 psi per inch of paper deflection. The gage was checked after each test, and no calibration changes were required.

Both the static and dynamic tests at WES were monitored by Norwood pressure transducers Model 211. These were statically calibrated prior to each test, and exhibited a generally linear response. They were ranged for about 250 psi/in. of paper deflection statically, and 125 psi/in. of paper deflection dynamically.

At least two gages were used in each test and the measured pressure for the gages was within ±5 percent of the average. A Bourdon gage was used to verify the peak static pressure and thereby made the static values more reliable; but the dynamic results probably varied either because of the use of a static calibration or because of the motions of the gage mounts. The gages were located between the firing tubes in the dynamic bonnet. A study by Kennedy and Sadler (1965) has shown that the surface pressure distribution is uniform within ±10 percent.

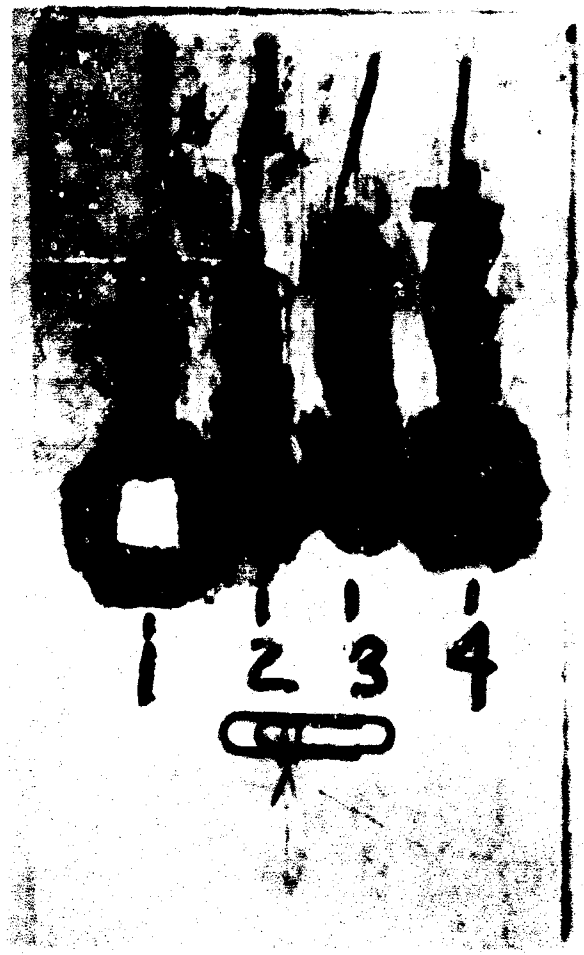

Fig. D.1 Strain Gage Test

Fig. D.2 Diameter Change Gage

VITA

Albert Francis Dorris was born in Utica, New York, on October 25, 1936. Following graduation from Utica Free Academy in 1955, he entered the United States Military Academy. He was named to the 1957 All-American Track and Field Team. In his senior year, he was appointed a Cadet Captain. He received the Bachelor of Science Degree in June 1959 and stood 6th in graduation order of merit out of a class of 499. Upon graduation he was commissioned as a regular officer in the United States Army, Corps of Engineers. He attended the Engineer Officers' Basic Course at Fort Belvoir, Virginia, and the U. S. Army's Airborne and Ranger courses at Fort Benning, Georgia, enroute to his initial assignment in Korea. From June 1960 to June 1961 he was with the 547th Engineer Company (Float Bridge) in Korea as a Platoon Leader and Company Commander. In August 1961 he entered the Engineer Officers' Advanced Course at Fort Belvoir and subsequently worked for a brief period in the Office of the Chief of Engineers before entering graduate training in Civil Engineering at the University of Illinois in June 1962. He received the Master of Science Degree from Illinois in June 1963 and from June 1964 to June 1965 was assigned to the U. S. Army Engineer Waterways Experiment Station, Vicksburg, Mississippi, as a Project Engineer. He currently holds the rank of Captain in the Corps of Engineers and is a member of the American Society of Civil Engineers, the Society of American Military Engineers, and the Association of the United States Army. He is an Engineer-in-Training in the State of Illinois.